TRIBOLOGICAL CHARACTERISATION OF ELECTROLESS Ni-P COATINGS UNDER HIGH TEMPERATURE

Thesis submitted by

SANJIB KUNDU

Doctor of Philosophy

(Engineering)

DEPARTMENT OF MECHANICAL ENGINEERING
FACULTY COUNCIL OF ENGINEERING & TECHNOLOGY
JADAVPUR UNIVERSITY
KOLKATA, INDIA

2019

JADAVPUR UNIVERSITY
KOLKATA-700032, INDIA

INDEX NO. 21/14/E

1. Title of Thesis:

Tribological Characterisation of Electroless Ni-P Coatings under High Temperature

2. Name, Designation & Institution of the Supervisors:

Prof. Prasanta Sahoo
Professor, Mechanical Engineering Department,
Jadavpur University, Kolkata-700032

Dr. Suman Kalyan Das
Assistant Professor, Mechanical Engineering Department,
Jadavpur University, Kolkata-700032

3. List of Publications (Referred Journals):

i. Sanjib Kundu, Suman Kalyan Das, and Prasanta Sahoo. "Tribological behaviour of autocatalytic Ni-P-B coatings at elevated temperatures." *Applied Physics A* 125 no. 520 (2019): 1-20. [SCI]

ii. Sanjib Kundu, Suman Kalyan Das, and Prasanta Sahoo. "Friction and wear behavior of electroless Ni-P-W coating exposed to elevated temperature."*Surfaces and Interfaces* 14 (2019): 192-207. [SCOPUS]

iii. Sanjib Kundu, Suman Kalyan Das, and Prasanta Sahoo. "Tribological behaviour of electroless Ni-P deposits under elevated temperature." *Silicon* 10, no. 2 (2018): 329-342. [SCIE]

iv. Sanjib Kundu, Suman Kalyan Das, and Prasanta Sahoo. "Tribological performance of electroless Ni-(high) P coatings under elevated testing temperature." *Materials Today: Proceedings* 4, no. 2 (2017): 379-387. [SCOPUS]

v. Sanjib Kundu, Suman Kalyan Das, and Prasanta Sahoo. "Influence of load and temperature on tribological behaviour of electroless Ni-P deposits." *IOP Conference Series: Materials Science and Engineering* 149, no. 1 (2016): 1-10. [SCOPUS]

vi. Sanjib Kundu, Suman Kalyan Das, and Prasanta Sahoo. "Friction and wear trends of electroless Ni-P coatings under high temperature test conditions." *BLB-International Journal of Science and Technology*, November, (2015): 84-91

vii. Sanjib Kundu, Prasanta Sahoo, and Suman Kalyan Das. "Optimization studies on electroless nickel coatings: a review." *International Journal of Manufacturing, Materials, and Mechanical Engineering (IJMMME)* 4, no. 4 (2014): 1-25. [SCOPUS]

viii. Sanjib Kundu, Suman Kalyan Das, and Prasanta Sahoo. "Properties of electroless nickel at elevated temperature-a review." *Procedia Engineering* 97 (2014): 1698-1706.

4. List of Patents: Nil

5. List of Presentations in National/ International Conferences:

i. Sanjib Kundu, Suman Kalyan Das, and Prasanta Sahoo (2018). Friction and wear characteristics of heat-treated Ni-P-W coatings under different velocity and temperature. 1st International Conference on Mechanical Engineering (INCOM), Jadavpur University, Kolkata, India, Paper ID 108.

ii. Sanjib Kundu, Suman Kalyan Das, and Prasanta Sahoo (2016). Tribological performance of electroless Ni-(high) P coatings under elevated testing temperature. 5th International Conference on Material Processing and Characterization (ICMPC-2016), GRIET , Hyderabad, India, Paper ID 210.

iii. Sanjib Kundu, Suman Kalyan Das, and Prasanta Sahoo (2016). Influence of load and temperature on tribological behaviour of electroless Ni-P deposits. International Conference on Advances in Materials and Manufacturing Applications (IConAMMA), Amrita Vishwa Vidyapeetham, Bangalore, India, Paper ID 036.

iv. Sanjib Kundu, Suman Kalyan Das, and Prasanta Sahoo (2015). Friction and wear trends of electroless Ni-P coatings under high temperature test conditions, National Conference on Product Design and Manufacturing (NCPDM), MNNIT, Allahabad, India, Paper ID 034.

v. Sanjib Kundu, Suman Kalyan Das, and Prasanta Sahoo (2014). Properties of electroless nickel at elevated temperature-a review, 12th Global Congress on Manufacturing and Management (GCMM), VIT University, Vellore, India, Paper ID HTM 260.

6. List of Book Chapters:

i. Sanjib Kundu, Suman Kalyan Das, and Prasanta Sahoo. "Friction and wear characteristics of heat-treated electroless Ni–P–W coatings under elevated temperature." In P. Sahoo and J. P. Davim (Eds), Advances in Materials, Mechanical and Industrial Engineering, Lecture Notes on Multidisciplinary Industrial Engineering, (2019): 59-82. Springer, Cham, Switzerland.

This page is left blank intentionally

Certificate from the Supervisors

This is to certify that the thesis entitled **"Tribological Characterisation of Electroless Ni-P Coatings under High Temperature"** submitted by **Shri Sanjib Kundu,** who got his name registered on **20.08.2014** for the award of **Ph.D. (Engineering)** degree of Jadavpur University is absolutely based upon his own work under our supervision and neither his thesis nor any part of the thesis has been submitted for any degree/ diploma or any other academic award any where before.

1. _____

(Prof. Prasanta Sahoo)
Signature of the Supervisor
and date with Official Seal

2. _____

(Dr. Suman Kalyan Das)
Signature of the Supervisor
and date with Official Seal

This page is left blank intentionally

Abstract

For many engineering applications such as power generation, metal forming operations and the aerospace industry, high temperature tribology plays a very important role. Electroless Ni-P coatings and its variants have shown tremendous potential as tribology material at room temperature. Hypophosphite reduced coatings show satisfactory results in many research studies concerning with friction and wear in dry and lubricated environment. These are also used as anti-corrosive coating. However, the performance of the same in high temperature field needs to be evaluated as investigation reveals the softening of most of the coating materials. This results in the deterioration of their wear resistant activity causing to shorten the life of the component. Controlling friction and wear at elevated temperatures is a challenge since the conventional lubrication methods are no longer effective above a certain temperature. Despite a good number of researches on Ni-P and its variant coatings particularly on evaluation of their properties at room temperature, very few are highlighted towards the behavior of the coating at elevated temperatures. Hence, the motivation to compare the tribological characteristics of hypophosphite reduced coatings at ambient as well as at elevated temperature is gained.

The basic focus is on the deposition of hypophosphite reduced Ni-P coating and evaluation of its tribological characteristics at room and high temperatures. Further the addition of W, B and Al_2O_3 in Ni-P matrix is considered for better tribological properties and thermal stability. Finally a comparative study is carried out between the developed coatings on the basis of tribological performances in high temperature conditions. The effects of test parameters such as load as well as sliding velocity at room and elevated temperature are studied. Further a detailed discussion is carried out based on the effect of different temperatures on friction and wear characteristics along with their wear mechanism. To assess the high temperature suitability of the Ni-P and its variant coatings, several characterisations such as SEM, AFM, EDAX and XRD are performed followed by tribological analysis through SEM and EDX. In addition, the wear mechanisms are further analyzed through AFM and elemental mapping. The coatings display the conventional nodular structure with no apparent surface defect in as-deposited condition. Except Ni-P-B, Ni-P and other variants show amorphous structure in as-deposited condition and turn crystalline on heat treatment. Ni-P shows stable bath with moderate deposition rate which decreases due to incorporation of third particles as W or Al_2O_3 . Though a reverse trend regarding the bath stability and deposition rate is observed for Ni-P-B. Use of borohydride in combination with hypophosphite as reducing agent provides higher reaction rate. The as-deposited coatings yield roughness values close to that of substrate. It increases slightly due to heat treatment because of increase in grain size. As-deposited Ni-P yields hardness around 600 $HV_{0.1}$ which increases due to incorporation of boron or tungsten or Al_2O_3 particles in the Ni-P matrix. The incorporation of Al_2O_3 in the Ni-P matrix yields highest hardness among all the developed Ni-P variants. Heat treatment causes increase in hardness of the each of the as-deposited coatings by precipitation of hard nickel phosphide phases. For Ni-P-B, the hard boride phases are also formed in conjunction with phosphide phases.

Both as-deposited as well as heat-treated coatings have been investigated for friction and wear behavior under room and high temperature conditions by varying applied load (10-50 N) and sliding velocity (0.094-0.22 m/s). It is found that COF of the as-deposited coating mostly increases with increase in load and decreases with increase in sliding velocity. Friction and wear performance of electroless Ni-P and its variants is evaluated at room (30°C) and elevated temperatures (100°C, 300°C and 500°C). Now, heat-treated coatings are harder than as-deposited coatings and are anticipated to exhibit better wear resistance compared to the latter. Again, at elevated temperature testing, the samples are expected to undergo a simultaneous heat treatment cycle (short duration) and as a result get somewhat harder. Hence, tests are conducted both on as-deposited samples as well as heat-treated (400°C, 1 hr) samples at various operating temperatures. The results of elevated temperature tests (particularly at 500°C) exhibit comparatively lower COF compared to others temperature. This may be because of in-situ heat-treatment due to the exposure at elevated test temperature which results in improved hardness of the coating. The heat-treated coatings also display almost analogous friction characteristics. In case of wear, behavior similar to friction study is observed. The worn surface displays a ploughing effect, coating detachment and cracks which indicate that both adhesion and abrasion phenomena govern the wear mechanism. The top surface of the coating after elevated tribology tests consists of a mechanically mixed layer of oxidation products. After the tests, the increase in hardness of the as-deposited coatings is quite high compared to the heat-treated ones. The effect of the short duration heat-treatment, due to high operating temperature tests is proven through XRD as well as hardness study of the post wear samples. The formation of hard phosphide phases are visible that yield increase in hardness as well as better wear resistance. Overall, the Ni-P and its variant coatings have potential to perform under elevated temperature conditions.

About the Author

Shri Sanjib Kundu completed his B.Tech in Mechanical Engineering in 2009 from Jalpaiguri Government Engineering College (under West Bengal University of Technology) and M.Tech in Production Engineering from Kalyani Government Engineering College (under West Bengal University of Technology) in 2011. Thereafter he was employed as Assistant Professor of Mechanical Engineering in Academy of Technology for two years. Due to his inclination towards higher studies, he left the job and joined as a Junior Research Fellow in CoE, TEQIP-II program of Jadavpur University. Along with research work in the designated project, he is pursuing his PhD in Engineering since 2014. He is currently employed as Assistant Professor in Mechanical Engineering Department, Academy of Technology, West Bengal.

This page is left blank intentionally

Acknowledgement

Pursuing Ph.D. is not an easy task. But it is absolutely one of the most productive and superb encounters in my life. I had the chance to work with significant number of individuals who extend their hands with caring assistance to accomplish the target. Therefore, I might want to thank every one of them, though it will not be sufficient to offer my gratitude in words. I would still prefer to give my many, many thanks to every one of them contributed and guided me to chase the right path.

Most importantly of all, I might want to unassumingly acknowledge my sincere regard and most profound appreciation to my supervisor, Prof. Prasanta Sahoo, who accepted me as his Ph.D. student decisively. His consistent direction, consolation, dynamic help and sagacious contributions helped this dissertation to be successful. I have been incredibly fortunate to work under the person with gigantic knowledge and experience who has given my profession a legitimate shape.

Next I would like to thank my co-supervisor, Dr. Suman Kalyan Das for his constant guidance, encouragement and active support. I truly feel honored to have received the chance to work under his direction. He is a perfectionist, never missed the slightest mistake in my papers. In particular he has continuously given a patient hearing to every one of my petulance. I've learned a lot from him starting from his cool, calm, composed personality, controlling adverse situation as well as to guide and counsel, without which completion of thesis work would have been extremely difficult.

I would also like to acknowledge COE, TEQIP – II program of Jadavpur University for providing financial assistance and costly equipments used in research work. I do heartily acknowledge the support received during characterisation studies of coating either in Department of Metallurgical Engineering, Jadavpur University, Kolkata or S.N. Bose National Centre for Basic Sciences, Saltlake, Kolkata. Moreover, I would like to thank all the researchers in this field whose published literatures have greatly helped me in getting an insight towards the experimental work. I could really acquire a lot of knowledge from these publications.

The experimental work was carried out in machine elements laboratory of the Department of Mechanical Engineering, Jadavpur University, Kolkata. Hence, thanks are also due to Shri Sunil Karmakar and Shri Aurobindo Jana for maintenance of the lab and furthermore for their genuine help constantly. I would like to convey my thanks to the Head of the Department, the Laboratory-in-Charge, Machine Elements Laboratory and all the academic and technical staffs of Mechanical Engineering Department, Jadavpur University, Kolkata. On this event, I should remember the name of Prof. Santanu Das (SD), Head, Mechanical Engineering Department, Kalyani Government Engineering College, who brought me into research. So, I want to convey my heartiest gratitude to SD sir from whom I learned a lot. I am also thankful to all the academic and technical staffs, specially Dr. Sujoy Saha, Amit Kumar Rana, Chiranjit

Guchait, Suchibrata Dutta and Dr. Sourav Kayal, of Mechanical Engineering Department, Academy of Technology, Hooghly.

The idea of pursuing Ph.D. from Jadavpur University was introduced to me by Dr. Bikash Panja, so a special thanks to my friend Bikash. Not only that, at the beginning of my research, starting from the coating deposition to tribological testing, at each point he stood beside me. There are few seniors like Dr. Shouvik Ghosh, Dr. Supriyo Roy, Dr. Milan Kumar Das and Dr. Prasanna Gadhari, who helped me a lot during my initial research work. Apart from that, thanks are due to the lab mates of machine elements lab, who constantly kept up a sincere and helpful environment in the lab.

Finally, I thank my beloved parents especially my mother whose unimaginable perseverance, unlimited love, and unapproachable commitment have been stupendous. Another person who plays a huge role in my life, my elder brother (shri Sujoy Kundu), without his support it is never possible to complete the journey of doctoral research. I'd like to thank my elder sister, Mamai, well-wishers and friends for their patience and constant support without which this work couldn't have been completed. Do excuse me if I have failed to spot any person who has been some segment of this shimmering experience called 'PhD'. Thanks again.

Sanjib Kundu

I would like to dedicate this work to my parents & teachers
from whom I've learned a lot.

This page is left blank intentionally

Contents

This page is left blank intentionally

List of Tables

This page is left blank intentionally

List of Figures

Page No.

This page is left blank intentionally

Chapter 1

Introduction

1.1 Tribology and Surface Engineering

Tribology is the study of friction, wear and lubrication of interactive surfaces in relative motion. Fundamental knowledge in tribology helps to improve service life, safety and reliability of mating components, and yields substantial economical benefits. Apart from improving the lifecycle of industrial machineries, it makes a major impact in a variety of modern applications, such as biomedical, nanotechnology, alternative energies and green methodologies.

Tribological phenomena are generally concerned with the surface of the material where interaction occurs between contacting pairs. A material with good surface as well as bulk properties may be very rare as well as costly. Again a material with good tribological behavior may lack certain bulk properties which can limit its application or vice versa. In this regard, the concept of surface engineering, which gives customized products are getting popular. Surface engineering involves treatment of the surface and near-surface regions of a material to allow the surface to perform functions that are distinct from those demanded from the bulk of the material. In many instances, it is either more economical or absolutely necessary to select a material with the required bulk properties and specifically engineer the surface to create the required interface with the environment, rather than to find one material that has both the bulk and surface properties required to do the job.

Nowadays immense research has been carried out on the development of surface engineering. Various techniques have been proposed (Mellor, 2006) such as techniques to cover a surface with a material of different composition or structure, techniques to modify an existing surface topographically, micro-structurally or chemically, techniques to modify the existing surface by inducing a change in composition of the surface layer, etc. The covering surface techniques have been used to protect bulk material from hostile environment and also to provide low or high friction resistance. Moreover, this method is highly suitable for providing required appearance to the metal surface and employ existing technology in order to obtain desired properties of the material. The said techniques are commonly known as painting, plating and coating. Apart from this, more diffused boundary between the substrate and the reaction layer have been developed by modifying the existing surface engineering method. This method include processes viz. carburizing, nitriding etc. However, it can be said that coating development is the most popular surface engineering technique. Deposition of coating is generally carried out in an aqueous medium. Through coating, required surface properties can

also be gained by depositing the respective metals or alloys. Among the available techniques of coating, electrolytic process grabs most of the application area though the potentials of electroless methods have well been recognized and they are being applied in many industrial and special applications where electrolytic method is inconvenient such as electronics, pumps, turbines, motor vehicles, machinery, valves, aerospace and nuclear industry etc.

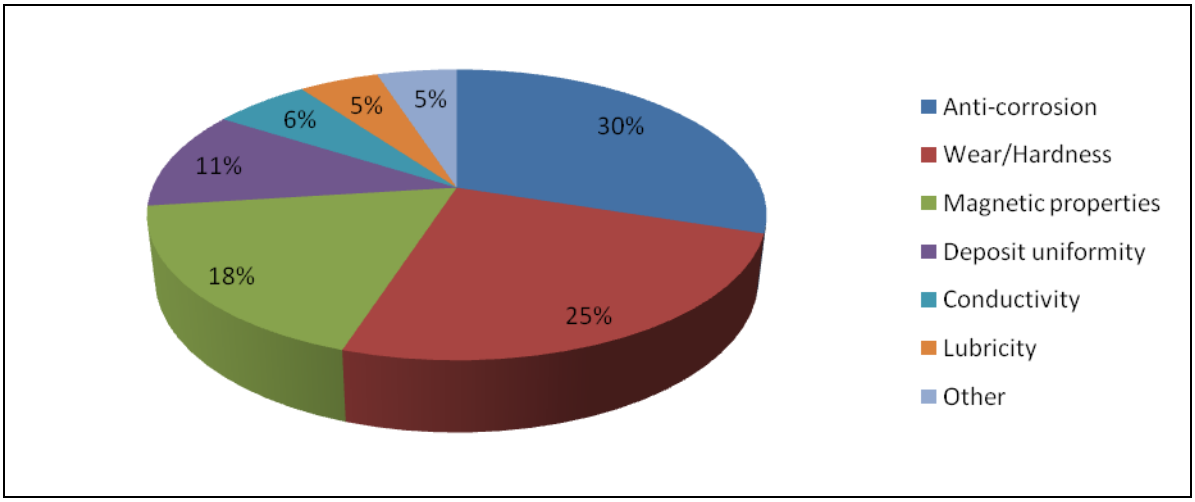

Figure 1.1 Pie chart representing the applications of electroless nickel based on properties (source – home page: www.pfonline.com)

1.2 Electroless Coating

Coating is a cover applied on the surface of any material, called substrate to protect it from any kind of tribological or environmental damage. Electroless coating is an electrochemical method of coating deposition in which metals are deposited from a liquid medium, generally aqueous, by autocatalytic means where reducing agent reduces the metal ions Though the electroless deposition of metals was first demonstrated in 1844 by Wurtz (Mallory & Hadju, 1990) but discovery of electroless coating is credited to Brenner & Riddell (Brenner and Riddell 1946). After the invention of electroless method, its use increased rapidly sometimes overshadowing other similar electrolytic methods. Possibility of deposition on electrically non conductive materials i.e., almost on any surface, which is steady in electroless coating solution may be the reason behind its wide acceptance. Moreover, this method provides very smooth surface with uniform thickness to any geometrical objects. The other reason, may be, it is a autocatalytic chemical deposition process, which is very simple, as the process is carried out without the aid of electricity. This method also provides better mechanical, chemical and magnetic properties compared to other methods.

Because of these host of advantages electroless coatings are applied in industries such as automobile, manufacturing, food processing, aerospace etc. Variety of characteristics provided by electroless coating is the possible reason for selecting it for many engineering applications. Figure 1.1 reflects the primary applications of electroless nickel with respect to its usability.

Electroless Nickel (EN) became the popular variant among this segment of coatings. Since invention, it is widely used because it provides uniformity in deposit, low porosity and requires low process temperature (Sahoo & Das, 2011). EN coatings have the added advantages of being hard and wear resistant besides being corrosion resistant as well.

1.3 Types of Electroless Nickel (EN) Coatings

Electroless nickel coating can be broadly classified into three categories viz. pure nickel coating, alloy/poly alloy coatings and composite coatings as shown in Figure 1.2. Reducing agent (i.e., hypophosphite, borohydride or dimethylamine borane and hydrazine) plays the deciding role in grouping of electroless nickel coatings as well as to decide the nature (acidic/alkaline) of the bath. Hydrazine is used as reducing agent for preparing super-hydrophobic surface on steel (Chen et al., 2008). But due to unstable bath, production of brittle and highly stressed part, pure nickel deposition is almost obsolete (Sudagar et al., 2013).The most common alloy coating is either Ni-P, originating from hypophosphite baths (Staia et al., 1996; Anik and Körpe., 2007; Sahoo, 2009; Mukhopadhyay et al., 2017)), or Ni-B which derives from borohydride baths (Sankara Narayanan & Seshadri, 2004; Anik et al., 2008; Das & Sahoo, 2011a; Mukhopadhyay et al., 2015; 2016). Apart from borohydride, Ni-B coatings are developed using amine borane (Velez et al., 1999; Contreras et al., 2006), which is available in two forms viz. N-dimethyl amine borane (DMAB)-$(CH_3)_2NH{\bullet}BH_3$, and H-diethyl amine borane (DEAB)–$(C_2H_5)_2NH{\bullet}BH_3$ (Agarwala & Agarwala, 2003). Further, Ni-P and Ni-B both are grouped as high, medium and low based on the weight percentage of phosphorus and boron respectively. The details are indicated in the classification block diagram (Figure 1.2).To improve the properties of electroless coatings, the introduction of a third/fourth element to form a poly nickel alloy has nowadays a demanding trend. Several metals such as W (Palaniappa & Seshadri, 2008; Roy & Sahoo, 2013; Duari et al., 2017), Cu (Ashassi-Sorkhabi et al., 2002; Balaraju & Rajam, 2005; Liu et al., 2015; Sahoo & Roy, 2017), Mo (Vargas Mendoza et al., 2006; Balaraju et al., 2014; Mukhopadhyay et al., 2018b), W and Cu (Balaraju et al., 2006; Balaraju & Rajam, 2009) are added to binary alloy (Ni-P/Ni-B) coating to prepare ternary and quaternary coatings to meet the industrial requirements. Choice of the particles depends upon the property which is desired. It is considered that the incorporation of a typical transition metal such as W, Co, Mn, Re and Mo in the binary alloy could lead to superior properties than the binary Ni-P/Ni-B coating.

Co-deposition of materials viz. diamond, silicon carbide (SiC), aluminum oxide (Al_2O_3), polytetrafluoroethylene (PTFE) particles, etc. with electroless coatings, gives rise to composite coating. Broadly electroless nickel composite coatings are either phosphorus based or boron based and depending upon the incorporation of particles, the coatings are either wear resistant or lubricating in nature as indicated in Figure 1.2. Wear-resistant composite coatings such as Ni-P-TiO_2 (John et al., 2005), Ni-P-Al_2O_3 (Novák et al., 2010; Gadhari & Sahoo, 2016) etc. can be produced by the co-deposition of fine hard particulate matter and lubricating composite coatings like Ni-P-PTFE (Ramalho & Miranda, 2005; Srinivasan & John, 2005), Ni-P-MoS_2 (Hu et al.,

2009) etc. can be produced by solid lubricants PTFE and MoS_2. Apart from progress of conventional types of EN coating, there are few emerging nickel coatings developed such as nano-coatings, duplex and multilayered coatings which provide remarkable mechanical and tribological characteristics. Dispersion of nano-particles into the EN matrix gives rise to electroless nano-coatings. Among these coatings, carbon nanotubes (CNTs) (Zhao & Deng, 2005) based coatings and nano TiO_2 (Li et al., 2006; Makkar et al., 2013) based coatings have received considerable attention. Several duplex coatings such as Ni-P/Ni-B (Sankara Narayanan et al., 2003; Vitry et al., 2012c; Bonin and Vitry., 2016), Ni-P/Ni-P-W ((Liu et al., 2012), Ni-P/Ni-P-Mo (Liu et al., 2016) along with multilayered Ni-P/Ni-B (Vitry and Bonin., 2017a) are found to be suitable in terms of tribological performances.

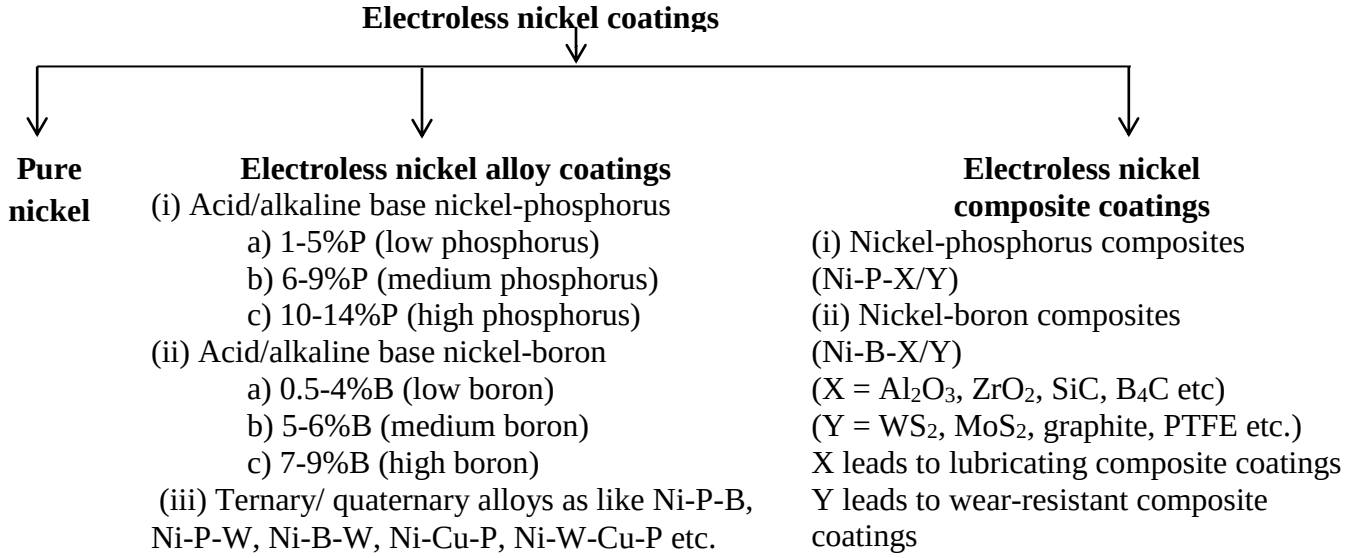

Figure 1.2 Block diagram representing classification of electroless nickel coatings

1.4 Basics of Electroless Nickel Bath

In case of electroless nickel (EN) coatings, base material which is also known as substrate acts like electrode where both the oxidation and reduction reactions take place. It is an autocatalytic process where the substrate develops a potential when it is immersed in electroless bath that contains a nickel source, reducing agent, complexing agent, stabilizer, surfactant, buffering agent, etc. (Sahoo & Das., 2011). The electroless nickel bath composition along with possible choice of chemicals and their functions are given in Table 1. The role of nickel source is to provide the nickel ions for deposition on the substrate, and reducing agent supplies the required electrons for the reduction process of nickel. On heating the solution, metal ions get reduced and are deposited on the substrate together with an element of the reducing agent. These types of coating can be deposited virtually over any material be it conductive or non-conductive. Among the common two variants of baths, hypophosphite reduced baths are the most popular due to higher stability and greater simplicity in bath control. Several hypotheses regarding

reaction mechanism of EN deposition (acid/alkaline) are available (Loto, 2016) but electrochemical and atomic hydrogen mechanism for hypophosphite reduced deposition are extensively used (Agarwala & Agarwala, 2003). In electrochemical mechanism, catalytic oxidation of the hypophosphite yields electrons at the catalytic surface that helps in reducing nickel and hydrogen ions (Sahoo & Das, 2011) in the deposition process as expressed by the following reactions :-

$$H_2PO_2^- + H_2O \rightarrow H_2PO_3^- + 2H^+ + 2e^- \quad (1.1)$$

$$Ni^{++} + 2e^- \rightarrow Ni \quad (1.2)$$

$$2H^+ + 2e^- \rightarrow H_2 \quad (1.3)$$

$$H_2PO_2^- + 2H^+ + e^- \rightarrow 2H_2O + P \quad (1.4)$$

Whereas in atomic hydrogen mechanism, catalytic dehydrogenation of hypophosphite molecule absorbed at the surface is responsible for releasing atomic hydrogen (Sahoo & Das, 2011). The mechanism involved in deposition process can be expressed as :-

$$H_2PO_2^- + H_2O \rightarrow HPO_3^- + H^+ + 2H_{ads} \quad (1.5)$$

$$2H_{ads} + Ni^{++} \rightarrow Ni + 2H^+ \quad (1.6)$$

$$H_2PO_2 + H_{ads} \rightarrow H_2O + OH^- + P \quad (1.7)$$

$$(H_2PO_2)^{--} + H_2O \rightarrow H^+ + (HPO_3)^{--} + H_2 \quad (1.8)$$

On the other hand borohydride reduced bath provides higher deposition rate (Krishnaveni et al., 2005) and provides better hardness and wear resistant surface. The corresponding reactions (Anik et al., 2008) involved in Ni-B deposition are as follows :-

Borohydride oxidizes through the electroless deposition process by the reactions as mentioned below :-

$$BH_4^- + 4OH^- = BO_2^- + 2H_2O + 2H_2\,(g) + 4e^- \quad (1.9)$$

$$BH_4^- = B + 2H_2\,(g) + e^- \quad (1.10)$$

Consequent reduction reactions in the coating bath can be represented as :-

$$Ni^{2+} + 2e^- = Ni \quad (1.11)$$

$$2H_2O + 2e^- = 2OH^- + H_2\,(g) \quad (1.12)$$

The reactions involved in mechanism as indicated above are affected by each of the bath components as indicated in Table 1.1. Coating performance is generally evaluated on the basis of hardness, surface roughness, friction, wear resistance, corrosion resistance, coating thickness and so on. Each of these characteristics of coating again highly depends on bath parameters. Moreover, heat-treatment post deposition, also changes the microstructure and hence plays a role on the mechanical and tribological characteristics of the coating (Sahoo & Das, 2011). Apart from the dependency on bath parameters, the tribological performance of the coating is also

dependent on the testing parameters viz. applied load, sliding speed and sliding duration (Krishnaveni et al., 2005; Li et al., 2008) which will be discussed in details in future sections.

Table 1.1 Electroless nickel bath components and their functions

Component	Choice of chemicals/temperature	Function
Nickel Ion	Nickel chloride, Nickel sulphate, Nickel acetates etc	Source of metal
Reducing agent	Sodium hypophosphite (for Ni-P), Sodium borohydride or N-dimethyl amineborane (DMAB) and N-diethyalmine borane (DEAB) (for Ni-B), Hydrazine (for pure Ni)	Source of electrons
Complexants	Monocarboxylic acids, Dicarboxylic acids, Hydrocarboxylic acids, Ammonia, Alkanolamines etc.	Stabilizes the solution by forming nickel complexes
Accelerators	Anions of some mono and di-carboxylic acids, Fluorides, Borates	Activates reducing agent and accelerates the deposition
Buffers	Sodium salt of certain complexants, choice depends on pH range used	Controlling pH (long term)
pH regulators	Sulphuric and hydrochloric acids, Soda, Caustic Soda, Ammonia	Regulates pH of solution (short term)
Stabilizer	Lead (Pb), Tin (Sn), Arsenic (As), Molybdenum (Mo), Cadmium (Cd) or Thorium (Th) ions, Thioures etc	Prevents solution breakdown
Wetting agents	Ionic and non-ionic surfactants such as sodium dodecyl sulfate (SDS) and cetyl trimethyl ammonium bromide (CTAB)	Increases wettability of the surfaces
Bath temperature	30-95°C	Supplies necessary energy for reaction

1.5 High Temperature Application

Electroless deposition has been acknowledged due to its ability to coat any material with uniform thickness, low porosity and low process temperature. Various metals like nickel, gold, copper etc. can be deposited by this method. However, deposition of nickel since its inception has gained immense popularity due to its superior tribological properties. Due to the distinct advantages of EN coatings such as deposition uniformity, coating of complex geometries without the need of electricity extends its uses over electrolytic and so many other coatings. Most of the valves, bores, internal surfaces, deep recesses, blind holes and threaded parts are suitable candidates for EN coating. EN coatings are mostly renowned for their higher hardness, better

corrosion resistance as well as excellent tribological characteristics. Because of that it has got variety of applications such as automotive to aerospace industries, chemical to textile industries, electrical to electronic industries and so on (Sahoo & Das, 2011; Loto, 2016).

High-temperature coatings often find applications in aerospace, manufacturing, military, power and petrochemical industries. Specific examples of applications for high-temperature coatings include jet engines, power plants/refineries, offshore assets, corrosion under insulation, fireproofing and original equipment manufacturer applications. For long time, automotive industries provide higher stress on quality, performance and efficiency on their components. The components mainly used are steel and aluminum, whose performances are usually enhanced by providing coating like electroless nickel. The use of electroless nickel and typical applications where high temperature arises in automobiles includes heat sinks, pistons, engine bearings, hose couplings, gear assemblies, carburetor parts, fuel injectors, shock absorbers and exhaust system components. Automotive companies have acknowledged the benefits of electroless nickel in all of these and other applications and also have their own provision for its use. These coatings have also been used on carburetor and clutch parts, engine valves, bearings and gears to extend their lifetime. For instance, the flexible bearing support for the Allison TF41 engine is subjected to heavy bearing loads at temperatures up to 480°C. Electroless nickel has been used extensively in the chlor-alkali industry, in which the two main products are chlorine and sodium hydroxide . The produced, chlorine has a temperature of 80°C. The life of a control valve used in the concentration of sodium hydroxide from a chlor-alkali cell was greatly increased by electroless nickel plating where solution temperature reached to 95°C. In some commercial and military aircraft, compressor section of gas turbine engines components are required to be protected from corrosive atmospheres and erosive particles at temperatures of 425°C. It also used in manufacturing unit for protecting mold surfaces from high temperature. These coatings offer great benefits when good wear and release properties are required on such items as molds and rolls used in food industries where it has to withstand temperatures in excess of 540°C. There are three major areas of oil and gas industry such as surface operations, subsurface operations and offshore operations. Equipment used for those operational areas are frequently exposed to temperatures as high as 250°C. Electroless nickel may help to improve the performance of each of the particular area which includes, surface, sub surface and offshore applications. Surface area covers brake assemblies, chokes, compressors, gas turbines, pump housings, pumps, connection manifolds and valves. Sub surface area includes couplings, logging tools, plungers, packers, pumps, safety valve units and tubing. Whereas offshore area is combined with gas turbines/compressors, heat exchangers, pumps, riser connectors and valves. Apart from these, the oil and gas industry has an enormous demand for tubular components, that are frequently exposed to severe, corrosive conditions at temperatures as high as 260°C (Parkinson, 1997).

Electroless nickel coatings has assumed the greatest commercial importance among the electroless coating mainly for high hardness and excellent corrosion and wear resistance (Agarwala & Agarwala, 2003; Sahoo & Das, 2011; Sudagar et al., 2013; Loto, 2016).The main

function of coatings is basically to provide protection to the component surface against phenomena viz. wear and corrosion (Mellor, 2006). However, keeping in mind the industrial demands, a need for thermal resistant coatings have cropped up lately. Now, mechanical parts undergoing tribological interactions under elevated temperature require coatings which would possess low friction characteristics, high corrosion resistance and high wear resistance and at the same time maintain its properties under high temperature. Several applications such as the hot metal working industry (hot forming, hot drawing, etc.), heat exchangers, turbines, tools, extruders, sealing surface of nuclear valves, plungers, rolls for rolling mills etc. require operations to be done at elevated temperature conditions (He et al., 2011). EN coatings have the potential to act as a thermal barrier to this adverse situations as nickel has a high melting point and is resistant to oxidation up to a temperature of 500°C (Li et al., 2013).

There are so many areas where electroless nickel coatings are used or may be used to protect components which are subjected to high temperature. As conventional lubrication also fails to work in the high temperature environment and generally fused away from the contacting zone, so the motivation to know about the electroless coating and its behavior under high temperature is a point of interest.

1.6 Evaluation of Electroless Nickel Coatings

So many research works have been carried out to attain enhanced properties of EN coatings. Electroless nickel performance is generally evaluated on the basis of deposition efficiency, hardness, surface roughness, corrosion, friction and wear. Since most of the industrial use of EN coatings is based on tribological applications (Sahoo & Das, 2011), a major stress is given to the study of tribological characteristics of the coatings and its enhancement. Initially each of the coating evaluation parameters such as plating rate, roughness, hardness, corrosion, surface morphology and microstructure are addressed since they affect the coating tribology. Thereafter, the tribological behaviors are discussed along with the wear mechanisms under room temperature as well as at high temperatures.

1.6.1 Plating rate and thickness

A coating may have several useful properties but unless it can be developed properly and easily, the deposition technique needs revision. Adequate coating thicknesses for various applications are essential together with a fast plating rate so that same can be developed very quickly. The deposition rate for optimal combination of coating parameters of electroless Ni-P coating yielded as high as 27.5μm per hour (Liu et al., 2011). Moreover, the coating surface quality was visually found to be very good. The effect of bath composition on the plating rate of electroless Ni-P (Qu et al., 2011) and Ni-Cu-P (Wang et al., 2012) coating on aluminum is also studied. For Ni-B coating on a copper substrate (Oraon et al., 2007), concentration of reducing agent increases the deposition up to a certain value beyond which the deposition experiences a drop.

A good prediction of the plating rate and %P was reported by Yating et al. (2008) which showed a splendid match for every design factor (shown in Figure 1.3). Their study further showed that increase in $Ni^{2+}/H_2PO_2^-$ ratio results in decrease in both the plating rate as well as %P.

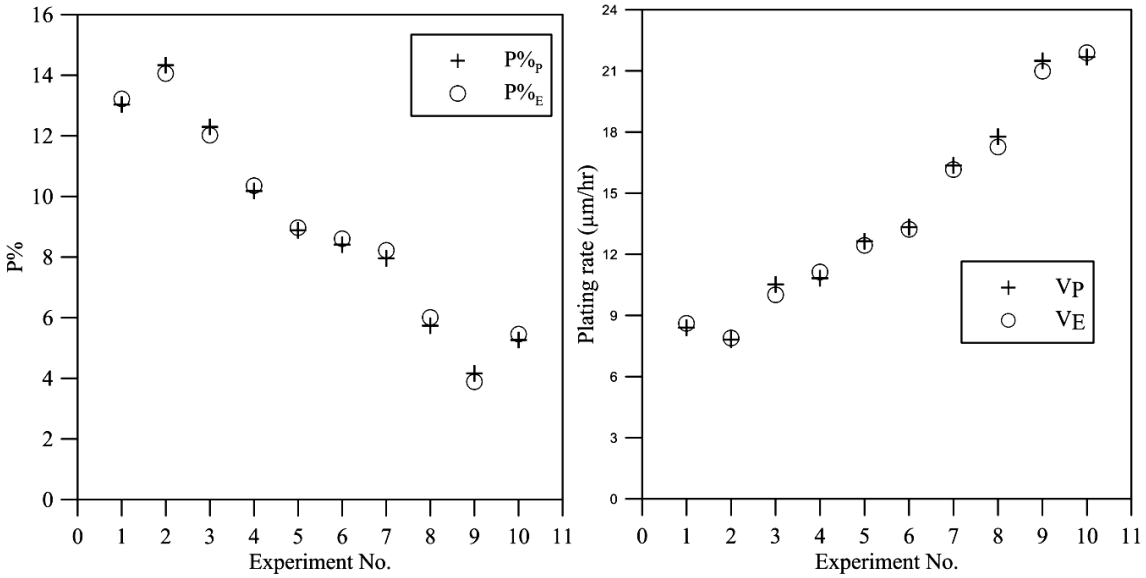

(a) (b)

Figure 1.3 Comparison between experimental and predicted values for (a) phosphorus % and (b) plating rate (adapted from Yating, W., Bin, S., Lei, L., & Wenbin, H. (2008). J Mater Process Technol., 205(1), 207-213)

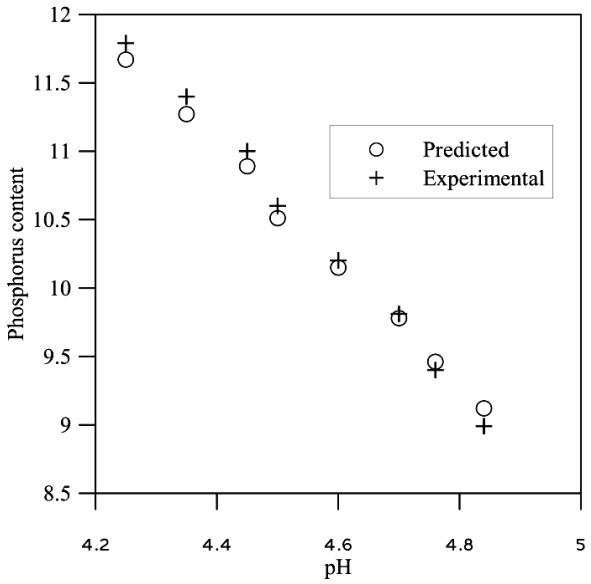

Figure 1.4 Phosphorus content vs pH (adapted from Vaghefi, S. Y. M., & Vaghefi, S. M. M. (2011). Neural Comput. Appl., 20(7), 1055-1060)

Moreover, the concentration of complexing agent and stabilizer showed a negative effect on the plating rate. However, pH of the bath had a positive effect over plating rate but a negative effect on P content. So, pH of the bath need to be adjusted properly because it is an important parameter and can affect phosphorus content in the deposit e.g., if the alkalinity of the solution increases, phosphorus content of the deposit decreases. Temperature of the bath has a considerable influence on the rate of deposition. The optimum bath was operated in the pH range 9-10, at a temperature between 75-85°C, with nickel salt to reducing agent ratio of 0.35 and nickel salt to complexing agent ratio of 1.4. Beyond this temperature, the quality of the coating deteriorates as it is difficult to maintain the pH of the solution (Beygi et al., 2012). The predicted and the actual plating rate also exhibited a good match. In a research (Vaghefi & vaghefi, 2011), Ni-P coating displayed an excellent match between the predicted and experimental results (Figure 1.4). They observed that the phosphorous content increases with both increase in bath loading as well as metal turn-over (MTO) but the same decreases with increase in pH.

1.6.2 Roughness and hardness

Electroless nickel coatings provide a very uniform deposit that follows the substrate surface profile rather than just filling the gaps between the surface asperities. Hence, in general, the roughness of the coating does not differ much from the roughness of the substrate. However, electroless coatings are believed to have some smoothening effect above a critical substrate roughness. Moreover, the micro-structure of the deposit may also play a role in defining the roughness of the coating. Now, surface roughness has large impact on the mechanical properties like fatigue behavior, corrosion resistance, creep life etc. It can also affect other functional attributes of machine components like friction, wear, light reflection, heat transmission, lubrication, electrical conductivity, etc. Nickel source is found to have the most significant influence over roughness of Ni-P (Sahoo, 2008a) while reducing agent and bath temperature has the most influence over roughness of Ni-B coating. Roughness is reduced by about 25% for Ni-P and about 15% for Ni-B by optimizing these parameters.

Roughness is normally characterized by three different types of parameters, viz., amplitude parameters, spacing parameters, and hybrid parameters. The vertical characteristics of the surface deviations viz. centre line average roughness, root mean square roughness, skewness, kurtosis, peak-to-valley height, etc. fall under the amplitude characteristics. The horizontal characteristics of the surface deviations viz. mean line peak spacing, high spot count, peak count, etc. fall under the spacing characteristics. The combination of both vertical as well as horizontal characteristics are incorporated in the hybrid parameters viz. root mean square slope of profile, root mean square wavelength, core roughness depth, reduced peak height, valley depth, peak area, valley area, etc. Among these, centre line average (R_a) value has been the most popular choice for defining roughness of EN coatings. However, a study is conducted for electroless Ni-P coating by considering five roughness parameters together (Sahoo, 2008b). The five roughness parameters are centre line average roughness (R_a), root mean square roughness (R_q), skewness (R_{sk}), kurtosis (R_{ku}) and mean line peak spacing (R_{sm}). It was found that concentration of the

reducing agent and its interaction with concentration of the nickel source solution, have significant influence in controlling the roughness characteristics of the coating. For Ni-B coating, concentration of reducing agent and nickel source is observed to have good amount of significance on the roughness. Incorporation of tungsten ion is found to influence the roughness characteristics of Ni-P coatings significantly (Roy & Sahoo, 2012b).

Addition of anionic surfactant viz. SDS to the electroless bath enables fine nickel particles to be dispersed uniformly on the substrate surface resulting in smoother surface finish of the deposited layer (Farzaneh et al., 2010). Increasing pH accelerated deposition rate and caused improvement in the surfactant effect as well as the microstructure of coating became finer.

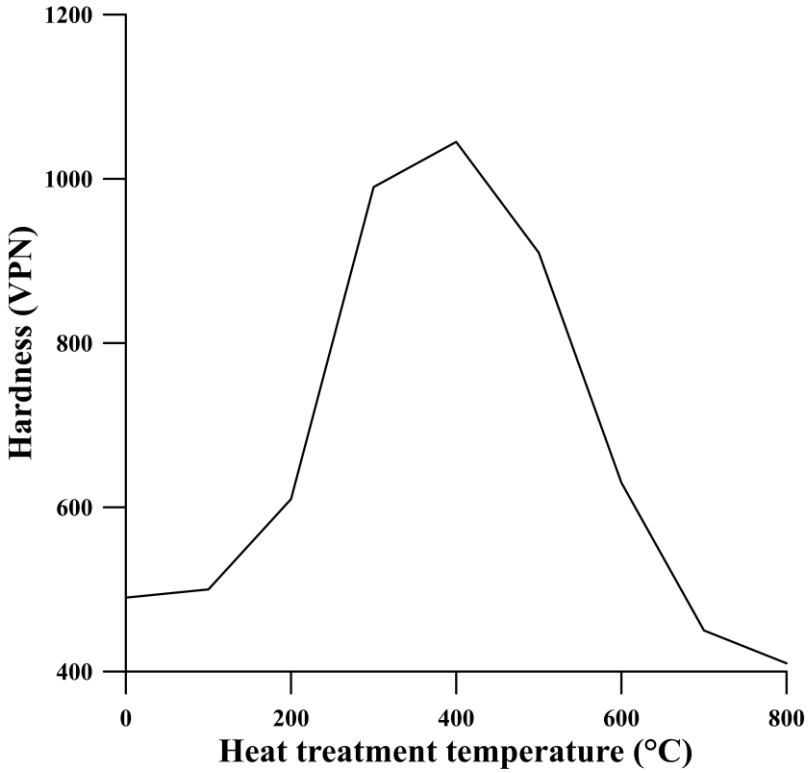

Figure 1.5 Effect of heat-treatment temperature on the hardness of Ni-P coatings (adapted from Higgs, C.E. (1974). Electrodep. and Surf. Treat., 2(4), 315-326)

Surface hardness is a critical property that governs wear and tear when one component rubs against another. This makes hardness a characteristic of materials that determines the safety and proper functioning of mechanical systems and constructions. Electroless nickel coating have already established itself in this respect and some of its types viz. Ni-B coatings can compete to the likes of tool steel and hard chromium coatings (Srinivasan et al., 2010). The hardness of electroless Ni-P and Ni-B coatings are dependent on the phosphorous and boron content respectively. However, the hardness of electroless Ni-P increases with decrease of phosphorous content while the hardness of Ni-B increases with the increase in boron content of the coating

(Anik et al., 2008). Different heat-treatment temperatures using one factor at a time approach is used by researchers and the highest hardness (about 1400 $HV_{0.1}$) is observed at a temperature of 300°C (Oraon et al., 2008). Further, increase in heat-treatment temperature reduces the coating hardness. High hardness can be incorporated in Ni-P deposits through a heat-treatment at 300-400°C, which converts Ni-P amorphous alloy into crystalline Ni and a hard nickel phosphide phase. This increases the hardness (Higgs, 1974) of the deposit (Figure 1.5), but also decreases the corrosion resistance. Upon heat-treatment, the increase in hardness occurs through formation of Ni_3P and Ni_5P_2 hard phases from the amorphous phase. Addition of surfactant viz. SDS is found to enhance the micro-hardness of Ni-P deposit (Farzaneh et al., 2010). It occurs due to the fact that addition of the surfactants results in a mixture of nano crystalline and amorphous structure The hardness of the Ni-P coatings increases from approximately 502 to 650 $HV_{0.1}$ with an increase in coating time (with decreased phosphorus content), and hardness of Ni–P rises with heat-treatment from 790 $HV_{0.1}$ to a maximum of 1045 $HV_{0.1}$ at 400°C (Ashassi-Sorkhabi et al., 2004).

Parametric study is conducted on the hardness of Ni-B coatings (Das & Sahoo, 2012) and hardness at the optimal condition is found to be 1252 $HV_{0.1}$. Heat-treatment temperature is identified as the most influencing factor and the optimum heat-treatment temperature was found to be 350°C. The enhanced hardness at the particular temperature is attributed to precipitation hardening phenomenon due to the precipitated nickel boride phases. Although Ni-P coatings exhibit lower hardness compared to Ni-B, several attempts were initiated to obtain improved hardness from Ni-P by optimizing the coating process parameters. The optimum hardness observed is 802 HV_1 and heat-treatment temperature was found to be the single most influencing factor (Panja & Sahoo, 2014). Study on microhardness of electroless Ni–B coating (Krishnaveni et al., 2005) reveals values in the order of 570 (HV_{100}) (for as-plated coatings) and 908 (HV_{100}) (for coatings heat-treated at 450°C for 1 hr). The hardness vs. heat-treatment temperature curve exhibits two maxima, one at 350°C and the other one at 450°C. The increase in hardness is due to the precipitation of nickel borides, Ni_3B and Ni_2B. Beyond 450 °C, coating begins to soften as a result of conglomeration of the Ni_3B particles and the hardness decreases. Heat-treated coated Ni-B samples at 500°C have the highest values of hardness (698 HV) (Contreras et al 2006).

Higher microhardness values were obtained for composite coatings due to the silicon nitride particle incorporation (Balaraju & Rajam, 2008). The hardness of the coating increases with the amount of tungsten in the deposit. This is due to the solid solution strengthening of the nickel matrix by the dissolved tungsten. The increase in the thickness of the electroless Ni–P coating and electroless Ni–P–B_4C composite coating results in an increase of the coating hardness (Ebrahimian-Hosseinabadi et al., 2006).

1.6.3 Surface morphology and microstructure

Tribology is a surface phenomenon. In this regard, surface morphology and microstructure are the two main attributes responsible for controlling the tribological

performance of EN coatings. Studying the microstructure of the coating in detail leads to better understanding of its macroscopic behavior by observing the changes occurring at the microscopic level of the coating. Electroless nickel coatings are in general very smooth and lubricious in nature thanks to their unique nodular micro-structure. The excellent tribological behavior of Ni-B coatings is attributed to its columnar growth (Pal et al., 2011). Ni-P coatings on the other hand display nodular structure. Heat-treatment causes inflation in grain size with prominent grain boundaries. Scanning electron micrographs of as-deposited and heat-treated (400°C for 1 hour) hypophosphite based Ni-P coatings and borohydride reduced as-deposited and heat-treated (350°C for 1 hour) Ni-B coatings is represented in Figure 1.6 and 1.7 respectively.

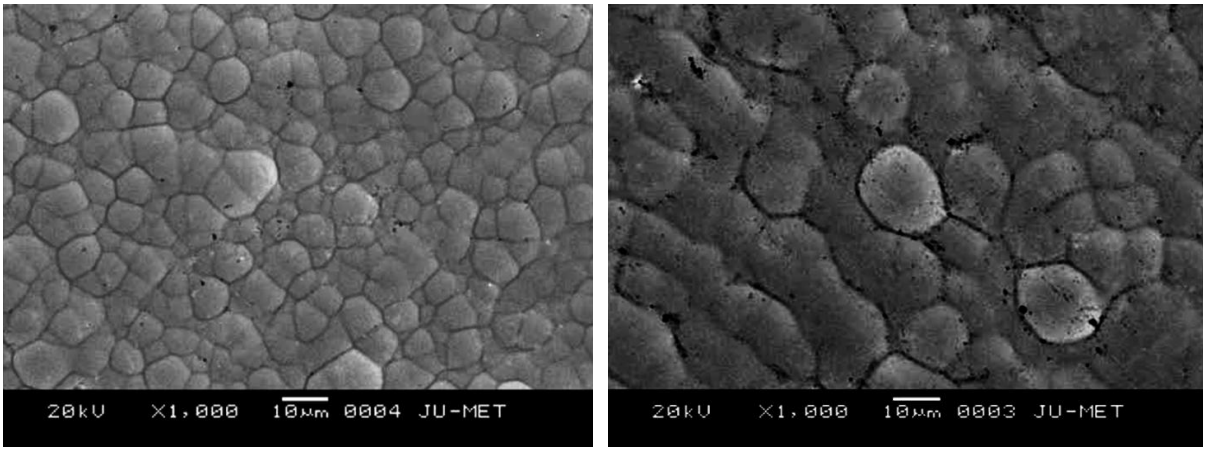

(a) (b)

Figure 1.6 SEM micrographs of Ni-P coating (a) as-deposited and (b) heat-treated at 400°C for 1hr (adapted from Sahoo, P. (2009). Mater. Des., 30(4), 1341-1349)

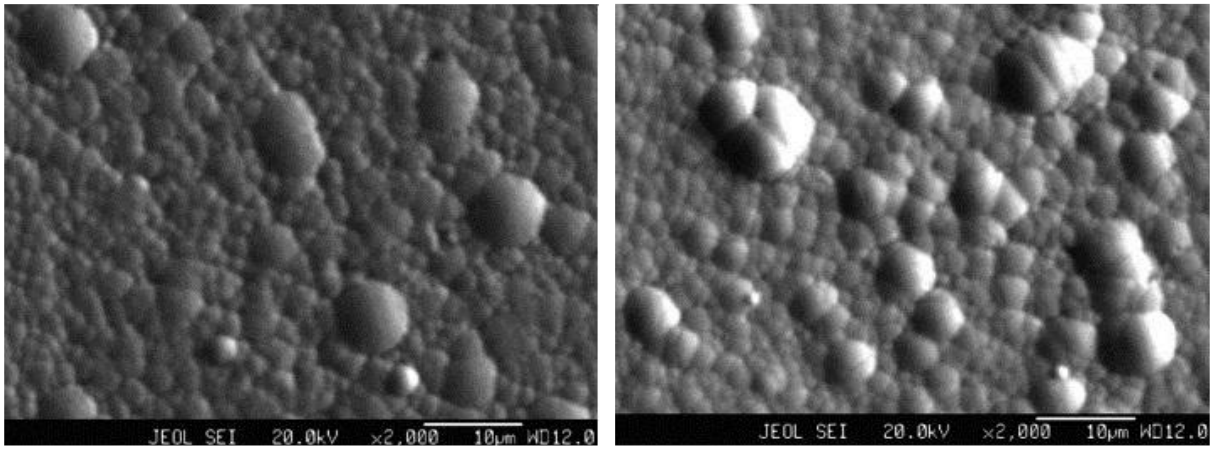

(a) (b)

Figure 1.7 SEM micrographs of Ni-B coating (a) as-deposited and (b) heat-treated at 350°C for 1hr (adapted from Das, S. K., & Sahoo, P. (2011). Mater. Des., 32(4), 2228-2238)

SEM micrograph of the as-deposited Ni-P surface reveals globular structure which is arranged in almost a series of rows. The coating generally provide a dense and defect free surface. The globule sizes are small in as-deposited case which doubles in size due to heat-treatment, giving rise to coarse grained structure. The nodular morphology implies the coating may exhibit low friction and wear characteristics. However, friction and wear characteristics of any material are not governed by the surface condition alone but by a host of others factors viz. the surface composition, material properties, etc. There is no visible surface damage and the coating appears to be of very low porosity which is again an indication of it possessing a good corrosion resistance

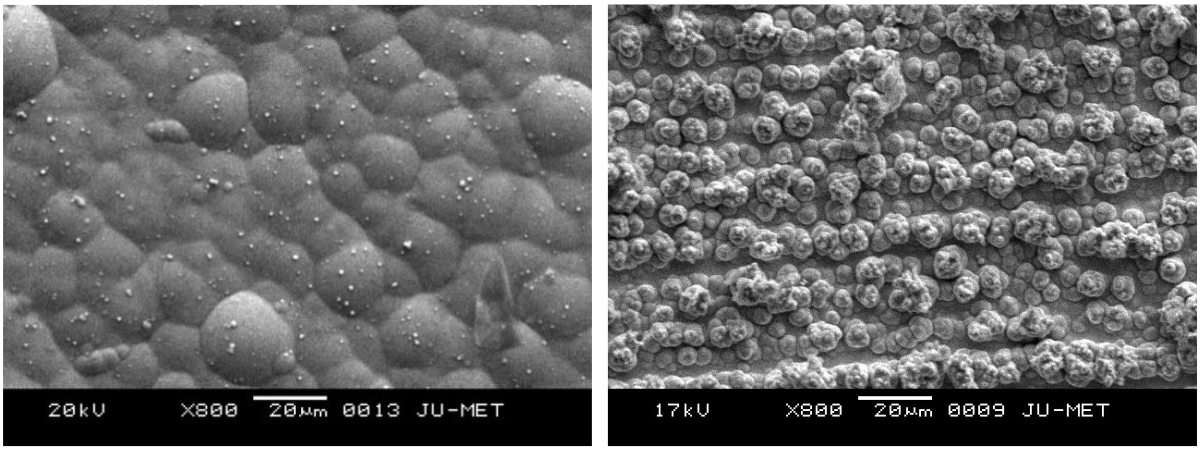

(a) (b)

Figure 1.8 SEM micrographs of EN poly alloy coatings from hypophosphite based bath (a) Ni-P-W and (b) Ni-P-Cu in as-deposited condition (adapted from **a.** Duari, S., Mukhopadhyay, A., Barman, T. K., & Sahoo, P. (2017). Surfaces and Interfaces, 6, 177-189.and **b.** Duari, S., Mukhopadhyay, A., Barman, T. K., & Sahoo, P. (2016). J. Mol. Eng. Mater., 04(04), 1640013, 13pp)

Cauliflower type surface morphology and columnar growth (Conteras et al., 2006) of Ni-B results in enhanced lubricity and thus improves the wear properties (comparable with hard chromium) due to reduction in the contact area (Riddle & Bailerare, 2005). The observed closely compacted nodular arrangement with cauliflower appearance (Fig 1.7) is similar to that as reported by many other researchers (Krishnaveni et al., 2005; Vitry et al., 2012b; Mukhopadhyay et al., 2018c). The tribological characteristics of Ni-B is superior to Ni-P coating mainly because of the columnar growths as it helps to reduce the actual area of contact and also retains lubricants (Vitry et al., 2012b).

Typical scanning electron micrographs of EN poly-alloy coatings obtained from hypophosphite based baths and borohydride baths in as-deposited condition is shown in Figure 1.8 and 1.9 respectively. Each poly-alloy coating has unique properties compared to their binary variants such as high hardness, wear resistance, corrosion resistance, low coefficient of friction

(COF), higher thermal stability, oxidation resistance, magnetic properties, electrical properties etc.

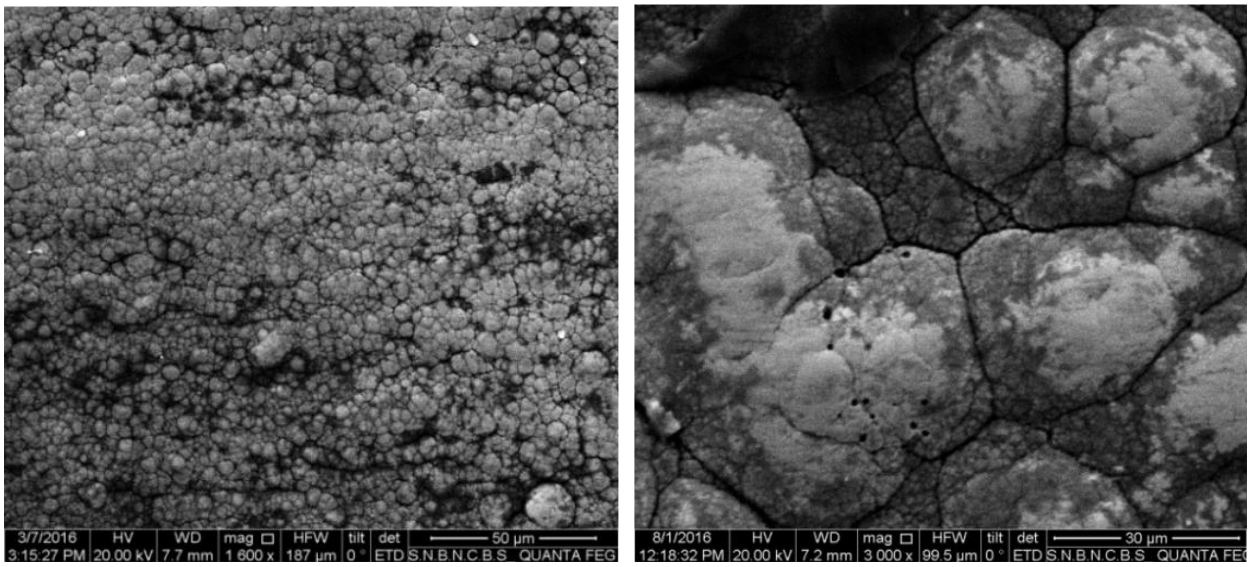

(a) (b)

Figure 1.9 SEM micrographs of EN poly alloy coatings from borohydride based bath (a) Ni-B-W and (b) Ni-B-Mo in as-deposited condition (adapted from **a.** Mukhopadhyay, A., Barman, T. K., & Sahoo, P. (2018), Proc. IMechE. Part J: J. Eng. Tribol., 232(11), 1450-1466 and **b.** Mukhopadhyay, A., Barman, T. K., & Sahoo, P. (2018), Surf. Rev. Lett.,1850175, 14 pp)

In general electroless nickel coating is amorphous or microcrystalline in as-deposited phase but turns crystalline with heat-treatment and phosphides and borides are precipitated. Upon heat-treatment, electroless Ni-P and Ni-B coatings precipitate hard particles such as nickel phosphide phase (Ni_3P) and nickel boride phase (Ni_3B) respectively (Keong & Sha, 2002; Sankara Narayanan, & Seshadri, 2004). When heat-treated at 400˚C, Ni-P deposits produce Ni_5P_2, Ni_2P and NiP_2 as major constituent compounds. The structure of electroless Ni-P coatings considerably changes during heat-treatment. A system consisting of mixture of two crystalline phases viz. nickel and nickel phosphide (mainly Ni_3P) forms as a result of heat-treatment (for both fine-crystalline and amorphous coatings).

Generally, the content of phosphorus or boron in EN coatings determines their crystallinity in as-deposited state. As the P content decreases, the crystallinity of the deposits changes from amorphous to a mixture of amorphous and nanocrystalline and finally to nanocrystalline structures. XRD plots of as-deposited and heat-treated Ni-P coatings is shown in Figure 1.10. Similar observations have also been made for Ni-B coatings. The B content also decides the cyrstallinity as higher B (>7 wt%) provides amorphous coating and lower B (<5 wt%) coatings are observed to be nanocrystalline (Krishnaveni et al., 2005). XRD plots of as-deposited and heat-treated Ni-B coatings is shown in Figure 1.11.

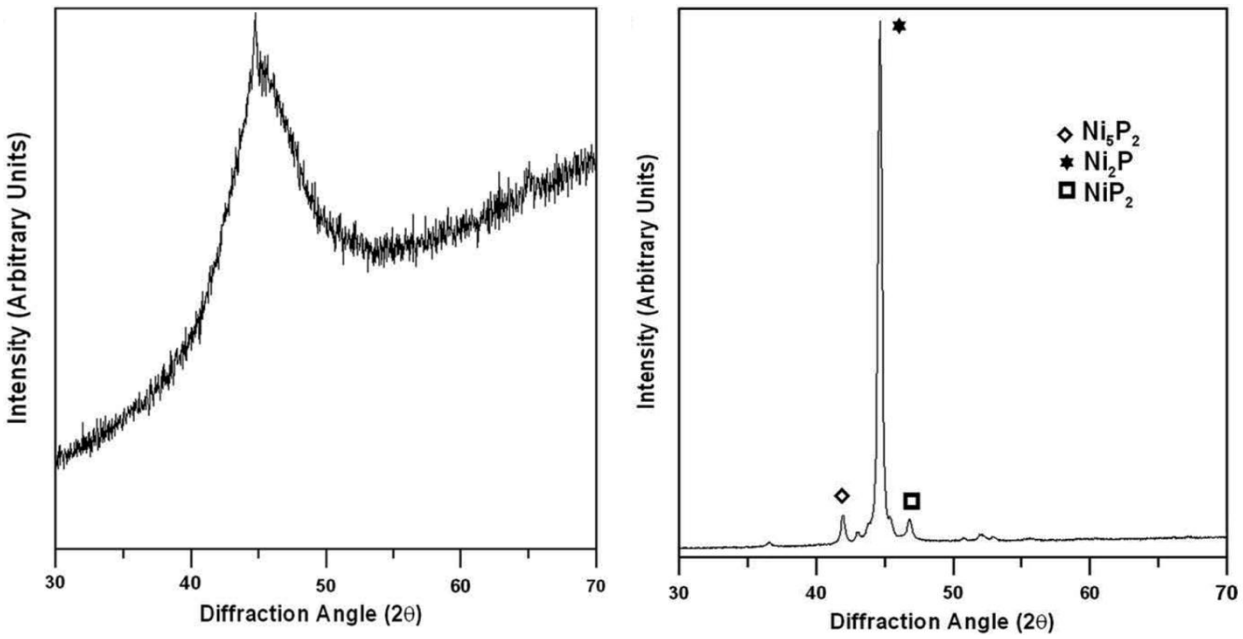

(a) (b)

Figure 1.10 XRD results of (a) as-deposited and (b) heat-treated electroless Ni-P coatings (adapted from Sahoo, P. (2009). Mater. Des., 30(4), 1341-1349)

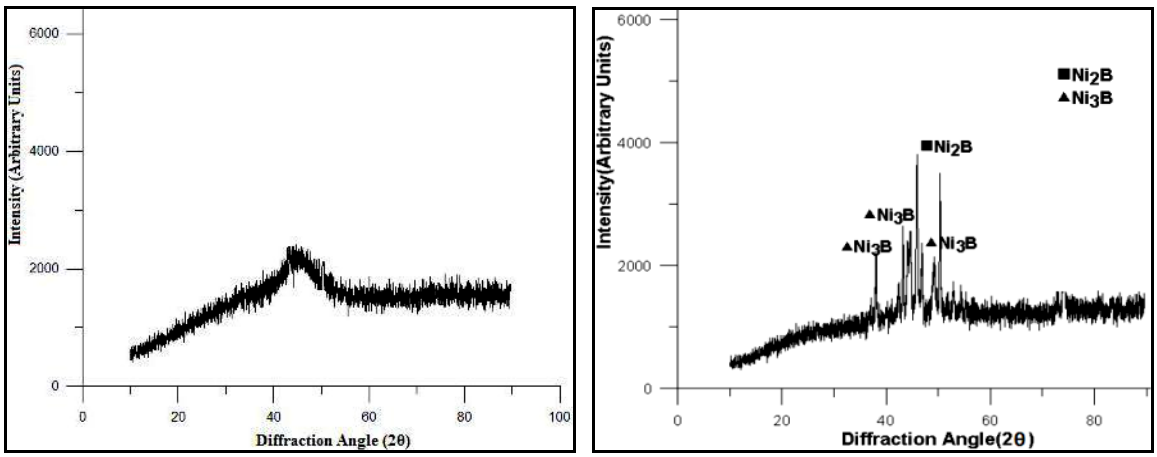

(a) (b)

Figure 1.11 XRD patterns of electroless Ni-B deposit (a) as-deposited and (b) heat-treated at 350ºC (adapted from Das, S. K., & Sahoo, P. (2011). Mater. Des., 32(4), 2228-2238)

Inclusion of alloying elements also influences the crystallinity of EN coatings mainly by affecting the P or B content of the coatings. X-ray patterns of as-deposited and heat-treated coatings of such alloy coating is shown in Figure 1.12. In as-deposited condition, the coating shows a mixture of amorphous and nano crystalline phases due to addition of W in Ni-P matrix but with heat-treatment it turns crystalline with the formation of nickel phosphide and Ni-W

solid solution. Similar nano-crystalline nature of the coating is also reported by Balaraju et al. (2012). Moreover, XRD results show a strong orientation towards Ni (111) plane pertaining to the sharp peak in the plot. These results exactly match the observations made by Osaka et al. (1982). With heat-treatment, as expected the coating turns completely crystalline with the appearance of nickel phosphide (Ni_3P) peaks (Fig 1.12b).

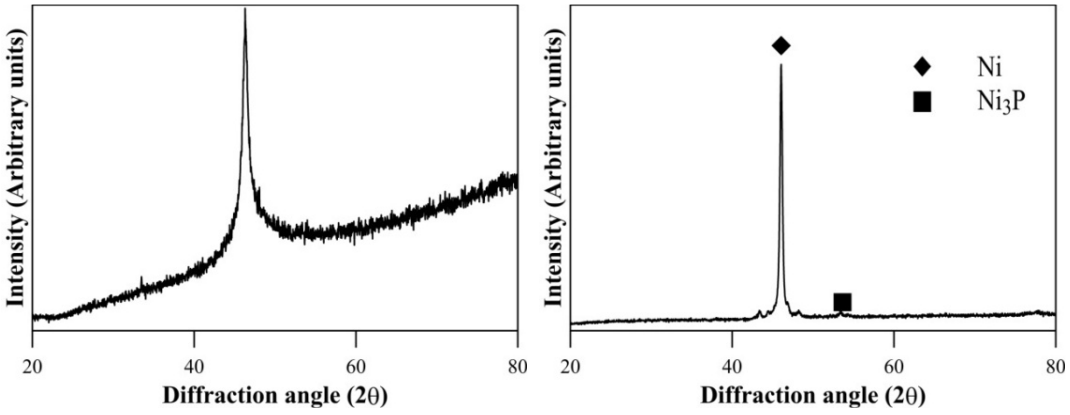

(a) (b)

Figure 1.12 XRD results of (a) as-deposited and (b) heat-treated electroless Ni-P-W coatings (adapted from Duari, S., Mukhopadhyay, A., Barman, T. K., & Sahoo, P. (2017). Surfaces and Interfaces, 6, 177-189)

1.6.4 Corrosion

Electroless Ni-P coatings are widely used for corrosion protection application in a variety of environments. They act as barrier coatings, protecting the substrate by sealing it off from the corrosive environments, rather than protecting by sacrificial action. Many factors are responsible for developing the corrosion resistance in the coating starting from the pre-processing stage of substrate preparation to the heat-treatment of the coating. Both Ni-P and Ni-P composite coatings demonstrated significant corrosion resistance in both acidic and salty atmosphere. Also proper post-heat-treatment (400°C and 1h) significantly improves the coating density and structure, giving rise to enhanced corrosion resistance (Huang et al., 2004). Again corrosion resistance of Ni-B is found to be lesser than Ni-P. The corrosion resistance evaluation of these Ni–B coated specimens shows two different behaviors; in acidic environment, Ni-B coating was more susceptible to the corrosion effects. It has a complex electrochemical behavior with three different time constants related to the corrosion phenomena. In neutral environment, the film has a protecting behavior and the substrate produces an instantaneous film of the same nature. A diffusion of ions through the film was detected at low frequencies (Contreras et al., 2006). Gou et al. (2010) developed Ni-P coating over magnesium alloy with $NiSO_4$ as the main nickel source and found the corrosion rate of Ni-P in 3.5% NaCl solution for 14h to be 0.76μm/h. Influence of anionic surfactant (SDS), pH, substrate finishing and annealing temperature on the corrosion

resistance of electroless Ni-P was studied (Farzaneh et al., 2010). Results indicate that SDS surfactant causes increase of corrosion resistance and improves surface morphology. The cause of the improvement in corrosion resistance is the lowering of the porosity of the deposit. Corrosion behavior of electroless Ni-B coatings was judged based on electrical impedance spectroscopy (EIS) (Das & Sahoo, 2011b) and potentiodynamic polarization experimentation (PPE). The effect of coating parameters on the electrochemical characteristics (charge transfer resistance and double layer capacitance for EIS and corrosion potential and corrosion current density for PPE) are studied and it was observed that bath temperature and concentration of nickel source have significant influence on the corrosion performance of the coatings. Sankara Narayanan et al. (2006) studied the formation of electroless Ni–P graded coatings, with varying nickel and phosphorus contents of the individual layers and evaluated their corrosion resistance. Comparison of the corrosion resistance of the coatings is found to be of the following order: EL graded Ni–P (LMH) > EL Ni–high P > EL Ni–medium P > EL graded Ni–P (HML) > EL Ni–low P (where L,M and H represents the Low, Medium and High phosphorous baths respectively).

Incorporation of copper in Ni-P alloy enhances its corrosion resistance (Huang et al., 2007). Other ternary alloys viz. Ni-P-W is developed for their improved wear resistance were compared to traditional Ni-P coatings (Roy & Sahoo, 2012a). Concentration of tungsten source is found to be the most important parameter that significantly affects the corrosion characteristics of Ni-P-W. Hosseini & Bodaghi, (2013) reported an experimental study of corrosion characteristics of electroless Ni-P-TiO_2 nano-composite coating. and incorporation of TiO_2 is found to increase the corrosion resistance and improve the surface morphology of the coating. Bath temperature is also found to play a significant role in influencing the corrosion behavior of Ni-P-TiO_2 coating.

1.6.5 Other properties

EN deposit has the ability to produce uniform thickness on parts with complex geometries and shapes. Density of electroless nickel depends on the inter atomic spacing and on the amount of porosity, which is comparable to electrodeposited nickel under identical circumstances of surface preparation and thickness. For same thickness value, corrosion resistance of EN deposits are more than electrodeposited ones because of lower porosity via heat-treatment. The density of EN deposits is lower than pure nickel due to the presence of phosphorus as an alloying constituent. The crystalline material is found to be denser than the amorphous type (Agarwala & Agarwala, 2003). The melting range of EN deposits vary widely depending upon the phosphorus/boron content for commercially available processes. Pure nickel melts around 1455°C but with addition of phosphorus as an alloying element, the deposit initiates to soften at lower temperatures (Sudagar et al., 2013). Lowest melting point of electroless Ni-P deposits is found to be 880°C (containing 11% P) and highest melting points, around 1200°C (for 3% P). The melting point of Ni-B is comparatively high. Melting point of

electroless Ni-B deposits (5% B) is 1080°C for sodium borohydride reduced bath and 1350–1360°C for DMAB reduced bath. Both internal stress and ductility vary with coating composition, specifically the percentage of phosphorus in the deposits. A linear relationship exists between internal stress and pH of the plating solution of EN deposits. Low phosphorus (Schwartz & Mallory, 1976) and high level of internal stress (Gaurilow, 1979) are the two important factors responsible for the reduction in ductility of the coating.

Fracture toughness is the material resistance against crack formation. It is very important for predicting the formation of cracks. Hence, there has been a lot of interest to determine the same for electroless nickel coatings. Indentation tests were used to determine the fracture toughness of Ni-P coatings and the same was found to be 1.5 MPa for 300°C heat-treatment and 2.1 MPa for 600°C heat-treatment (Roman et al 2002). Fracture toughness of electroless Ni-P coatings has been measured (Zhou et al., 2006a; 2006b) using a notch tensile specimen made of stripped film. The fracture toughness was found to decrease with increasing treatment temperature, i.e., degree of crystallization. The average fracture toughness was found to be 7.1 MPa for as-deposited Ni-P coatings, 5.2 MPa for 300°C treatment, 3.7 MPa for 330°C treatment and 1.2 MPa for 400°C treatment (corresponding to complete crystallization).

The electrical resistivity of electroless nickel alloys is higher than that of pure nickel (Keong & Sha, 2002). With the increase in phosphorus content, the electrical resistivity of the deposit also increases. The thermal conductivity, which is proportional to the electrical conductivity, can be easily calculated as the reciprocals of the electrical resistivity. The magnetic properties of the deposits depend on their nature of crystallization. Crystalline deposits are ferromagnetic, while those having an amorphous structure are essentially non-magnetic (Schwartz & Mallory, 1976).

1.7 Tribological characteristics

Since invention, electroless nickel coating is widely used because of its superior tribological characteristics. In this section the friction and wear behavior of electroless nickel alloy/composite coatings under room temperature and their evolution over testing time is discussed. Further, the same under high temperature are discussed along with recent progresses.

1.7.1 Tribology under dry condition

Electroless nickel (EN) coatings have proven their aptness for the improvement of the performance of base materials. This is due to the coating possessing splendid hardness, wear resistivity and corrosion resistance. The deposition rate, properties of coated components and the structural behavior of deposits mainly depend upon the plating bath constituents/conditions such as the type and concentrations of the reducing agent, stabilizer, pH and the temperature of the bath, etc. The electroless bath typically comprises an aqueous solution of metal ions, complexing agents, reducing agents and stabilizers, operating in a specific metal ion concentration,

temperature and pH ranges (Sahoo & Das, 2011). Each process parameter has its specific role on the process and influences the process response variable and is also responsible for the efficiency and crystallinity of EN deposits (Jappes et al., 2005). Temperature also affects the deposition significantly and for lower bath loading, deposition is significantly high (Oraon et al., 2006). Heat-treatment is an important factor that affects the thickness, hardness, structure and morphology of deposit (Ashassi-Sorkhabi & Rafizadeh et al., 2004). Among the variety of EN coatings, Ni-P has got attention by so many researchers because of its widespread applicability as well as wear resistant and anti corrosive property. Electroless Ni-P coating is an autocatalytic deposition of a Ni-P alloy from an aqueous solution onto a substrate without the application of electric current. Generally acknowledged optimal heat-treatment regime is 400°C for 1 h as it results in maximal hardness of electroless nickel phosphorous coatings. The hardness increase is attributed to the crystallization of nickel and to the precipitation of fine particles of Ni_3P phase. Use of higher heat-treatment temperatures and longer times leads to the progressive decrease in hardness, which can be attributed to the nickel grain growth and to the grain coarsening. There is an increase of as-deposited hardness with decreasing phosphorus content and highest hardness is observed with heating temperature 400°C whereas further heating at higher temperatures would decrease the hardness values (Keong et al., 2003). It has been seen that the highest wear resistance was obtained for samples heat-treated at 400°C for 1h (Staia et al., 1996). It was found from another research that the heat-treatment decreases the abrasive wear resistance of the Ni-P coatings (Staia et al., 1997).

The mechanism of wear of electroless Ni-P deposit depends on the attractive force that operates between the atoms of nickel from the coating and iron from the counter disk. A negative wear depth curve is also observed in some cases (Palaniappa & Seshadri, 2008) as a result of the buildup of oxide debris at the interface of the coated pin and counter disc. Wear is strongly dependent on the applied load and it increases along with increasing load (Ramalho & Miranda, 2005) irrespective of whether specimen is Ni-P coated or Ni-P coated and tempered. The optimization of the coating parameters (Krishnaveni et al., 2005) reported that annealing temperature and bath temperature have the most significant influence in controlling wear characteristics of electroless Ni-P coating. Whereas Ni-B coating is used to provide higher hardness and higher wear resistance which is equivalent to high chromium coatings. Compared to as-deposited condition, both heat-treated Ni-P and Ni-B shows higher wear resistance because of high hardness achieved through precipitation of hard phosphide (Staia et al., 1996) and boride phases (Das & Sahoo, 2011a) respectively. Tribological characteristics of both Ni-P and Ni-B highly depends upon the process parameters and can be controlled via modifying the bath parameters. Frictional properties also change with heat-treatment and phosphorus/boron content. The coefficient of friction for electroless nickel/boron against steel is found to be 0.12-0.13 for lubricated condition and 0.43-0.44 for dry condition (Agarwala & Agarwala, 2003). Hardness combined with smoothness is the feature present behind the use of electroless nickel coatings for tribology based applications. Adhesive and abrasive wear are the primary mechanisms of wear at

room temperature under dry conditions and the rate of wear varies depending on the dominant mechanism (Sahoo & Das, 2011).

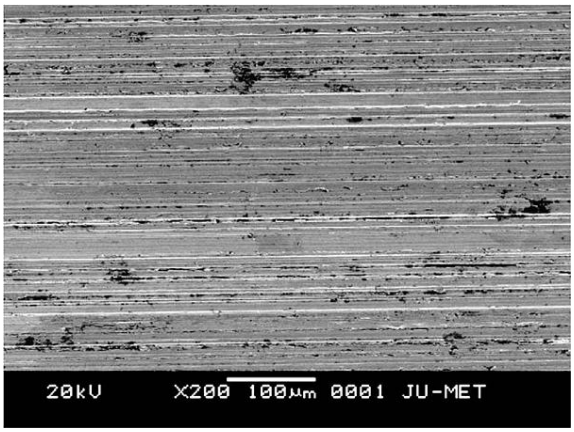

(a)

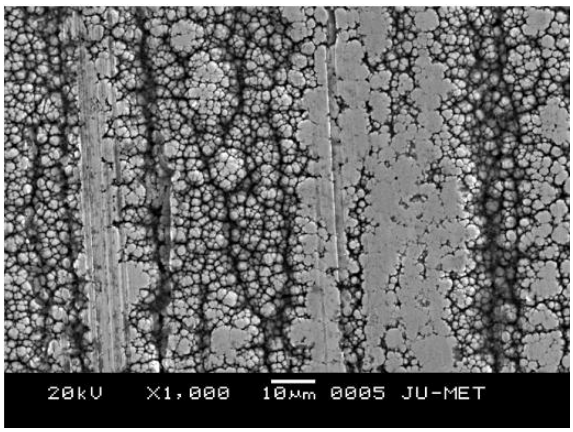

(b)

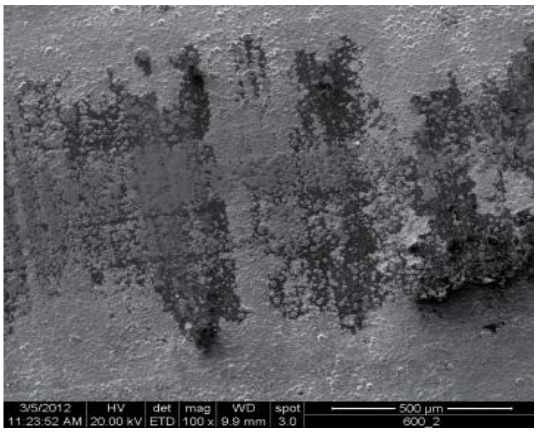

(c)

Figure 1.13 SEM of coatings post wear testing: (a) Ni-P (adapted from Sahoo, P. (2009). Mater. Des., 30(4), 1341-1349.) (b) Ni-B (adapted from Das, S. K., & Sahoo, P. (2011). Mater. Des., 32(4), 2228-2238.) and (c) Ni-P-W (adapted from Roy, S., & Sahoo, P. (2013). J. of Coatings, 608140, 13pp)

Remarkable improvement in the wear resistance of EN coatings has been reported when hard particles are incorporated. Choice of the particles depends on the property which is desired. It is considered that the incorporation of a typical transition metal such as W, Co, Mn, Re and Mo in the binary Ni-P alloy could lead to superior properties than the binary Ni-P coating. So the research could be extended for the ternary Ni-P-T alloy where the T is the transition metal. For ternary coatings, which besides nickel and phosphorous, contain elements like Cu, W, Zn also show an amorphous structure after a certain limit of phosphorous content is exceeded. Ni–Cu–P coatings are amorphous at a phosphorous content above 7 wt. %. When the phosphorous content is below 3.9 wt. %, a crystalline Ni–Cu phase is visible (Yu et al., 2001). In Ni–Zn–P coatings, an increase in zinc content up to 23 wt. % does not alter the crystalline structure of the nickel (Bouanani et al., 1999). The tribological behavior of Ni-B coatings is also influenced by alloying

with tungsten or molybdenum (Aydeniz et al., 2013; Serin & Göksenli, 2015). Electroless nickel coatings (Ni-P and Ni-B) exhibit predominantly abrasive wear phenomenon (Sahoo, 2009; Das & Sahoo, 2011a) as depicted in Figure 1.13 (a) and (b) respectively. Wear behavior of Ni-P coating is studied by Sahoo, (2009) and it is found that interaction of bath temperature and nickel source solution has significant influence on wear. Also it is observed that the wear mechanism does not change with the variation in coating process parameters. However, ternary alloys viz. Ni-P-W exhibit adhesive nature (shown in Figure 1.13c) of wear (Roy & Sahoo, 2013).

To obtain better tribological, chemical, mechanical, physical, magnetic, and other properties from the same coatings, sometimes other elements are added into the chemical deposition process, giving rise to the idea of composite coating. To meet the challenges for the development of material with enhanced characteristics such as high temperature sustainability, higher hardness, lubricity, wear and corrosion resistance, etc. is the main cause behind the merger of particles. Many soft particles such as WS_2, MoS_2, PTFE (polytetrafluoroethylene), graphite as well as hard particles viz. WC, SiC, Al_2O_3, B_4C, TiO_2, diamond etc. are generally used as additional particles in Ni-P matrix (Dong et al., 2009; Gadhari and Sahoo, 2016; 2017). The similar approach is also adapted for electroless Ni-B coatings (Ghaderi et al. 2016a; Niksefat & Ghorbani, 2015). Each of the particles has a unique characteristic and because of that fact it affects the overall properties and performance of the developed coating. A study on the effect of heat-treatment on the microhardness of electroless Ni-P composite coating (Apachitei et al., 1998) showed that the particles incorporated into the Ni-P matrix increase the hardness of the coating and such composite coatings are much harder than the Ni-P coating and after heat-treatment at 400°C the hardness of both Ni-P and composite coatings increases where composite coatings showed higher hardness than comparing to the electroless Ni-P coating. Peak profile analysis of electroless nickel coatings (Martyak & Drake, 2000) showed that the amorphous and crystalline components of the EN coatings changed with the heat-treatment.

The adhesion of both deposits is similar as in an as-plated state, yet in a heat-treated condition and it was seen that the ternary alloy was stronger than the binary one (Tsai et al., 2001).Friction coefficient of EN coating is increased due to missing of natural lubricity because of the addition of hard particles viz. B_4C (Ebrahimian-Hosseinabadi et al., 2006) and SiC (Araghi & Paydar, 2010) in the deposits. Whereas addition of softer particles viz. PTFE (Wu et al., 2006) and MoS_2 (Zou et al., 2006) in the electroless deposition provides a drastic reduction in the friction coefficient value. Wear resistance and hardness of a coated surface are correlated, though wear properties of the coatings are affected by many other factors such as the nature of the applied stress and the surface morphology. Phosphorus content and heat-treatment are the two main parameters that affect wear resistance of Ni-P coating a lot. An attractive force is generated in between nickel atoms and the counterface material during the rubbing activity that causes the wear of electroless nickel phosphorus coating. Sometimes wear depth curve moves in negative direction that may be because of the formation of buildup oxide debris in between the coated sample and counterface material (Palaniappa & Seshadri, 2008). Gadhari and Sahoo

(2016) made a detailed discussion on electroless composite coatings and corresponding tribological behavior under ambient condition.

Comparative study between sliding wear behavior and friction coefficients of electroless Ni-P and Ni-P-BN(h) composite deposits reported that composite coating with 35% BN(h) incorporated particles presented a wear factor which is nearly two orders of magnitude smaller than the wear factor reported for a BN(h)-free electroless Ni-P (León et al., 1998). The friction and wear behavior of several electroless Ni-P composite deposits have been investigated (Straffelini et al., 1999). In addition to Ni-P deposit, deposits containing SiC, PTFE, MoS_2 and BN particles are produced. Duplex coatings are also developed (Sankara Narayanan et al., 2003) with Ni-P and Ni-B in order to study the friction and wear behavior and to compare with individual Ni-P and Ni-B coatings of similar thickness. It is found that the duplex coatings are uniform and the micro-hardness, wear resistance and corrosion resistance of the duplex coating is higher than Ni-P or Ni-B coating of similar thickness. Among the two types of duplex coatings studied, hardness and wear resistance is higher for coating having Ni-B coating as the outer layer whereas better corrosion resistance is offered by coatings having Ni-P coating as the outer layer. Friction and wear behavior of electroless Ni-P and Ni-P/PTFE is studied simultaneously (Ramalho & Miranda, 2005). The introduction of PTFE particles produces a significant rise in the wear resistance. The dry friction and wear behavior is studied in case of Ni-P and Ni-P matrix with PTFE and/or SiC particles under a high load of 150N (Wu et al., 2006). It is seen that Ni-P-PTFE offers lowest friction coefficient whereas Ni-P-SiC offers the lowest wear rate.

Besides the development of binary Ni-P and Ni-B and its possible variants in the alloy or composite category, some other techniques have been developed such as duplex Ni-P/Ni-B (Sankara Narayanan et al., 2003; Vitry et al., 2012c; Bonin and Vitry., 2016), Ni-P/Ni-P-W ((Liu et al., 2012), Ni-P/Ni-P-Mo (Liu et al., 2016) along with multilayered Ni-P/Ni-B (Vitry and Bonin., 2017a). These coatings provide better wear resistance in comparison to simple Ni-P or Ni-B coatings. In case of duplex coating, usually Ni-P is provide as the inner layer for better corrosion resistance and Ni-B as outer layer for its superior wear resistance. The tribological behavior of both Ni-P/Ni-P-W and Ni-P/Ni-P-Mo shows better characteristics than Ni-P coatings which is further improved by additional treatments. The multi-layered coatings are developed for combining high corrosion resistance of Ni-P and high wear resistance of Ni-B.

There are many situations in industrial applications, where a particular material has to undergo sliding and rubbing under harsh environments. These type of situations inflict both wear and corrosion on the material surface. Keeping this aspect in mind, some studies have been conducted to assess the effect of bath components on the tribological behaviors of Ni-P coatings and that too under various corrosive environments (Panja et al., 2016; Panja & Sahoo, 2014). Panja et al. (2016) conducted a detailed comparative study on the tribological behavior of the electroless Ni-P coating under three corrosive environments such as acidic, brine and alkaline media. They found that the friction coefficient of Ni–P coating decreases with increase in load for all environments. Wear rate of Ni–P coating gradually increases with increase in load for all

mediums but the same decreases after 40N in brine and alkaline mediums. But in acidic solution, the wear rate shows a continuous increasing trend. It is observed that alkaline and brine environments are favorable from friction and wear point of view of the coating, respectively. Typical SEM micrographs of post wear test coatings as obtained by them in different corrosive medium are shown in Figure 1.14.

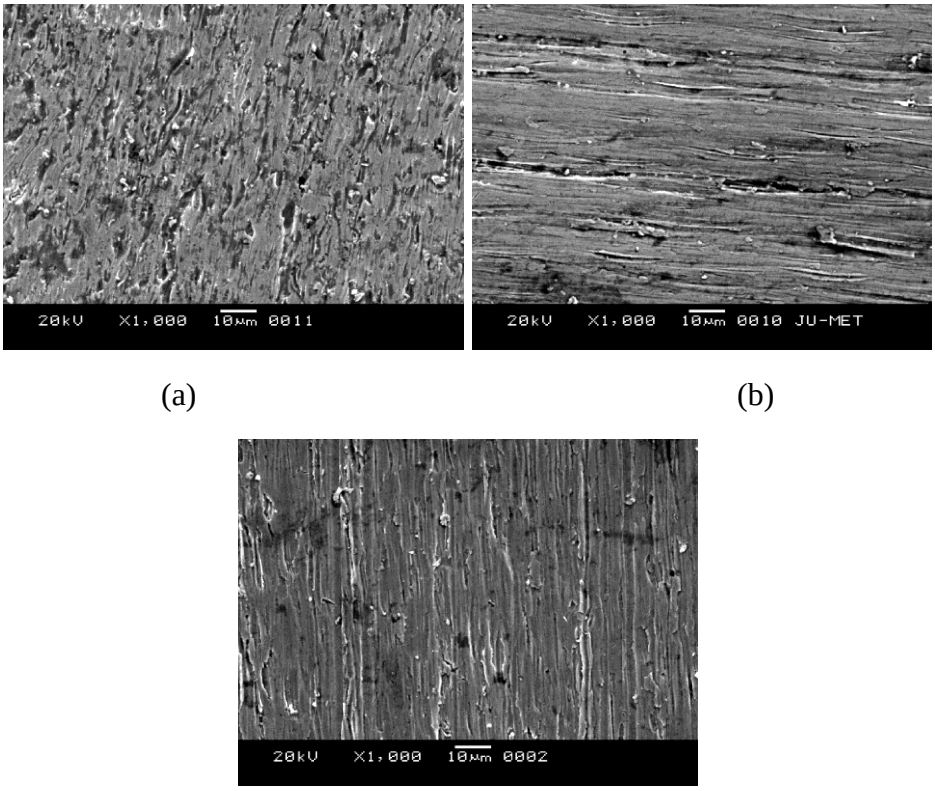

Figure 1.14 SEM micrograph of Ni-P coatings after wear friction test under (a) acidic (b) brine and (c) alkaline environment (adapted from Panja, B., Das, S. K., & Sahoo, P. (2016). Surf. Rev. Lett., 23(05), 1650040, 18pp)

1.7.2 Tribology under high temperature

A thorough literature survey reveals that research work in the field of electroless nickel and its alloy coatings has been focused mostly on the study of tribological behaviors under ambient test conditions. But there is very limited number of examinations that addresses application of EN coatings under elevated temperature. The present investigation is a humble attempt in that direction. The main focus is to identify the parameters that affects the friction wear mechanism under high temperatures.

Electroless Ni-P coatings are found suitable in room temperature applications but very few investigators have worked on their high temperature use. In many fields like aerospace and automobile, the coating may be subjected to operation at elevated temperatures. Hence,

investigation on the properties of EN coatings at elevated temperature is quite relevant. Hardness value of as-deposited coated samples tested at 550°C is increased by 70% due to the high temperature transformation of the Ni-P amorphous phase to a mixture of hard Ni_3P and nickel which normally occurs due to heat-treatment (Masoumi et al., 2012). Formation of an oxide layer on contacting surfaces is the main reason for as-deposited electroless Ni-10% P coatings to exhibit the best wear resistance and the lowest friction coefficient in the wear test at 550°C. With heat-treatment, wear resistance of electroless Ni-10% P coating improved at room temperature test because of the crystallized structure, though it shows an opposite nature in the wear test at 550°C (Masoumi et al., 2012).

Amalgamation of hard particles(X) (e.g. SiC, WC, ZrO_2, diamond, Al_2O_3, Si_3N_2 or BN (cubic) and TiO_2) or soft lubricants (X) (e.g. PTFE, BN (h), graphite, MoS_2 and carbon nanotube) into Ni-P matrix can enrich the mechanical and tribological behavior of Ni-P composite coatings. The hardened composite coating has a wear resistance two orders of magnitude higher than that corresponding to the traditional Ni-P coating in room temperature test (heat-treated in the same conditions, i.e. for 1h at 400°C). However, very limited data on the influence of temperature on the tribological behavior of the Ni-P-X coatings are available.

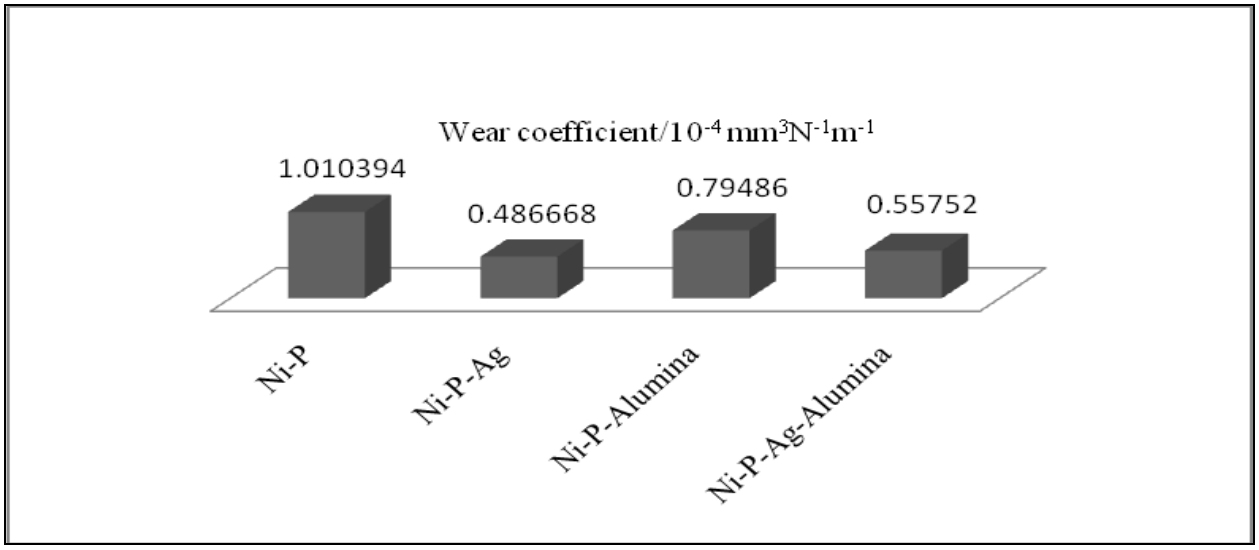

Figure 1.15 Wear rate of heat-treated Ni-P and Ni-P-X coatings at high temperature (adapted from Alirezaei, S., Monirvaghefi, S. M., Saatchi, A., Ürgen, M., & Motallebzadeh, A. (2013). Trans. IMF, 91(4), 207-213)

Applications of heat-treatment to other composite coatings are available in the literatures. Heat-treatment helps Ni-P-SiC composite coatings to improve its wear resistance by 135% compared to that of as-deposited condition because of precipitation hardening (Staia et al., 2002). León et al. (2003) studied the high-temperature tribological behavior of Ni-P-BN autocatalytic coatings deposited on AISI 316L stainless steel and found that the incorporation of solid lubricant BN did not reduce friction and wear. The friction coefficient and wear of the composite

coatings found to increase with increasing operation temperature because of the change in wear mechanism i.e. a transition to a more severe wear, characterized by gross plastic deformation and larger amount of material transfer to the counter face part. But different judgment was made by Li et al. (2013) as MoS_2 plays a key role in the friction and wear rate reduction at higher temperature upto 500°C; best at 400°C due to the formation of the lubricious oxide film composed of NiO and MoO_3, continuing till the softening of the coating. Technological expansion has put forward the claim for tribological systems that possess low wear rates and low friction coefficients under operation at elevated temperatures. At temperatures above 350°C and especially, in oxidizing environments, conventional liquid lubricants and most conventional solid lubricants (e.g., graphite and MoS_2) degrade rapidly. A number of solid materials, such as noble metals (e.g., Au, Ag, and Pt) useful under moderate temperatures and some metal oxides (e.g., NiO, and MoO_3) that are lubricious at elevated temperatures have been employed as solid lubricants due to their high stability and low shear strength (Sliney, 1992). Silver has been used nowadays as a solid lubricant because it yields decent thermo-chemical stability over a wide range of temperatures and possesses low shear strength over a moderate range of temperatures (DellaCorte, 1996). It has been used in composite coatings due to its large diffusion coefficient and high mobility at elevated temperatures. High temperature helps it to diffuse out of the matrix to open surface and form a lubricating film at the sliding interface. The high temperature tribological performance is strongly dependent on the diffusion of silver and its transfer to the counterface. Alirezaei et al. (2013a) works with silver composite coating and found that entrapment of silver particles in Ni-P matrix increases the lubrication and wear resistance of Ni-P coating at room and elevated temperatures operations. The formation of a silver thin layer on the sliding surface led to the decrease of the friction coefficient of Ni-P-Ag coating which makes it suitable to use in high temperature sliding applications such as aerospace industries. Ni-P-Ag coatings have lower wear rate and friction coefficient than other composite coatings at high temperature. A comparison in between various composite coatings with respect to wear rate is shown in Figure 1.15. High temperature wear rate of Ni-P coating is found to be about 10 times more than room temperature wear, but this value reduces by about two times for nanocrystalline Ni-P-Ag composite coating. Alirezaei et al. (2013b) showed that tribological properties of the Ni-P-Ag-Al_2O_3 coating were similar to those of the Ni-P-Ag composite coating. As mentioned by Voevodin & Zabinski, (2005), this type of Ag-based composite coating can be considered as a 'chameleon' coating, due to the formation of self–lubricating thin film from silver at sliding contact conditions for high temperature applications.

Ni-B coatings and its variants are well known for their hardness and wear resistance in ambient conditions. But there are also few studies concerning their high temperature tribological characterisation. Mukhopadhyay et al. (2018a; 2018b; 2018c) conducted several studies concerning borohydride reduced Ni-B and its alloy variants under elevated temperature conditions whose details along with their outcomes are discussed in this section. Mukhopadhyay et al. (2018c) carried out tribological test and found that electroless Ni-B coating shows excellent wear resistance at 300°C, which again degrades at 500°C due to severe oxidation and softening

of the deposits. Within the chosen temperature range (room and elevated temperatures of 100, 300, and 500°C), the wear mechanism changes from adhesive to a combination of adhesive and abrasion as the temperature rises from ambient condition to 100°C, post which the wear mechanism is predominantly abrasive. They also suggest tribological behavior of the coatings at high temperature is affected by tribo chemical oxide film formation during the tests. The tribological behavior of as-deposited and heat-treated Ni–B–W coatings are investigated at room and elevated temperatures (100°C, 300°C, and 500°C) and show an improvement in the wear resistance and coefficient of friction at 300°C and 500°C in comparison to 100°C (Mukhopadhyay et al., 2018a). Microstructural changes occur in the coating due to the in situ heat-treatment at high temperature. The tribological behavior of the coatings at 100°C and 300°C is mainly governed by the loose wear debris and formation of debris patches, respectively. Whereas at 500°C, formation of protective tribo-oxide patches is also observed which is similar to that of Ni-B coatings. Post wear scanning micrograph images of Ni-B and Ni-B-W coatings tested under 500°C is displayed in Figure 1.16.

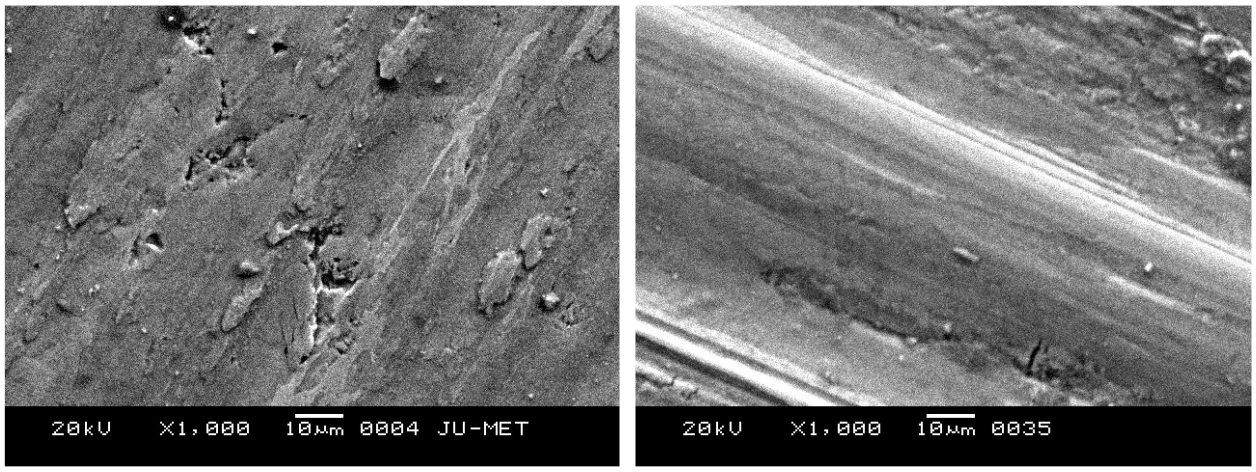

(a) (b)

Figure 1.16 SEM micrographs of high temperature (500°C) post wear test of as-deposited (a) Ni-B (adapted from Mukhopadhyay, A., Barman, T. K., & Sahoo, P. (2018), Tribol. T., 61(1), 41-52.) and (b) Ni-B-W (adapted from Mukhopadhyay, A., Barman, T. K., & Sahoo, P. (2018), Proc. IMechE. Part J: J. Eng. Tribol., 232(11), 1450-1466.) coatings

Tribological behavior and associated tribo-mechanisms at different temperatures under dry sliding condition for Ni–B–Mo coatings is studied and wear shows an increasing trend with an increase in applied normal load and speed at room temperature, 100°C and 300°C (Mukhopadhyay et al., 2018b). At 500°C, the wear increases with load but with speed it first increases up to 80 rpm and then decreases. The COF does not show a similar behavior like the wear with varying load and speed at different temperatures. Instead, it is controlled by the accompanying wear mechanisms, formation of oxide debris and oxide layers of Ni and Mo.

1.8 Summary

EN deposits are classified as a functional class of coatings used primarily to enhance the surface characteristics of a variety of substrates. EN plays a great role primarily on surface engineering and corrosion-resistant fields resulting in an extension in the useful life of the component. Nickel coating is a good alternative to hard chromium for applications in several industries because of toxic nature of the latter. The performance of electroless nickel coating is generally evaluated on the basis of hardness, surface roughness, friction, wear, fractal dimension and corrosion. Electroless coatings are formed as a result of a chemical reaction between reducing agent present in the solution and the metal ions. The properties of electroless nickel depend upon various process parameters, composition, heat-treatment temperature, etc. The mechanical and tribological properties of EN deposits can further be enhanced by the incorporation of different materials as well as by suitable surface treatments (heat-treatment, laser treatment, etc.). The most common material to be added along with nickel is phosphorus or boron, which gives birth to two well-known coatings such as Ni-P and Ni-B. Apart from deposition of these two materials inclusion of various transition metals (tungsten, copper, molybdenum, etc.) as well as particles (TiO_2, Al_2O_3, SiC, etc.) leads to poly alloy or composite coatings which are also investigated by various researchers. Heat-treatment also plays as an important factor for improving the performance of EN coating by affecting the thickness, hardness, structure and morphology of the deposit.

For many engineering applications such as power generation, metal forming operations and the aerospace industry, high temperature tribology plays a very important role. Controlling friction and wear at elevated temperatures is a challenge since the conventional lubrication methods are no longer effective above a certain temperature. Despite a good number of researches on Ni-P coating particularly on evaluation of their properties at room temperature, very few are highlighted towards the behavior of Ni-P coating at elevated temperatures. Hence, the motivation to compare the tribological characteristics of hypophosphite reduced coatings at ambient as well as at elevated temperature is obtained.

1.9 Present Work

The present work deals with high temperature tribological behavior of electroless Ni-P coatings and its variants. The basic focus is on the deposition of hypophosphite reduced Ni-P coating and its tribological characteristics evaluation at room and high temperatures. Further, the addition of W, B and Al_2O_3 in Ni-P matrix is considered for better tribological properties and thermal stability. Finally, a comparative study is carried out in between the developed coatings on the basis of tribological performances in high temperature conditions. The effects of test parameters such as load as well as sliding velocity are studied both at room and elevated temperature. Further, a detailed discussion is carried out based on the effect of different temperatures on friction and wear characteristics along with the wear mechanism. To assess the

high temperature suitability of the Ni-P coatings, several characterisation tests are performed followed by tribological analysis and wear mechanism as illustrated in Figure 1.17.

1.10 Structure of the Thesis

There are eight chapters in the current thesis. The first chapter presents the basics of electroless coating process and its tribological aspects focusing high temperature applications and the motivation of the present work. The experimental details including substrate preparation, film deposition, equipment used in coating characterisation, etc. along with the detailed work plan are introduced in second chapter. The third chapter deals with the deposition, characterisation of electroless Ni-P coating and its tribological performance evaluation in room and high temperatures. Chapter four, five and six presents the effort to improve the tribological characteristics of hypophosphite reduced electroless Ni-P coating by inclusion of W, B and Al_2O_3 respectively. Seventh chapter presents a comparative study on high temperature tribological behavior of Ni-P coatings and its variants and suitability of their use in high temperature applications. The final chapter (eight) highlights the conclusion stating the future possibility of the present work.

1.11 Contribution of the Thesis

Electroless Ni-P coatings and its variants have established themselves as a good tribological material for room temperature applications. Hypophosphite reduced coatings shows satisfactory results in many research studies concerning friction and wear in dry and lubricated environments. It also indicates a remarkable stand as anti-corrosive coating. However, the performance of the same in high temperature field needs to be evaluated as investigation reveals the softening of most of the coating materials at temperatures above a certain value. This results in the deterioration of their wear resistant activity causing to shorten the life of the component. Despite a good number of researches on Ni-P coating particularly on evaluation of their properties at room temperature, very few are highlighted towards the behavior of Ni-P coating at elevated temperatures. Hence, the motivation to compare the tribological characteristics of hypophosphite reduced coatings at ambient as well as at elevated temperature is gained. Thermal stability of coatings is usually determined through heat-treatments at different temperatures and durations. Post heat-treatment analysis explores thermal stability of Ni-P coatings (Biswas et al., 2017). The similar pattern of study is also conducted for the other variants of the EN coatings (Pal et al., 2018) But in the current work, thermal stability of the coatings has been predicted from the tribological characteristics of the coatings This may aid future researchers in exploring the potential of Ni-P and its variants as a high temperature coating material which may in turn find its applications in suitable industrial domains.

Substrate (block/pin) preparation through cleaning and activation

Chemicals

Film deposition

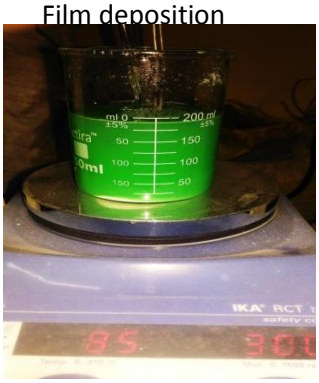

Heat-treatment

Preparation of hypophosphite based Ni-P and its variant coatings

Characterization of developed coating

a) Vicker's microhardness test
b) Scanning electron microscopy
c) Atomic force microscopy
d) Energy dispersive X-ray analysis
e) X-ray diffraction

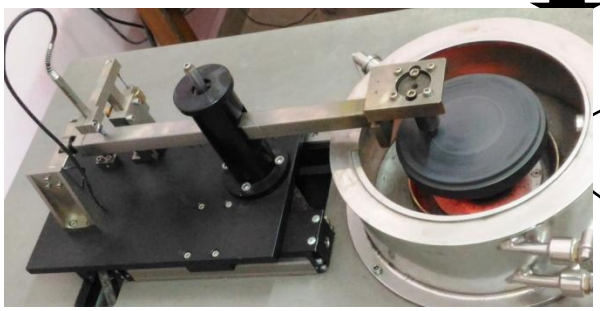

Stage I: Effect of test parameters on tribological behavior

Stage II: Effect of test temperatures on coating tribology

Friction and wear tests at room and elevated temperatures

Tribological mechanism and characterization

Structure, phase transformation and wear mechanism

Figure 1.17 Schematic representation of the present work

1.12 Closure

The present chapter tells about the basics of electroless coating process and its tribological aspects with particular emphasis on high temperature applications. Among all variants of electroless nickel coating, Ni-P has got wide acceptance because of its high anti-corrosion and anti-wear property. An extensive literature review mainly on tribological characterisation of Ni-P coatings and its variants are discussed focusing its applicability in high temperature domain. The motivation for the present work comes out as Ni-P coatings and its variants have already proven their excellent tribological characteristics at room temperature condition. There is opportunity for further evaluation and improvement of the friction and wear characteristics at high temperatures. Finally, a short description of the present work along with the thesis structure and its contribution is presented.

This page is left blank intentionally

Chapter 2

Experimental details

2.1 Introduction

Experiment is a scientific test in which series of actions are performed and their effects are carefully observed in order to learn about something. With proper planning and execution of an experiment, definite and meaningful inferences can be drawn which enhances the human perception of nature. The present chapter deals with the planning of experiments required to develop Ni-P and its variant coatings. Furthermore, the method of substrate preparation and the methodologies used for different tests (roughness, hardness, friction, and wear) are also discussed in this chapter.

2.2 Coating Development

2.2.1 Substrate preparation

Carbon steel (AISI 1040) is used as the material for preparation of blocks (15×15×2 mm) for characterization and pin (30 mm length and 6 mm diameter) specimens for tribological test in the pin on disk apparatus. The carbon steel used in the present work consist of carbon (0.36-0.41%), manganese (0.65-0.82%), phosphorous (~0.03%), sulphur (~0.04%), silicon (~0.02%) and rest Fe. All the substrates before coating are subjected to roughness evaluations (center line average values, Ra) and the substrates which showed as little as 0.1% variation in roughness are selected for electroless depositions. The roughness measurements are carried out using a surface profilometer (details in Section 3.5). The blocks and pins those confirm roughness grade N5 (Ra=0.40μm) are selected as substrate for electroless nickel deposition as EN coatings follow the surface of the substrate and friction characteristics are dependent on surface roughness. The substrates are initially cleaned using soap water. After that, acetone is employed to clean off any remaining organic particles. Finally the substrates are cleaned with methanol. Before coating, the subjects are subjected to pickling treatment with 50% HCl acid for one minute in order to remove rust and other surface oxide layers. Lastly, the cleaned substrates are activated in palladium chloride solution at 55ºC temperature and placed in the electroless bath. Schematic chart showing steps engaged with substrate preparation and coating deposition is illustrated in Figure 2.1. This activation step is required to overcome the initial energy barrier and kick start the deposition process. Subsequently, they are rinsed in distilled water prior to coating. When the pretreatment steps are finished, the substrates are immersed in the electroless bath for desired

duration with the assistance of a customized sample holder which is dormant to the bath chemicals. The schematic setup for electroless nickel deposition is appears in Figure 2.2.

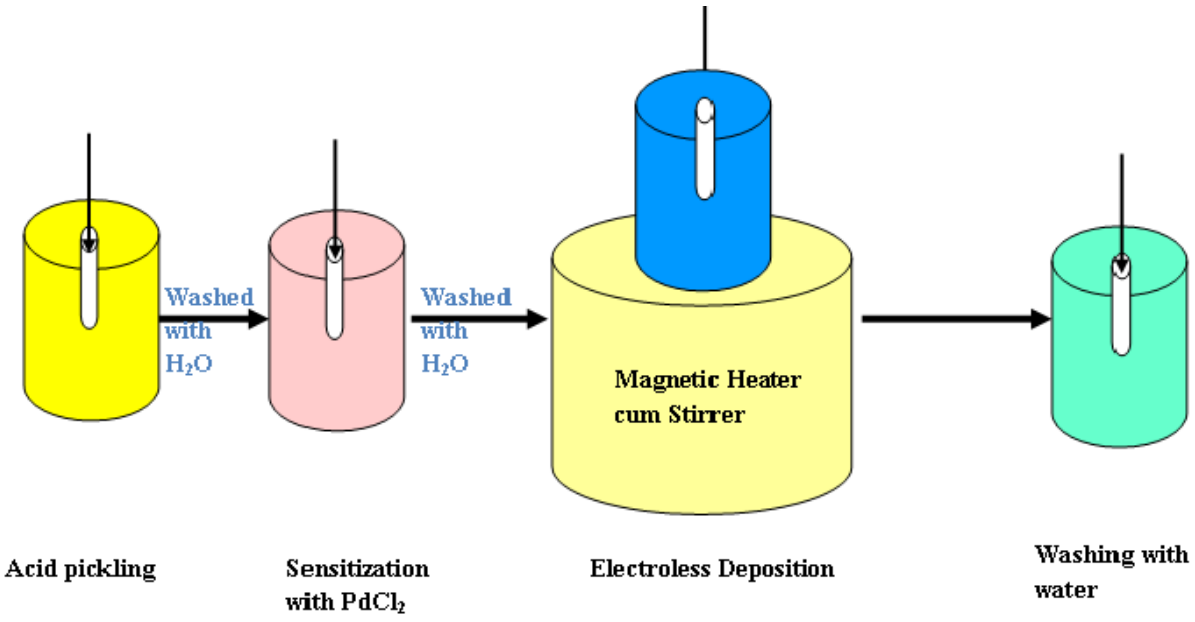

Figure 2.1 Schematic representation of steps for electroless coating on substrate surface

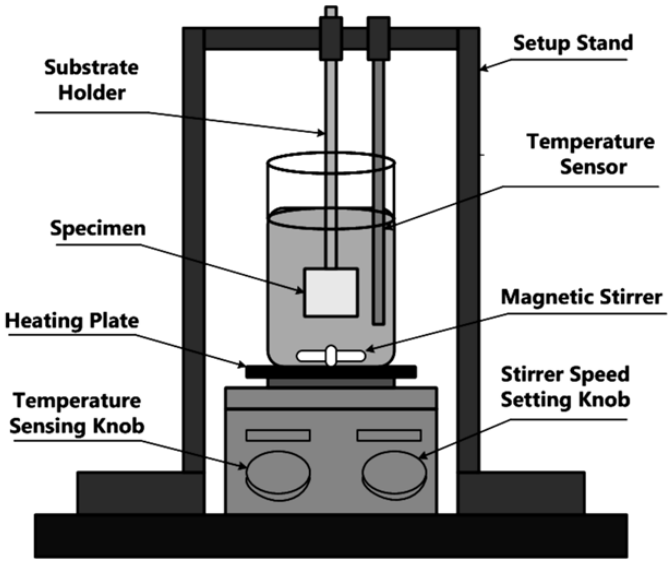

Figure 2.2 Schematic representation of setup for electroless nickel deposition

2.2.2 Film deposition

Hypophosphite reduced electroless Ni-P and its three other variants were chosen for the deposition purpose. Initially large number of experimental trials were performed to decide the bath composition of each coating with the proper selection of coating process parameters. A

general discussion on coating deposition indicating the chemicals used for each bath prosecuted here viz. Ni-P-W, Ni-P-B, Ni-P-Al_2O_3. Bath composition and operating conditions for Ni-P and its three variants are discussed in chapter 3, 4, 5 and 6 respectively. The pH of the solution was measured by a pH meter (EUTECH Instrument, South Korea, ISO 90001) and was adjusted to the desired value either by adding sodium hydroxide (NaOH) for acidic bath or adding ammonium hydroxide (NH_4OH) for alkaline bath. The coating is carried out for desired duration so that a considerable coating thickness can be achieved which is necessary for carrying out the tribological tests. A double bath deposition technique is employed for this purpose. Deposition time and bath volume is kept same for all specimens of each category of coating so that the coating thickness and bath loads remains approximately constant. After the deposition, the samples are taken out of the bath and washed in distilled water. As some heat-treated samples are required for the tests, a few coated specimens undergo heat-treatment in a furnace at 400ºC for 1 hour and then cooled to room condition (approximately 30°C). This particular temperature is selected as most researchers have acknowledged it as the best heat-treatment condition for EN coatings with respect to tribological behavior.

Figure 2.3 Precision weighing balance

Figure 2.4 Digital pH meter

2.2.3 Instruments and chemicals used for film deposition

Usually, basic and low cost instruments are required for any electroless deposition. The following instruments are used for bath preparation and deposition of prosecute coatings:

Electronic weighing balance: High precision electronic balance (AFCOSET, Model No. ER-182A, SL. No. 0108017, Max^m range 180 gram, Min^m range 0.01 mili-grams, refer Figure 2.3).

Magnetic stirrer: Magentic stirrer is used for proper mixing of bath solution (2MLH Magnetic stirrer, Manufactured by Remi Instruments).

pH meter: A digital pH meter is used to measure the pH of the electroless bath (Electronic India, Model No. 181, SL. No. 11505265, Max^m range 14 pH, Min^m range 0.01pH, refer Figure 2.4).

Electoless bath heater: Used for heating of electroless Ni-P and its variants alloy and composite baths (IKA® RCT basic, refer Figure 1.x).

Infrared thermometer: Used to maintain the electroless bath temperature during coating deposition process (HTC, MT4, Max^m range 530°C, Min^m range -50°C, refer Figure 2.5).

Muffle furnace: Used for heat treating the coated samples (10×10×25) Max^m Range 1200°C (refer Figure 2.6).

Glass beaker: Used to hold the electroless bath solution (Merk).

Figure 2.5 Infrared thermometer

Figure 2.6 Muffle furnace

Chemicals used in general for electroless nickel phosphorus and its variants baths are:

- Nickel Chloride **($NiCl_2.6H_2O$)**, Merck Specialties Pvt. Limited, Mumbai, No. 61761305001046, B.N. MC5M532009, UN 3288, CAS No. 7791-20-0, 6.1/III (IMDG – Code).

- Nickel (II) Sulphate Hexahydrate Purified **($NiSO_4.6H_2O$)**, Merk Specialities Private Limited. B. N. MF8M580868, No. 61756705001730. CAS No. 10101-97-0, 9/III (IMDG-code), UN 3077.

- Sodium Hypophosphite (**$NaH_2PO_2.2H_2O$**), Merck Specialties Pvt. Limited, Mumbai, India, No. 0590500500 Lot: # SL06951303, CAS No. 10039-56-2.

- Sodium Succinate **($C_4H_4Na_2O_4.6H_2O$)**, LOBA CHEMIE PVT LTD., Mumbai, Art. No. 6010, Batch No. V007303, CAS No. 6106-21-4.
- Sodium Tungstate Dihydrate GR **[Na_2WO_4]**, Merk Specialities Private Limited, B. N. ML3M532516, No. 61761202501046.
- Tri-Sodium Citrate Dihydrate GR **[$C_6H_5Na_3O_7$. $2H_2O$]**, Merk Specialities Private Limited, B. N. MF8M581342, No. 61770905001730. CAS No. 6132-04-3.
- Ammonium Sulphate GR **[$(NH_4)_2SO_4$]**, Merk Specialities Private Limited, B. N. M17M572322, No. 61783405001730, CAS No. 7783-20-2.
- Lactic Acid, min. 88% GR **[$C_3H_6O_3$]**, Merk Specialities Private Limited, B. N. AF6G560264, No. 61779105001730, CAS No. 50-21-5.
- Sodium Borohydride (powder 98+%, Natrium Borhydrid, nitrogen flushed) **($NaBH_4$)** : ACROS ORGANICS, New Jersey, USA, No – 189301000, Lot : A017697501, CAS No. 16940-66-2, EINECS : 241-004-4.
- Sodium Hydroxide pellets (G.R.) **(NaOH)** : Merck Specialities Pvt. Ltd., Mumbai, India, No. 61843805001730, B.N. MG8D580159, UN 1823, CAS No 1310-73-2 8/11 (IMDG-Code).
- Ethylenediamine (pure, min. 99%, M.W. – 60.10) **($C_2H_8N_2$)**: SISCO Research Laboratories Pvt. Ltd., Mumbai, India, No. 052753, Batch No. TT533140.
- Lead Nitrate (A.R.) **($Pb(NO_3)_2$)** : S.d. fine-chem Limited, Mumbai, India, Prod. No. - 20145, Batch No. LO2Z/0602/2711/31, UN 1469, IATA 5.1, 5.1/11 (IMDG –Code).
- Sodium acetate anhydrous GR (**CH_3COONa**): Merck Specialties Pvt. Limited, Mumbai, India, No. 61795202501730, B. N. QD3Q630867, CAS No. 127-09-3.
- Aluminium oxide active, neutral Activity I-II, (acc. To Brockmann for column chromatography), (**Al_2O_3**): No. 61768405001730, B. N. MD8m580835, CAS No. 1344-28-1.
- Sodium Lauryl Sulphate (Sodium Dodecyl Sulphate0 (Needle Shape) (**$C_{12}H_{25}NaO_4S$**) Art. 5925: LOBA CHEMIE PVT. LTd.. Mumbai, India, B. N. LB217809, Cas No 151-21-3
- Lead (II) acetate trihydrate GR (pro analysi) [**$(CH_3COO)_2Pb.3H_2O$**]: Merck Specialties Pvt. Limited, Mumbai, India, No. 7375, B. N. CF933658, UN 1616 6.1/III (IMDG-Code).

- Paladium (II) Chloride anhydrous (**$PdCl_2$**): Merck Specialties Pvt. Limited, Batch No. ML8M583408, UN – 32608/III (IMDG - CODE).

- Acetone (**CH_3COCH_3**): Merck Specialties Pvt. Limited, CAS No. 67-64-1 3.1/II (IMDG-CODE), UN 1090.

- Methanol GR pro analysi (**CH_3OH**): Merck Specialties Pvt. Limited, CAS No. 67 56-1 3.2/II (IMDG-Code), SA7SF57012, UN 1230.

2.3 Determination of Coating Thickness

Earlier coating thickness was used to be measured by following weight gain method. However, this method involves the density of developed coating which again varies depending on the process parameters. Thus, calculation of thickness considering constant density results in errors. Thickness of the coating can accurately be determined by observing the cross cut surface of the coated substrate under SEM (Scanning Electron Microscope). In any case, before observing under the microscope, the sliced surface is well ground to get a smooth area, for better and accurate result. This techniques help to provide precise estimation of the coating thickness.

2.4 Surface Roughness Measurements

Surface roughness is a bulk measure of the average size of the hills and valleys. Some surfaces appear smooth and planar to the naked eye when in fact the real shape is composed of a semi-infinite number of irregular forms. Surface roughness is critical to the performance of wear-resistant and lubricant coatings, stress corrosion and fatigue. Wear and friction are strongly affected by surface roughness and in many instances, an optimum roughness can be found which provides a minimum of wear and friction. The geometrical parameter of a coating that is its surface roughness has a key effect on the mechanical integrity of the covering. Exact estimation of roughness is subsequently basic to the assessment of any layer. The contact strategy which depends on a stylus crossing the surface is utilized to quantify the surface roughness of the developed electroless nickel phosphorus and its variant coatings. A Talysurf profilometer (Make – Taylor Hobson, UK) is utilized to quantify the roughness parameter R_a considered in the present thesis (appeared in Figure 2.7). The Talysurf instrument (Surtronic 3+) is a compact, independent stylus and slide type instrument for the estimation of surface texture. In this instrument the amplifications of the signal created by the stylus is done electrically. The parameter assessments are microprocessor based. The results are shown on a LCD screen and can be fed to a printer or another PC for further assessment. The instrument is controlled by non-rechargeable alkaline battery (9V). It is outfitted with a diamond stylus having a tip radius of 5 µm. The estimating stroke begins from the outward position. Toward the finish of the estimation, the pickup comes back to the position, prepared for the next assessment. The choice of cut-off length decides the traverse length. Normally as a default, the traverse length is five times the cut-off length, however the amplification factor can be changed suitably.

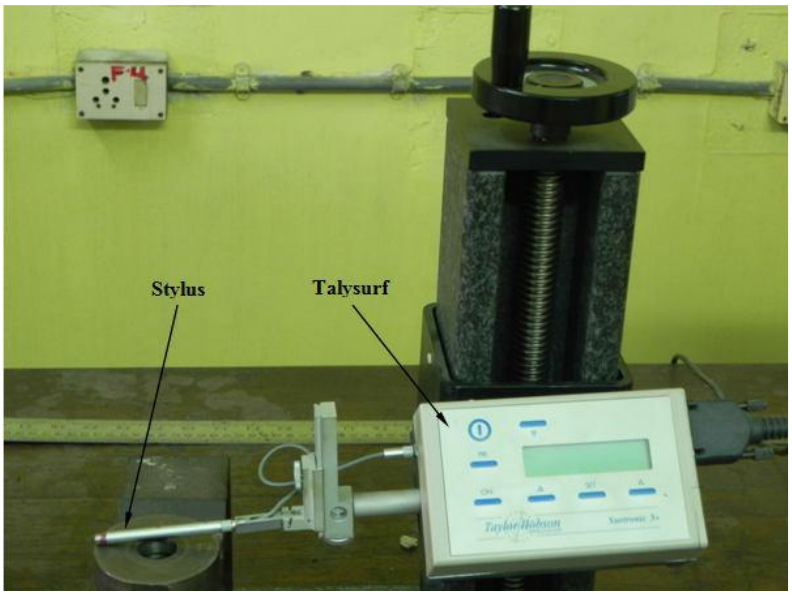

Figure 2.7 Talysurf Profilometer

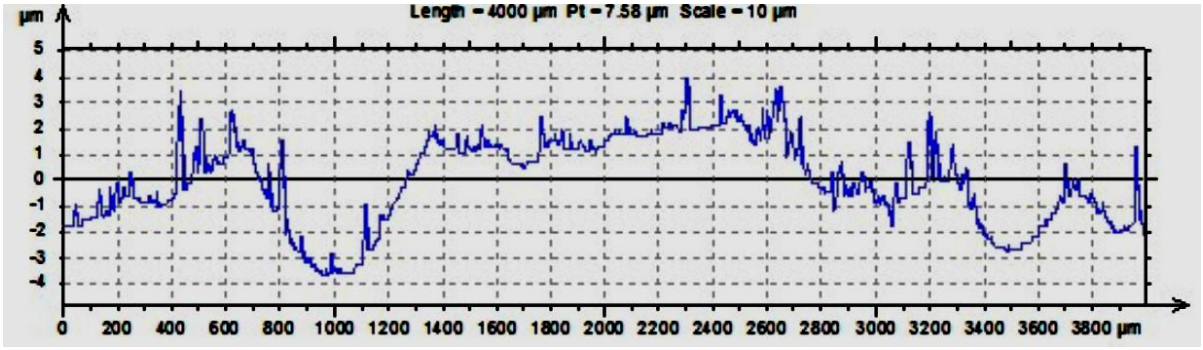

Figure 2.8: Typical surface profile of a substrate captured in profilometer

In the present work, the roughness (centre line average) of as-deposited and heat-treated specimens are measured using Talysurf (Surtronic 3+) profilometer (stylus type with a tip of radius 5 µm, made of diamond) by considering sampling length, traverse length and traverse speed of 0.8mm, 4mm and 1 mm/s respectively. Talyprofile software (Taylor Hobson, Leicester, UK) is employed to process the readings and average of six such readings is considered as the roughness value R_a for a particular specimen. The surface profile of a substrate obtained by the stylus profilometer is shown in Figure 2.8.

2.5 Hardness Evaluation

Hardness is the property of the material by virtue of which it offers resistance to plastic deformation under the application of load. The possible techniques applied to finding this resistance is usually scratch, indentation, penetration or rebound. The most adopted process for metals/alloys is indentation and the response or the resistance that is offered by the material

against the load is typically expressed by hardness number. Different hardness techniques are available with various load ranges and scales, but Vickers hardness test is the most renowned one because of its wide load range facility. Hardness is a parameter which solely depends on the material's chemical composition and its structure. So for coating structure, hardness highly depends on bath composition and corresponding process parameters. As thickness of coatings mostly lie in millimeter-micrometer range, the most preferred choice of hardness is micro hardness but nowadays with the development of nano coatings the concept of nano hardness is also applied.

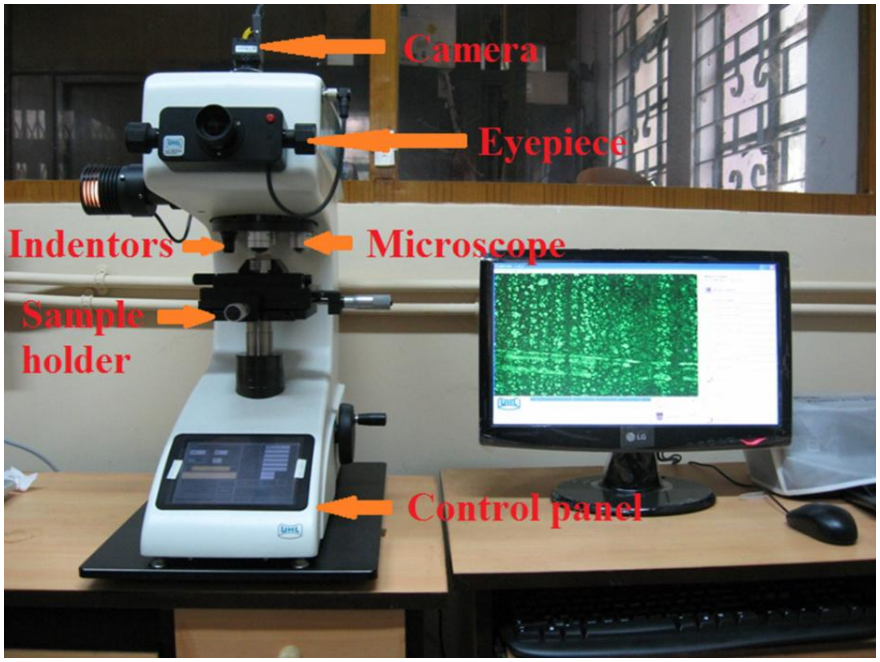

(a)

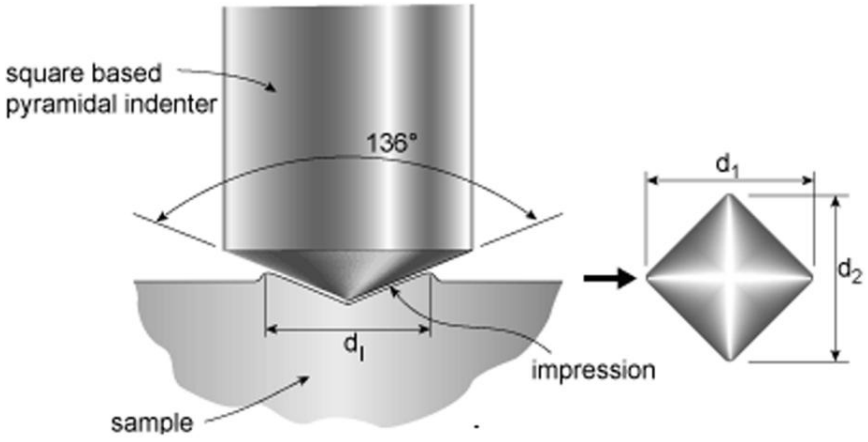

(b)

Figure 2.9 (a) Vicker's Microhardness tester with (b) zoomed view of its indenter

Since, in the present thesis, the materials to be examined are thin coatings (about 25-50µm), micro hardness testing approach, by means of a precise diamond indenter with low load (100

gram force) is used. Vicker's microhardness of the developed coatings (both as-deposited and heat treated) is performed following ASTM standard E384-16. Hardness analyzer (VMHTOT, Technische Mikroskopie) as shown in Figure 2.9 (a), along with a pyramidal diamond indenter (Figure 2.1(b)) is used for finding hardness by applying an indentation load of 100 g, dwell period of 15s and a speed of 25 μm/s. Now, the load application in micro-hardness tester is done in two speeds — a "fast speed" to bring the indenter close to the test piece, and a "slow" speed to contact the work and apply the load. The "stroke" of the indenter is usually set with a measuring device. The speed of 25 μm/s mentioned here is the approach speed of the indenter. On the other hand depth of the indentation depends on the indentation load and the dwell time both of which have been carefully selected based on the thickness of the coating and after several trials. Hence, there is no danger of perforation of the coating by the hardness indenter. The micro hardness analyzer is controlled through a touch screen based framework and length of the diagonal of the indent surface is measured to provide hardness result. That length is measured by a low amplification optical magnifying instrument which is attached to the hardness analyzer. Five indentations are done on each face of the coated specimen and their average is recorded.

2.6 Friction and Wear Evaluation

Pin-on-disc type tribotester is being used to evaluate friction and wear characteristics of the EN coated specimens under high temperature following ASTM G99-05 (2010) standard. The room temperature was about 30ºC with a relative humidity at 85%. The effects of loads under dry, non-lubricated conditions on tribological performance in different test temperature (room and 100-500°C) are studied in a pin-on-disc type tribotester (TR-20-M56, DUCOM, INDIA). A pictorial view of the setup is illustrated in Figure 2.10. Both as-deposited and heat-treated coated samples are held vertical and slid against a EN31 counterface disk (diameter 110 mm×8 mm thickness) made of hardened steel (58-62 HRC) at 60 mm track diameter and rotating at the desired speed. The loading of the pin is done precisely through a stepper motor and load cell arrangement. Constant torque is applied to the disc with the help of a servomotor drive. The rotating counter face disc is heated inductively to the desired temperature and the test is conducted in a closed chamber. Wear can be measured in terms of displacement with the help of linear voltage resistance transducer. The wear displacement sensor allows obtaining direct measurement of the pin's movement which corresponds to the wear of the specimen plus the wear of the counter face surface. The bottom disc being fully hardened (1680 $HV_{0.1}$ hardness) undergoes negligible wear, and thus the measured wear is essentially the wear of the coated pin specimen. However, in the current thesis, wear is evaluated by the conventional weight loss method. The frictional force is measured by frictional force sensor that uses a button type load cell of 100 N capacity. Friction coefficients were recorded by a computer across the entire test duration. The wear rate is calculated by the mass loss that occurs during the tribo-test. Precision weighing balance (AFCOSET, ER 182A) having a readability of 0.01 mg is used to measure the mass loss. A pyrometer (least count=1°C) is used to monitor and control the disk temperature. Tests are conducted for all relevant temperatures to evaluate the tribological behavior of the

coatings properly. Every single one of the tribo- tests was repeated at least twice, and the average values were recorded.

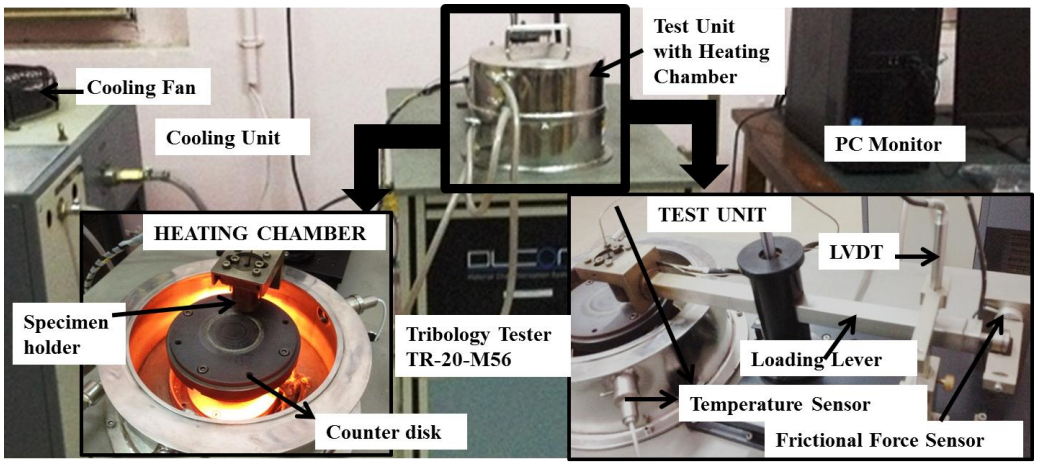

Figure 2.10 Pictorial view of wear and friction set up with test unit and heating chamber (inset)

For the present study, considering the low thickness of the coating (about 25-50 μm), the load and speed ranges are fixed after conducting some trials. The fixed ranges of applied load and sliding velocity are 10-30 N and 0.094-0.220 m/s respectively. The duration of the tests is limited to 5 minutes. For the first phase, the effects of load (10, 30 and 50N) and sliding velocities (0.094, 0.157 and 0.22 m/s) on tribological behavior at room and elevated temperature (500°C) are studied. In second phase, selecting proper load and velocity, a detailed temperature profiling (100-500°C) is carried out to understand the friction and wear characteristics of the electroless Ni-P and its variants in high temperatures domain. A schematic indicating high temperature test of developed coating is shown in Figure 2.11.

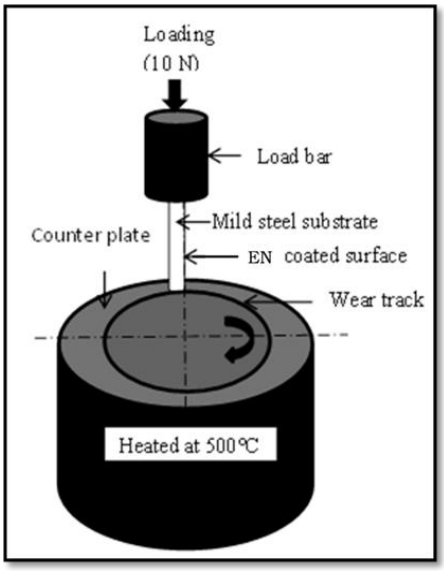

Figure 2.11 Schematic diagram for high-temperature friction wear test

2.7 Micro structural Analysis

Morphological characterization are conducted after deposition of the coating to ensure about the proper development of the coating as well as after the tribological test to evaluate the nature of failure. In the present study, surface morphology study of the electroless Ni-P and its variant coatings is done by using field-emission scanning electron microscopy (FESEM-FEG Quanta 250) under high vacuum at 20 kV and equipped with phosphor cathode ray tube screen, in order to observe the microstructure as well as wear mechanism of the coatings. FESEM (Figure 2.12) is used to investigate the microstructure of both as-deposited and heat-treated coatings along with the wear tracks. The cross-section investigations are done to confirm the coating thickness as well as to detect the interfacial interaction in between the coating and substrate material. Everhart Thornley secondary electron (SE) detector is used to investigate the morphology of the coatings as well as wear modes and mechanisms.

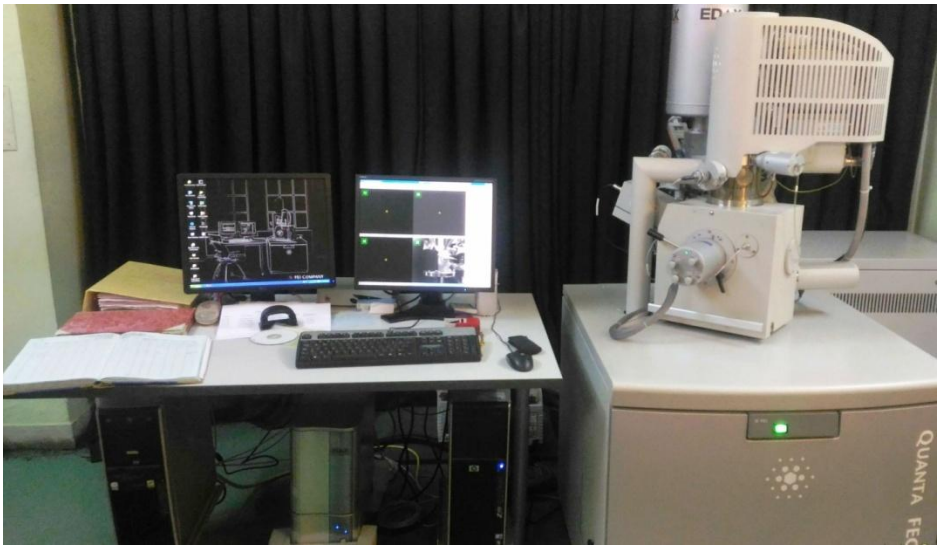

Figure 2.12 Quanta FEG 250 field-emission scanning electron microscope (FESEM)

Further Atomic Force Microscopy (AFM) is employed to examine the surface heterogeneities of the coated specimens in details. In addition to that this high resolution scanning probe microscopy is used to confirm the observations made through SEM. The 2D and 3D illustration of Ni-P and its variant coatings in as-deposited and heat-treated conditions have been inspected with AFM in contact mode with a scan area of 10 μm × 10 μm. In the present study, AFM (Digital Instruments CP-II Veeco Company, USA) is conducted with a machine equipped with silicon cantilevers (Al reflex coated with a spring constant 0.9Nm-1, resonant frequency 22kHz) in contact mode (Figure 2.13). Apart from that, few post wear specimen with 100 μm × 100 μm area is analysed for better understanding the high temperature wear mechanism. Further it helps to correlate the tribological behavior with the corresponding wear modes and mechanism.

Figure 2.13 Veeco atomic force microscope (AFM)

2.8 Compositional Analysis

Energy dispersive X-ray investigation (EDX) is utilized in conjunction to a Scanning Electron Microscope (SEM) as both use the same electron source. EDX under high vacuum at 15 kV is done in conjunction with FESEM having an Everhart Thornley secondary electron detector (Figure 2.12), to study the composition of the Ni-P and its variants coatings in terms of the weight percentages of nickel, phosphorous, boron, tungsten, etc. The penetration of electrons into a specimen is commonly in the range of 0.1 to 1 μm and hence the elemental composition of coatings with this scope of thickness can be precisely distinguished from the substrate. EDX can be either used to investigate composition at a point or over a wide zone. Explicit components can likewise be mapped over a test surface by examining for X-beam outflow at a predetermined energy. In the present study, EDX is conducted both before and after the high temperature test for proper surveillance and to check the thermal stability of the coatings. Different forms of EDX such as in the form of point, line or area is performed as per requirement of a proper investigation.

2.9 Phase Structure Analysis

A diffractometer comprises of a X-beam source, a sample holder with capacity for revolution and a progression of counter to screen the diffracted force is used for phase structure study. Oxides, nitrides, carbides and sulfides of metals are noticeably recognized by this strategy. The phase structure of the coating is studied with the help of X-ray diffraction (XRD) analysis (Rigaku, Ultima III) with CuKα source (λ = 0·15418 nm) and outfitted with Inel CPS 120 hemispherical detector (Figure 2.14). XRD is performed for 2θ value ranging from 20–80° and with a scanning speed of 0.03°/min. Now, angular position of the diffraction peaks in a diffraction plot is determined by the distances in between parallel planes of atoms (dhkl)

following Bragg's law. XRD is best applied to bulk samples but can be used to analyze thicker coatings and powder samples. Identification of compounds can be obtained by comparing the X-ray diffraction graph of unknown sample with JCPDS file. For the developed electroless Ni-P and its variant coatings, the crystalline compounds anticipated to be formed are expected to manifest themselves in the diffraction range of 20–80°. The same range has also been repeatedly used in many works related to electroless nickel coatings and hence has been used in the present study. XRD is also carried for some worn out samples to detect the changes (if any) with respect to structure and grain size compared to unworn state.

Figure 2.14 Rigaku, Ultima III X-ray diffractometer

2.10 Work plan

Experiments are performed in an orderly manner and in a sequence so that proper and logical inferences can be drawn from the experimental results and unwanted errors could be prevented. At first the substrates are very meticulously prepared according to the specified dimensions then processed for electroless Ni-P deposition. Developed coating are characterized ensuring proper deposition and then moved for tribological characteristics evaluation at room and high temperatures. The tribological evaluation of the coatings is planned to be carried out in two phases. In the first phase, the effects of the applied load and sliding velocity on the tribological behavior of the coating both at room and elevated temperature (500°C) is studied. Based on these results, the combination of load and velocity which gives more or less minimum friction and wear is selected. In the second phase, the effect of elevated temperatures (RT to 500°C) on the tribological behavior of the coatings at the selected test parameters is investigated. Further, the addition of W, B and Al_2O_3 in Ni-P matrix is considered for better tribological properties and thermal stability. Each of the developed coating are then evaluated based on their high temperature tribological performances and finally a comparative study is undertaken. The details of the thesis work indicating the steps involved are depicted by Figure 2.15.

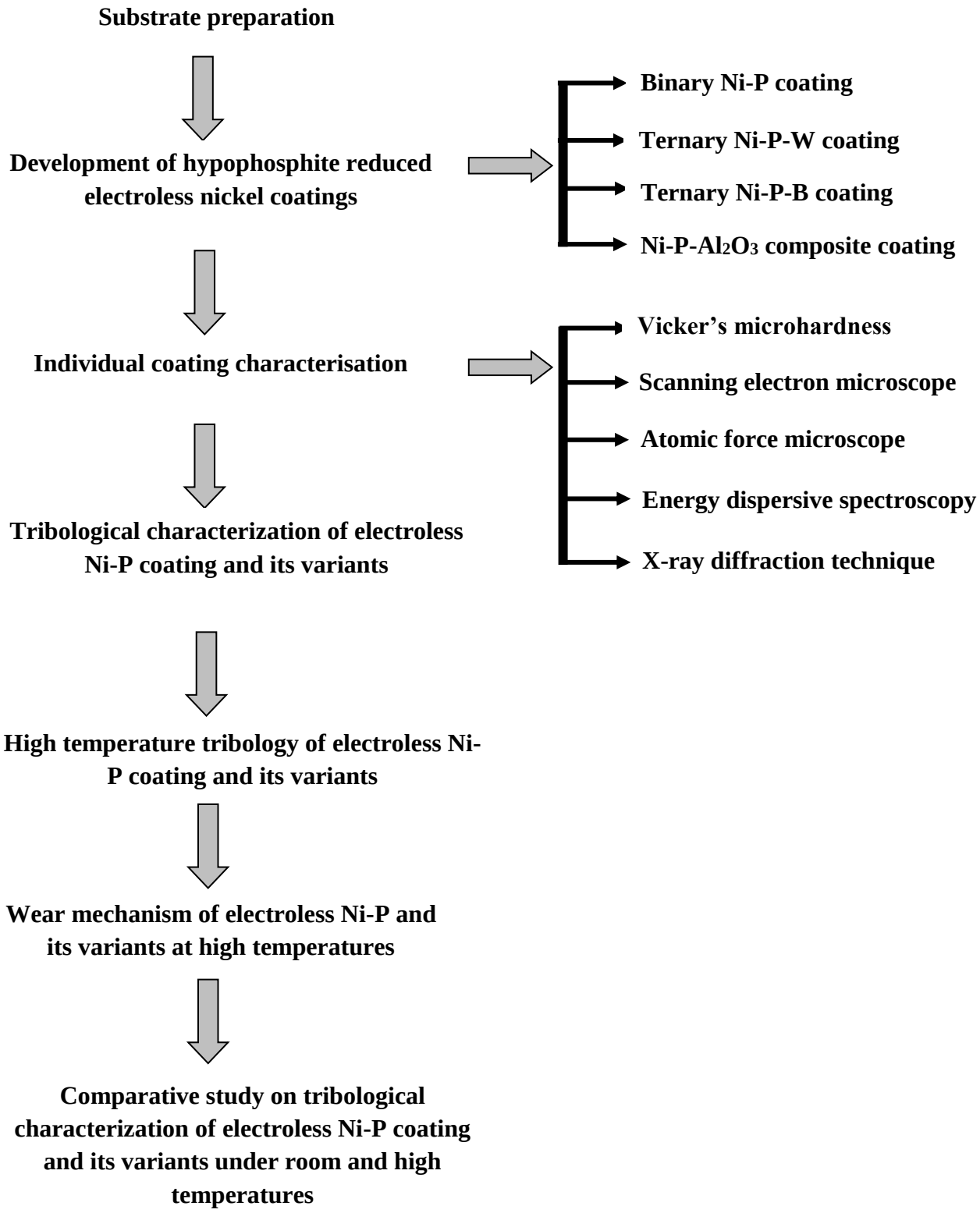

Figure 2.15 Block diagram representing steps involved in the thesis work

2.11 Closure

This chapter outlines the details of the experimental methods along with the sequence of experiments used in the thesis work. Initially it starts with the development of electroless coating, in general, considering the chemicals and basic set up of electroless bath. After that different evaluation techniques such as viz. roughness, hardness, friction, wear are discussed with detailing on the machines used for the analysis. Several coating characterization techniques such as morphological (involving SEM and AFM), compositional (EDX) and phase structural (XRD) studies are presented along with their equipment details. Finally, the steps involved in smooth conduction of the thesis work is discussed.

Chapter 3

High temperature tribology of Ni-P coating

3.1 Introduction

Electroless Ni-P, among the EN coatings takes the governing role in industry as well as research works due to their inherent characteristics. Application of coating in high temperature field reveals the softening of the material and deterioration in the wear resistant activity causing the shortening of life of the component. Despite a good number of studies on EN coatings particularly on the tribological properties of such coatings, it is seen that there are few studies which tried to discuss tribological characteristics in elevated temperature. In this chapter, a systematic study of the high temperature friction and wear performance of electroless Ni-P coatings is presented. Both as-deposited and heat-treated coatings are evaluated for their microstructural and tribological characteristics. The applied load and sliding velocity are varied in order to capture the exact trends of friction and wear under room and high temperature. Hardness tests are performed before and after tests in order to note the changes in the physical characteristics of the coating. Finally, microstructural tests are performed to know about the wear mechanism encountered by the coating in high temperature tests.

3.2 Experimental Investigations

3.2.1 Substrate preparation and Ni-P film deposition

Both the types of substrates (block and cylindrical) as discussed in section 2.2.1 are chosen for Ni-P deposition. The pre-processing steps and deposition procedure is also as per the discussion presented in the same section. Bath composition and operating conditions (refer Table 3.1) are decided after several trial experiments and following literature review keeping in mind the thickness and hardness of Ni-P coating. The pH of the electroless solution is measured using a pH-meter and maintained throughout the period of the coating. The coating is carried out for a total period of four hours so that a considerable coating thickness can be achieved which is necessary for carrying out the tribological tests. A double bath deposition each of two hours duration is employed for this purpose. Deposition time and bath volume is kept same for all specimens so that the coating thickness and bath loads remains approximately constant. After the deposition, the samples are taken out of the bath and washed in distilled water. As heat-treated samples are required for the tests, some coated specimens undergo heat-treatment in the box furnace at 400ºC for 1 hour and then cooled naturally. This particular temperature is selected as most researchers have acknowledged it as the best heat-treatment condition for EN coatings with respect to tribological behavior.

Table 3.1: Bath composition and operating conditions of hypophosphite-reduced Ni-P bath

Bath composition		**Working conditions**	
Nickel chloride and Nickel sulphate (1:1)	30 gl^{-1}	pH	4.5
Sodium hypophosphite	10 gl^{-1}	Time	4 h
Sodium succinate	12 gl^{-1}	Deposition temperature	80 ± 1°C
		Bath Vol.	200 ml

3.2.2 Characterization of Ni-P coating

All the micro structural analysis, roughness, microhardness and tribological tests for Ni-P coating are performed as per the detailed discussions presented in sections 2.4 to 2.9. As already discussed, tribological experiments are conducted in two phases. The values of tribo-testing parameters for the first phase is given in Table 3.2. Every single friction and wear test is repeated at least twice and the average of the two values reported.

Table 3.2: Experimental parameters along with their ranges for first phase

Normal load (N)	**Sliding speed (rpm)**	**Sliding velocity (m/s)**	**Test temperature (°C)**
10, 30, 50	30, 50, 70	0.094, 0.157,0.22	30, 500

In the second phase, suitable load and sliding velocity selected from first stage of study is subjected to high temperature tests by varying the temperature starting from room temperature to high temperature with other two interval as presented in Table 3.3. Experiments are carried out for all combinations of the values of test temperatures laid down in Table 3.3 to accurately estimate the high temperature profiling of Ni-P coatings and compare the same with ambient condition. Effect of various test temperatures on wear (in terms of mass loss/distance) and friction coefficient are evaluated under constant load and sliding velocity. The associated wear mechanism are also studied for room and high temperature tests for both as-deposited and heat-treated specimens through SEM and EDX. To highlight the effects of elevated temperature test as well as to maintain brevity, samples post test 500°C are further considered for AFM and elemental mapping study. In this way, the effect of test parameters as well as the test temperatures on the tribological characteristics of the deposits is ascertained in a organized manner.

Table 3.3: Tribological test parameters for second phase

Normal load (N)	Sliding speed (rpm)	Sliding velocity (m/s)	Test temperature (°C)
10	70	0.22	30, 100, 300, 500

3.3 Results and Discussions

3.3.1 Ni-P coating configuration

Ni-P coating is developed by using sodium hypophosphite as the reducing agent which provides a stable bath with moderate deposition rate. To achieve the required thickness for the thesis work, deposition is carried out for four hours with each of two hours duration. The deposition thickness versus time plot is presented in Figure 3.1 which indicates a higher slope for the first two hours and a diminishing trend for the next two hour. The average plating rate for Ni-P deposition is found to be 12-14 μm/h. To achieve higher thickness for tribological tests, as already discussed, double bath deposition technique is adapted.

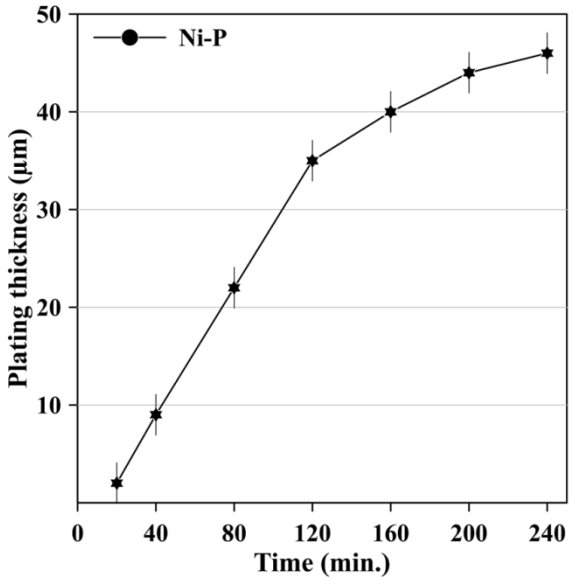

Figure 3.1 Deposition rate of Ni-P coating

Compositional analysis is performed on several points on the surface of as-plated and heat-treated Ni-P via EDX analysis as shown in Figure 3.2. This spectrum is used to identify the percentage by weight of the individual elements present in the coating. The weight percentage of P is 9-9.5% while the remaining is Ni. The weight percentage of phosphorus is quite high in the present coating and hence considered as high phosphorus coating. The coating is further investigated through SEM and XRD. With heat-treatment, structural changes may occur but no significant change is observed in phosphorus content apart from the observation of oxygen

around 2.5 %. The source of oxygen may be supported by the fact of entrapment of air in the furnace cavity during heat-treatment.

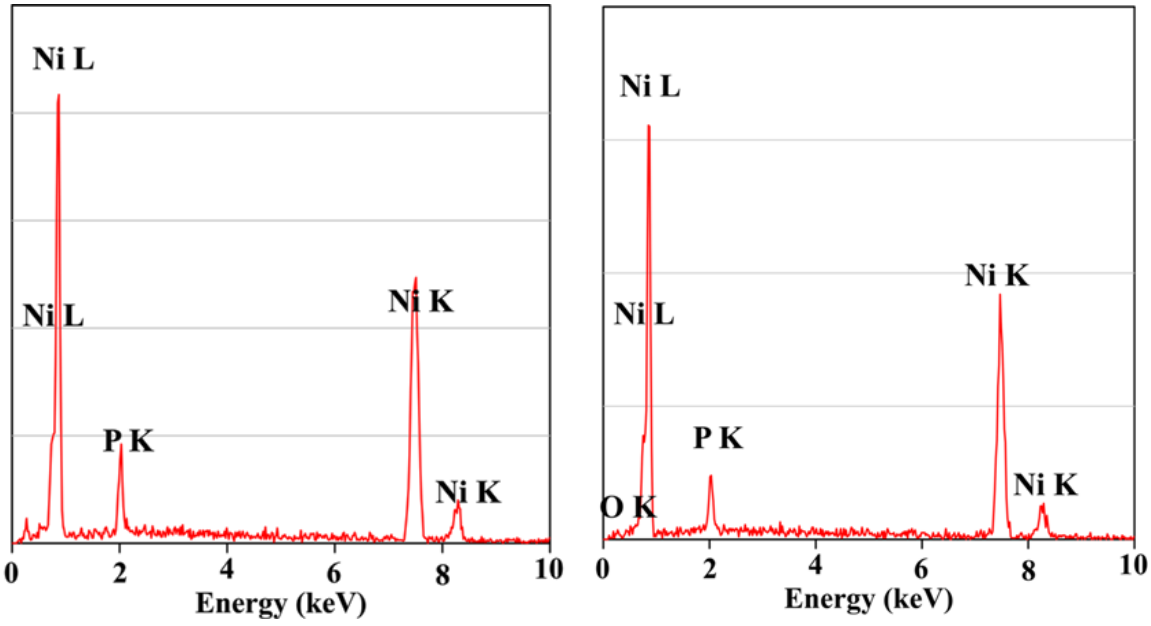

(a) (b)

Figure 3.2 EDX spectrum of (a) as-deposited and (b) heat-treated electroless Ni-P coating

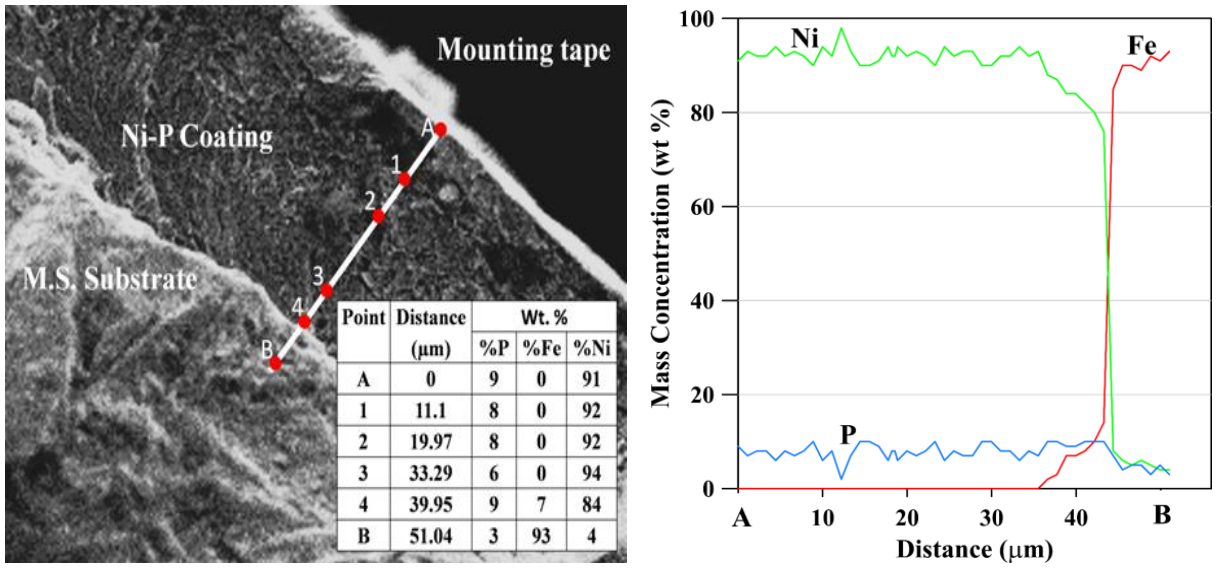

(a) (b)

Figure 3.3 (a) SEM image showing line EDX (quantitative analysis included in table) and (b) detailed composition profiles of elements presents measured along the thickness of the Ni-P

Apart from elemental analysis at points, EDX line scan is also performed on the cross cut section of the coating for better understanding of elemental distribution. The detail line scan is represented in Figure 3.3. The quantitative results indicating weight percentage of Ni, P and Fe is given in table inside Figure 3.3 (a). Composition profiles of Ni, P and Fe measured along the thickness of Ni-P (Figure 3.3 (b)) coatings are performed through line EDX for detailed understanding of the elemental variation across the cross section.

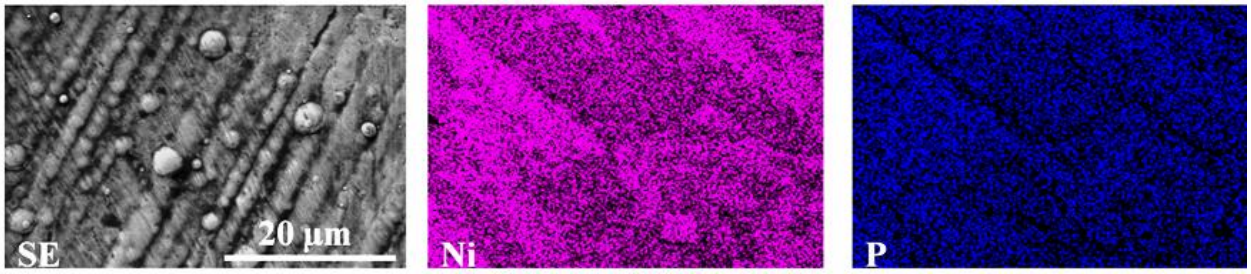

(a) (b) (c)

Figure 3.4 EDX mapping analysis on the surface of the as-deposited Ni-P coating indicating (a) SE image (b) Ni and (c) P

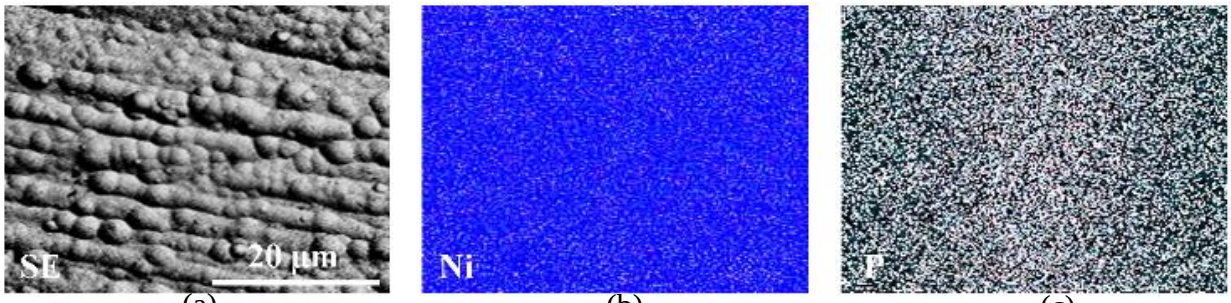

(a) (b) (c)

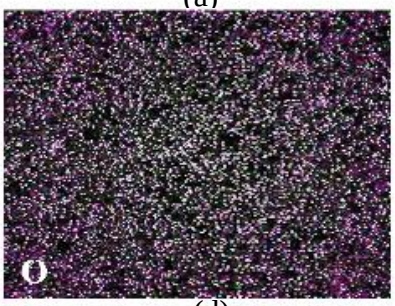

(d)

Figure 3.5 EDX mapping analysis on the surface of the heat-treated Ni-P coating indicating (a) SE image (b) Ni (c) P and (d) O

EDX mapping is used in random areas over the surface of the coating to find the distribution of the element as mentioned by point analysis earlier. EDX maps showing each element for as-deposited and heat-treated Ni-P coating is illustrated in Figure 3.4 and Figure 3.5 respectively. The secondary electron (SE) image of as-deposited and heat-treated coating layer

where scanning is done is shown in Figure 3.4a and 3.5a respectively. The EDX mapping proves that the nickel and phosphorus are uniformly and homogeneously distributed in the Ni-P matrix shown in Figure 3.4 and Figure 3.5 for as-deposited and heat-treated coatings respectively. Presence of oxygen is seen for heat-treated coatings as seen in Figure 3.5d. The mapping results are well in agreement to that of EDX spectrum with regards to presence of oxygen (Figure 3.5) for heat-treated sample. It may be because of oxide scale formation in muffle furnace in the presence of air.

3.3.2 Surface texture of coating

The surface morphology of as-deposited and heat-treated Ni-P coating is also captured through optical microscope, scanning electron microscope and atomic force microscope. Surface morphology of the coating is studied with various intensities and with the help of different types of microscopes in order to properly evaluate the surface features o that the same could be interlinked to its tribological behavior.

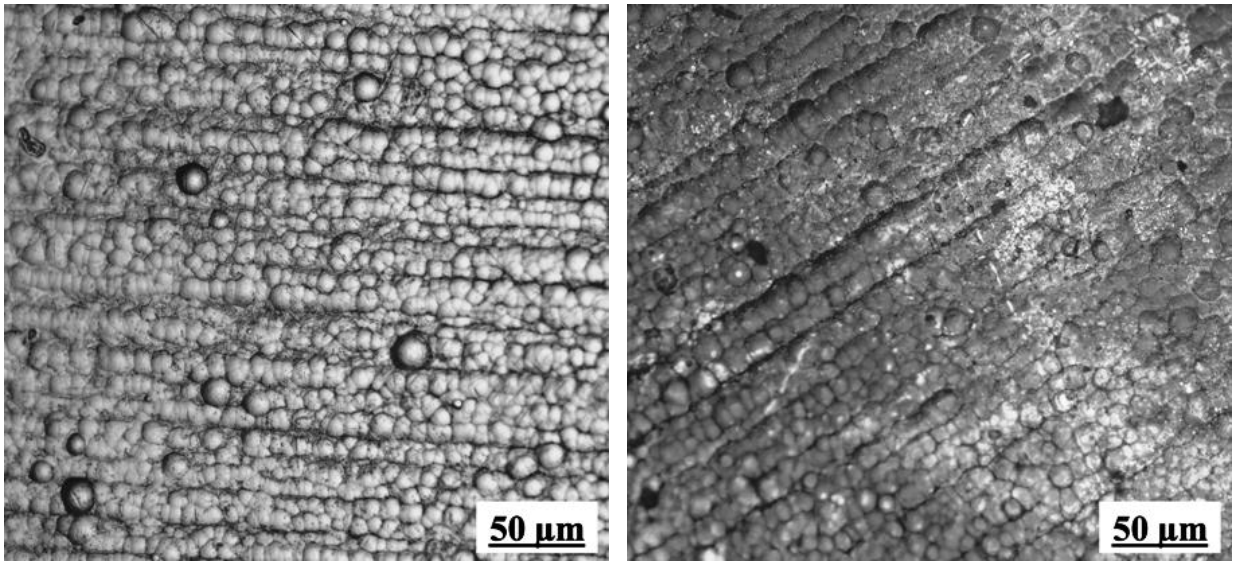

(a) (b)

Figure 3.6 Optical micrograph of (a) as-deposited and (b) heat-treated electroless Ni-P coating

Optical micrograph for both as-plated and heat-treated Ni-P coating shows a globular structure which is arranged in almost a series of rows indicating a columnar growth of the coating from the substrate surface as indicated by Figure 3.6. The same kind of results in higher resolution (SEM) is observed which is shown in Figure 3.7. The as-deposited coating as captured via both optical or scanning microscope, reveal the coating to be dense and without any surface defect. Whereas the same for heat-treated (at 400°C) condition consists of nodules, larger in size. This may be because of coating crystallization at the mentioned temperature which causes to raise the granule size. The average size of the globules in the as-deposited phase is found to be

around 10 μm (Figure 3.7a).With heat-treatment, the globules increased in size to a maximum of around 25 μm (Figure 3.7b) giving rise to a coarse grained structure. Few dark spots are visible on heat-treated coating surface as seen in Figure 3.7b, owning to the oxide scale development as confirmed through EDX (Figure 3.2b) and elemental mapping (Figure 3.5) results. As an indicative of substrate adhesion and coating thickness which lies in the range of 43-50 μm, cross cut geometry of Ni-P coating is depicted in Figure 3.8. For achieving the mentioned thickness, Ni-P is deposited for four hours with double bath deposition technique with a single interval.

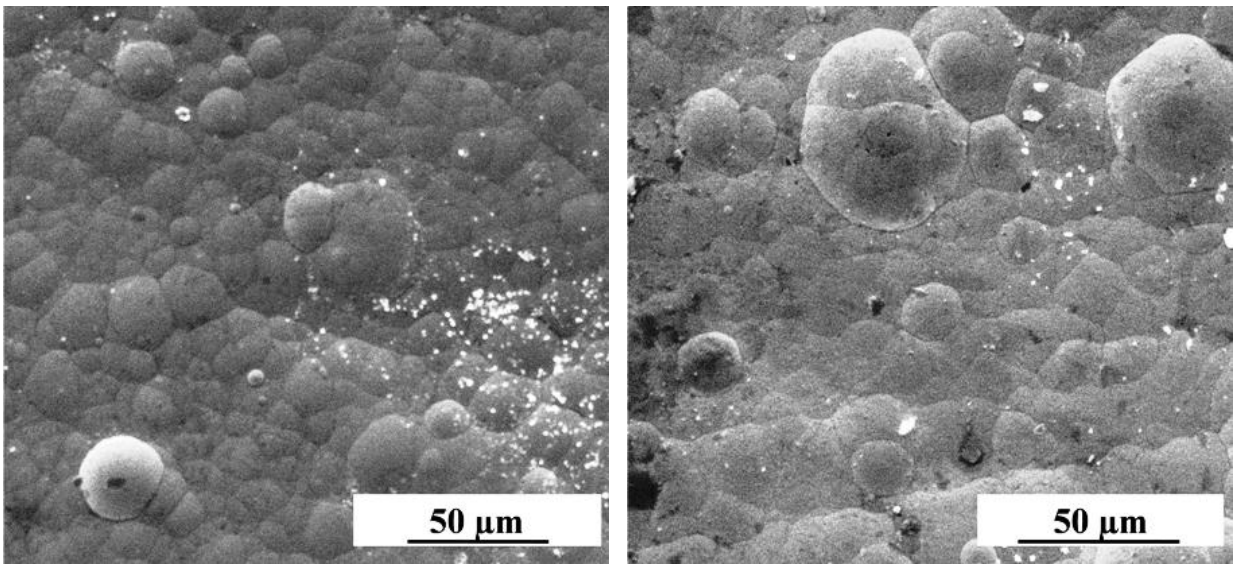

(a) (b)

Figure 3.7 SEM micrograph of (a) as-deposited and (b) heat-treated electroless Ni-P coating

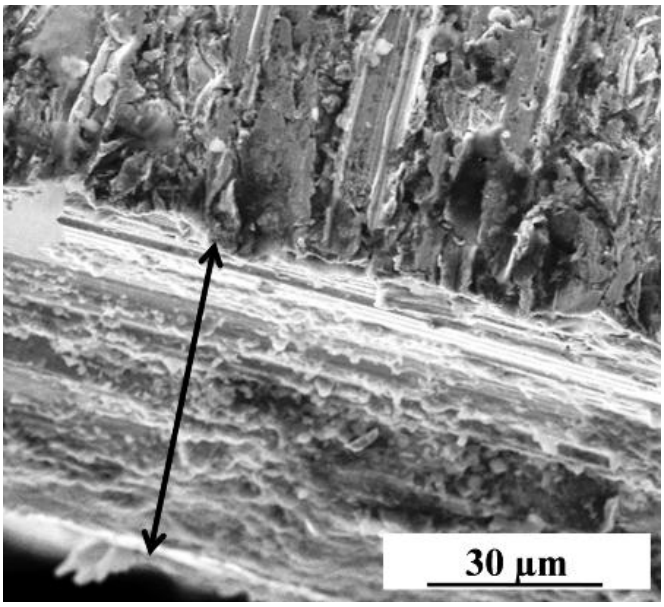

Figure 3.8 A cross-cut section of the Ni-P coating

Further atomic force microscopy (AFM) is employed to evaluate the surface of the coated specimens at nanometer level. The 2D and 3D illustration of Ni-P coatings in before and after heat-treatment conditions have been inspected with AFM in contact mode. A scan area of 10 μm ×10 μm is chosen for the purpose of surface analysis. Figure 3.9 and 3.10 show atomic force microscopic (AFM) images of as-deposited and heat-treated specimens Ni-P coatings, respectively, where topographical image (2D) is marked as (a) and three dimensional (3D) image marked as (b). In 2D figure, x axis and y axis both have a dimension of 10μm each whereas in 3D figure along with the existing two axis, the third z axis is introduced representing the heterogeneities present on the surface in nanometer level. Surface texture of as-deposited coatings shows regular nodular morphology composed of finer grains highly dense and compact. This observations are used to reiterate the SEM results as presented in Figure 3.7. Nodular feature is very common in electroless deposition which arise due to fast nuclei creation and its successive growth. Apart from that, bath constituents, coating environment and substrate surface mainly surface irregularities play a deciding role in formation of nodule. The arrangement of nodules in almost a series of rows indicate towards the columnar growth of the coating from the substrate surface as clearly indicated in Figure 3.9. Deposition of coating per unit time is directly involved in deciding the nodular structure by controlling the supply of atoms. Nodule growth (mainly in z direction i.e. normal to the substrate) directly depends on available number of atoms which is again proportional to the rate of deposition. The series of rows are little bit deflected with few humps for heat-treated Ni-P coatings as indicated by Figure 3.10. It may be because of the increment in grain size due to heat-treatment as indicated earlier in SEM analysis. The proper justification about phase transformation, can be given after observing the XRD results. The grain coarsening because of heat-treatment causes to increase the surface irregularities which indicates a higher roughness of heat-treated specimen in compare to as-deposited samples. From the AFM observation (Figure 3.10), each grain of heat-treated samples consists of higher number of smaller grains analogous to diffused-like morphology.

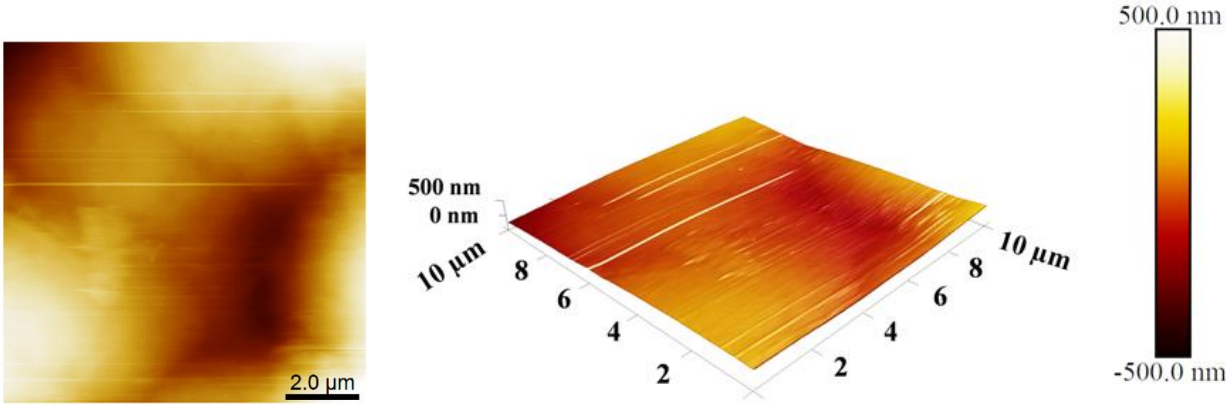

(a) (b)

Figure 3.9 Typical AFM morphologies of as-deposited Ni-P surfaces in (a) 2D and (b) 3D

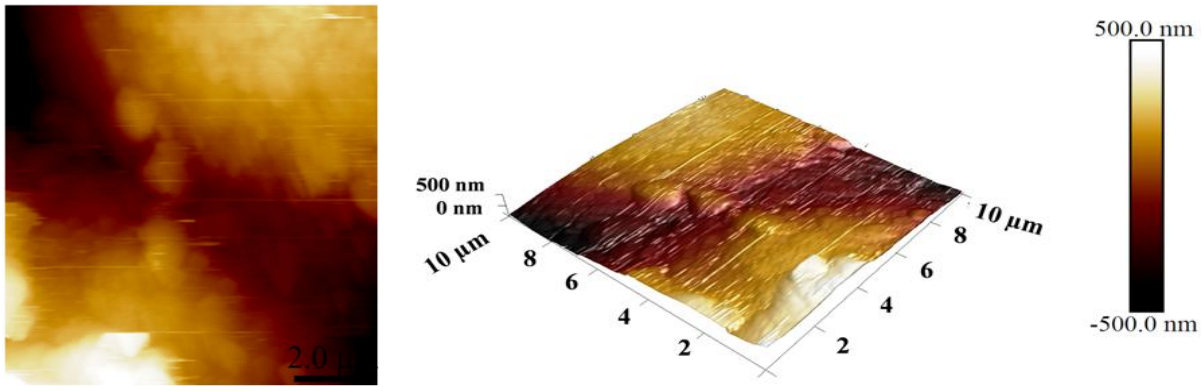

(a) (b)

Figure 3.10 Typical AFM morphologies of heat-treated Ni-P surfaces in (a) 2D and (b) 3D

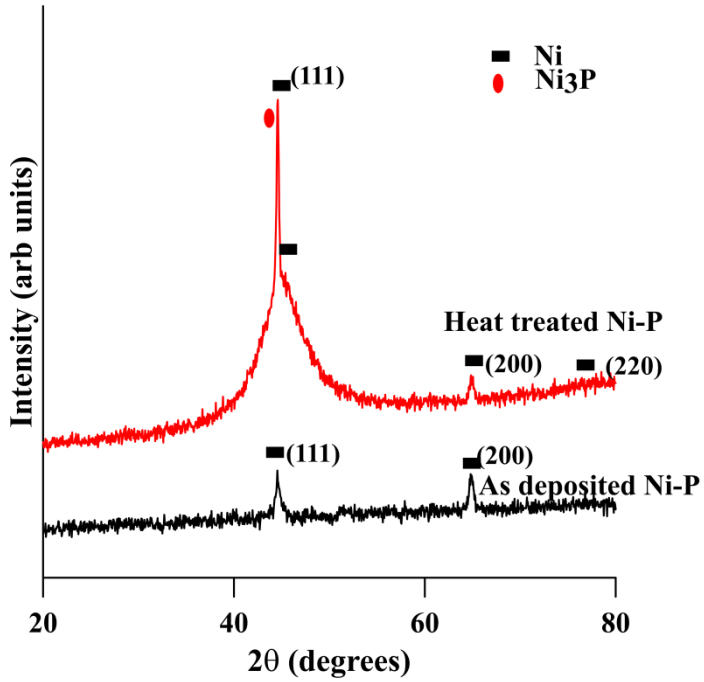

Figure 3.11 XRD spectra obtained for as-deposited and heat-treated electroless Ni-P coating

3.3.3 Structural aspects of Ni-P coating

From XRD analysis (Figure 3.11), it is found that the coating is largely amorphous in the as-deposited phase which is represented by a series of small peaks very close to each other. After heat-treatment (400°C, 1hr) the coating turns crystalline with the formation of nickel phosphide phases, the major phase being Ni_3P. Thus heat-treatment brings structural changes of the Ni-P matrix from an amorphous to crystalline phase. Heat-treatment actually causes to decrease FWHM resulting in increased grain size. Formation of phosphide phases as well as increase in grain size as a outcome of heat-treatment is already established by other researchers (Masoumi et

al., 2012; Duari et al., 2016; 2017). For Ni-P, heat-treatment provides crystalline Ni (111) at ~44.6° (2θ) and nickel phosphides (shown in Figure 3.11) that results in increase of hardness for heat-treated samples than as-deposited ones.

3.3.4 Roughness and microhardness evaluation

Roughness of Ni-P samples are tested via Talysurf profilometer as well as AFM and expressed in terms of centre line average value (Ra). The outcomes of each of the characterisation studies for determination of roughness are very close to each other. The maximum Ra value observed for as-deposited coating is close to 0.46 µm which is very close to that of substrate. Heat-treatment causes to increase the value slightly but it never exceeds 0.52 µm, because of the inflation of granules size due to heating at the particular temperature. The observed roughness value of coated samples are close to the substrate roughness, which is good enough for the majority of applications.

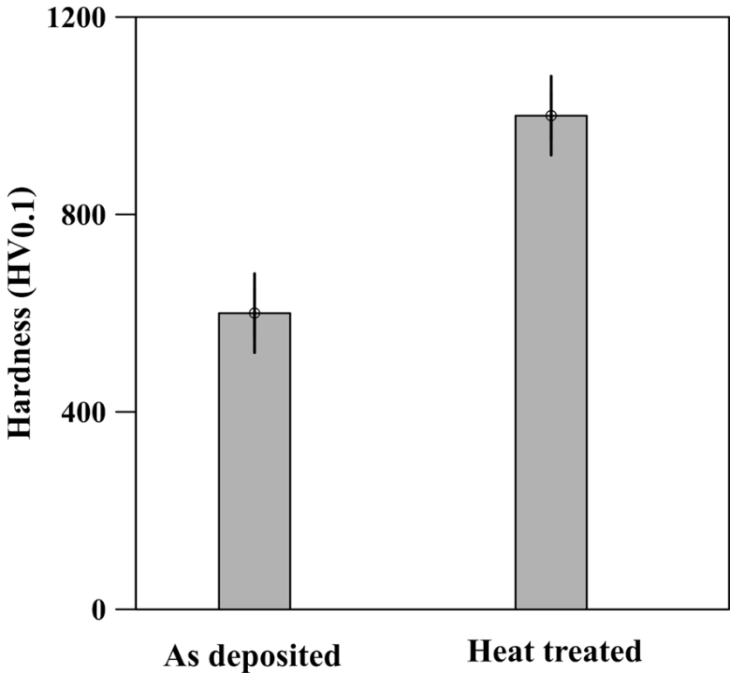

Figure 3.12 Microhardness obtained for as-deposited and heat-treated electroless Ni-P coating

As tribological characteristics are largely dependent on the hardness, the microhardness of binary Ni-P coatings before and after the heat-treatment are evaluated as presented in Figure 3.12. Electroless deposition Ni-P provides average microhardness to be around 600 $HV_{0.1}$ working with a substrate having hardness of 140 $HV_{0.1}$. Substrate hardness is increased nearly by 4 times by using a layer of Ni-P coatings and makes it suitable for further tribological interactions. Further, the effect of heat-treatment at 400°C on the coating is included in the same figure. Heat-treatment causes to increase the hardness of Ni-P to 1000 $HV_{0.1}$. The effect of heat-treatment is prominent in Ni-P as it causes to increase hardness by 67%, compared to as-

deposited Ni-P coating hardness. The effect is solely because of phase transformation and the formation of hard phosphide phases during the heat-treatment in muffle furnace, as is also shown in XRD study. The results of hardness obtained for Ni-P coatings are well in agreement with that of existing literature (Balaraju & Rajam, 2005).

3.3.5 Tribological characterization based on test parameters

3.3.5.1 Friction under different load and sliding velocity

The effect of load and sliding velocity under ambient and high temperature on the friction performance of as-deposited and heat-treated Ni-P coatings are studied. The experiments are arranged in an incremental manner by varying one factor at a time. The COF of as-deposited as well as heat-treated coatings as a function of load and sliding velocity separately under two different working temperature are shown in Figure 3.13a and 3.13b respectively. The samples are slide in different load by choosing a uniform sliding velocity of 0.22 m/s. In general, COF increases with increase in applied load which is attributed to the increase in contact area and subsequent higher force required to break them. Similar observations have already been made by other researchers (Chowdhury et al., 2011). However, apart from the RT test, the increase of COF is more for the increase of load from 10-30N but there is a decrease observed for load varied from 30–50 N. For a particular load however, COF decreases with increase in the operating temperature for as-deposited samples. The low friction may be due to the in situ oxide formation on sliding surfaces at high temperature. The oxide layer is soft and presents low shear properties resulting is lesser friction. Tests at RT for as-deposited coating show a monotonically increasing trend for COF with the applied load but for heat-treated coating it shows similar trend to that of test conducted at high temperature. For heat-treated coatings, COF increases with increase in load, but decreases beyond 30 N. Further, the test at RT for heat-treated coatings also reveals a similar trend as the high temperature tests which is quite different compared to the as-deposited coatings tested at RT.

The sliding tests are conducted at a uniform load of 10 N. Except at RT, increase in sliding velocity results in lowering of COF. However, apart from the highest level of sliding velocity (0.22 m/s), the COF displayed by the coating at RT is lower compared to that displayed at higher temperature. Hence, it can be seen that both sliding velocity as well as operating temperature have a significant effect over the COF of EN coatings. Now, during sliding, the contact points change rapidly depending on the sliding velocity as new points come in contact and existing contacts break. The more the area of contact, the higher is the friction at the interface. At higher operating temperature, the coating gets a real time heat-treatment and hence becomes hard. Due to increase in hardness, the real area of contact formed is less which shows up in the form of a decrement of friction.

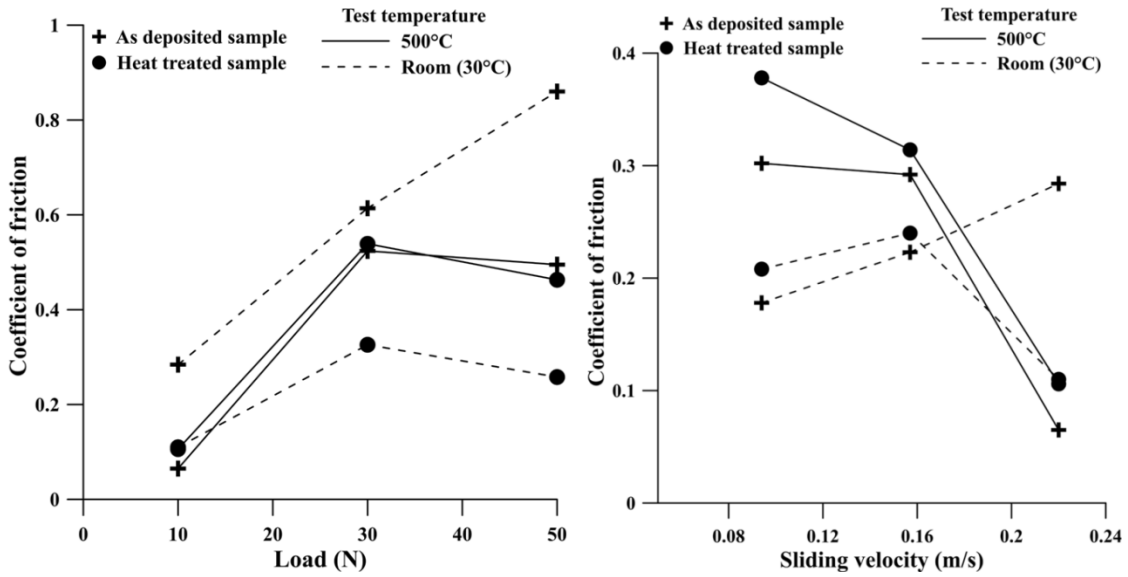

Figure 3.13 Friction performance of Ni-P coating for room and high temperature under different (a) load and (b) sliding velocity

The decreasing trend of COF with sliding velocity may be due to the change of shear rate which can in turn affect the mechanical properties of the mating materials (Bhushan & Jahsman, 1978). Moreover, higher sliding velocity will contribute to a larger normal momentum transfer in the upward direction. This results in an increased separation between the coating and the counterface which further results in decreased real area of contact. This may also serve as an explanation for the lower friction coefficient at higher sliding velocity in the high temperature situation. Again, higher P coatings display increased passivity. The passive films formed in Ni-P coatings are phosphorus enriched layers which obviously have a tendency to increase with higher phosphorous content in the coating. The present coatings being of high P grade, operating under high temperature, cause the passive films to adhere effectively improving the lubrication action of the coating thus exhibiting a reduced friction coefficient (Lee, 2009). The friction behavior of heat-treated coatings under room and high temperature for different sliding velocities are also included in Figure 3.13b. The effects of sliding velocity and high temperature on COF are analogous to the results of as-deposited coatings.

3.3.5.2 Wear under different load and sliding velocity

Wear behavior of EN coatings is investigated under ambient and high temperature by varying the testing parameters viz. normal load and sliding velocity. The effects of each parameter on the wear of the coating are investigated in detail here. Wear is represented by the ratio of weight loss to the distance traversed so that the effect of sliding speed on wear can be truly realized. The effect of load and sliding velocity on wear under two working temperatures for as-deposited along with heat-treated EN coatings is shown in Figure 3.14a and 3.14b

respectively. For Figure 3.14a, sliding velocity is fixed as 0.220 m/s whereas for Figure 3.14b, load is fixed as 10N. From Figure 3.14a, it is found that wear rate increases with increase in applied load. Several researchers (Panja et al., 2016) have made similar observations for coatings tested at RT. For the current study, under RT for both as-deposited and heat-treated coatings, wear is found to increase by almost six times within the load range 10–50N. Whereas under elevated temperature conditions, within the same load range, the increase of wear is about ten times (500°C plot) for as-deposited coatings though for heat-treated coatings, the effect is less. Lesser wear rate also occurs for 500°C conditions for the two test temperatures. It is already known that the phase transformation temperature of EN coatings lies around 335°C (Das et al., 2007). Hence, the higher wear resistance found at 500°C can be attributed to the increase in hardness of the coating due to heat-treatment at the test temperature. This result can be further supported by post wear phase transformation and hardness study to understand and correlate the reason behind the better wear resistance of Ni-P as-deposited coatings at high temperature (500°C) test.

The relation between wear rate and sliding velocity for varying test temperatures for a particular load (10N) is shown in Figure 3.14b. It is found that under elevated temperature conditions wear reduces with increase in sliding speed. For variation of speed from 30-70 rpm, wear is found to decrease by about eight times in both room temperature as well as tests conducted at 500°C. The behavior of both as-deposited and heat-treated coatings are very similar to each other.

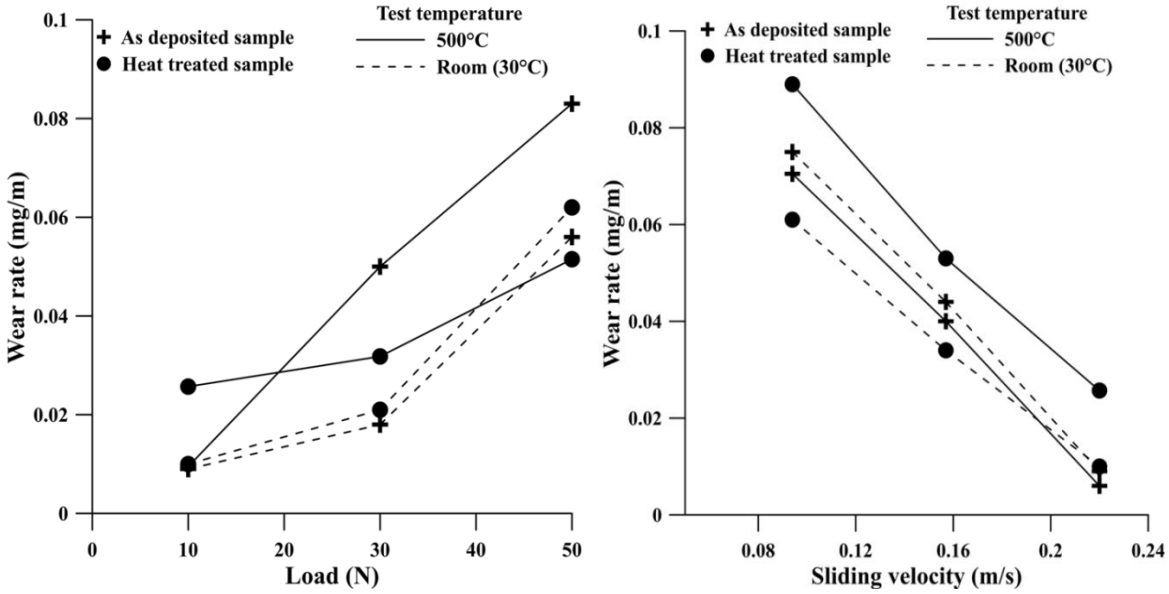

(a) (b)

Figure 3.14 Wear performance of Ni-P coating for room and high temperature under different (a) load and (b) sliding velocity

It is observed that the increase in load results in higher wear for any working temperature as in the case of as-deposited samples. High temperature test at 500°C yields lesser wear, though that at RT is even lower. Also similar to the as-deposited sample, increase in sliding velocity results in decrease in the wear rate of the heat-treated coating. However, when compared to that of the RT test, wear rate is observed to be higher in high temperature conditions. From Figure 3.13 and Figure 3.14, it can be seen that 10N and 0.22 m/s is the best combination of load and sliding velocity respectively which yield low COF and wear from the coating. So, the further temperature profiling and detail discussion on as-deposited and heat-treated Ni-P coating is presented in the next section based on these load and velocity combination.

3.3.6 Study of tribological behavior of Ni-P coating at various test temperatures

3.3.6.1 Friction performance of as-deposited and heat-treated Ni-P coating at different test temperatures

Friction and wear performance of electroless Ni-P coating is evaluated at various temperatures (R.T.-500°C). Now, heat-treated coatings are harder than as-deposited coatings and are anticipated to exhibit better wear resistance compared to the latter. Again, at elevated temperature testing, the samples are expected to undergo a simultaneous heat-treatment cycle (short duration) and as a result get somewhat harder. Hence, tests are conducted both on as-deposited samples as well as heat-treated (400°C, 1 hr) samples at various test temperatures.

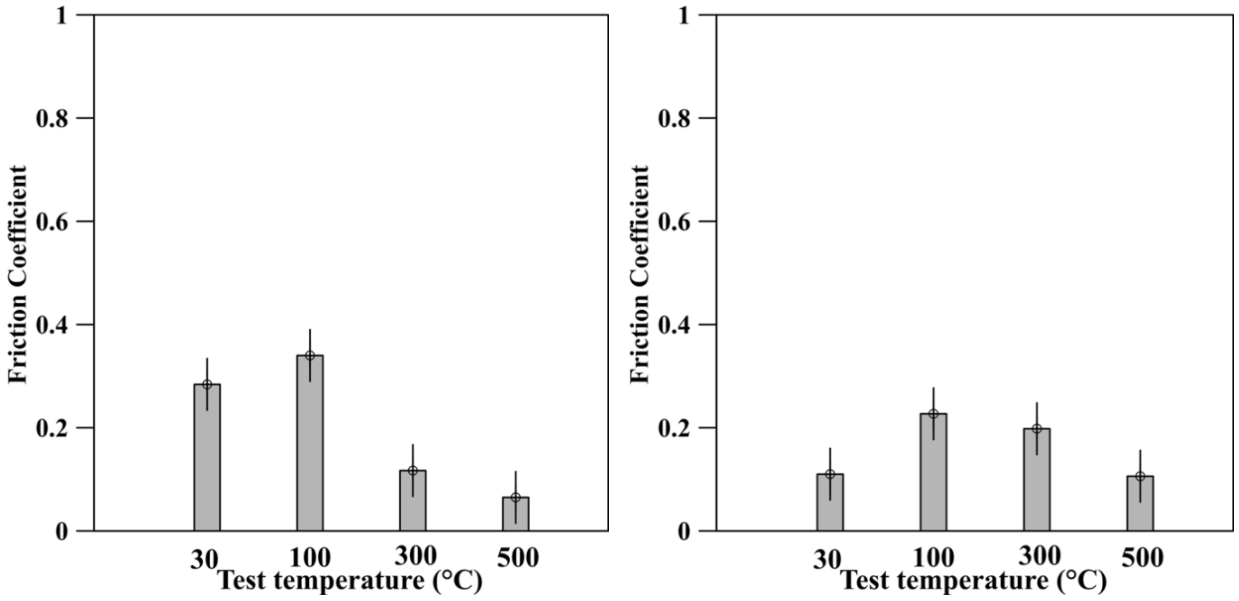

(a) (b)

Figure 3.15 Friction as a function of test temperature for (a) as-deposited and (b) heat-treated Ni-P coating

It is interesting to note that unlike as-deposited sample, for heat-treated samples, even the tests carried out at R.T. exhibit low value of friction (around 0.1- 0.2). This may partly be attributed to the fact that as-deposited coatings are ductile and hence allow the formation of debris. Besides, it is a known fact that as-deposited Ni-P coatings exhibit lower hardness compared to heat-treated samples (Sahoo & Das, 2011) and hence contribute to an increase in the area of contact between the tribological pair. As a result, more friction force is required for shearing of the contact points formed (Masoumi et al., 2012). The formation of surface oxides at test temperature around 500°C may be providing a lubricating effect lowering the COF at the same test temperature. The mean friction values at different test temperatures, both for as-deposited and heat-treated samples are shown in Figure 3.15. For as-deposited samples, as discussed previously, friction shows a decreasing trend with the increase of the test temperature. Higher friction is encountered in tests conducted at R.T. and 100°C with COF value around 0.3 while lowest COF is encountered at 500°C with a COF of value below 0.1. For heat-treated samples, the highest COF (around 0.25) is found at test temperature of 100°C and the lowest friction (around 0.1) is observed at R.T. and temperatures of 500°C.

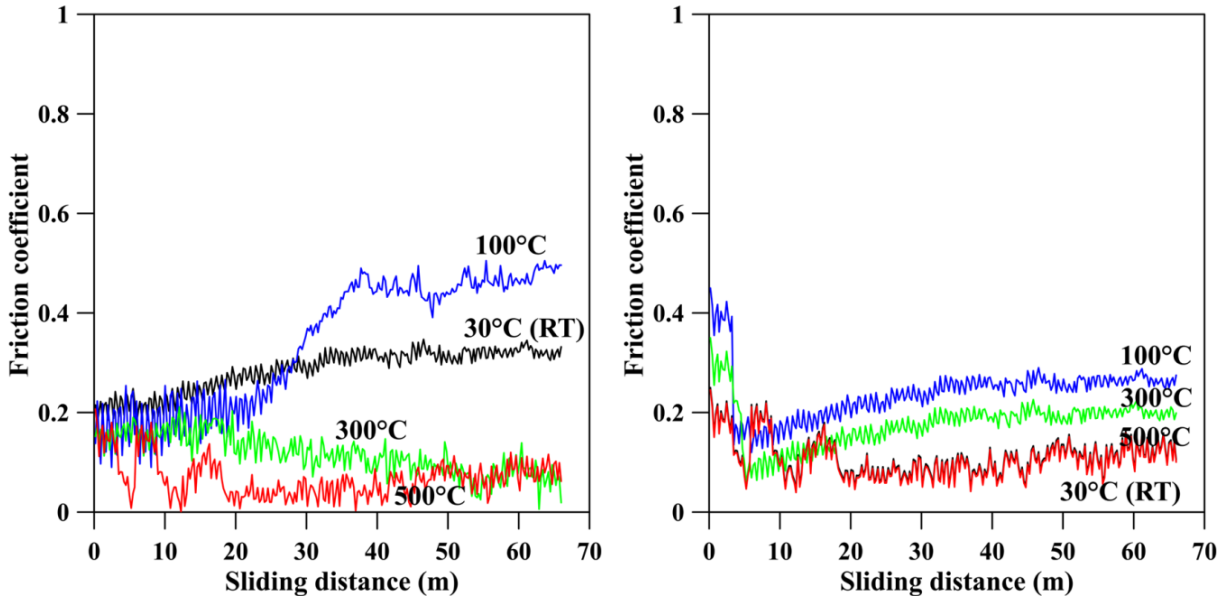

Figure 3.16 Evolution of COF of at room and elevated temperatures for (a) as-deposited and (b) heat-treated Ni-P coating

The variation of coefficient of friction (COF) with distance traversed for tests conducted at different temperatures is illustrated in Figure 3.16. It is observed that for as-deposited sample (Figure 3.16a), COF in general doesn't suffer huge variation with distances at all temperatures except at R.T and at 100°C. At. 100°C, COF increases by about 3 times from the start of the test to end. Friction is also found to be lower for tests conducted at higher temperatures. For heat-

treated case, the variation in friction is much less and the minimum value of friction belongs to tests conducted at R.T and 500°C.

3.3.6.2 Wear performance of as-deposited and heat-treated Ni-P coating at different test temperatures

Wear performance of Ni-P coating both in as-deposited as well as heat-treated state at various testing temperature is studied. Here, wear is represented by the ratio of weight loss to the distance traversed. Figure 3.17 shows the wear rates at different test temperatures, both for as-deposited and heat-treated samples. Contrary to the common belief, it is observed that wear rate doesn't show a continuously increasing trend with the increase in test temperature. In case of as-deposited samples, wear rate increases with increase in test temperature and then suddenly drops at 500°C. For heat-treated samples, R.T. exhibits the lowest wear rate with a sudden jump in the wear rate at test temperature of 100°C which is similar at 300°C, but again wear rate slightly increases at test at 500°C.

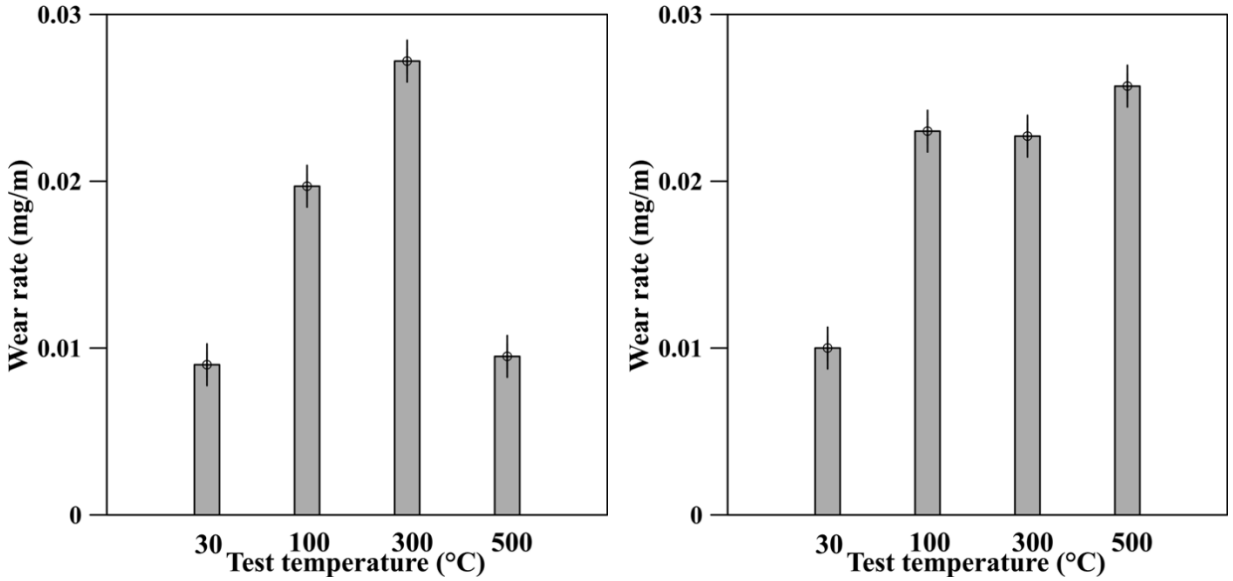

(a) (b)

Figure 3.17 Wear as a function of test temperature for (a) as-deposited and (b) heat-treated Ni-P coating

SEM image indicating the wear along with the direction for Ni-P as-deposited coatings tested at 500°C is represented in Figure 3.18. The coating clearly exhibits linear wear tracks as soft coating is subjected to abrasion by harder counter face. Along with that, few removal of material in the form of pits and prows is also detected which arise due to breakage of bonding between coating and counter face asperities. Linear tracks are prominent which is an indication of abrasive wear pattern. Pits and prows which are symbolic for adhesive wear mechanism are also observed. So, the wear mechanism at 500°C for the coating is mostly governed by abrasive

and partly by adhesive wear mechanism. The linear tracks and removal of coating is clearly visible from Figure 3.18a. The dark spots indicates the formation of oxide layer during the test conducted at high temperature. Further to prove the fact as well as to indicate the other elemental distribution line EDX (as shown by line AB in Figure 3.18a) is carried out. The results indicating the detail variation of each element across the chosen line (AB of approx 200 µm) is provided in Figure 3.18b for Ni-P coating. Presence of oxygen implies high temperature oxide formation as claimed by other researchers (Masoumi et al., 2012; Mukhopadhyay et al., 2018a; 2018b; 2018c). Existence of nickel and the other primary coating elements after test proves the survival of those coatings at elevated temperature. Amount of Fe comes as a result of interaction with counterface material which may provide a mixed mechanical layer. It may also be the reason behind the lower wear rate at elevated temperature.

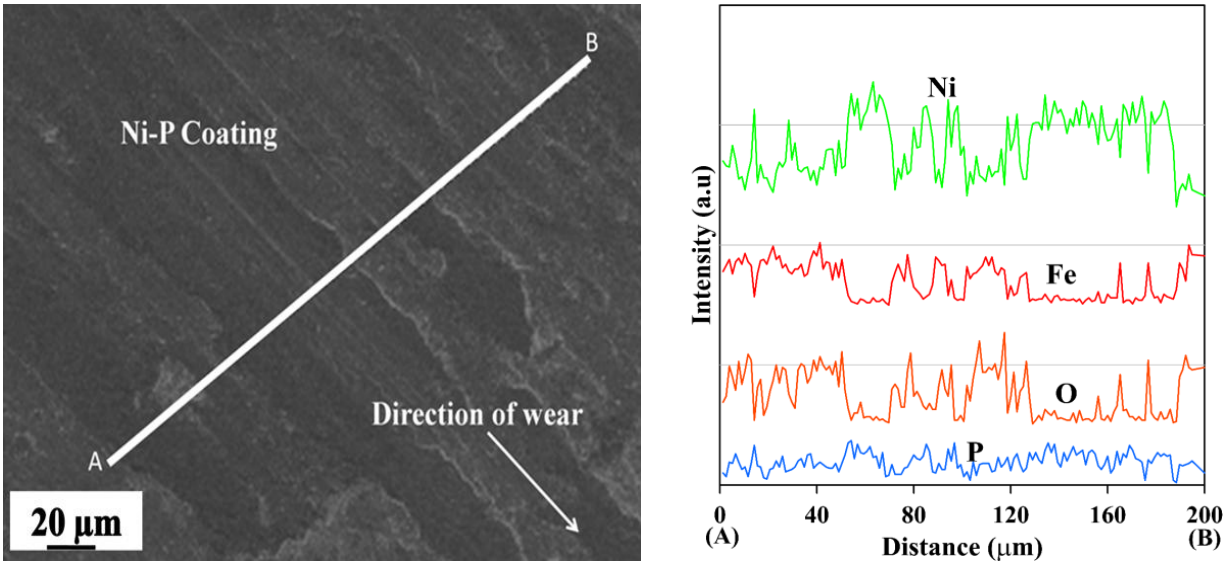

(a) (b)

Figure 3.18 SEM image indicating (a) the line for EDX study and direction of wear and (b) corresponding EDX line analysis for Ni-P coating

3.3.6.3 Wear mechanism study

The wear mechanism of EN coatings depends to a large extent on the attractive force that operates between the atoms of nickel from the coating and iron from the counter face surface (hardened steel). To further understand the role of elevated temperature on the wear mechanism, the worn out surface of the as-deposited samples are observed by SEM (Figure 3.19). The as-deposited coating tested at room temperature shows a flattened nodular structure (Figure 3.19a). Most of the asperities are compressed under the application of load and few fragmented nodules are spread over the whole surface area of contact. This wear particles playing the role of solid lubricants causes to provide low wear as indicated by Figure 3.17a. The coating is mostly intact

after the room temperature test as clearly visible in Figure 3.19a with a small number of patches. Removal of coating in the form of patches is a significant characteristics of adhesive wear.

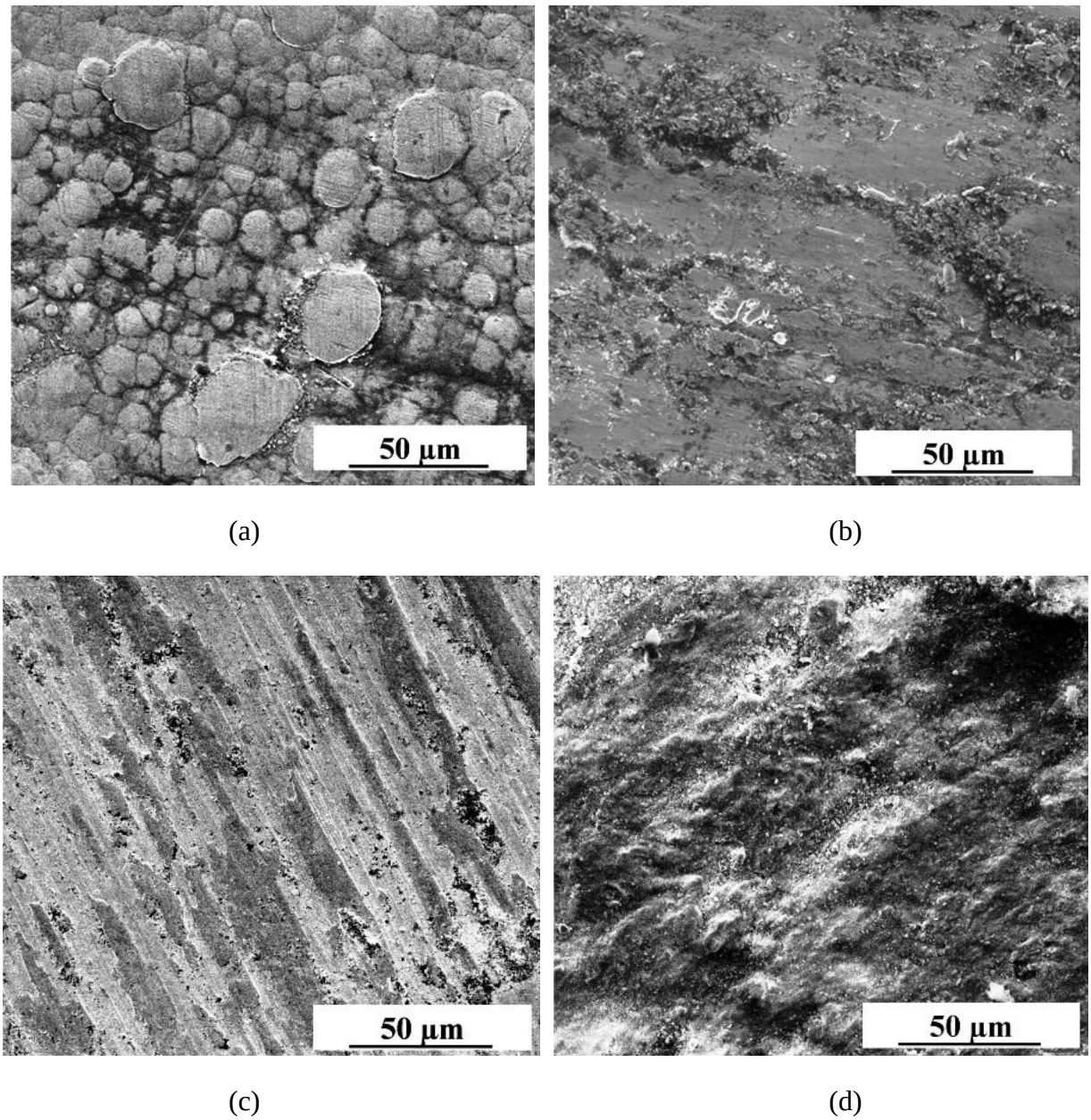

Figure 3.19 SEM (secondary electron) micrograph of worn specimen of as-deposited electroless Ni-P coating tested at (a) 30°C (b) 100°C (c) 300°C and (d) 500°C

The intactness of the post test coatings are verified through EDX study (Figure 3.20a) which clearly indicates the existence of two major constituents Ni and P. The nodular morphology seems to disappear and rough surface with several pits and prows are observed for coating tested at 100°C (Figure 3.19b). This is a predominant feature of adhesive wear which causes to increase the COF and wear of as-deposited samples and also justifies the results

obtained in Figure 3.15a and 3.17a respectively. Mutual force of attraction between nickel and counter face material plays the lead role in material removal process.

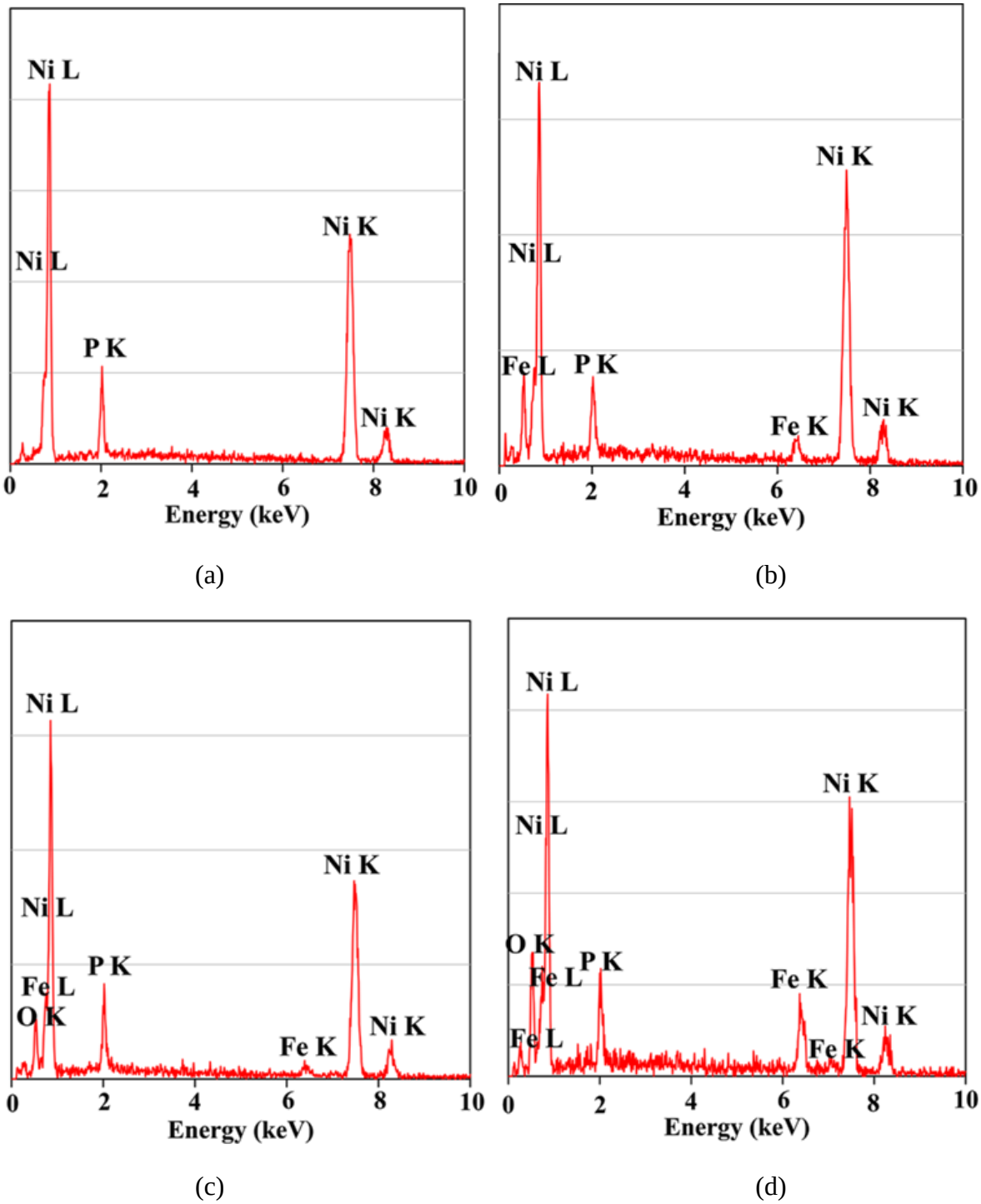

Figure 3.20 EDX spectrum of worn specimen of as-deposited electroless Ni-P coating tested at (a) 30°C (b) 100°C (c) 300°C and (d) 500°C

The presence of Fe along with the chief constituents in EDX study (Figure 3.20b) backs the claim of interaction of iron particles during 100°C test temperature. Plastic deformation is observed in almost all the samples with appearance of blackish spots especially in samples tested at 300°C and beyond. These black areas may be due to the formation of oxides at high temperature as the test enclosure contains air.

The EDX analysis (Figure 3.20) of the tested samples at 300°C and 500°C also detects elemental oxygen which is again an indication of the formation of oxides. EN coatings exhibit clear wear tracks especially at lower testing temperatures which are indicative of the ploughing effect by the counterface as well as by the wear debris formed which are strain hardened. The ploughing effect is representative of the abrasive wear phenomenon. However, it is not the sole phenomenon governing the wear mechanism of the coatings.

The SEM images of the as-deposited coatings tested at 300°C (Figure 3.19c) clearly show the presence of torn patches and in some places even detachment of the coating. Along with that few torn patches leads to adhesion , black spot indicating heavy oxidation are clearly visible in Figure 3.19(d). Formation of tribo oxidative layer during the 500°C test causes to decrease in COF as presented in Figure 3.15a results in COF with lesser fluctuation (Figure 3.16a). Presence of Oxygen (Figure 3.20d) confirms the tribo oxidative layer as well as oxidation of the coating during the elevated test. Presence of Fe in the post test samples may be because of two reasons, either it is because of adhesion (high mutual solubility of iron and nickel atoms) or diffusion of iron from the steel substrate during test. The chances of diffusion is very less as the test is subjected to high temperature for a very short time. Therefore, adhesive wear in conjunction with abrasive wear governs the wear mechanism of as-deposited Ni-P coating tested at 500°C.

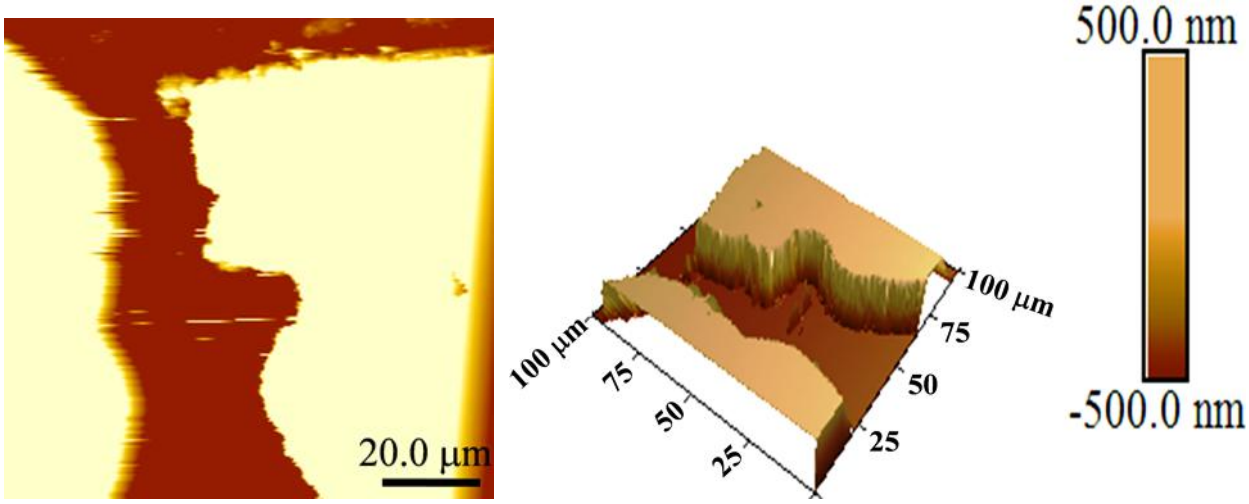

(a) (b)

Figure 3.21 AFM morphology (a) 2D and (b) 3D of as-deposited Ni-P coating tested at 500°C

To highlight the effects of elevated temperature test as well as to maintain brevity, samples post test at 500°C are further considered for AFM and elemental mapping study and the corresponding results are indicated by Figure 3.21 and 3.22 respectively. The 2D and 3D surface morphology of post test samples is represented by Figure 3.21a and b respectively. It clearly indicates a deep groove along with micro-ploughing. Wear tracks in the direction of sliding along with material removal is also noticeable. The elemental maps along with secondary electron (SE) image of worn as-deposited Ni-P coating tested at 500°C is shown in Figure 3.22. SE image of worn out specimens also indicates the linear wear tracks, indicating abrasive wear trend, in the direction of sliding and its very close to that of Figure 3.18a. Uniform allocation of nickel and phosphorous can be seen from the images (Figure 3.22) which mean the survival of coating even after the wear test. The existence of oxygen proves the development of tribo-oxide film as discussed earlier. The oxide layer surrounds over the whole surface of the coating as evident from the mapped image (Figure 3.22) which is the main reason for lesser fluctuation and a reduced amount of COF. For the 500°C, iron shows very strong signal (Figure 3.22) in the image which implies occurrence of adhesive wear whose remnants can be observed from torn patches on the coating post test.

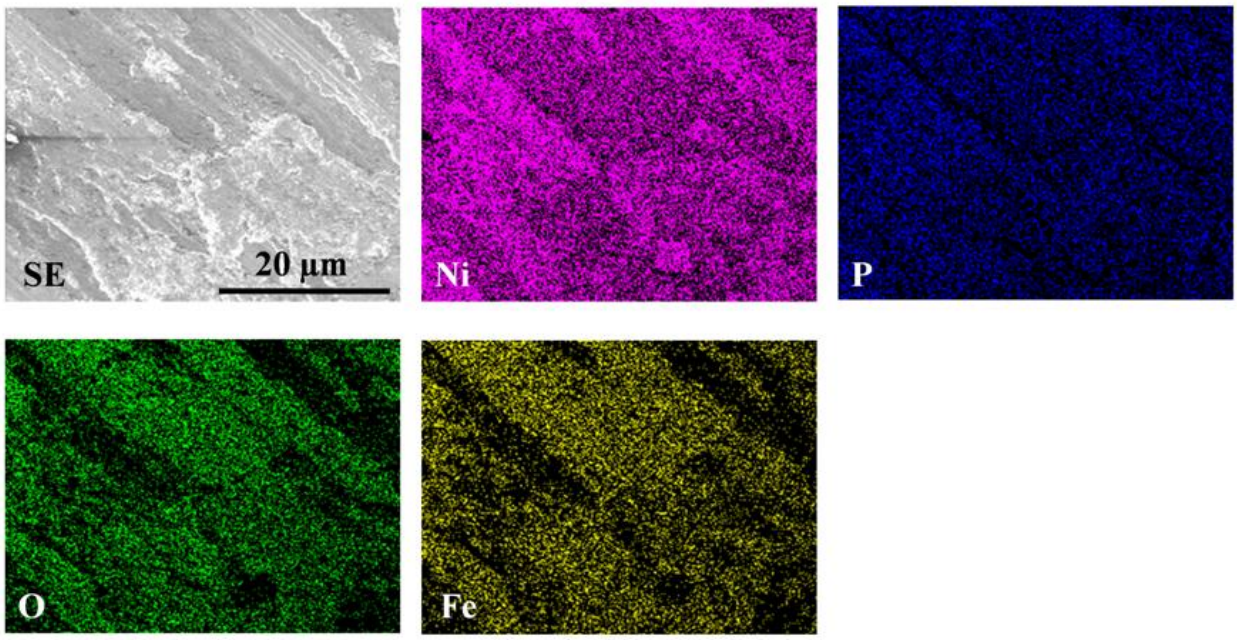

Figure 3.22 EDX maps of worn specimen of as-deposited Ni-P coating tested at 500°C

Post wear test, heat-treated Ni-P samples are evaluated through SEM and EDX investigations to understand the mechanism and effects of wear on coating. Further, a detailed study is consolidated by AFM and elemental mapping analysis for as-deposited and heat-treated coating tested at 500°C. SEM micrographs (Figure 3.23) and EDX findings (Figure 3.24) of worn out heat-treated Ni-P samples tested at various temperatures (30°C, 100°C, 300°C and 500°C) are presented in this section. The heat-treated coating tested at room temperature shows a

flattened nodular structure (Figure 3.23a). Most of the asperities are compressed under the application of load and few fragmented nodules are spread over the whole surface area of contact.

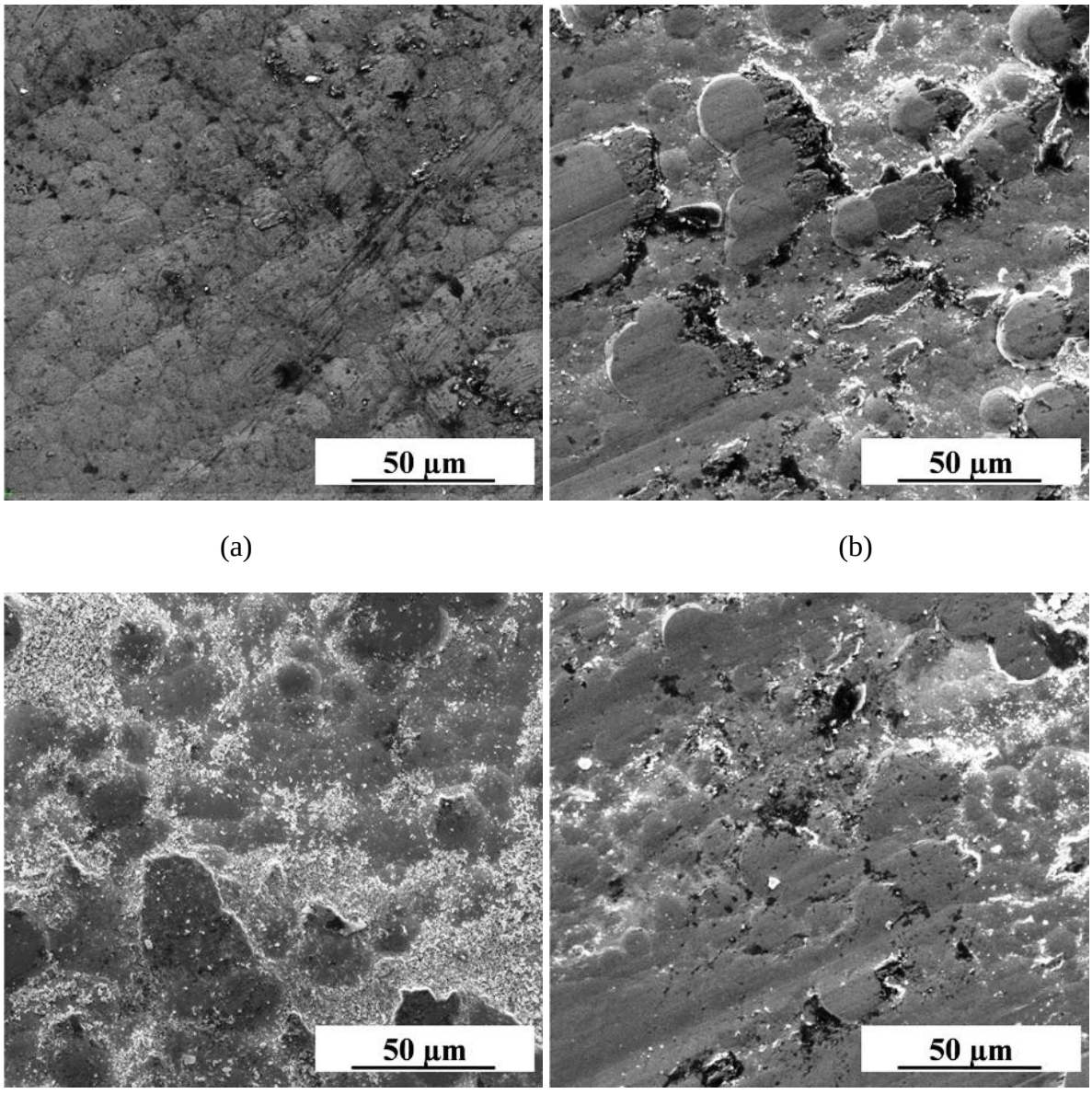

Figure 3.23 SEM (secondary electron) micrograph of worn specimen of heat-treated electroless Ni-P coating tested at (a) 30°C (b) 100°C (c) 300°C and (d) 500°C

As discussed before this split particles play the role of solid lubricants and causes to provide low COF and wear as indicated by Figure 3.15b and 3.17b respectively. The coating is mostly intact after the room temperature test as clearly visible in Figure 3.23a with a small number of patches. Removal of coating in the form of patches is a significant characteristics of

adhesive wear. The intactness of the post test coatings are verified through EDX study (Figure 3.24a) which clearly indicates the existence of two major constituents Ni and P. The oxidation of wear zone may be represented by the EDX outcomes through the presence of oxygen.

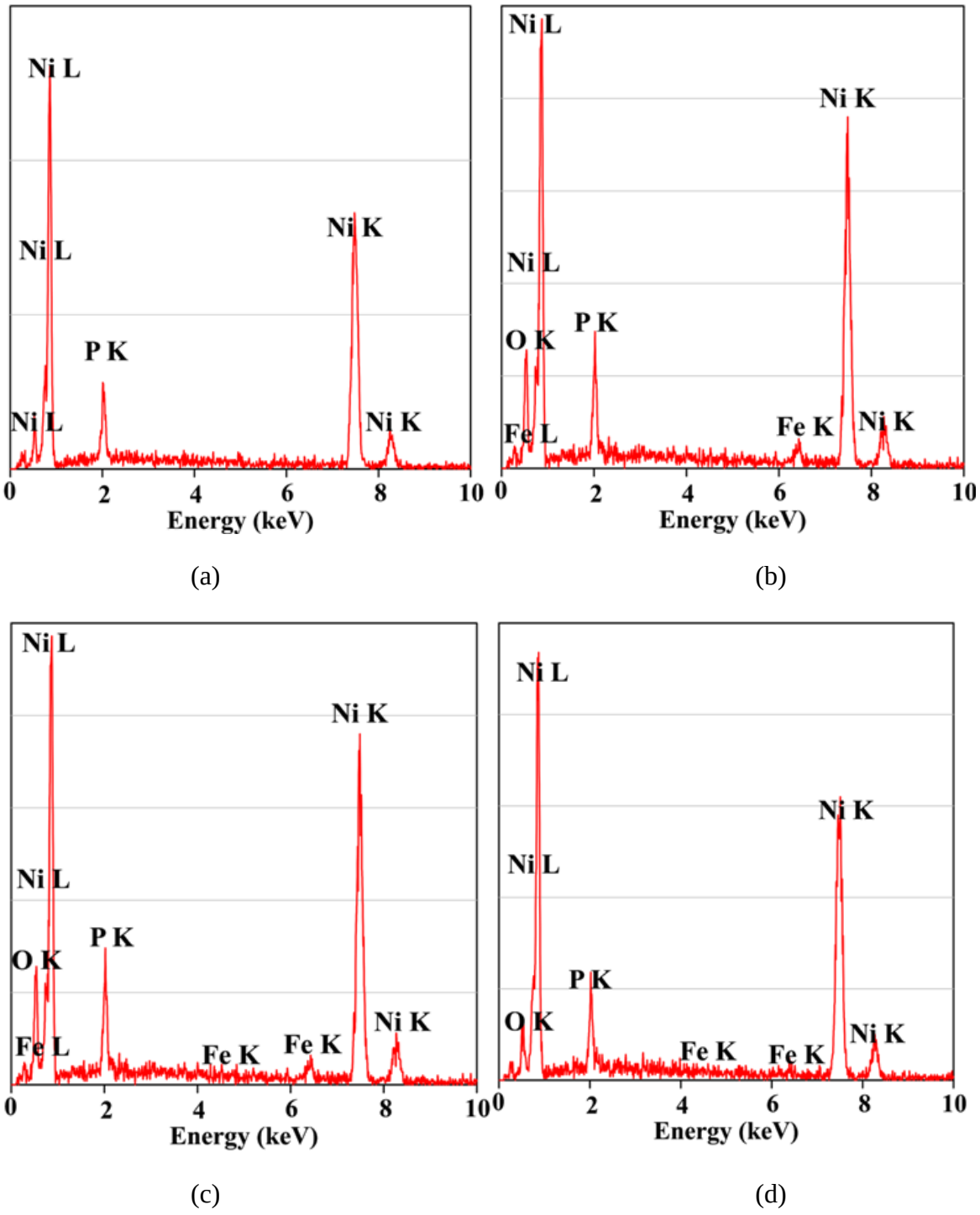

Figure 3.24 EDX spectrum of worn specimen of heat-treated electroless Ni-P coating tested at (a) 30°C (b) 100°C (c) 300°C and (d) 500°C

Micro-cutting and micro-ploughing together with torn patches (Figure 3.23b) are encountered in the wear test at 100°C. Though the coating surface appears to suffer ductile failure with high level of plasticity in the direction of sliding. EDX results again indicates the existence of oxygen and iron (Figure 3.24b). Ploughing with torn patches in the direction of sliding can also be observed for coating tested at 300°C (Figure 3.23c) which again point towards a mixed wear mechanism. The severe adhesive wear and rough surface supports towards the high COF observed at this condition (Figure 3.15b).

The EDX of the post wear sample (Figure 3.24c) shows iron which yields abrasive wear owing to high mutual solubility of nickel and Fe atoms. The presence of micro cracks is noticed on the worn surface (Figure 3.23d) as a result of the shear stress transmitted to the sub-surface layer and the variation of the load experienced at the area of contact (Le´on et al., 2003). This type of morphological feature, commonly known as "prows", is reported for adhesive wear failure of EN coatings by several researchers (Staia et al., 1996; Gawne & Ma, 1987). All this evidence points towards the occurrence of adhesive wear phenomenon in the coatings.

The EDX of the wear tested specimen (Figure 3.24d) also shows the presence of iron (Fe) peaks which have definitely come from the steel counterface. This indicates the high mutual solubility of nickel and iron atoms. The adhesive wear mechanism is in agreement with literature reports (Staia et al., 2002). Overall, the wear mechanism encountered in the test is a mixture of adhesive and abrasive wear phenomena.

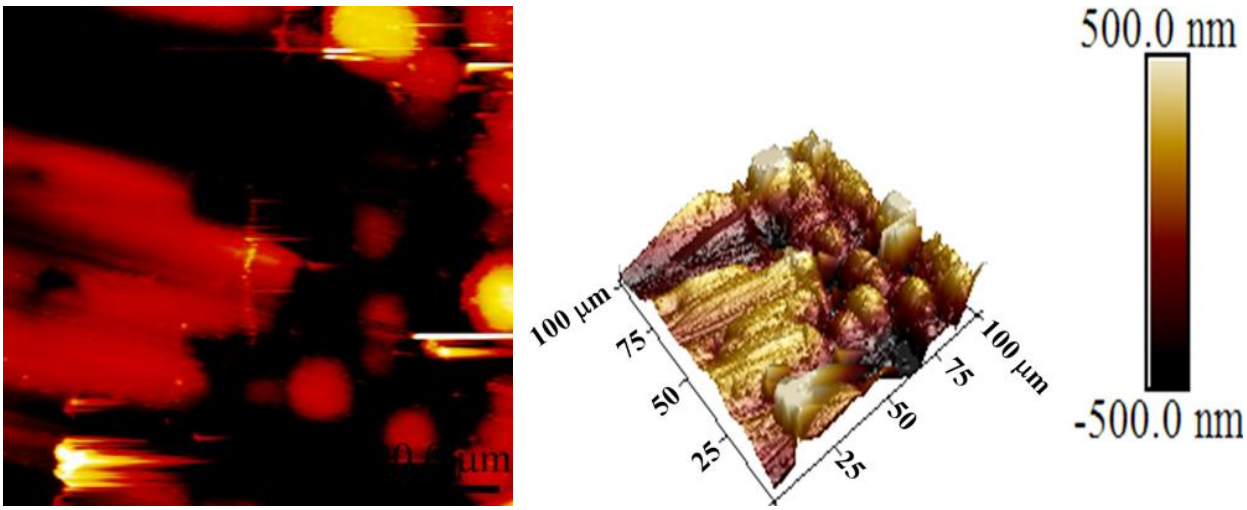

(a) (b)

Figure 3.25 AFM morphology (a) 2D and (b) 3D of heat-treated Ni-P coating tested at 500°C

To understand the underlying facts of elevated temperature test in better way as well as to maintain brevity, heat-treated samples post test at 500°C are consolidated via AFM and elemental mapping assessment and the corresponding results indicated by Figure 3.25 and 3.26 respectively. The 2D and 3D surface morphology of post test samples is represented by Figure

3.25a and 3.25b respectively. It clearly indicates a rough surface along with micro-ploughing. Wear tracks in the direction of sliding along with material removal is also noticeable. The elemental maps along with SE image of worn heat-treated Ni-P coating tested at 500°C is shown in Figure 3.26. Uniform allocation of nickel and phosphorous can be seen from the images (Figure 3.26) which mean the survival of coating even after the wear test. The existence of oxygen proves the development of tribo-oxide film as discussed earlier. The oxide layer surrounds over the whole surface of the coating as evident from the mapped image which is the main reason for lesser fluctuation and a reduced amount of COF compared to 100°C and 300°C tests. For the 500°C, iron shows very strong signal (Figure 3.26) in the image which implies occurrence of adhesive wear whose remnants can be observed from torn patches on the coating post test.

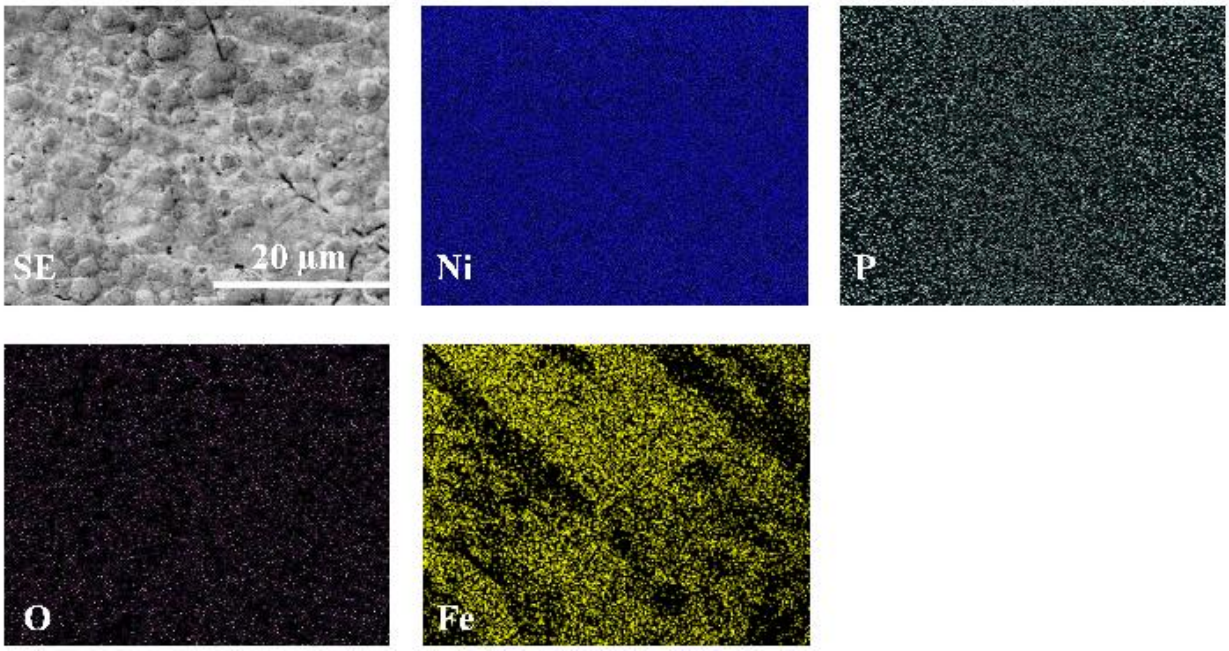

Figure 3.26 EDX maps of worn specimen of heat-treated Ni-P coating tested at 500°C

3.3.6.4 Phase transformation and hardness change

Several researchers claims commencement of phase transformation because of in situ heat-treatment during elevated temperature test of EN coatings (Franco et al., 2016; Mukhopadhyay et al., 2018a; 2018c). Detailed XRD study of post wear Ni-P coatings are conducted to understand the reality of the claim. Phase transformation study of mainly as-plated coatings tested at elevated temperature are examined and explained through Figure 3.27. Heat-treated specimens are excluded for XRD analysis, as they are already in crystalline state and it is so complicated to identify the effect of elevated temperature test. The samples subjected to room temperature test causes small effects in crystal structure and the same is observed similar to that presented by as-deposited coating as indicated in Figure 3.11. Wear behavior of as-plated

coatings during room temperature test is solely controlled by the plastic deformation that occurs during the test as stated earlier.

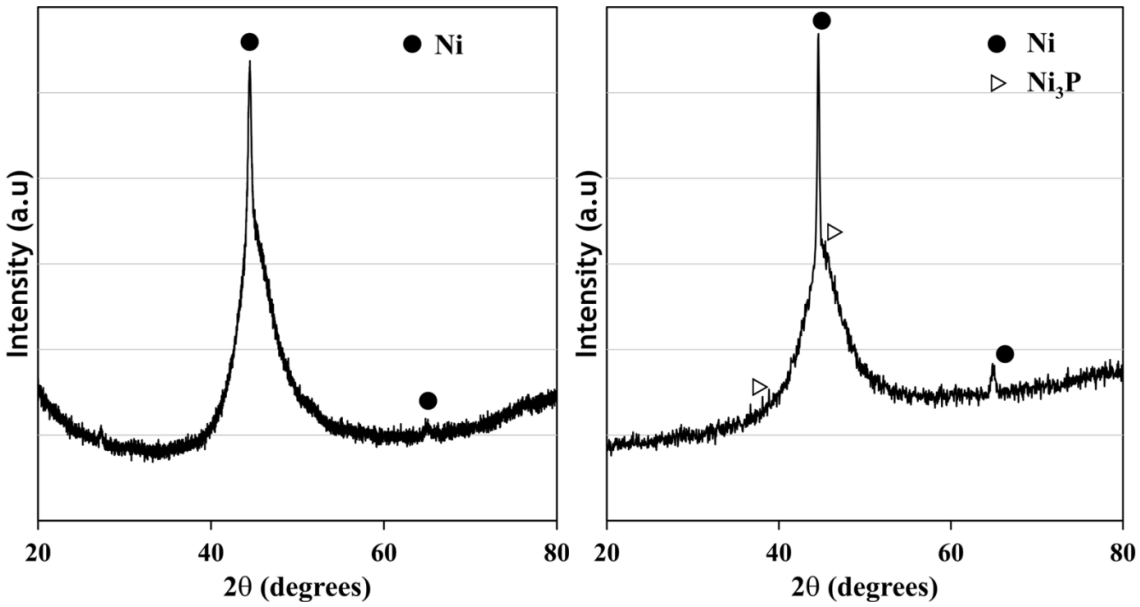

(a)

(b)

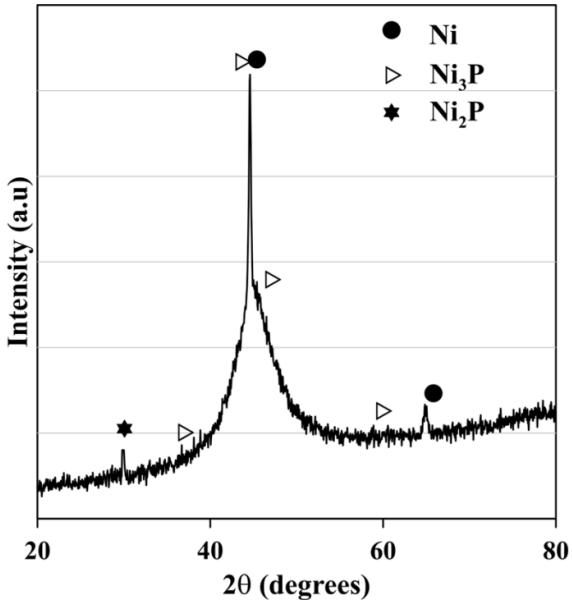

(c)

Figure 3.27 XRD analysis of as-deposited Ni-P coating post-wear test at (a) 100°C, (b) 300°C, and (c) 500°C

Figure 3.27a represents the phase structure of post wear Ni-P coatings tested at 100°C. Nickel peak (111) gets sharper compared to as-plated coating. Microstructural changes that

occurs at 100°C is due to the combined effect of plastic deformation and test temperature. Further crystallographic change is observed for coatings tested at 300°C as illustrated by Figure 3.27b. Crystalline Ni_3P is visible which clearly indicates the phase transformation of the as-plated coating during the 300°C wear test. The formation of phosphide phases of nickel are accelerating with the increase in test temperature which reflects in Figure 5.27c. The existence of Ni_3P along with Ni_2P proves the same. These harder phases may act as a barrier against the dislocation which leads to improvement in the tribological performance at elevated temperature. High temperature causes to decrease wear because of precipitation of nickel phosphides phases. Further the phase transformation effects are justified through post wear hardness evaluation of as-deposited and heat-treated samples, presented in the next part of this section.

The results obtained through post wear XRD of as-deposited Ni-P coating is well in agreement with the earlier results as is mentioned in the wear mechanism section. The point EDX (Figure 3.20c and 3.20d) clearly indicates the presence of inter diffused Fe particle. Though the presence of Fe particles or inter diffusion phenomenon is not clear in XRD study. The detailed wear mechanism is also explained by the EDX maps (Figure 3.22) of post wear test sample of as-plated coatings tested at 500°C, clearly indicating the presence of each element including Ni and P, and thus justifying the existence of the coating at elevated temperature. The present discussion thus proves the phase transformation scenario as an outcome of short duration heat-treatment during the elevated temperature wear test. The present study provides a qualitative idea about high temperature tribology of Ni-P coatings. Further studies such as X-ray photoelectron spectroscopy (XPS) can be conducted for thorough examination on oxide layer formation, that controls tribological performance of the coatings.

It is already known that the phase transformation temperature of EN coatings lies around 335°C (Das et al., 2007). Hence, the higher wear resistance found at 500°C can be attributed to the increase in hardness of the coating due to heat-treatment at the test temperature. This is also supported from the hardness data of the samples pre and post test. The percentage increase of hardness of the samples after test is illustrated in Figure 3.28. It is found that for as-deposited samples, the maximum increase of hardness (>40 %) is for the samples subjected to the 500°C test. EN coatings gain hardness after elevated temperature tests. It is interesting to note that the percentage increase in hardness for as-deposited coatings is more compared to heat-treated ones. This is again indicative of the real time heat-treatment of the samples and changes in the microstructure. However, the increased hardness (maximum 874 $HV_{0.1}$ after 500°C test) is lower compared to the hardness achieved by proper heat-treatment (around 1000 $HV_{0.1}$ for 400°C, 1 h).

It is also observed that for as-deposited samples, the hardness increase is more for higher test temperature compared to the lower ones. In the case of heat-treated coatings, the test at 100°C yields negligible enhancement of hardness. Hence, it can be concluded that the tests at elevated temperatures act as short duration heat-treatment, which have quite a positive impact on the hardness of the as-deposited coating. The effect of the aforesaid heat-treatment is already

proved through XRD study of the post wear samples where the formation of hard phosphide phases are visible as is indicated earlier by Figure 3.27. Overall, the hardness results are found to fairly match the tribological performance of EN coatings at elevated temperature tests.

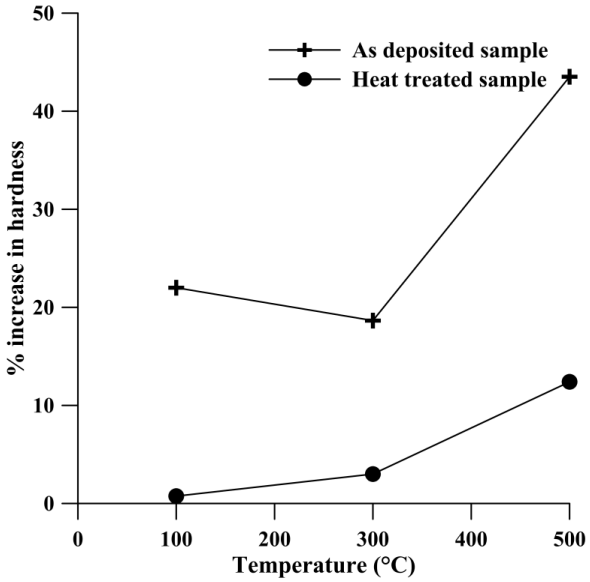

Figure 3.28 Percentage increase in hardness after high temperature tests of Ni-P coating

3.4 Conclusion

EN coatings are developed in the laboratory with the available chemistry and found to be of high phosphorous category. The coatings display the conventional nodular structure with no surface defect. Both as-deposited as well as heat-treated coatings have been investigated for friction and wear under different temperature conditions by varying applied load and sliding velocity. It is found that the COF of the as-deposited coating mostly increases with increase in load for all temperatures and decreases with the increase in the sliding velocity. The results of elevated temperature tests particularly at 500°C exhibit comparatively lower COF than the others. This may be because of the in situ heat-treatment due to the exposure to the elevated test temperature which results in improved hardness of the coating. The heat-treated coatings also display almost analogous friction characteristics. In the case of wear, behavior similar to the friction study is observed. The worn surface displays a ploughing effect, coating detachment and cracks which indicate that both adhesion and abrasion phenomena govern the wear mechanism. The top surface of the EN coating after elevated temperature tribology tests consists of a mechanically mixed layer of oxidation products. After the tests, the hardness increase of the as-deposited coatings is quite high compared to the heat-treated ones. The effect of the short duration heat-treatment, due to high temperature tests is proven through XRD as well as hardness study of the post wear samples where the formation of hard phosphide phases are visible that results in increase of hardness as well as represents better wear resistance Overall the EN coatings have potential to perform under elevated temperature conditions.

Chapter 4

High temperature tribology of Ni-P-W coating

4.1 Need for Tungsten (W) Inclusion

Electroless Ni-P deposit is a supersaturated alloy in the as-deposited state, and can be strengthened by the precipitation of nickel phosphide crystallites by suitable heat-treatment. However, the hardness of Ni-P film degrades with excessive heat-treatment due to grain coarsening. Another method to enhance the strength and properties of the coating is to incorporate certain metals and particulates into it. Tungsten and its alloys are recognized due to their specific tribological, magnetic, electrical and electro-erosion properties. They may compete even with ceramics and graphite by virtue of their high thermal resistance. It has been observed that incorporation of tungsten in EN coatings increases its wear resistance which has brought it in focus of numerous investigations (Balaraju & Rajam, 2005; 2006; Palaniappa & Seshadri, 2008; Tsai et al., 2001). This could be attributed to the solid solution strengthening by provided by tungsten into nickel matrix. The addition of tungsten into nickel enhances its properties like hardness and high temperature stability. The as-deposited Ni-P and Ni-P-W coatings exhibit amorphous structure. Phosphorus and tungsten are dissolved in the nickel matrix and exhibit a (111) preferred orientation under phase structure analysis. For Ni-P-W coatings, it is believed that inclusion of W promotes mechanical and thermal properties due to its relatively high hardness and high melting point of 3410°C (Wu et al., 2004). The presence of tungsten retards the crystallization of coatings during heat-treatment process. The temperature of crystallization is determined to be around 400 °C for electroless Ni-W-P coatings (Tsai et al., 2001). Higher hardness obtained at 400°C temperature for Ni-P-W deposits has been ascribed to the formation of Ni-W solid solution apart from nickel phosphide precipitation (Balaraju & Rajam, 2006).

A thorough literature survey reveals that despite a good number of studies on electroless Ni-P-W coatings, there is a dearth in studies concerning its tribological behavior under elevated temperature. The present study is a humble attempt in that direction. Several applications such as the heat exchangers, turbines, tools, extruders, sealing surface of nuclear valves, plungers, rolls for rolling mills etc. require operations to be done at elevated temperature conditions (He et al., 2011). The present chapter thus attempts to investigate the friction and wear behavior of Ni-P-W coating under high temperature since EN coatings find scope as a potential surface coating for applications working under such demanding conditions.

4.2 Experimental Details

AISI 1040 steel pins is used for the deposition of electroless Ni-P-W coating. After preparation of the substrate as mentioned in section 2.2.1 of chapter 2, the substrate is ready for the deposition of coating. The bath composition and operating conditions for Ni-P-W coating are selected after several trials and proper ranges of the bath parameters which yield a stable deposit are chosen. Sodium tungstate solution is used as the source of tungsten ion and bath concentration and deposition conditions are indicated by Table 4.1. The pH of the solution is maintained at by continuous monitoring with a pH meter. All depositions are carried out for a period of three hours with mild agitation (stirred at 150 rpm) and same volume of the solution is used, so that the coating thickness and bath load remain approximately same for all the specimen. No replenishment for the salts were done during the plating. However, as an alternative of replenishment as well as to maintain sufficient thickness for tribological test, double bath deposition technique (1.5h each) is used. After the deposition, the samples are taken out of the electroless nickel bath and washed in distilled water.

After deposition, rest of the tests viz. roughness, hardness, tribological testing and microstructural characterisations are conducted with the same plan as discussed in sections 2.4 to 2.9 of chapter 2. Tribological tests are conducted by considering two phases which are already described in Table 3.2 and Table 3.3 of chapter 3.

Table 4.1: Bath composition and working conditions for Ni-P-W coating

Bath constituents	**values**	**Operating conditions**	**values**
Nickel sulphate (g/l)	20	pH	7-8
Sodium hypophosphite (g/l)	20		
Sodium citrate (g/l)	35	Temperature (°C)	90 ± 2
Ammonium sulphate (g/l)	30		
Lactic acid (g/l)	5	Duration of coating (hour)	3
Sodium tungstate (g/l)	20		
		Bath volume (mL)	200

4.3 Results and Discussions

4.3.1 Ni-P-W coating configuration

Sodium hypophosphite is used as the reducing agent for the electroless deposition of Ni-P-W coatings. Inclusion of W in Ni-P matrix causes to decrease the deposition rate compared to Ni-P coating. The deposition thickness versus time plot is presented in Figure 4.1 which indicates a moderate slope and the average deposition rate is close to 10-12 μm/h. Thus to

achieve required thickness for further tribological tests, instead of replenishment double bath deposition technique is adapted for Ni-P-W deposition.

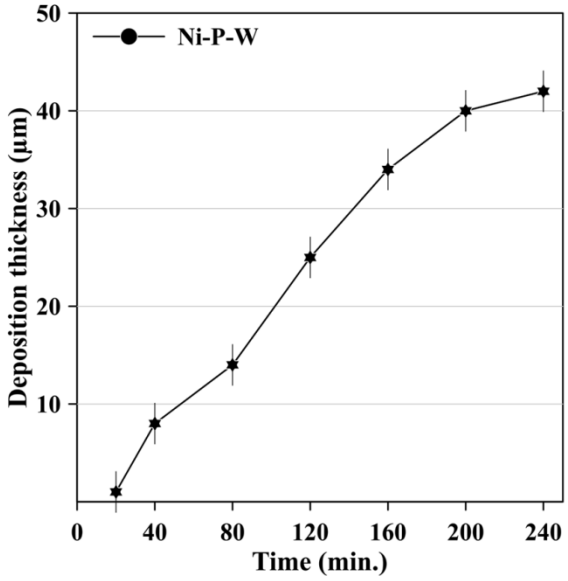

Figure 4.1 Deposition rate of Ni-P-W coating

Tungsten added to the coating as a third particle is expected to have positive effect on the tribological behavior of the coating. Composition analysis of as-deposited Ni-P-W coating is done using EDX and the spectrum shown in Figure 4.2. The analysis reveals that the tungsten content in terms of weight percentages, lie in the range of 3.8-4.7 and phosphorous content, in the range of 7.6-8.3 while the remaining is nickel. This confirms that the developed coating is a ternary alloy of nickel, phosphorous and tungsten as desired. Now, the phosphorus percentage of the deposit determines its crystallinity. In general, for the binary Ni-P alloy system, the coatings are seen to be amorphous in the high phosphorus (10-13 wt% P) range, while a mixture of nano-crystalline and amorphous phases exist for the medium phosphorus (6-9 wt% P) deposits. It has been seen from the literatures that incorporation of W improves the crystallinity of the coatings due to the reduction in phosphorus content, and the coatings are transformed more to a mixture of amorphous and nano-crystalline phases (Balaraju et al., 2009). The reduction in P content may be explained on the basis of the increase of metals ions ratio to hypophosphite ions in the electroless bath. This may also depend on the complexing ability of the sulphamate ions in the present alkaline citrate based bath. Overall, tungsten and phosphorus incorporations are found to be lower in the case of sulphamate based baths. EDX of Ni-P-W coating heat-treated at 400°C for 1 h is shown in Figure 4.2b and the presence of Oxygen (around 2%) is observed. Hence, the formation of oxide scales due to heat-treatment could be confirmed from EDX results. Rest of the elements do not exhibit much variation in their composition. The oxide scale may be present as oxides of Ni and W.

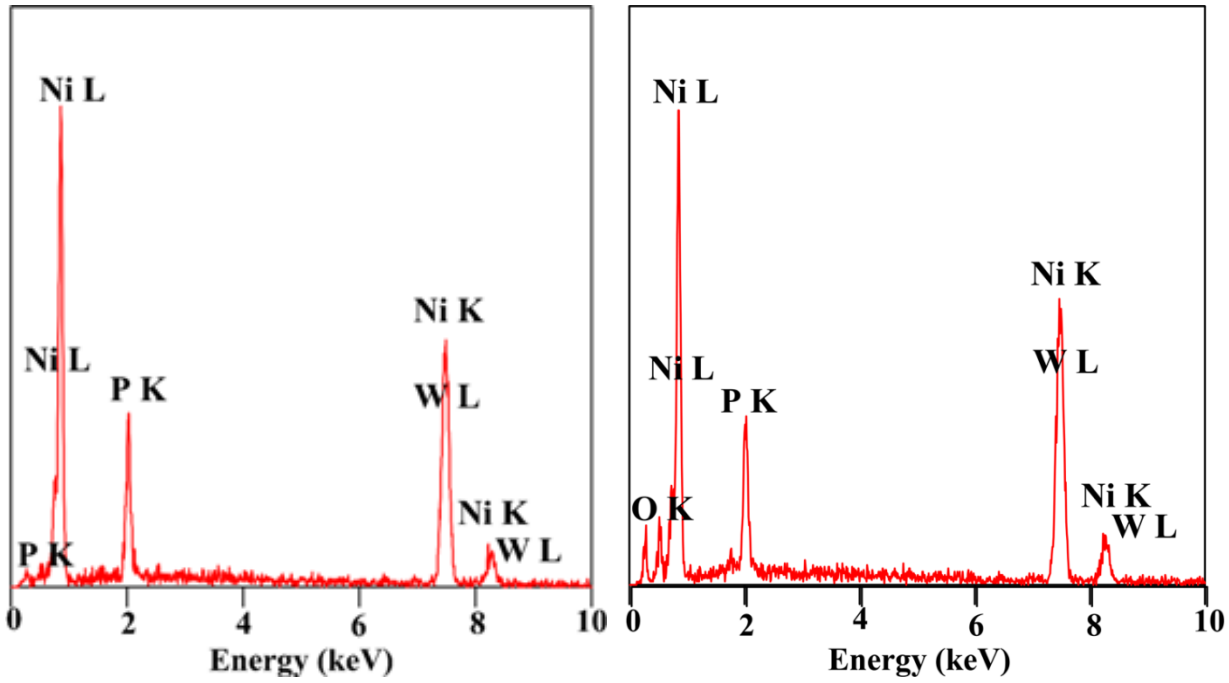

(a) (b)

Figure 4.2 EDX spectrum of (a) as-deposited and (b) heat-treated electroless Ni-P-W coating

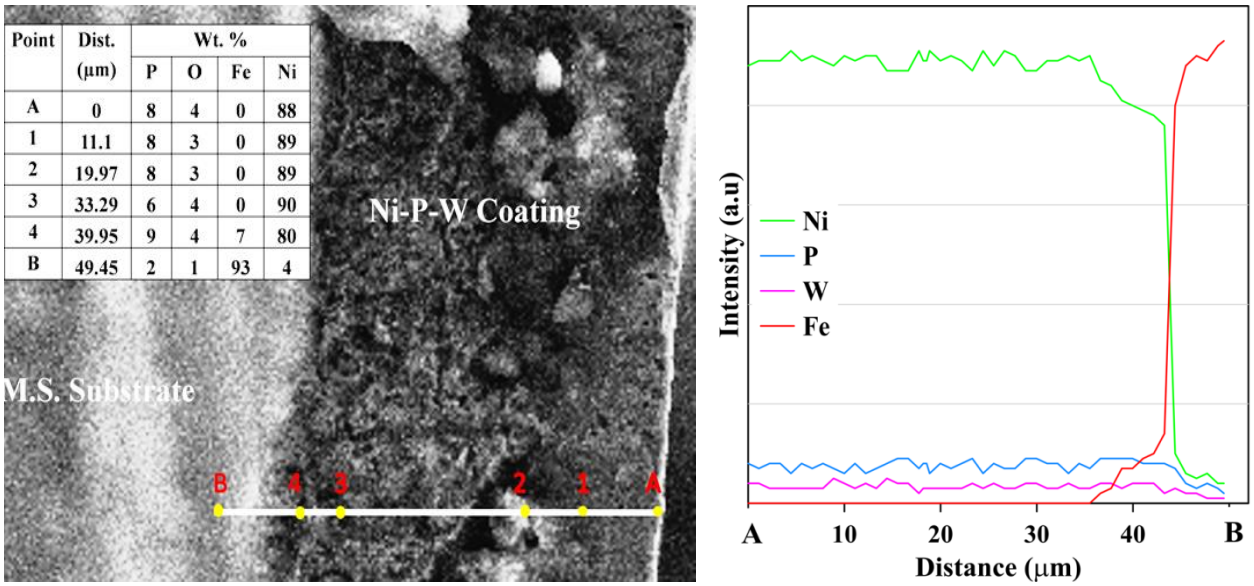

(a) (b)

Figure 4.3 (a) SEM image showing line EDX (quantitative analysis included in table) and (b) detailed composition profiles of elements present measured along the thickness of coating

Apart from point elemental analysis, EDX line scan is also performed on the cross cut section of the coating for better understanding of elemental distribution. The detail line scan is

represented in Figure 4.3. The quantitative results indicating weight percentage of Ni, P, W and Fe is given in table inside Figure 4.3a. Composition profiles of Ni, P, W and Fe measured along the thickness of Ni-P-W (Figure 4.3b) coatings are performed through line EDX for detailed understanding of elemental variation across the cross section.

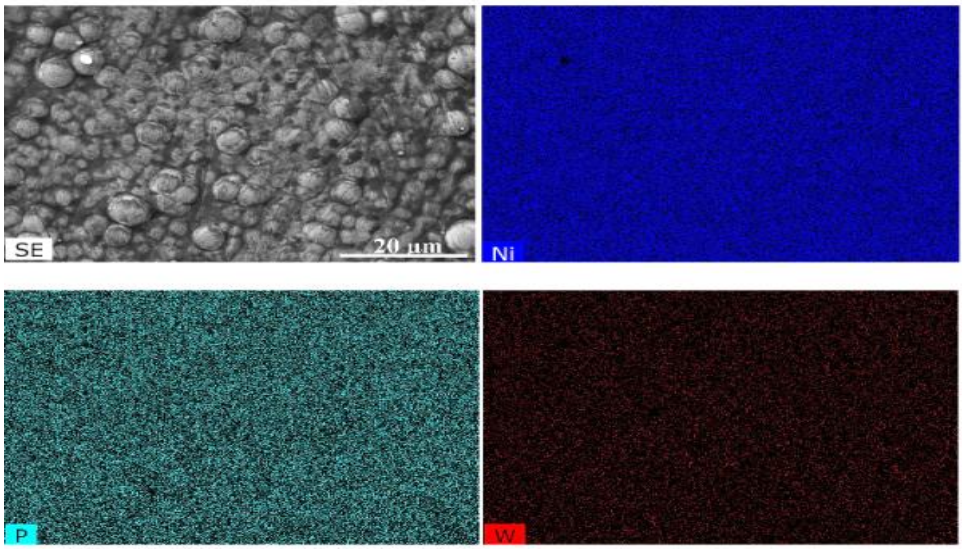

Figure 4.4 EDX mapping analysis on the surface of the as-deposited Ni-P-W coating

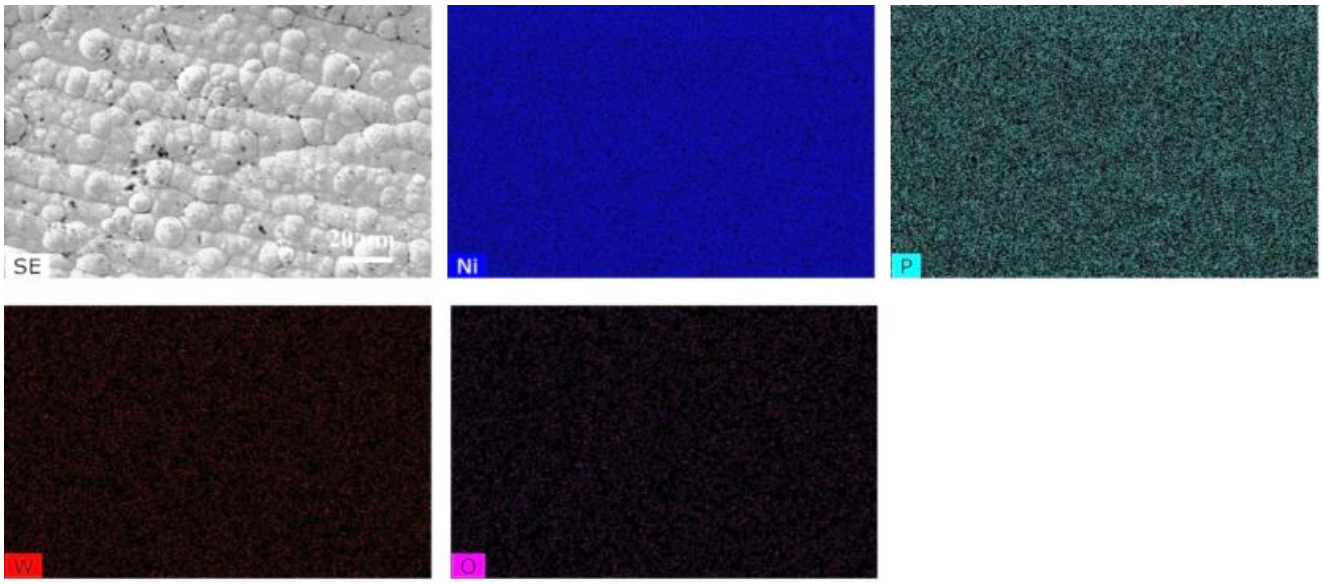

Figure 4.5 EDX mapping analysis on the surface of the heat-treated Ni-P-W coating

Figure 4.4 and 4.5 shows the elemental mapping of the as-deposited and heat-treated coating surfaces respectively. It is noticed that the constituent elements of the coating are distributed almost homogenously throughout the surface of the coating. In case of heat-treated

coating (Figure 4.5), oxygen is detected as an additional constituent which indicates the formation of an oxide film on the coating surface.

4.3.2 Surface texture of coating

Optical micrograph of as-deposited and heat-treated Ni-P-W specimen is presented in Figure 4.6, proclaiming surface morphology qualitatively. The detailed analysis is carried out by SEM micrograph of the samples revealing its surface morphology and cross-cut section as shown in Figure 4.7 and 4.8 respectively. The densely packed nodulated morphology is observed for Ni-P-W coatings in as-deposited condition in the high-magnification SEM micrograph (Figure 4.7). Nodulated surface characteristics with low porosity is very common in EN coatings (Alirezaei et al., 2013b; Palaniappa & Seshadri, 2007; Wu et al., 2004). The rapid formation of nuclei and subsequent growth of the EN deposits promote the nodularity. Some pores in the coatings may result from the evolution of hydrogen during the electroless deposition. Pores appear as dark regions, but these are very small in size and may not have penetrated to the substrate surface. Such structures augment the self-lubricating capability of the coatings by acting as pocket for retaining lubricants. A cross-cut section of the as-deposited Ni-P-W coating is shown in Figure 4.8. It seems that the coating is connected closely to the substrate exhibiting good adhesion to the substrate.

The SEM micrographs (Figure 4.7) of as-deposited and heat-treated Ni-P-W coating depict a globular morphology. The size of the globules is almost uniform with their diameters ranging between 20-25 µm. By careful observation of the coated surface, it can be seen that the globules are arranged in a columnar pattern which again indicates towards the columnar growth of the electroless nickel coating. The coating appears dense and compact with light grey in colour. There is no visible surface damage and the coating appears to be of very low porosity which is again an indication of it possessing a good corrosion resistance. White particles are found to be scattered all over the coating surface due to the excess growth of nickel alloy over the nodules. Similar results are obtained by Selvi et al. (2014), they explained that this excess growth could be due to the mixed complex in the electroless bath which acts as a precursor for the deposition of the alloy. Upon heat-treatment however, there is an increase in the size of the nodules making the surface of the coating coarse. The nodular morphology implies the coating may exhibit low friction and wear characteristics. However, friction and wear characteristics of any material are not governed by the surface condition alone but by a host of others factors viz. the surface composition, material properties, etc., which would be investigated in the present study. Thickness of the deposits is found to be around 45-50µm as shown in Figure 4.8 with a deposition rate of nearly 10-12µm/h. Diamond cutter is used for cross-cutting followed by polishing of the cut surface with various grades of emery paper. The present coating is also found to have a good adhesion to the substrate. Balaraju et.al (2006) found numerous lamellar lines throughout the cross cut of the coating which they attributed to the variation in the composition of binary and ternary electroless nickel alloys with thickness from interface of the

deposit/substrate to the surface of the deposits. Formation of laminates is due to the periodical fluctuations in the pH of plating solution (due to hydrogen evolution) adjacent to the deposit surface. Although double bath deposition technique is followed for the present coating, no lamellar or parting line is observed on the coating cross section.

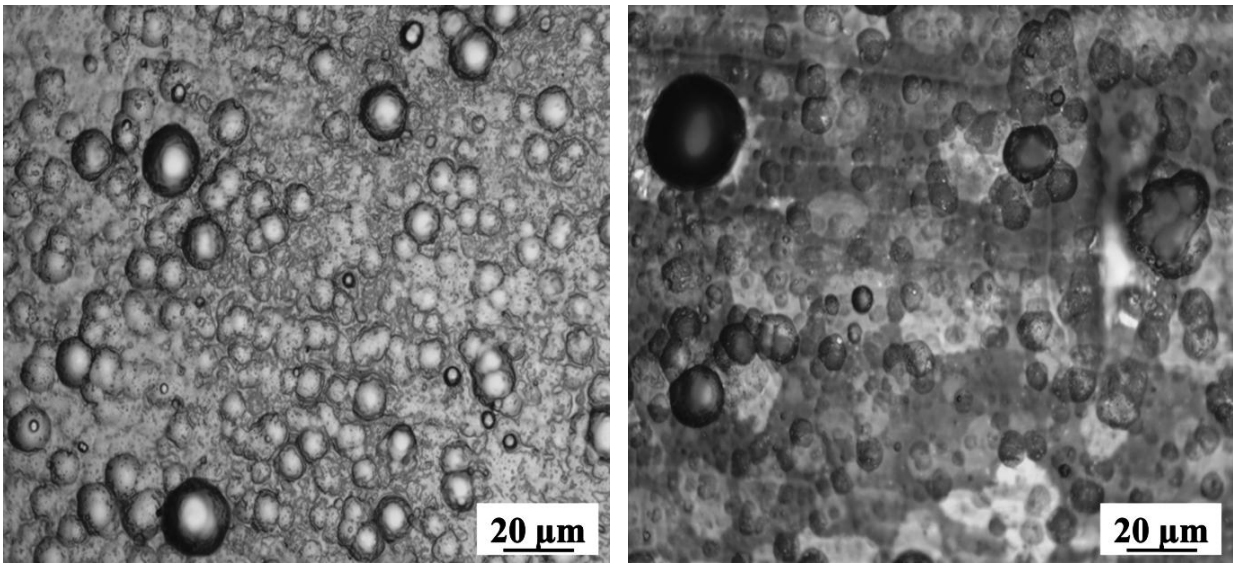

(a) (b)

Figure 4.6 Optical micrograph of (a) as-deposited and (b) heat-treated electroless Ni-P-W coating

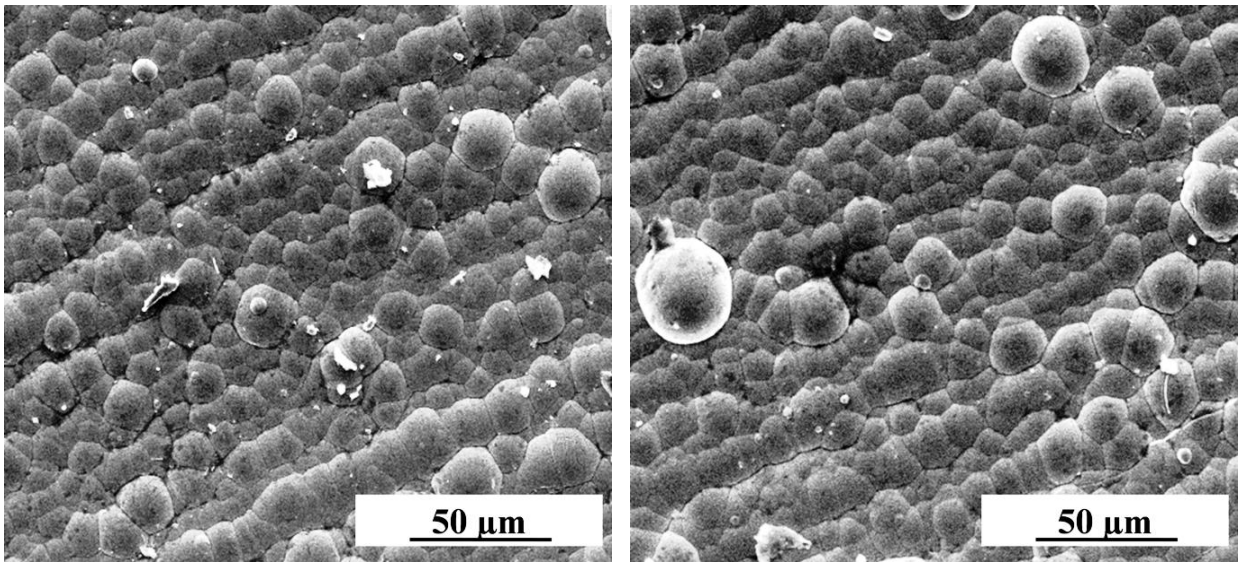

(a) (b)

Figure 4.7 SEM micrograph of (a) as-deposited and (b) heat-treated electroless Ni-P-W coating

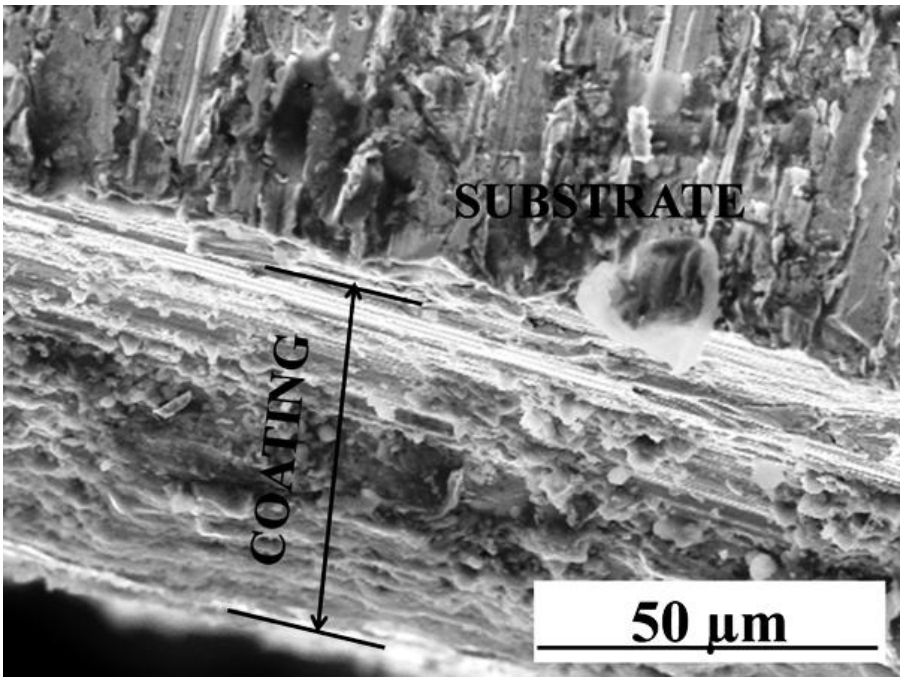

Figure 4.8 A cross-cut section of the Ni-P-W coating

The surface texture of the coating, both as-deposited and heat-treated is investigated in more details through AFM and the corresponding plots appear in Figure 4.9 and 4.10 respectively. The AFM results reiterate the observations made through SEM. As usual nodular morphology for the both as-deposited and heat-treated coatings are observed. The as-deposited coatings display regular array of the nodules yielding a more homogeneous surface texture. It can be noted that nodule formation is a common feature in electroless nickel deposits. The rapid formation of nuclei and subsequent growth of the electroless nickel deposit promote the nodular feature. Deposition rate plays an important role in the formation of nodules which may be due to the fast supply of atoms that enables the nodules to grow preferentially in the Z-direction (normal to the substrate) than the X and Y directions. Besides, the surface diffusion of as-deposited atoms may also be inhibited to a certain extent by the rapidly arriving atoms. However, nodule formation also depends on the bath constituents as well as particles on the substrate surface. The particles can come from many different sources: dirt and debris from the air, blasting or grinding media, machining damage, tank plate-out, dirty water, Ni-P-W particles from an overactive or old bath, poor cleaning, etc. In case of heat-treated coatings (Figure 4.10), again grain coarsening is observed making the surface texture more irregular.

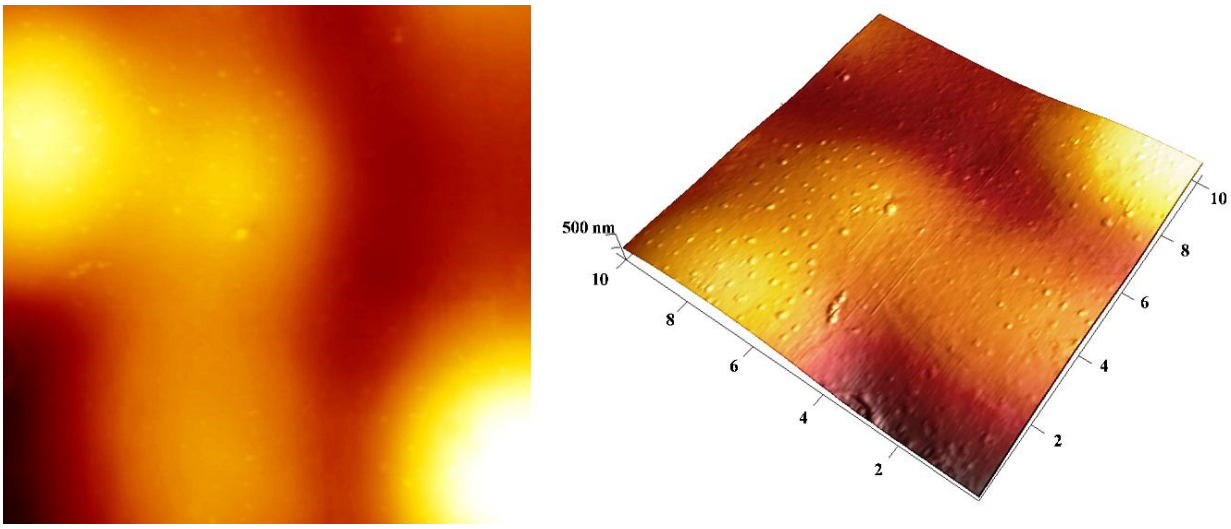

(a) (b)

Figure 4.9 Typical AFM morphologies of as-deposited Ni-P-W surfaces in (a) 2D and (b) 3D

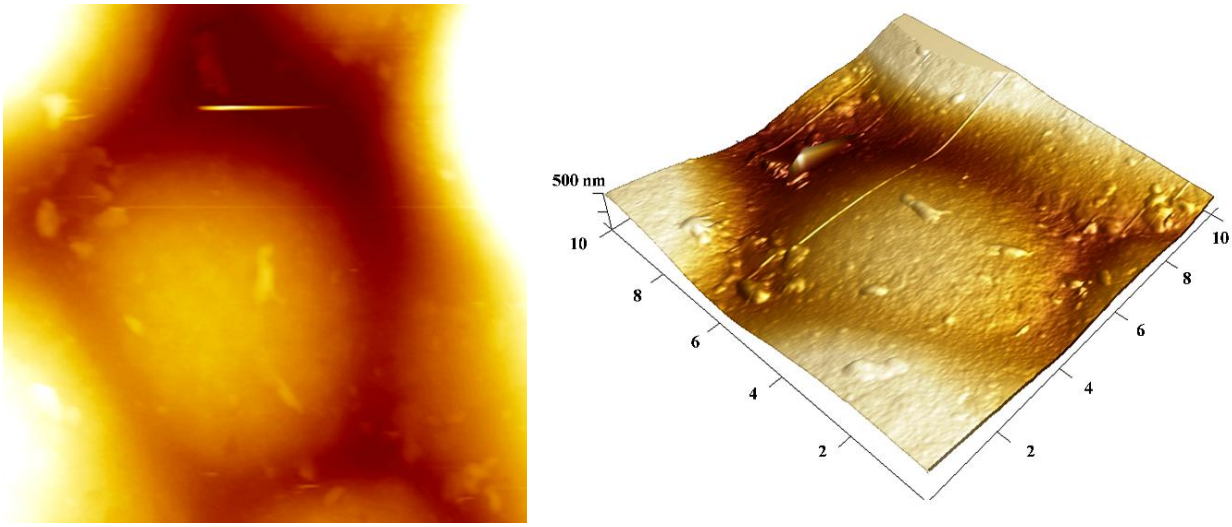

(a) (b)

Figure 4.10 Typical AFM morphologies of heat-treated Ni-P-W surfaces in (a) 2D and (b) 3D

4.3.3 Structural aspects of Ni-P-W coating

XRD analysis (Figure 4.11) of the present as-deposited Ni-P-W coating is seen to support the fact of crystallinity improvement due to W incorporation. The distribution of each element is indicated by the elemental maps of as-deposited and heat-treated specimen. From SEM and XRD data, both reveals that in as-deposited condition the coating shows a mixture of amorphous and nano crystalline phases due to addition of W in Ni-P matrix but with heat-treatment it turns crystalline with the formation of nickel phosphide and Ni-W solid solution. Similar nano-

crystalline nature of the coating is also reported by Balaraju et al. (2012). Moreover, XRD results show a strong orientation towards Ni (111) plane pertaining to the sharp peak in the plot. These results exactly match the observations made by Osaka et al. (1982). With heat-treatment, as expected the coating turns completely crystalline with the appearance of nickel phosphide (Ni_3P) peaks (Figure 4.11). The range of interest (40-55°) is zoomed (inset) so that the main peaks are manifested which are found to be consisting of Ni_3P only. This phenomenon is also observed in case of binary Ni-P alloy. However, it is interesting to note the presence of Ni-W which manifests itself as the major peak in XRD plot. Now, W is dissolved in the nickel matrix and shows a (111) preferred orientation in phase structure study with the formation of Ni-W solid solution. The effect of W is mostly substitutional as solute atom (W) is larger than the solvent atom (Ni). Thus, W replaces Ni in the crystal lattice. Apart from this, in comparison to Ni-P, Ni-P-W provides lesser atomic weight percentage of Ni and P, which also indicates substitutional solution.

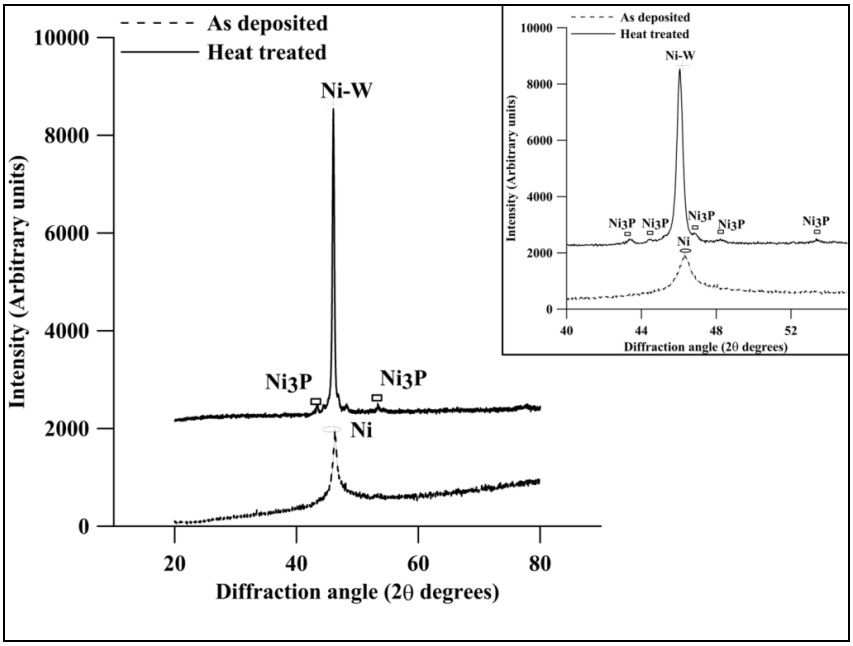

Figure 4.11 XRD spectra obtained for as-deposited and heat-treated electroless Ni-P-W coating with zoomed view (inset)

Thus, the preferential orientation towards Ni (111) in as-deposited condition is not maintained upon heat-treatment of the coating which may be due to the introduction of tungsten which in turn forms an intermetallic compound with nickel due to heat-treatment. Now, Ni-W is considered to be a very hard material and hence expected to contribute to the hardness and wear resistance of the coating. Full width at half maximum (FWHM) is measured before and after the heat-treatment process and Debye–Scherrer's equation (Balaraju & Rajam, 2009) is employed to determine the crystallite size. Heat-treatment is found to result in a decrease in the FWHM and a consequent increase in grain size. A sharp peak with Ni (111) plane is found to have FWHM

value of 1.52613 and the corresponding crystallite size measures 5.914 nm. The grain size of the coatings heat-treated at 400°C based on Ni-W (111) is found to be 21.62 nm for a FWHM value is 0.4196. The existence of Ni_3P is noticeable after heat-treatment with an average FWHM of 0.6185 and crystallite size of 14.71 nm. The grain size obtained in the current study is quite consistent with that obtained by other researchers (Palaniappa & Seshadri, 2007). They further found that heating the deposit at 600°C, results in large grain coarsening where grain size was found to have grown to approximately 100-500 nm.

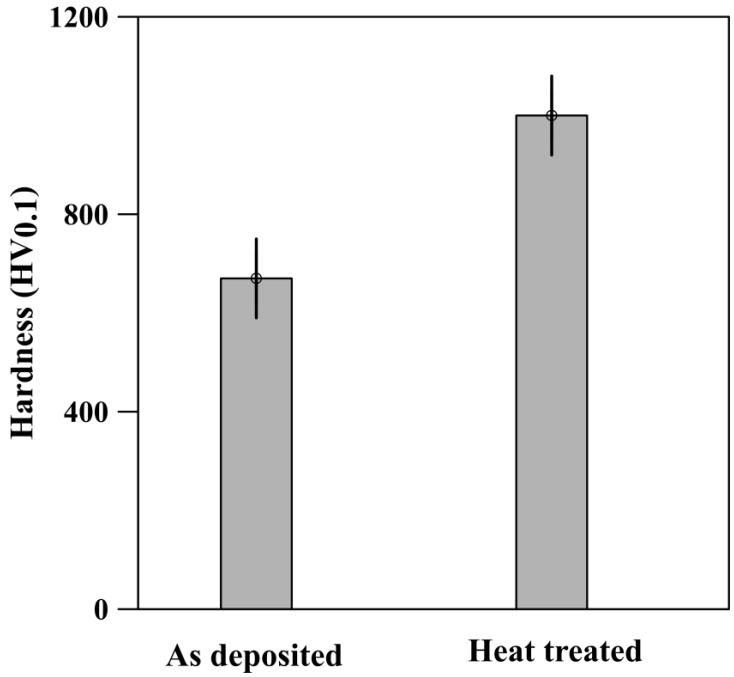

Figure 4.12 Microhardness obtained for as-deposited and heat-treated electroless Ni-P-W coating

4.3.4 Roughness and microhardness evaluation

The center line average roughness (Ra) value of present electroless Ni-P-W coating is seen to lie around 0.42 μm which is quite closer to the substrate roughness. Due to constant bath composition, most of the coated specimens are found to possess the same roughness with a variation of ±1%. The specimens exceeding the variation limit are rejected.

The incorporation of W in Ni-P coatings is also reflected in the micro hardness results of the as-deposited coatings (Figure 4.12). When compared to that of Ni-P coatings which has as-deposited hardness around 600 $HV_{0.1}$ (as presented in chapter 3), Ni-W-P is found to have hardness around 670 $HV_{0.1}$. This improvement in hardness is definitely due to the incorporation of tungsten which itself has a relatively higher hardness. There is a significant rise (more than 60%) in the average hardness of the coating post heat-treatment (400°C, 1h). This remarkable improvement in hardness is observed due to solid solution strengthening of the EN matrix by W

addition as also reported by Wu et al. (2004). However, the hardness of the heat-treated Ni-W-P coatings is marginally higher when compared to that of heat-treated Ni-P coating (average hardness around 1000 $HV_{0.1}$) (as indicated in chapter 3). The present coating being harder than the substrate material (AISI 1040 steel), definitely improves its surface hardness. Moreover, since all the samples are subjected to a uniform deposition condition, a very low variation in micro-hardness between the specimens is ensured. The hardness result obtained in the present study agrees well with that reported in literatures (Palaniappa & Seshadri, 2008).

4.3.5 Tribological characterization based on test parameters

4.3.5.1 Friction under different load and velocity

From Figure 4.13a, it is observed that friction behavior of both as-deposited and heat-treated Ni-P-W coatings is quite similar with the variation of applied load. It is further observed that except for 500°C test, COF increases with the increase in applied load for both the set of coatings. This increase in COF is in general attributed to the increase in contact area (due to higher applied load) which subsequently requires higher force to break. Similar observations have already been made by other researchers (Chowdhury et al., 2011). In case of as-deposited coating, the increase in COF is very marginal in case of elevated temperature conditions compared to that at RT. At lower load (10 N), RT yields the lowest COF of around 0.45. Increase of 40 N in the applied load (10 – 50 N) results in an increase of COF to 0.75. Thus, it can be concluded that the friction behavior of the coating is defined by more than one factor. When test is carried out at elevated temperatures (500°C), an oxide layer is formed on the surface of the coating (as atmospheric air is trapped inside the test chamber) which governs its friction behavior. The presence of oxygen is confirmed by EDX analysis of worn out coating as indicated later. Due to the formation of phosphates and oxides, the phosphorus and oxygen contents tend to increase at the coating surface, which partly governs the friction and wear characteristics of the coating. One notable observation from Figure 4.13a is the minimal variation of COF (at elevated temperatures) which implies that the surface layers of the coating maintains its nature over the load regime considered for the present study. The softening phenomenon at higher temperature (500°C) results in soft interfacial layer that presents low shear properties. This result in the coating display lesser friction at higher temperatures even for higher applied load. This observation is highly significant from the viewpoint of application of the coatings at elevated temperature conditions.

The effect of sliding speed under room and high temperatures is investigated to know its effect on tribological characteristics of Ni-P-W coatings. The friction and wear results are illustrated in Figure 4.13b and Figure 4.14b respectively. The sliding tests are conducted at a uniform load of 10N. RT test exhibits the minimum COF at most of the sliding velocity compared to the elevated temperature test. Sliding velocity in general is found not to be significant in controlling the COF of the coatings. Now, during sliding, the contact points change rapidly depending on the sliding velocity as new points come in contact and existing contacts

break. The more the area of contact as well as the time, the higher is the friction at the interface. Grain softening at elevated temperatures leads to increase in the contact area at the interface resulting in the coating displaying a marginal increase in COF. The friction behavior of the coating is mainly governed by the superficial layer of the coating without any influence from the sub-surface properties. The increasing trend of COF with sliding velocity for RT tests may also be due to the change of shear rate which can in turn affect the mechanical properties of the mating materials (Bhusan & Jahsman, 1978).

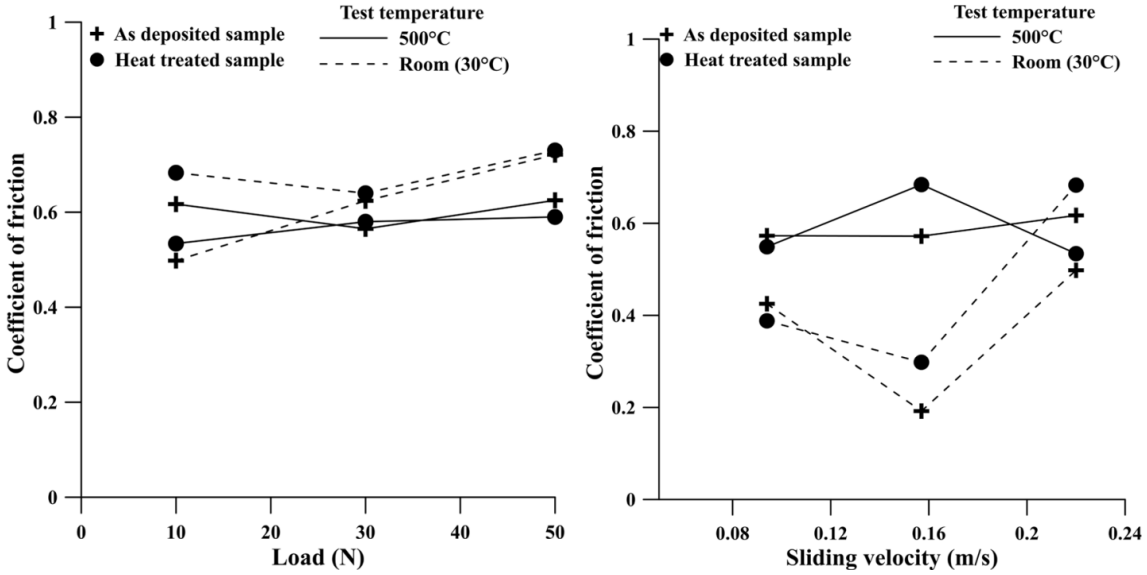

(a) (b)

Figure 4.13 Friction performance of Ni-P-W coating for room and high temperature under different (a) load and (b) sliding velocity

4.3.5.2 Wear under different load and velocity

The wear results (Figure 4.14a) are found to be significantly dependent on the applied load especially for RT and the results are gain quite similar for as-deposited and heat-treated coatings. From Figure 4.14a, it is observed that with increase in the applied load, wear rate at the two conditions escalate by about 8-10 times compared to that at low load (10N). Similar results have been obtained by other researchers (Le´on et al., 2003; Panja et al., 2016). The coatings mostly experience lower wear rates at higher test temperatures viz. 500°C. Now, the established phase transformation temperature of electroless nickel coatings is around 320-350°C (Wu et al., 2004; Das et al., 2007) which lead to the formation of harder crystallization phases in the coating thus increasing the overall hardness of the coating and decreasing the wear rate. The coatings subjected to real time heat-treatment provided by the higher temperature tests may be experiencing similar metallurgical changes which show up as lower wear rate in the plot. This can be further proven by providing supporting results such as post wear phase transformation and hardness analysis.

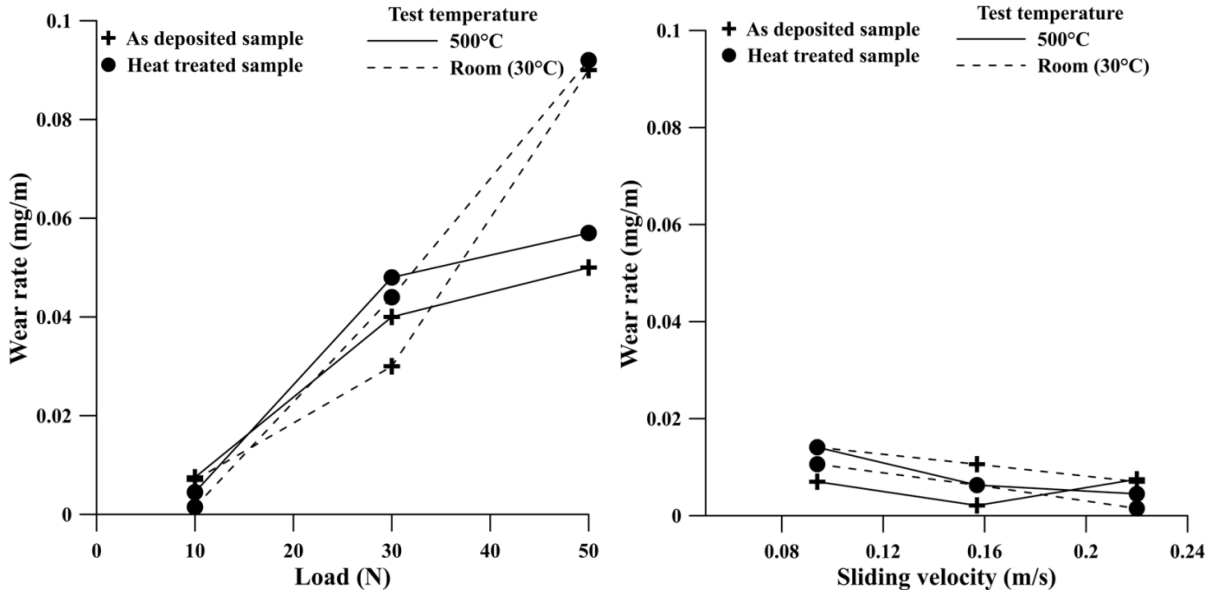

(a) (b)

Figure 4.14 Wear performance of Ni-P-W coating for room and high temperature under different (a) load and (b) sliding velocity

In the present study, wear is represented by the ratio of weight loss to the distance traversed so that the effect of sliding speed on wear can be truly realized. The effect of sliding velocity on wear for both as-deposited and heat-treated coatings is displayed in Figure 4.14b. The wear trends for both set of coatings are found to significantly differ from each other. It is interesting to note that for as-deposited coatings, except RT test, the elevated temperature conditions exhibit minimum wear rates at 0.22 m/s sliding velocity. Both as-deposited and heat-treated samples exhibit a monotonous decreasing trend in the wear rate with the increase in sliding velocity. Now, wear rate depends on the hardness of the two bodies in contact, together with friction-induced transformations and chemical changes. In the present case external heating is another factor affecting the wear performance of electroless Ni-P-W coating. One of the possible reasons for decreasing wear rate for higher sliding velocity is the lack of time to establish welded contact which is true considering adhesive wear being the dominant phenomenon for the present case. This can be confirmed only by observing the wear zone under microscope.

From the present study of both as-deposited and heat-treated coating, sliding speed of 0.22 m/s, which shows the best wear performance may be an optimum speed considering the properties of the mating surfaces under the room and high temperature test conditions as well as the applied load (10N). This particular value are considered to be constant for the next phase of study.

4.3.6 Study of tribological behavior of Ni-P-W coating at various test temperatures

4.3.6.1 Friction performance of as-deposited and heat-treated Ni-P-W coating at different test temperatures

The tribological performance of as-deposited Ni-P-W coating is studied under various working temperature for a particular load (10 N) and sliding velocity (0.220 m/s). Coefficient of friction (COF) of as-deposited and heat-treated coatings at various test temperatures are shown in Figure 4.15a and 4.15b respectively. It is found that friction performance of both set of coatings is quite similar. The COF at RT and 100°C is minimum and maximum respectively for both the coatings. Beyond 100°C, COF is found to decrease progressively with temperature. The COF at RT for heat-treated coatings is lower due to the higher hardness of the coating which results in lower area of contact at the interface. However, for elevated temperature tests, the grain softening phenomenon results in reduced shear strength of the interfacial layer. This also induces the grain boundary sliding thus reducing the friction of the coating.

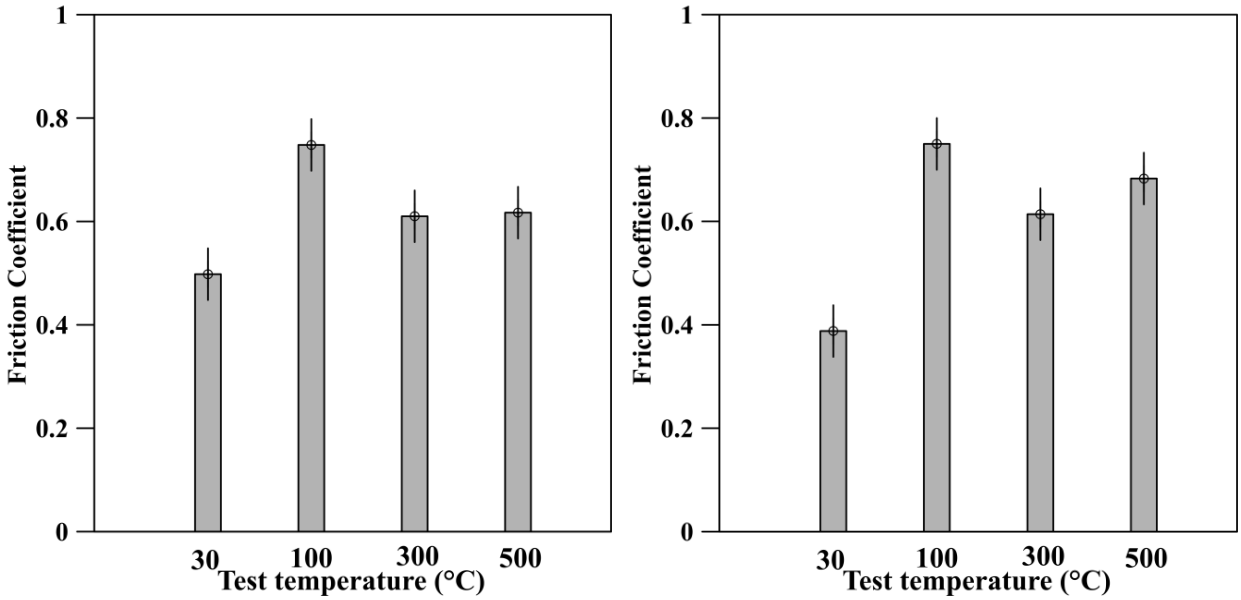

(a) (b)

Figure 4.15 Friction as a function of test temperature for (a) as-deposited and (b) heat-treated Ni-P-W coating

Figure 4.16 represents the evolution of COF with respect to sliding duration for the Ni-P-W coatings tested under different temperatures at a constant sliding velocity (0.220 m/s) and load (10N) for duration of 300s. It is found that COF remains quite stable (between 0.4 to 0.8) for the entire test duration. The maximum variation is observed for 100°C test temperature. For 300°C and 500°C tests particularly, COF exhibits remarkable stability after the initial transient run-in

time for both as-deposited and heat-treated coatings. It is interesting to know that the structural changes encountered by the coating because of exposure to high temperature, although influences the hardness and wear performance of the coating, does not affect its friction performance

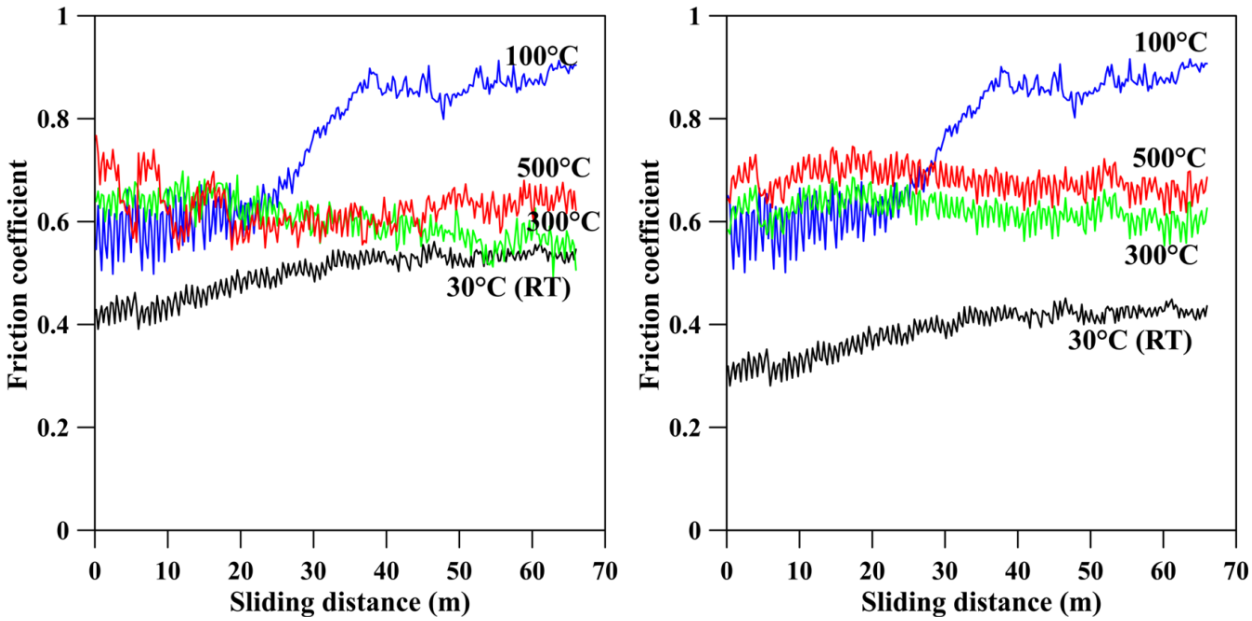

Figure 4.16 Evolution of COF of at room and elevated temperatures for (a) as-deposited and (b) heat-treated Ni-P-W coating

4.3.6.2 Wear performance of as-deposited and heat-treated Ni-P-W coating at different test temperatures

Figure 4.17 illustrates the wear results of the coatings. From the figure, it is evident that heat-treatment increases the wear resistance of electroless Ni-P-W coating which is reflected in the lower wear rate of heat-treated coatings. The reduction in the wear rate of heat-treated coatings is seen to reach up to 50% of that of as-deposited coatings. The wear rate of heat-treated coatings is lowest at RT and its same for as-deposited coatings. This may be explained based on the microstructural state of the coating. As it is seen that the present coating is amorphous/nano-crystalline in as-deposited condition with hardness around 670$HV_{0.1}$, the coating offers descent wear resistance under room temperature test. But at elevated temperature tests, due to real time heat-treatment, the coating gains sufficient hardness which increases its wear resistance. However, considering the heat-treated coating, where the coating has already gained the necessary hardness due to precipitation of harder phases, the test at RT show low wear rate. Increase in test temperature causes massive scale deformation of the surface that lead to an applied stress value crossing the yield strength of the material. This acts result in severe adhesion and causes lower wear resistance. Similar kind of phenomenon is also observed with an increase

in the heat-treating temperature higher than 400°C which contributes to the increase of the matrix ductility and, therefore, to its softening and massive wear.

It is interesting to note that the as-deposited coating at 100°C experiences the highest wear rate. In case of heat-treated coatings, a progressive increase in the wear rate is observed with the increase in the operating temperature. The wear rate at higher operating temperature is found to be almost double of that at RT for this coating. However, apart from 100°C test, as-deposited coatings exhibit similar wear rate for all the temperatures. For a better understanding of the friction and wear characteristic of Ni-P-W coatings, SEM and EDX are conducted on the post test samples. Moreover, micro hardness tests before and after wear tests are done in order to observe the presence of any correlation between the hardness results and that of wear results.

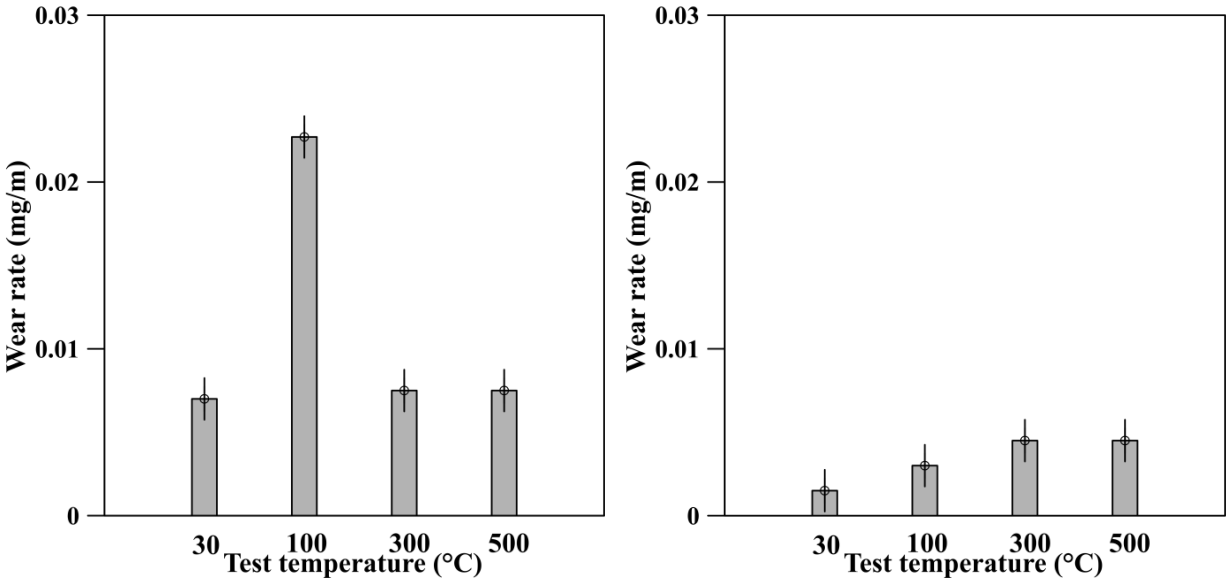

Figure 4.17 Wear as a function of test temperature for (a) as-deposited and (b) heat-treated Ni-P-W coating

SEM image indicating the wear along with the direction for Ni-P-W as-deposited coatings tested at 500°C is represented in Figure 4.18. The coating clearly exhibits linear wear tracks as soft coating is subjected to abrasion by harder counter face. Along with that, few removal of material in the form of pits and prows is also detected which arise due to breakage of bonding in between coating and counter face asperities. Linear tracks are prominent which is an indication of abrasive wear pattern as well as pits and prows are symbolic for adhesive wear mechanism. So, the wear mechanism at 500°C for the coating is mostly governed by abrasive and partly by adhesive wear mechanism. Few dark spots is visible, indicating the formation of oxide layer during the test conducted at high temperature. Further to prove the fact as well as to indicate other elemental distribution, line EDX (as shown by line AB in Figure 4.18a) is carried

out. The results indicating the detail variation of each element across the chosen line (AB of approx 200 µm) is provided in Figure 4.18b for Ni-P-W coating. Presence of oxygen signifying the fact of high temperature oxide formation as claimed by other researchers (Masoumi et al., 2012; Mukhopadhyay et al., 2018a; 2018b; 2018c) in the field of high temperature coatings. Existence of nickel and the other primary coating elements proves the survival of those coatings at elevated temperature. Amount of Fe comes as a result of interaction with counterface material which may provide a mixed mechanical layer. It may be also the reason behind the lower wear rate at elevated temperature.

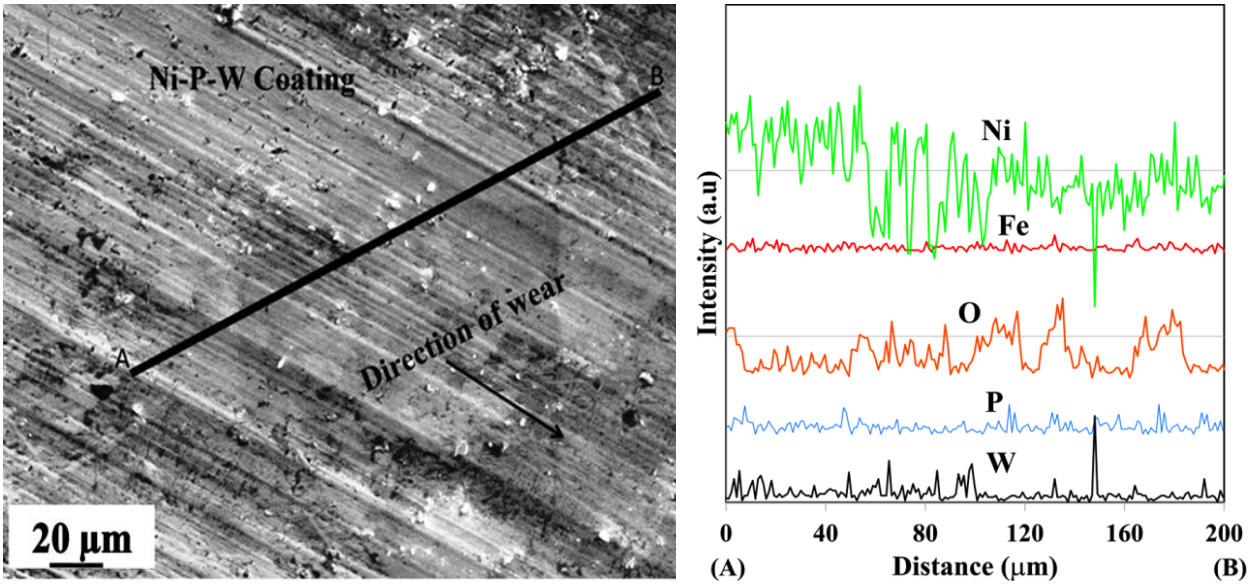

(a) (b)

Figure 4.18 (a) SEM image indicating the line for EDX study in the direction of wear and (b) corresponding EDX line analysis for Ni-P-W coating

4.3.6.3 Wear mechanism study

In order to understand the underlying mechanisms defining the tribological behavior of the coating, the worn out surface of the samples are observed under SEM (Figure 4.19). This is also significant in assessing the wear mechanism via EDX (Figure 4.20) that the coating experiences with its counterpart. The as-deposited coatings exhibit linear wear tracks which indicate the occurrence of abrasive wear mechanism (Figure 4.19a). Abrasive wear occurs when hard rough surface or particles scratches across a softer surface. In the present case, the hard counterface having a defined roughness (Ra = 0.20) abrades the softer coating. Besides the wear track, small patches are also found to be distributed over the coating surface. These small pits and prows are because of removal of material due to breakage (shear) of bonding between the coating and the counter face asperities. This indicates that adhesive wear mechanism is also partly responsible in governing the wear of the coating. The adhesive wear is mainly dependent

on physical and chemical factors such as material properties, presence of corrosive atmosphere or chemicals, as well as the dynamics such as the velocity and applied load.

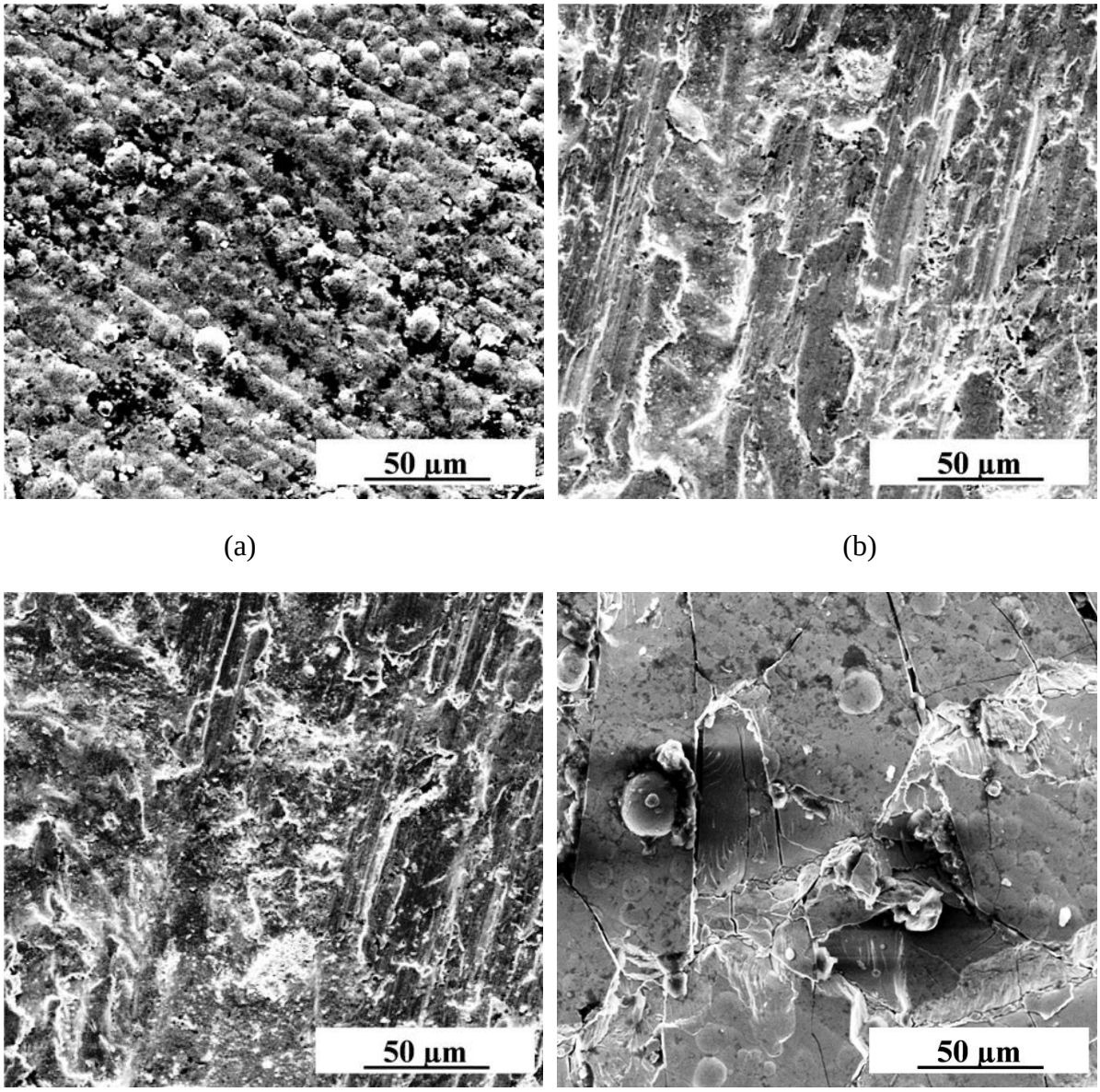

Figure 4.19 SEM (secondary electron) micrograph of worn specimen of as-deposited electroless Ni-P-W coating tested at (a) 30°C (b) 100°C (c) 300°C and (d) 500°C

To further establish the role of elevated temperature on the wear mechanism, the worn out surface of the samples are observed under SEM. For brevity, only the samples exhibiting pertinent and interesting features post wear test are presented in this section. The SEM images of as-deposited samples are shown in Figure 4.19. The nodular morphology of the coating is no longer visible post wear test. For samples tested at elevated temperature (100°C and 300°C),

random torn patches typical to delamination is visible which again directs towards adhesive wear mechanism. Now, adhesive wear is a very serious form of wear characterized by high wear rates and a large unstable friction coefficient (Stachowiak & Batchelor, 1993).

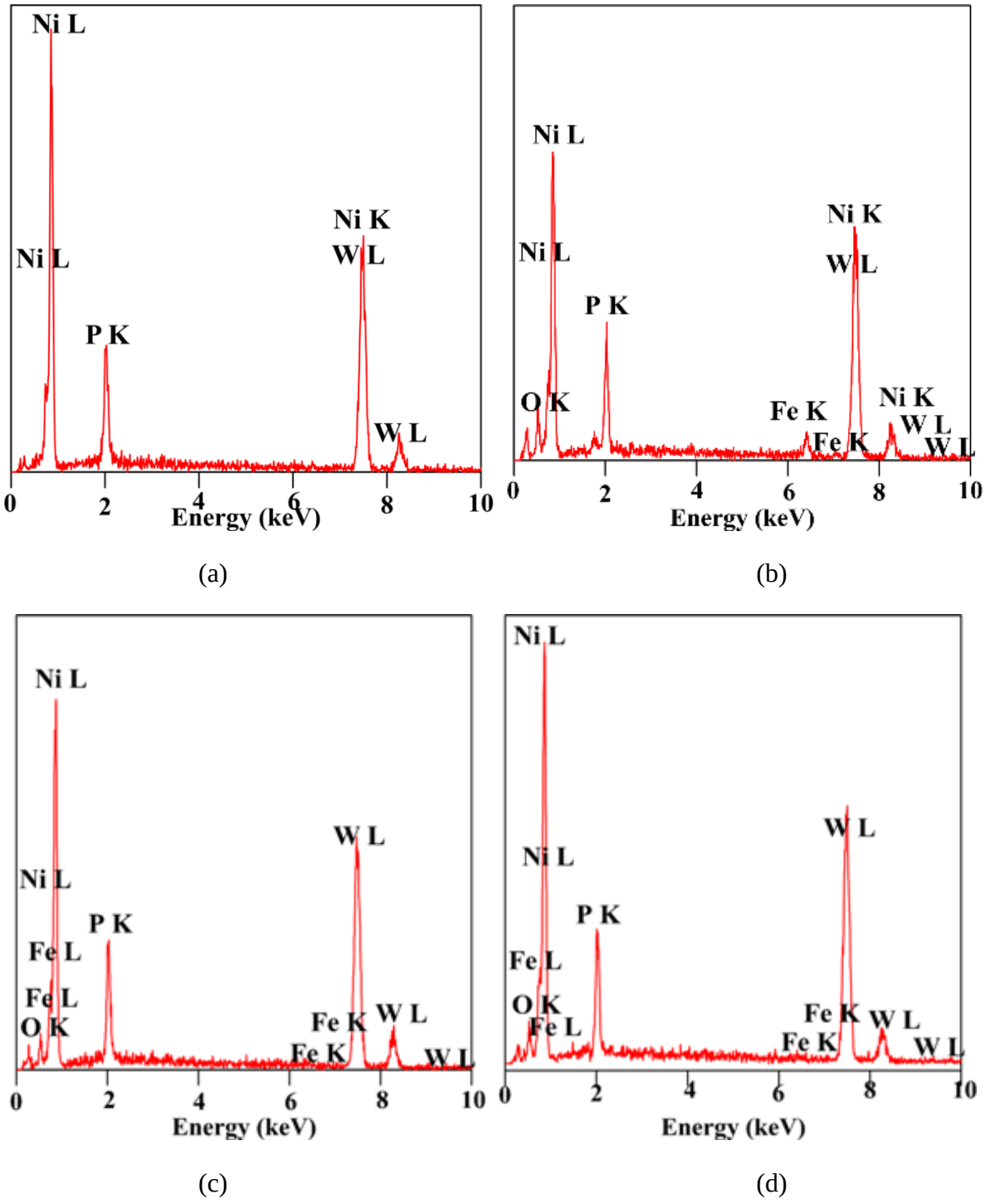

Figure 4.20 EDX spectrum of worn specimen of as-deposited electroless Ni-P-W coating tested at (a) 30°C (b) 100°C (c) 300°C and (d) 500°C

Thus, the present analysis explains the abrupt rise in COF and wear rate of the samples tested particularly at 100°C as seen from Figure 4.15a and Figure 4.17a. Now, adhesive wear increases as the hardness of the bodies in contact decreases (Stachowiak & Batchelor, 1993). Now, it is quite natural that during sliding, high amount of heat is generated at the interface which is further aided if the operating temperature is elevated. Thus, it can be said that the as-deposited sample during the test at 100°C is exposed to conditions which forces it to display a higher wear rate. The relatively higher wear resistance at 300°C compared to 100°C might have occurred due to the formation of harder phosphide phases. Coupled with this is the stable lubrication provided by the oxide layer formed during the test. The presence of oxide layer can be confirmed by the detection of oxygen in EDX results (Figure 4.20).

The worn morphology of the coatings at 500°C does not exhibit signs of much delamination but instead micro cracks start to appear on the coating surface (Figure 4.19d). These cracks may have appeared as a result of the high thermal stress coupled with shear stress transmitted to the sub-surface layer (during testing) due to the variation of the load experienced at the area of contact (Le´on et al., 2003).

The EDX of the worn surface of the sample tested at 500°C (Figure 4.20d) shows the presence of both oxygen as well as iron. Now, existence of oxygen indicates towards formation of oxide layers as also observed for the 300°C tested sample. However, iron in the coating may have come through two pathways. Firstly, adhesive wear may indicate high mutual solubility of nickel and iron atoms (from the ferrous counter face). Secondly, the iron may have come from the steel substrate itself through diffusion. Now, diffusion is a result of the interactions between the coating and the substrate interface and which is propelled by thermal energy. However, chances of the diffusion are remote as the exposure of the coating to high temperature is for a very short duration. Hence, it can be confirmed that adhesive wear co-exist along with abrasive wear while governing the wear behavior of Ni-P-W coatings which is in agreement with the observation of other researchers (Staia et al., 2002).

To highlight the effects of elevated temperature test as well as to maintain brevity, samples post 500°C test are further considered for AFM and the corresponding results indicated by Figure 4.21. The 2D and 3D surface morphology of post test samples is represented by Figure 4.21a and b respectively. It clearly indicates a rough surface with deep grooves along with micro-ploughing. Wear tracks in the direction of sliding along with material removal is also noticeable. The elemental map of worn as-deposited coating tested at 500°C is shown in Figure 4.22. Uniform distribution of nickel, phosphorous and tungsten can be seen from the images which imply the proper existence of coating even after the wear test. The presence of oxygen proves the formation of tribo-oxide film as discussed previously. The oxide film also uniformly covers the surface of the coating as evident from the mapped image.

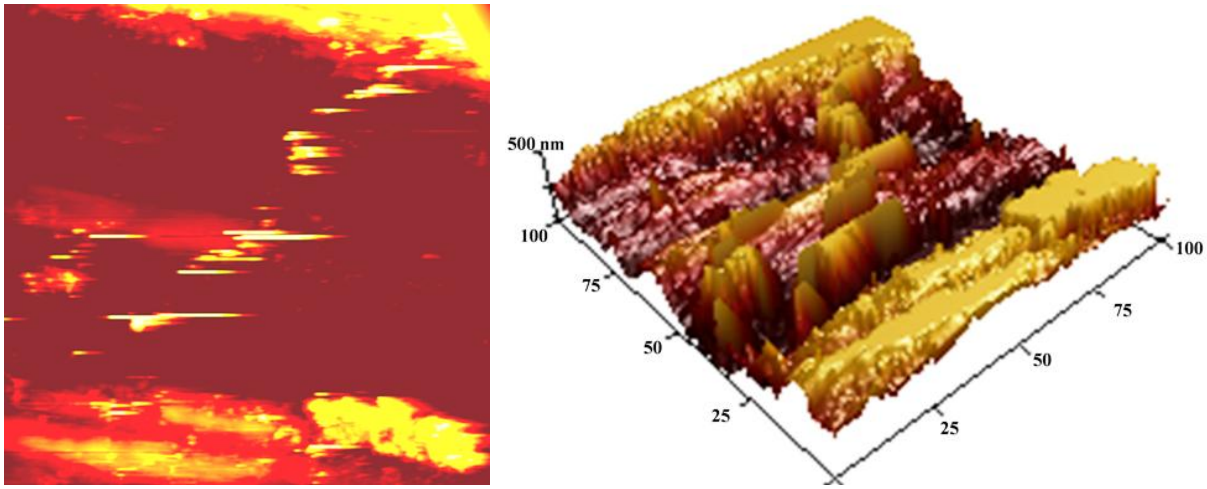

(a) (b)

Figure 4.21 AFM morphology (a) 2D and (b) 3D of as-deposited Ni-P-W coating tested at 500°C

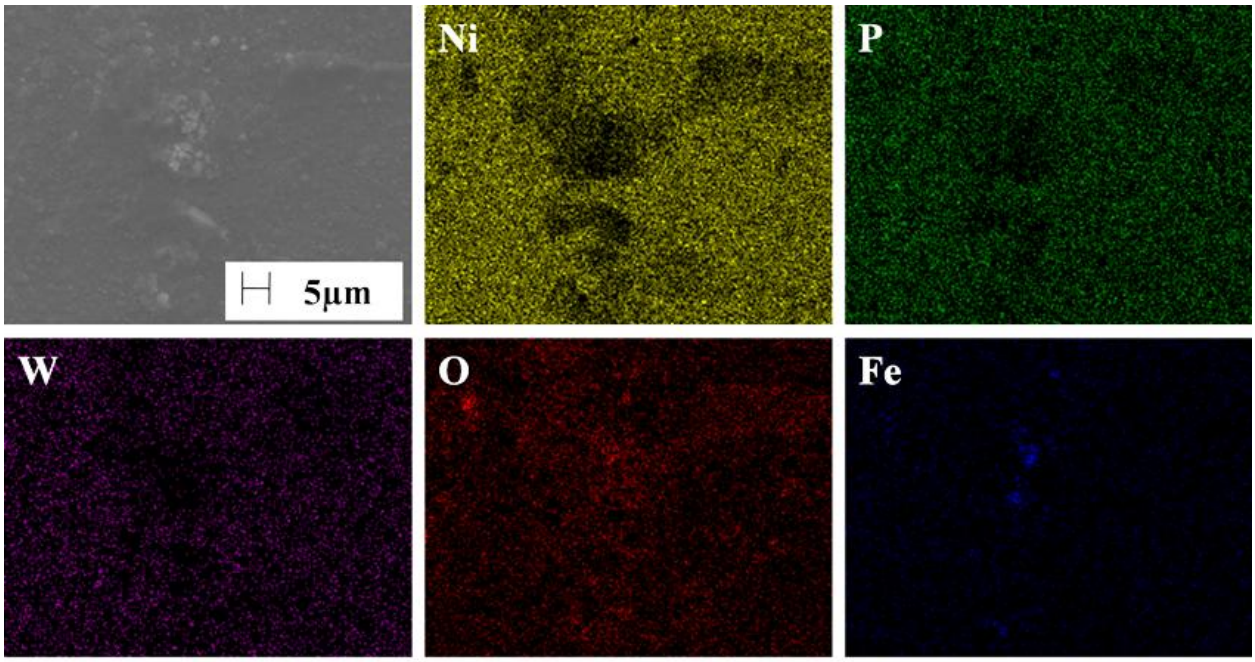

Figure 4.22 EDX maps of worn specimen of as-deposited Ni-P-W coating tested at 500°C

The wear mechanism of the heat-treated Ni-P-W coatings at room temperature (30°C) and at elevated temperatures of 100-500°C is investigated through SEM micrographs and EDX of the worn surfaces. The trends of tribological behavior of the coatings exhibited in Figure 4.15-4.17 are further consolidated by the SEM images of the wear scars and its corresponding EDX results. The presence of pits and prows over the wear tracks are quite easily noticed for the sample tested at room temperature (Figure 4.23a). Pits and prows are characteristic of adhesive

wear mechanism whereas wear tracks denote the occurrence of abrasive wear phenomenon. Hence, it can be said that the coating encounters a mixed wear mechanism under room temperature tests. SEM micrograph of the wear zone of the sample (tested at room temperature) and corresponding EDX spectrum is presented in Figure 4.23a and Figure 4.24a respectively.

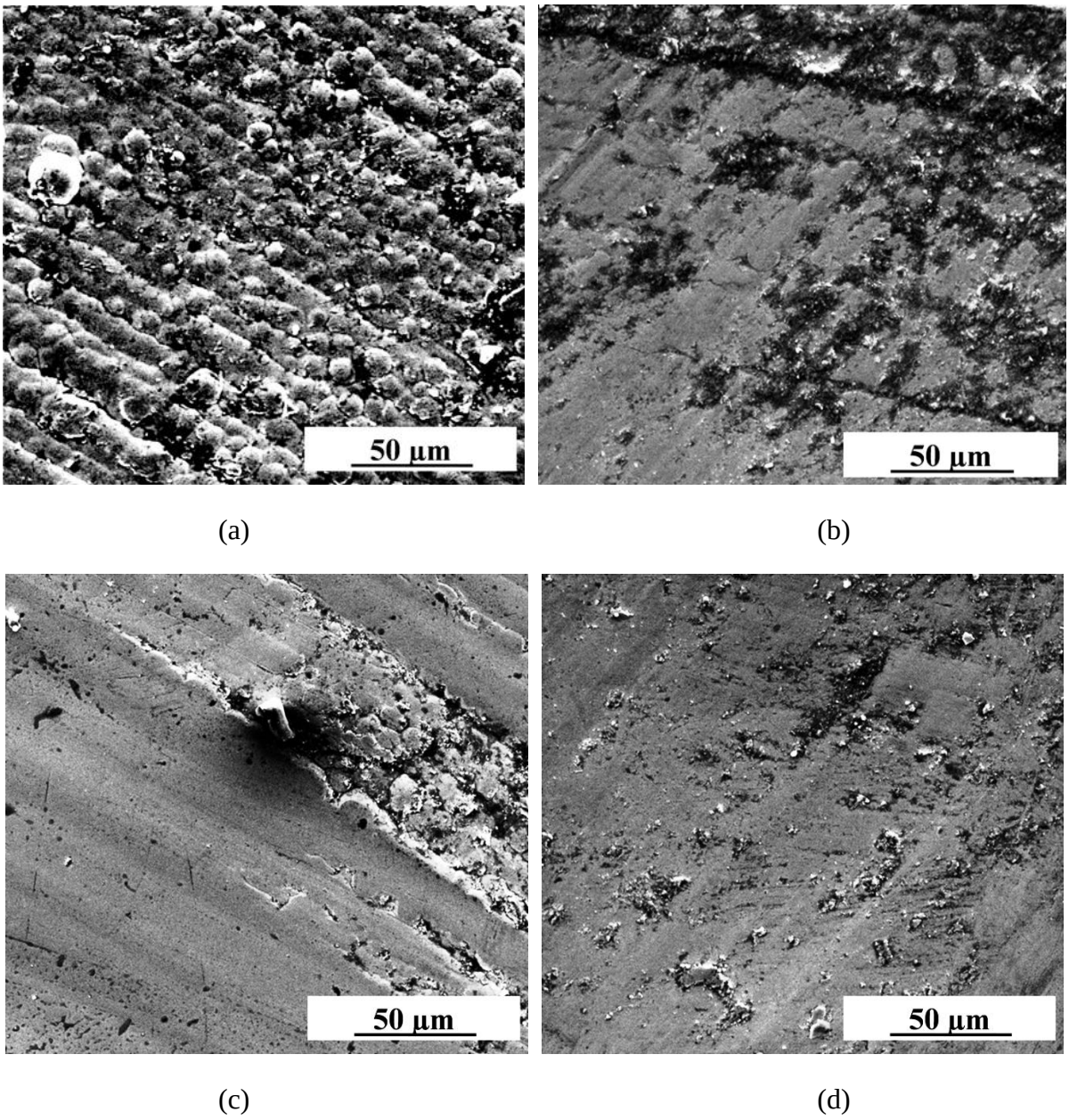

Figure 4.23 SEM (secondary electron) micrograph of worn specimen of heat-treated electroless Ni-P-W coating tested at (a) 30°C (b) 100°C (c) 300°C and (d) 500°C

The EDX plot indicates the post wear elemental distribution which consists of mostly the original coating constituents. Ploughing and micro cutting together with torn patches in the direction of sliding can also be observed for coating tested at 100°C (Figure 4.23b) which again

point towards a mixed wear mechanism. The uneven wear zone also supports towards the high COF observed at this condition (Figure 4.15b). The EDX of the wear zone (Figure 4.24b) shows the presence iron which supports the occurrence of abrasive wear as the iron must have come from the counterface (steel part) due to high mutual solubility between nickel and iron. Thus, adhesive wear seems to be the dominant wear mechanism at this test condition. Moreover, the presence of oxygen in EDX results point towards the formation of oxides in the wear zone. At 300°C, test temperature the wear surface again exhibits micro-cutting and micro-ploughing together with torn patches (Figure 4.23c). However, overall coating surface appears to suffer ductile failure with a high degree of plasticity in the direction of sliding. The EDX spectrum (Figure 4.24c) again exhibits the presence of oxygen and iron. The coating tested at 500°C again exhibits parallel grooves along with micro-ploughing (Figure 4.23d) which is again an indication of an abrasive wear phenomenon. However, there is a distribution of materials in the form of small spots on the entire coating surface which may be the wear debris being welded to the coating surface due to the pressure at the contact surface and under immense heat coming from the heated counterface. There are also some blackish regions which indicate towards heavy oxidation under 500°C (corresponds mainly to NiO), as the same observed by several researchers (Masoumi et al., 2012; Li et al., 2013; Alirezaei et al., 2013b; Franco et al., 2016).

The presence of oxygen in the EDX plot (Figure 4.24d) also supports this claim. Overall, it can be said that both adhesive as well as abrasive wear govern the wear mechanism of the Ni-W-P coatings tested at elevated temperatures. High temperature is generated at the coating-counterface contact region due to the heated counterface which is augmented by friction heating due to sliding of the workpiece. Thus, the wear debris generated undergoes local hardening and getting trapped between the coating and the counterface are responsible for creating the grooves on the coating surface. At the highest temperature (500°C) however, the debris tend to get attach to the coating surface as observed from Figure 4.23d. The presence of oxygen in the EDX spectrums (Figure 4.24b, 4.24c and 4.24d) confirms oxidation of the coatings and the formation of a tribo-oxide layer during sliding wear tests at 100°C, 300°C and 500°C respectively. From the investigation of the wear mechanism of heat-treated Ni-P-W coatings it can be seen that the mechanism changes from adhesive to a mixture of adhesive and abrasive from RT to 500°C.

To understand the underlying facts of elevated temperature test in better way as well as to maintain brevity, heat-treated samples post 500°C test are consolidated via AFM and elemental mapping assessment and the corresponding results indicated by Figure 4.25 and 4.26 respectively. The 2D and 3D surface morphology of post test samples is represented by Figure 4.25a and 4.25b respectively. It clearly indicates a rough surface along with micro-ploughing. Wear tracks in the direction of sliding along with material removal is also noticeable.

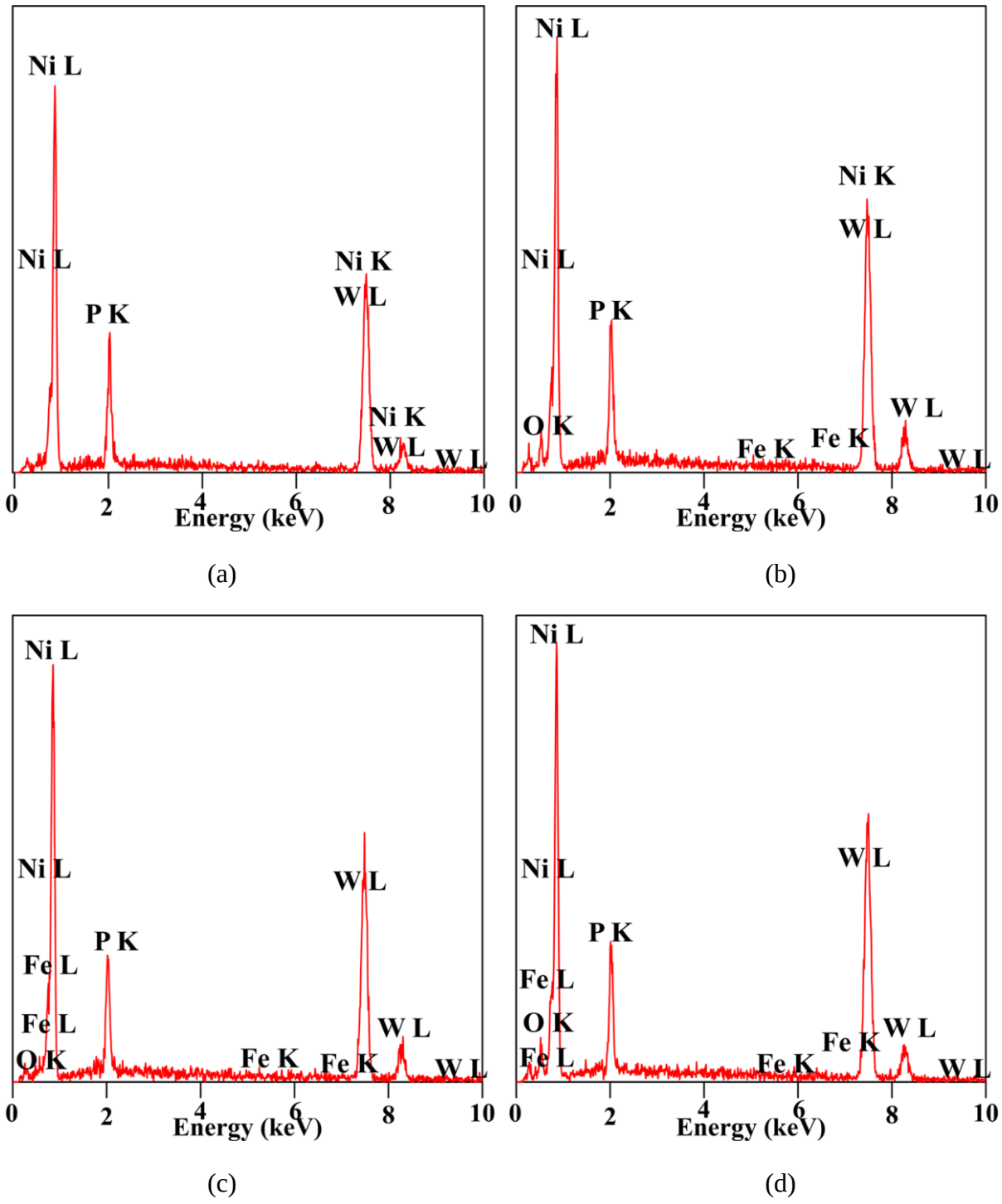

Figure 4.24 EDX spectrum of of worn specimen of heat-treated electroless Ni-P-W coating tested at (a) 30°C (b) 100°C (c) 300°C and (d) 500°C

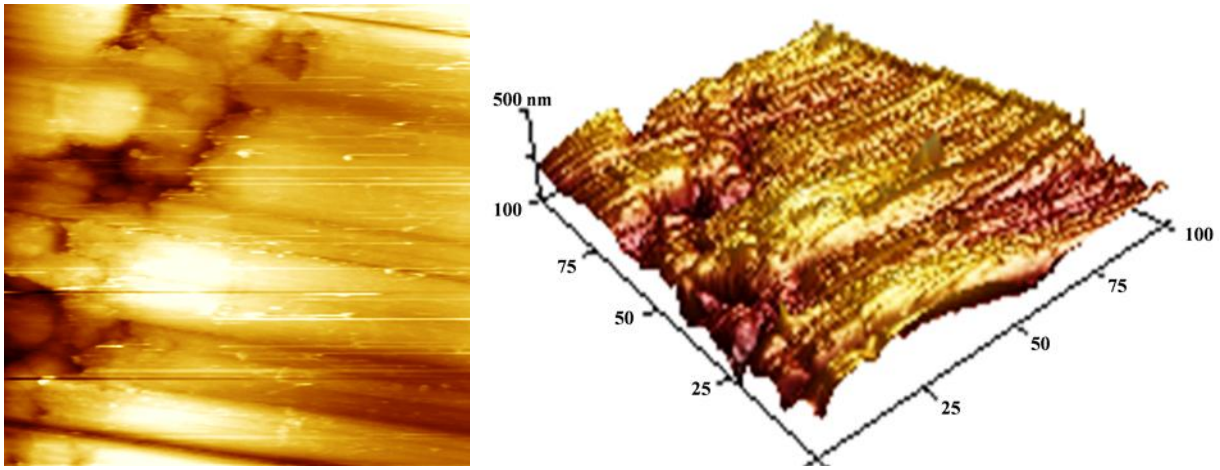

(a) (b)

Figure 4.25 AFM morphology (a) 2D and (b) 3D of heat-treated Ni-P-W coating tested at 500°C

The elemental map of worn heat-treated coating tested at 500°C is shown in Figure 4.26. Uniform distribution of nickel, phosphorous and tungsten can be seen from the images which imply the proper existence of coating even after the wear test. The presence of oxygen proves the formation of tribo-oxide film as discussed previously. The oxide film also uniformly covers the surface of the coating as evident from the mapped image. For the 500°C, iron shows very weak signal (Figure 4.26) in the image which implies very less occurrence of adhesive wear whose remnants can be observed from discrete small patches on the coating post test.

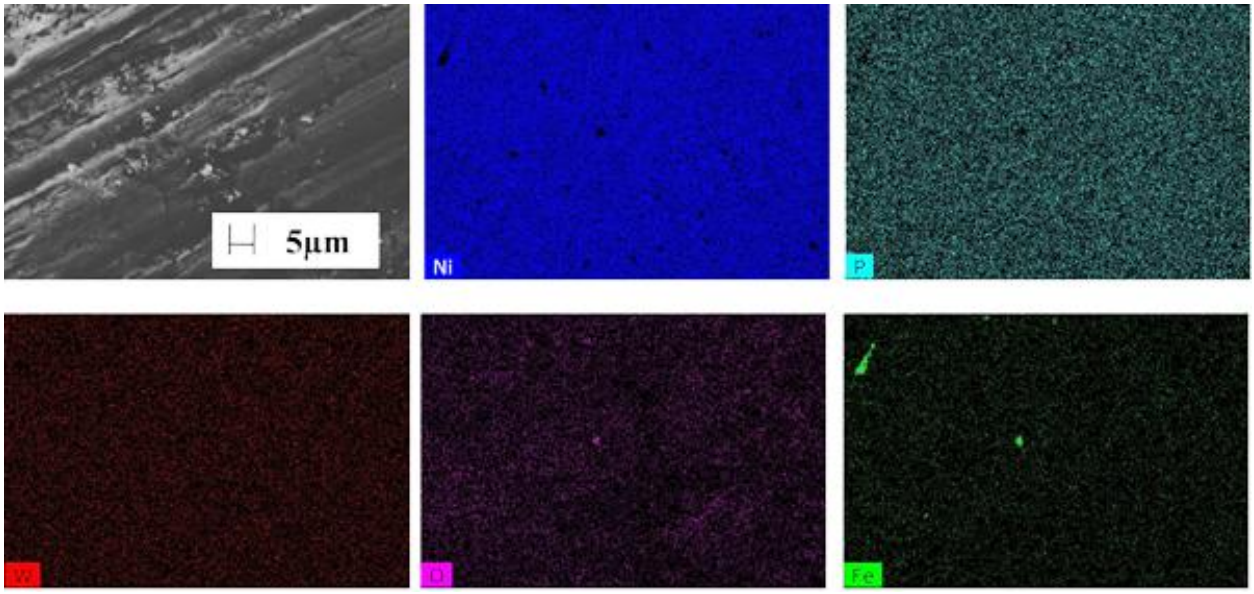

Figure 4.26 EDX maps of worn specimen of heat-treated Ni-P-W coating tested at 500°C

4.3.6.4 Phase transformation and hardness change

Several researchers claim commencement of phase transformation because of in situ heat-treatment during elevated temperature test of EN coatings (Franco et al., 2016; Mukhopadhyay et al., 2018a; 2018c). Detailed XRD study of post wear Ni-P-W coatings are conducted to understand the reality of the claim. Phase transformation study of mainly as-deposited coatings tested at elevated temperature are examined and explained in Figure 4.27. Heat-treated specimens are excluded for XRD analysis, as they are in crystalline state, so complicated to identify the effect of elevated temperature test. The samples subjected to room temperature test causes insignificant changes in crystal structure and observed similar to that presented by as-deposited coating as indicated in Figure 4.11. Wear behavior of as-deposited coatings during room temperature test is solely controlled by the plastic deformation occurs during the test as stated earlier. Figure 4.27a represents the phase structure of post wear Ni-P-W coatings tested at 100°C. Nickel peak (111) is getting sharper compared to as-deposited coating, may be because of phase transformation. Microstructural changes occurs at 100°C is due to combination effect of plastic deformation and test temperature. Further crystallographic change is observed for coatings tested at 300°C, illustrated by Figure 4.27b. Crystalline Ni_3P is visible along with Ni-W solid solution which clearly indicates the phase transformation of the as-deposited coating during the 300°C wear test. The formation of phosphide phases of nickel along with Ni-W solid solution formation are accelerating with the increase in test temperature which reflects in Figure 4.27c. It may act as a barrier against dislocation which leads to improve the tribological performance at elevated temperature.

High temperature causes to decrease wear because of precipitation of nickel phosphides phases along with Ni-W solid solution. Further the phase transformation effects are justified by thorough post wear hardness evaluation of as-deposited and heat-treated samples, presented in the next part of this section. The results obtained through post wear XRD of as-deposited Ni-P coating is well agreement with the earlier results as is mentioned in the wear mechanism section. The point EDX (Figure 4.20c and 4.20d) clearly indicates the presence of inter diffused Fe particle. Though the presence of Fe particles or inter diffusion phenomenon is not clear in XRD study. The detailed wear mechanism is also explained by the EDX maps (Figure 4.22) of post wear test sample of as-deposited coatings tested at 500°C, clearly indicating the presence of each element including Ni, W and P, and thus justifying the existence of the coating at elevated temperature. The present discussion thus proves the phase transformation scenario as an outcome of short duration heat-treatment during the elevated temperature wear test. The present study provides a qualitative idea about high temperature tribology of Ni-P-W coatings. Further studies such as X-ray photoelectron spectroscopy (XPS) can be conducted for thorough examination on oxide layer formation, that controls tribological performance of the coatings.

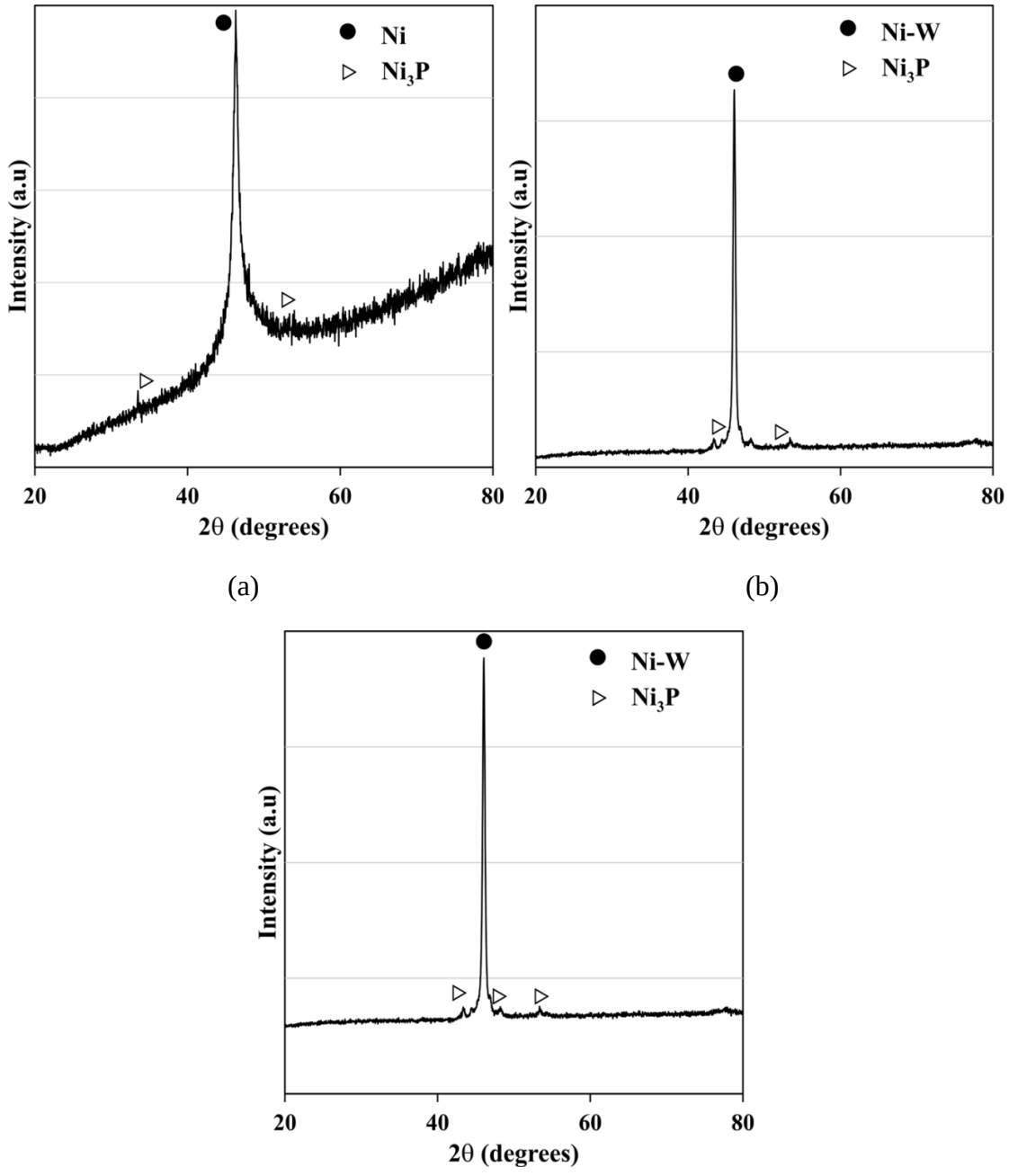

Figure 4.27 XRD analysis of as-deposited Ni-P-W coating post-wear test at (a) 100°C, (b) 300°C, and (c) 500°C

The hardness of the coatings before and after wear test for all the temperatures is measured and exhibited in percentage increase form in Figure 4.28. It is seen that hardness increases in almost all the cases after the test. Another interesting thing to note is that in general increase of hardness is more for as-deposited coatings compared to heat-treated ones. Moreover, hardness enhancement is more at higher operating temperatures with almost 46% increase at

500°C compared to the RT test. These observations indicate that tribological tests at higher temperatures is similar to short duration heat-treatment which induces structural changes in the coating especially at temperatures higher than crystallization temperature. Nickel phosphide and nickel tungstate are formed for the samples tested at 500°C as evident from the XRD analysis of post test samples. Formation of harder phases provides a barrier to the movement of the dislocations which show up as increased hardness and wear resistance of the coating. From Figure 4.28, it can also be seen that increase in hardness for as-deposited sample is more compared to heat-treated samples which is quite obvious considering that heat-treated coatings have already gained the necessary hardness and further improvement in hardness is less. Based on this however it would be improper to assume that as-deposited Ni-P-W coating are also suitable for high temperature tribology based applications as the initial hardness of as-deposited coatings is far lesser compared to that of heat-treated coatings. Moreover, tribological operations at elevated temperature can never be a substitute for proper heat-treatment cycle as the maximum hardness gained for as-deposited sample is quite less compared to that for heat-treated ones.

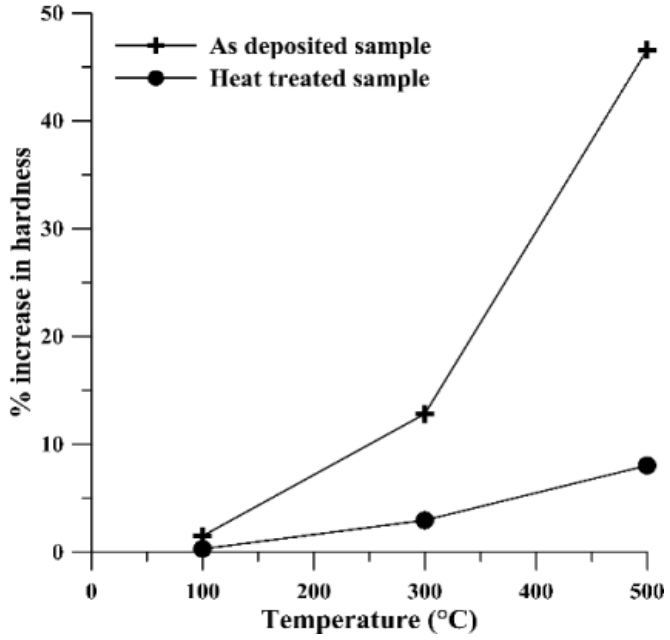

Figure 4.28 Percentage increase in hardness after high temperature tests of Ni-P-W coating

4.4 Conclusion

This chapter attempts to present in a detailed manner the tribological behavior of electroless Ni-P-W coatings under elevated temperature conditions. The coatings are developed in the laboratory and friction and wear tests are carried out in a pin on disc tribometer. Both the as-deposited and heat-treated coatings exhibit a uniform distribution of the constituent elements. Upon heat-treatment the coatings turn crystalline with increase in the grain size. The Ni-P-W coating showed an amorphous structure in the as-deposited state and exhibited a relatively low hardness of approximately 670 $HV_{0.1}$. As temperature was raised to 400°C, the hardness

increased to 1090 $HV_{0.1}$ due to the precipitation of Ni and Ni_3P in the amorphous matrix. Presence of stable Ni and Ni_3P was identified for the heat-treated deposits (400°C/1 h) containing lower amount of W and higher amount of P. Higher crystallization temperatures were obtained due to W co-deposition in Ni-P matrix. Ni-P-W coatings are found to display good hardness and they are found to remain stable under elevated temperature tests. In fact the exposure to high temperature during the tests act like short duration heat-treatment inducing microstructural changes in the coating (especially for as-deposited coatings) which further increase the hardness and wear resistance of the coating. The as-deposited samples tested at 500°C display an increase of about 46% hardness compared to that before the test. Heat-treated coatings on the other hand display a stable tribological performance under elevated temperature tests. Friction performance of the coatings does not seem to be highly affected by the elevated operating temperatures. However, elevated temperature is found to affect the wear behavior of as-deposited coatings. Interestingly, coatings display low wear rate when subjected to high operating temperatures. Again applied load and sliding velocity also exhibit marginal influence over the friction and wear behavior behavior of the coatings particularly at higher temperatures. In high temperature tests it is observed that wear rate increases with the increase in test temperature. The increase in applied load is also found to negatively impact the wear resistance of the coating. However, wear rate is almost inversely proportional to the sliding velocity under a constant value of load. Coefficient of friction does not seem to be affected very much under elevated temperature tests. The SEM micrograph of the corroded and worn surface of the coating reveals that both abrasive and adhesive wear phenomenon is present as wear mechanism for elevated temperature. Oxide formation is another interesting phenomenon for the coatings tested under elevated temperatures. Study of worn surface reveals that the wear is governed by both abrasive and adhesive wear mechanisms. Moreover, the formation of oxide layers on the coating at high temperature is observed which is also believed to influence the tribological behavior of the coating.

Chapter 5

High temperature tribology of Ni-P-B coating

5.1 Need for Boron (B) Inclusion

Essential characteristics of hypophosphite reduced electroless nickel baths (Ni-P) are ease of control, low cost and good corrosion resistance. Whereas, borohydride based baths (Ni-B) provides better reduction efficiency as well as plating rate but probability of decomposition and cost of operation is higher. The major advantages of borohydride-reduced baths are its hardness and better wear resistance in the as-deposited condition (Duncan & Arney, 1984). Electroless Ni-P and Ni-B coatings both are found to be amorphous in as-deposited condition but transformed to crystallite with heat-treatment through precipitation of hard particles such as nickel phosphide phase (Ni_3P) and nickel boride phase (Ni_3B) respectively (Guo et al., 2003; Keong & Sha, 2002; Sankara Narayanan & Seshadri, 2004). Cauliflower type surface morphology and columnar growths of Ni-B causes to enhances lubricity and thus improves the wear properties (comparable with hard chromium) due to reduction in the contact area (Contreras et al., 2006; Riddle & Bailerare, 2005). Ni-B coating has decent anti-corrosive (0.058 mm/year) properties but not satisfactory in comparison with Ni-P (0.019 mm/year). Heat-treatment in vacuum provides an improvement in hardness but is associated with further decrease in corrosion rate (0.135 mm/year) for Ni-B coating (Dervos et al., 2004).

Both Ni-P and Ni-B coatings proved their supremacy individually and accepted globally in different areas like automotive, chemical, aerospace, electrical and electronics sectors. But the idea to gather up properties of both the coatings for improvement of surface brings electroless Ni-P and Ni-B in the form of duplex coatings. Hardness, wear strength and corrosion properties of the duplex coating is better than Ni-P and Ni-B coatings in both as-deposited and heat-treated condition but it largely depends on outer layer (Sankara Narayanan et al., 2003; Zhang et al., 208; Vitry et al., 2012c).To facilitate all the complementary properties provided by both types of coating simultaneously, electroless Ni-P-B can be considered as a reasonable choice. There are few number of research articles available which works on development and characterization of ternary electroless Ni-P-B coating (Venkatkrishna & Sankara Narayanan, 2013; Venkatkrishna et al., 2014). Role of boron is dominating phosphorus throughout the Ni-P-B coating and characteristics are mostly similar to Ni-B. Most of the studies related to as-deposited and heat-treated Ni-P-B coatings report the development with coating characterization and mechanical property evaluation at room temperature. The friction and wear performance of Ni-P-B coatings at high temperature mostly remains unaddressed. Thus, the present investigation is aimed to gather knowledge of the tribological phenomenon at ambient condition and elevated temperature for Ni-P-B coatings. The results of both room temperature and high temperature operations are

compared. The morphology, composition, surface topography and microstructural evolution of the developed coating and worn surface are examined along with wear mechanism investigation.

Table 5.1: Bath composition and operating conditions of Ni-P-B bath

Bath composition		**Working conditions**	
Nickel Sulphate ($NiSO_4.6\ H_2O$)	30 gl^{-1}	pH	14.0
Sodium Hypophosphite ($NaH_2PO_2.H_2O$)	18 gl^{-1}	Time	2h
Sodium Borohydride	0.8 gl^{-1}	Deposition temperature	95 ± 1°C
		Bath Vol.	200 ml
Sodium Hydroxide	90 gl^{-1}	Stirring speed	600 rpm
Ethylenediamine	90 gl^{-1}		
Lead Nitrate	14 mgl^{-1}		

5.2 Experimental Details

The order of the experiments used to develop the coating starting from substrate preparation and evaluation of the developed Ni-P-B coating through several characterisations are same as mentioned earlier in chapter 2. The basic components and operating conditions of Ni-P-B bath is provided in Table 5.1, where 0.8g/L sodium borohydride is added as a reducing agent as a source of boron electrons. Thus the development of Ni-P-B is arise from a combined hypophosphite and borohydride based bath, which causes an increase in reduction efficiency as well as deposition rate (Venkatkrishna et al., 2014). Activated samples are dipped into the prepared bath along with a magnetic stirrer and temperature sensor. The Ni-P-B bath kept at a temperature of 95°C in a hot plate cum stirrer for 1 hour at 600 rpm, as it decompose quickly due to borohydride concentration. After 1 hour the samples are deposited again in a fresh bath and total time for coating development is 2 hours. The approximate thickness comes as close to that of Ni-P after 2 hours of deposition for Ni-P-B coating. For constant thickness and bath load, coating development time and bath volume hold equal for all the samples. After proper development of the coating, it removed from the bath and washed in distilled water. Few specimen are placed in muffle furnace for 1 hour at 400°C followed by air cooling, for the purpose of heat-treatment. Effect of test parameters such as load and sliding velocity on wear (in

terms of mass loss/distance) and friction coefficient are evaluated under room temperature (30°C) and at high temperature (500°C) as following Table 3.2. From this analysis, suitable load and sliding velocity are decided after which they are subjected to a detail high temperature tribological tests by varying the temperature as mentioned in Table 3.3. The associated wear mechanism are also studied for high temperature tests for both as-deposited and heat-treated specimens through SEM and EDX. To highlight the effects of elevated temperature test as well as to maintain brevity, samples post test 500°C are further considered for AFM and elemental mapping study. Details XRD study of post wear Ni-P-B coatings are conducted to understand the commencement of phase transformation because of in situ heat-treatment during elevated temperature test of as-deposited coatings. The changes in hardness due to high temperature test for both kind of samples are also reported.

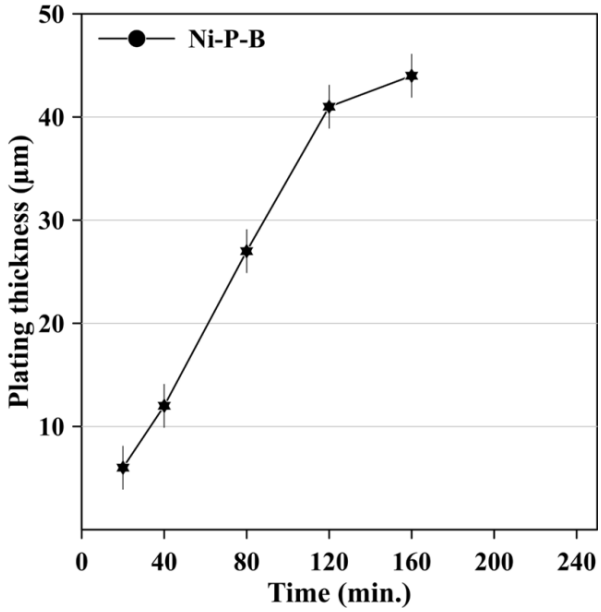

Figure 5.1 Deposition rate of Ni-P-B coating

5.3 Results and Discussions

5.3.1 Ni-P-B coating configuration

To deposit both “P” and “B” on the substrate surface use of sodium borohydride is essential in combination with the hypopsohphite agent(Venkatkrishna & Sankara Narayanan, 2013). Role of reducing agent is very important in determining film development rate as it is controlled via reduction efficiency. Plot of plating rate of Ni-P-B is presented in Figure 5.1, where it shows an increasing slope which means better deposition rate. The experiments after 2 hours causes no further improvement in coating thickness and the average deposition rate for Ni-P-B coating is found to be 18-21 μm/hour. The higher slope may be because of superior reducing agent, borohydride which provides higher reaction rate compared to other reducing agent.

Replenishment is not used for the salts but continuous monitoring of pH level is maintained throughout electroless plating process. Instead of replenishment over and above to maintain sufficient thickness for tribological assessment, double bath deposition method is used.

EDX analysis is performed on several points on the surface of as-plated and heat-treated Ni-B-P to determine the percentage by weight of the individual elements deposited in coating and the spectrum shown in Figure 5.2. The weight percentage of P is around 0.6-0.7% while that of B is 3.3-3.5% and the remaining is mostly Ni. The weight percentage of boron is higher than that of phosphorus and it is expected to play a dominating role. The B content also decides cyrstallinity as higher B (>7 wt%) provides amorphous and lower B (<5 wt%) is observed to be nanocrystalline (Vitry & Bonin, 2017b). In the present work (low-B range), it is therefore predictable that as-deposited coatings will exhibit nanocrystalline phases and which has been further investigated by carrying out SEM and XRD. Heat-treatment does not provide significant changes in P and B content but 2.9 % oxygen is observed probably because of oxide scale of Ni.

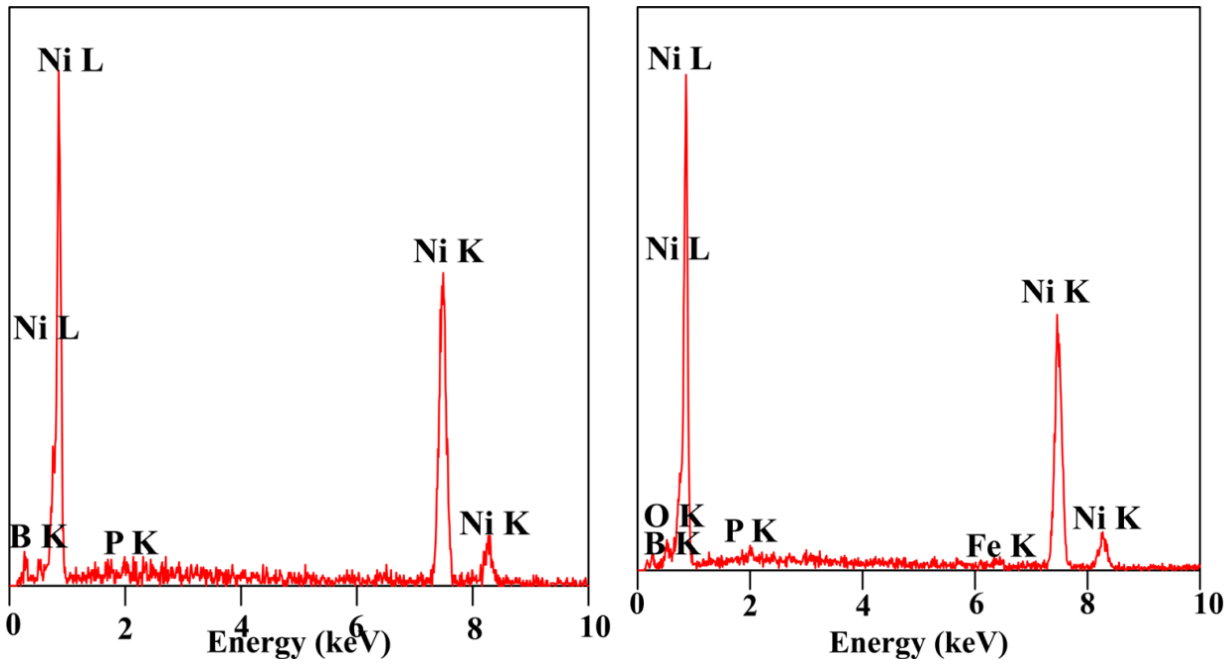

(a) (b)

Figure 5.2 EDX spectrum of (a) as-deposited and (b) heat-treated electroless Ni-P-B coating

To justify the result, further line EDX is conducted on the cross cut section of coating and the result is illustrated in Figure 5.3. The quantitative results indicating weight percentage of Ni, B, P, O and Fe is given in table inside Figure 5.3 (a). Composition profiles of Ni, P, B and Fe measured along the thickness Ni-P-B (Figure 5.3 (b)) coatings are performed through line EDX for detailed understanding of the elemental variation across the cross section.

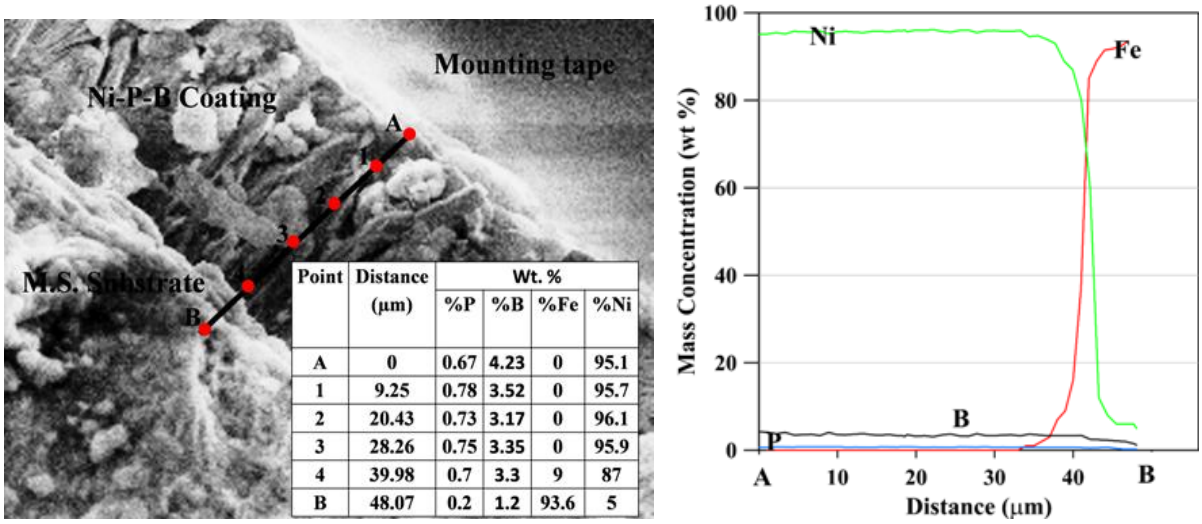

Point	Distance (μm)	Wt. %			
		%P	%B	%Fe	%Ni
A	0	0.67	4.23	0	95.1
1	9.25	0.78	3.52	0	95.7
2	20.43	0.73	3.17	0	96.1
3	28.26	0.75	3.35	0	95.9
4	39.98	0.7	3.3	9	87
B	48.07	0.2	1.2	93.6	5

(a) (b)

Figure 5.3 (a) SEM image showing line EDX (quantitative analysis included in table) and (b) detailed composition profiles of elements presents measured along the thickness of the Ni-P-B

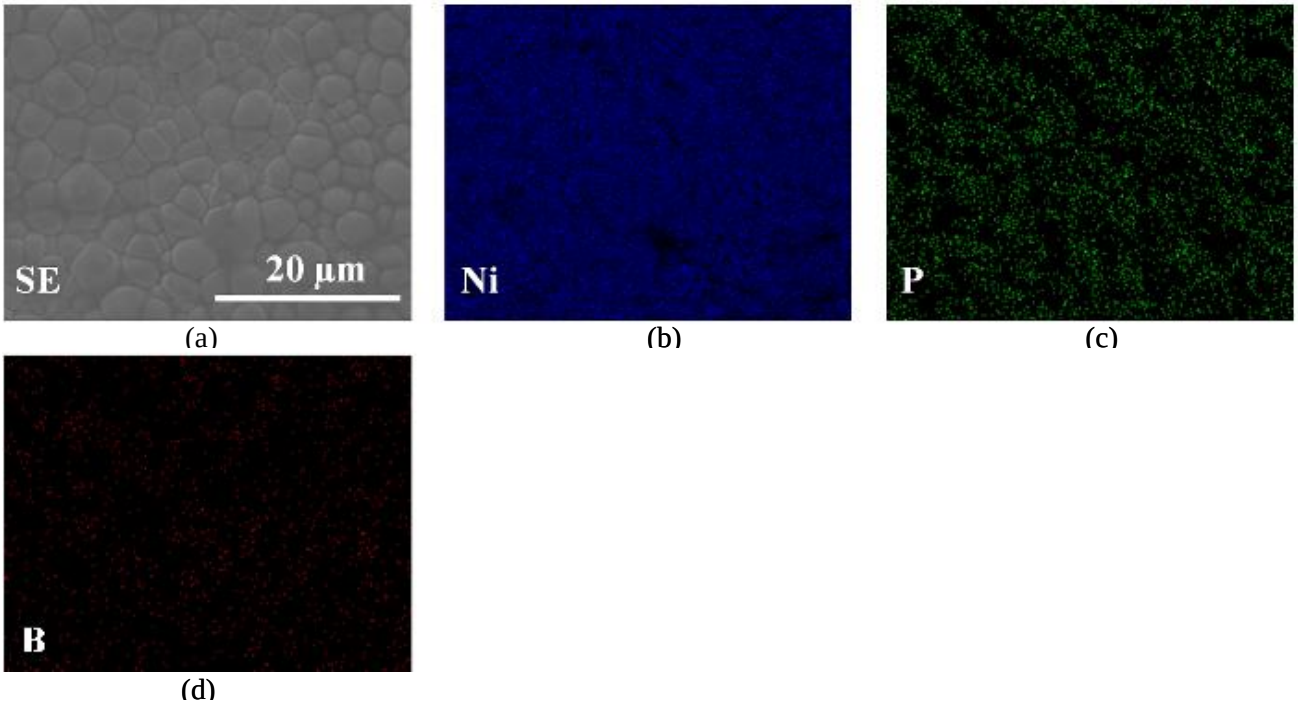

(a) (b) (c) (d)

Figure 5.4 EDX mapping analysis on the surface of the as-deposited Ni-P-B coating indicating (a) SE image (b) Ni (c) P and (d) B

Furthermore to confirm the presence of individual elements in the respective coatings, EDX mapping is carried out for as-deposited and heat-treated Ni-P-B coating and presented in Figure 5.4 and Figure 5.5 respectively. The cross-sectional SE image of as-deposited and heat-treated coating layer is shown in Figure 5.4a and 5.5a respectively. For more illustration, the

EDX mapping proves that the nickel, phosphorus, and boron are uniformly and homogeneously distributed in the Ni-P-B matrix as shown in Figure 5.4 for as-deposited and the same for heat-treated as presented in Figure 5.5.

The mapping results are well in agreement with that of EDX spectrum in regards of presence of oxygen (Figure 5.5) for heat-treated sample. It may have happened because of heat-treatment process that is performed in muffle furnace which contains air.

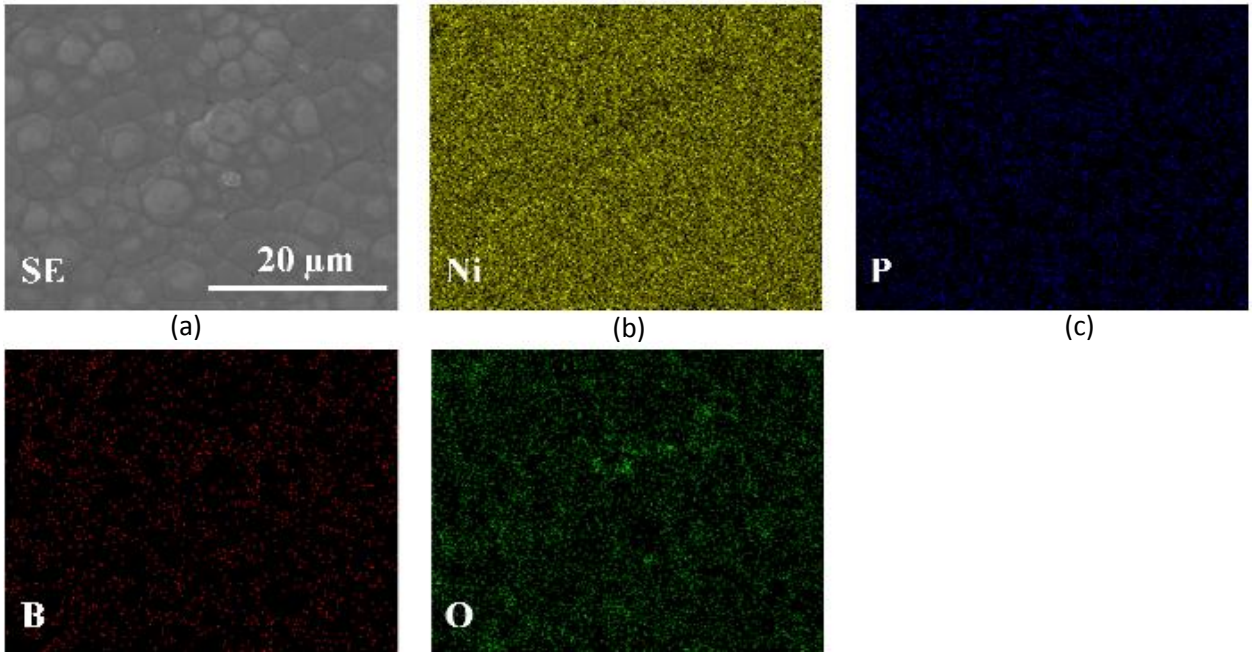

(a) (b) (c)

(d) (e)

Figure 5.5 EDX mapping analysis on the surface of the heat-treated Ni-P-B coating indicating (a) SE image (b) Ni (c) P (d) B and (e) O

5.3.2 Surface texture of coating

Optical micrograph of as-deposited and heat-treated Ni-P-B coating is presented in Figure 5.6. The same captured via scanning electron microscope is shown in Figure 5.7. The as-deposited coating as captured via optical or scanning microscope, both reveals the similar closely compacted nodular structure in different magnification. Whereas the same for heat-treated (at 400°C) condition consists of nodules, larger in size. This may be because of coating crystallization at mentioned temperature which results in increase of granule dimension. Common cauliflower like appearance as of borohydride reduced baths can be identified. The observed closely compacted nodular arrangement with cauliflower appearance is similar to that as reported by many of the researchers (Mukhopadhyay et al., 2018c; Krishnaveni et al., 2005; Vitry et al., 2012b). This kind of structure is preferred as it helps to reduce friction and work as lubricant retainer. Few dark spots are visible on heat-treated coating surface shown in Figure 5.7(b), owing to the oxide scale development as confirmed through EDX (Figure 5.2(b)) and

elemental mapping (Figure 5.5) results. As an indicative of substrate adhesion and coating thickness which lies in the range of 35-42 µm, cross cut geometry is depicted in Figure 5.8.

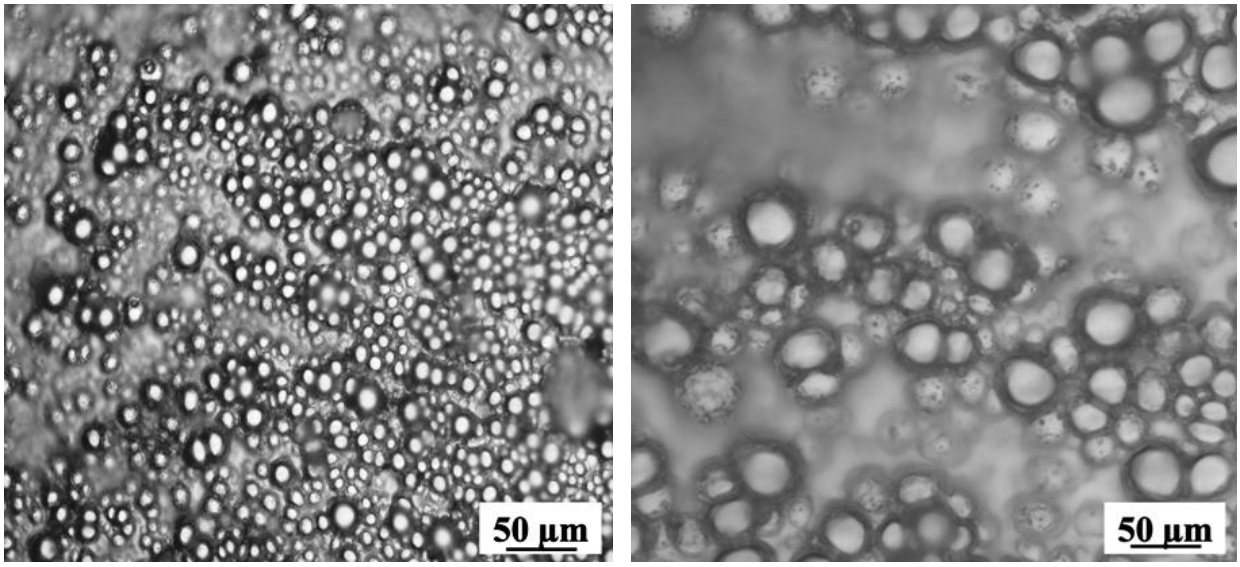

(a) (b)

Figure 5.6 Optical micrograph of (a) as-deposited and (b) heat-treated electroless Ni-P-B coating

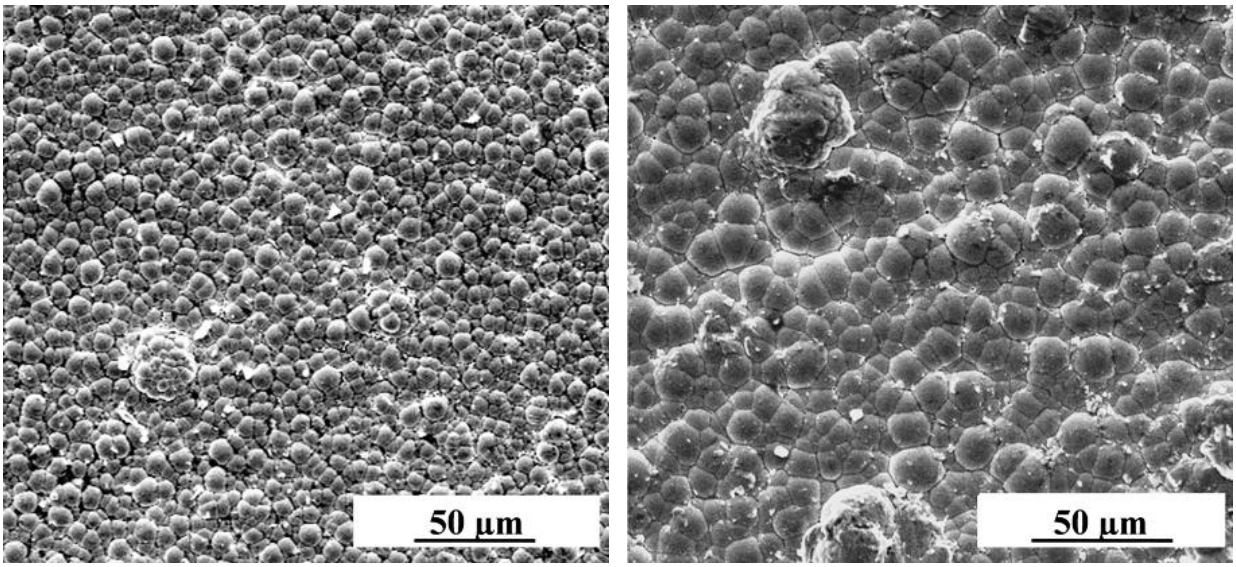

(a) (b)

Figure 5.7 SEM micrograph of (a) as-deposited and (b) heat-treated electroless Ni-P-B coating

A portion of the coating as shown by a rectangle in Fig. 5.8(a) is chosen and zoomed as shown by Figure 5.8(b) for better understanding of the surface morphology. As seen in Figure 5.8(b) columnar growth of Ni-P-B coating is clear which is again an obvious phenomenon in

borohydride based baths (Mukhopadhyay et al., 2018c; Vitry et al., 2012b). This phenomenon helps to reduce the actual contact area and thus improving tribological performances. Ni-P-B shows the typical dense structure which is analogous to both Ni-P and Ni-B coating.

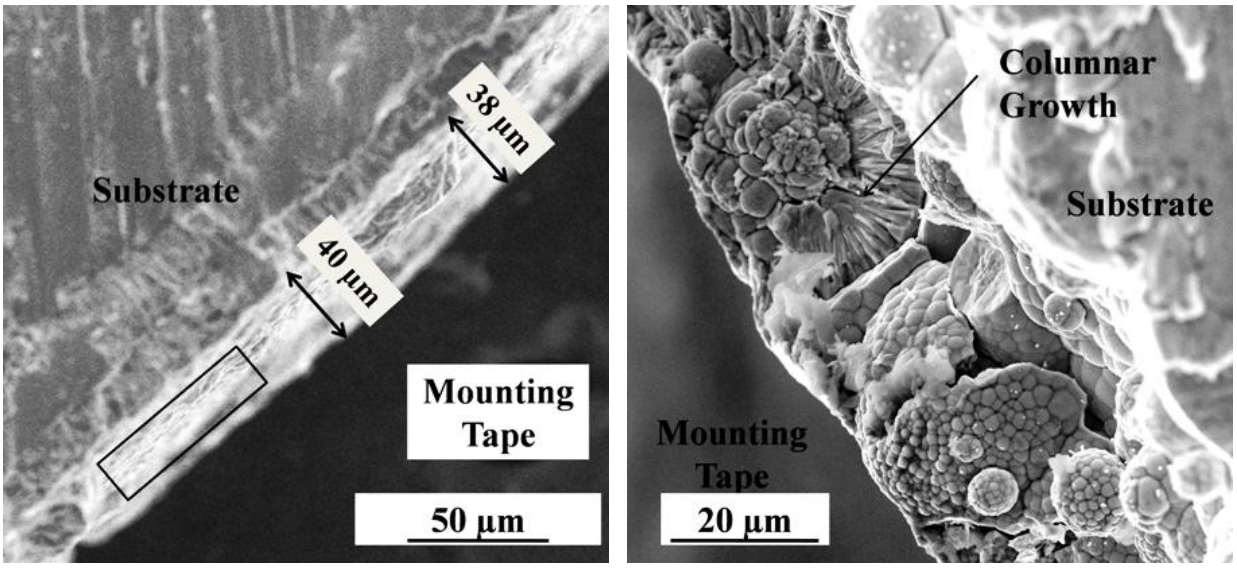

(a) (b)

Figure 5.8 A cross-cut section (a) of the Ni-P-B coating with (b) detailing of the growth pattern of deposition

Further, Atomic Force Microscopy (AFM) is employed to examine the surface heterogeneities of the coated specimens in details. The 2D and 3D illustration of Ni-P-B coatings in before and after heat-treatment conditions have been inspected with AFM in contact mode with a scan area of 10 µm × 10 µm. Figure 5.9 and 5.10 show atomic force microscopic (AFM) images of as-deposited and heat-treated specimens Ni-P-B coatings, respectively, where (a) topographical image (2D) and (b) three dimensional (3D) image. Surface texture of as-deposited coatings shows regular nodular spherical morphology composed of finer grains highly dense and compact. This observations used to reiterate the SEM results as presented by Figure 5.7 and greatly in Figure 5.8(b). Nodular feature is very common in electroless deposition which arise due to fast nuclei creation and its successive growth. Apart from that, bath constituents, coating environment and substrate surface mainly surface irregularities play a deciding role in formation of nodule. The common nodular structure is formed by joining crystals each other on the surface of the substrate as clearly visible in Figure 5.9. Deposition of coating per unit time is directly involved in deciding nodular structure by controlling the supply of atoms. Nodule growth (mainly in Z direction i.e. normal to the substrate) directly depends on available number of atoms which is again proportional to the rate of deposition. Ni-P-B (Figure 5.9) shows increased nodules, may be because of higher plating rate of Ni-P-B, as indicated earlier (Figure 5.1). Heat-treatment causes to increase the grain size in Ni-P-B as indicated in Figure 5.10, which may be because of phase transformation that is expected in XRD analysis. The grain coarsening because

of heat-treatment causes to increase the surface irregularities which indicates a higher roughness of heat-treated specimen compared to as-deposited samples. From the AFM observation (Figure 5.10), each grain of ht samples consists of higher number of smaller grains analogous to diffused like morphology.

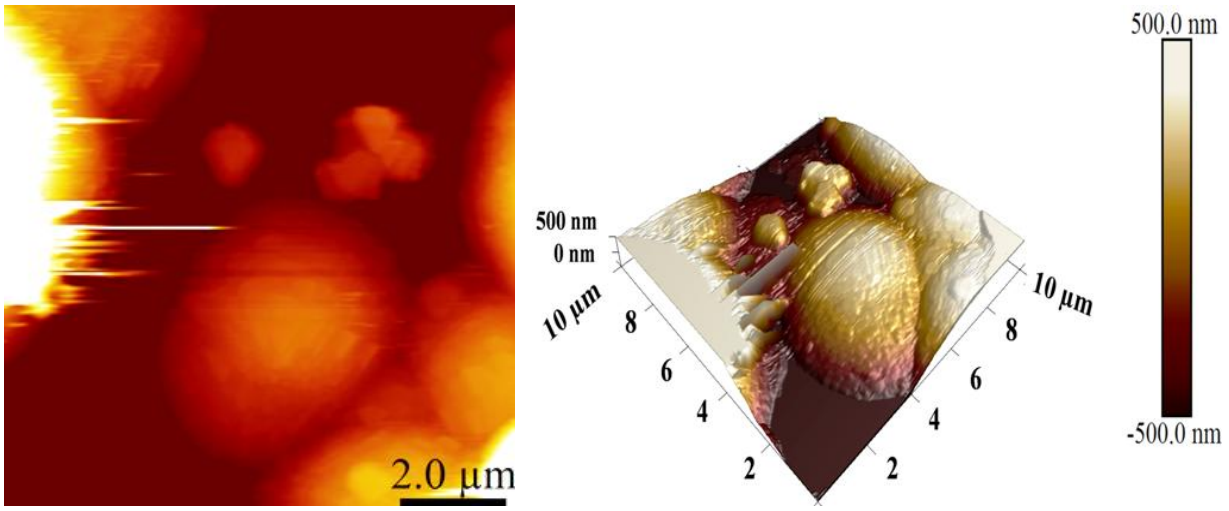

(a) (b)

Figure 5.9 Typical AFM morphologies of as-deposited Ni-P-B surfaces in (a) 2D and (b) 3D

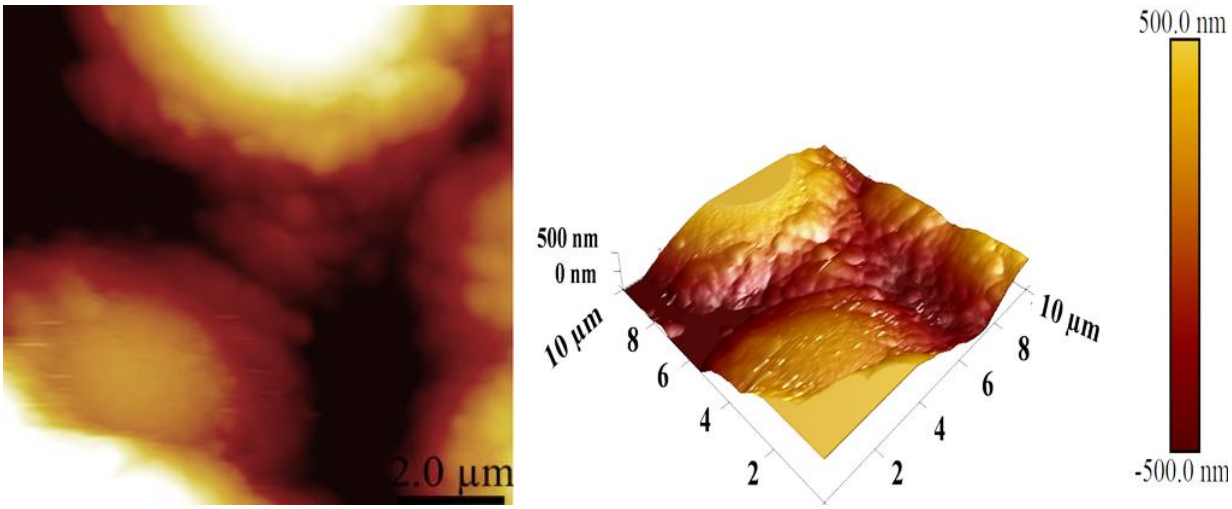

(a) (b)

Figure 5.10 Typical AFM morphologies of heat-treated Ni-P-B surfaces in (a) 2D and (b) 3D

5.3.3 Structural aspects of Ni-P-B coating

XRD patterns of the Ni-P-B coatings is shown in Figure 5.11. Under as-deposited condition, there is no hump observed in Ni-P-B coating. A wider FWHM (full width half

maximum) corresponding to nanocrystallite structure (crystallite size of approximately 2nm) is observed. The developed coating (3.3-3.5 wt% B) lies in the low-B range and shows the nanocrystallite structure in accordance to literature (Vitry & Bonin, 2017b). For as-deposited Ni-B coating, Balaraju et al. (2016) worked with 5.37 wt.% B and found a grain size of 19 nm whereas Niksefat and Ghorbani (2015) obtained 11 nm size worked with 4-7wt.% B. Heat-treatment provides crystalline Ni for Ni-P-B coating as observed at ~46.2° (2θ) with its borides (Ni_3B and Ni_2B) and phosphides (Ni_3P) phases. Formation of borides and phosphide phases are clearly indicating the phase transformation and lead to higher hardness. The role of boron is dominating phosphorus in Ni-P-B as EDX study reveals a lower (0.6-0.7) wt % of P in the total structure. Ni-P-B coatings heat-treated at 400°C reveals crystallite size of 27±2 nm, calculated using Debye Scherrer's formula (Vitry et al., 2012c), which shows increased grain size compared to as-deposited condition. Heat-treatment causes to decrease FWHM and results in increased grain size. Formation of boride phases as well as increase in grain size as outcomes of heat-treatment is already established by other researchers (Mukhopadhyay et al., 2018a; 2018b; 2018c).

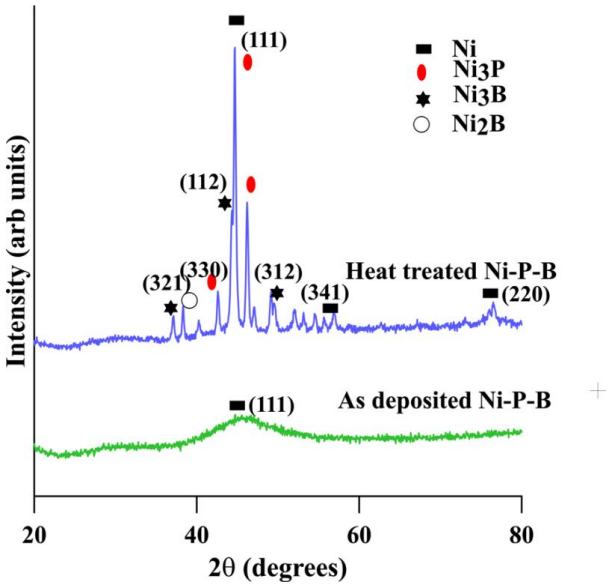

Figure 5.11 XRD spectra obtained for as-deposited and heat-treated electroless Ni-P-B coating

5.3.4 Roughness and microhardness evaluation

Roughness of Ni-P-B samples are tested via Talysurf profilometer as well as AFM and expressed in terms of centre line average value (R_a). The maximum R_a value observed for as-deposited coating is close to 0.53 µm which is very close to that of Ni-B. Heat-treatment causes to increase the value slightly but it never exceeds 0.57 µm, because of the inflation of granule size due to heating at particular temperature. The observed roughness value of coated samples are close to the substrate roughness (less than N6 grade), which is sufficient for majority of applications.

The microhardness of ternary Ni-P-B coatings before and after the heat-treatment were performed as illustrated in Figure 5.12. Electroless deposition Ni-P-B provides average microhardness of 690 $HV_{0.1}$ working with a substrate having hardness of 140 $HV_{0.1}$. The hardness obtained is nearly 15% more than that of Ni-P (as compared with chapter 3) and 3% higher compared to Ni-B (Mukhopadhyay et al., 2018c). Addition of boron in Ni-P matrix may be the reason behind hardness increment. It may be concluded that developing coating through combined hypophosphite and borohydride bath is better than that of solely developed hypophosphite or borohydride bath. Further the effect of heat-treatment at 400°C on the coating is included in the same figure. Heat-treatment causes to increase the hardness of Ni-P-B to 1080 $HV_{0.1}$. The effect of heat-treatment is pronounced in Ni-P as it is indicated in chapter 3; in comparison to Ni-P-B. However, inclusion of P and B results in a ternary coating with high microhardness and is higher than that obtained from sole hypophosphite based-baths (Balaraju & Rajam, 2005) and borohydride reduced EN alloy coatings obtained by other researchers (Mukhopadhyay et al., 2018c; Vitry & Bonin, 2017b).

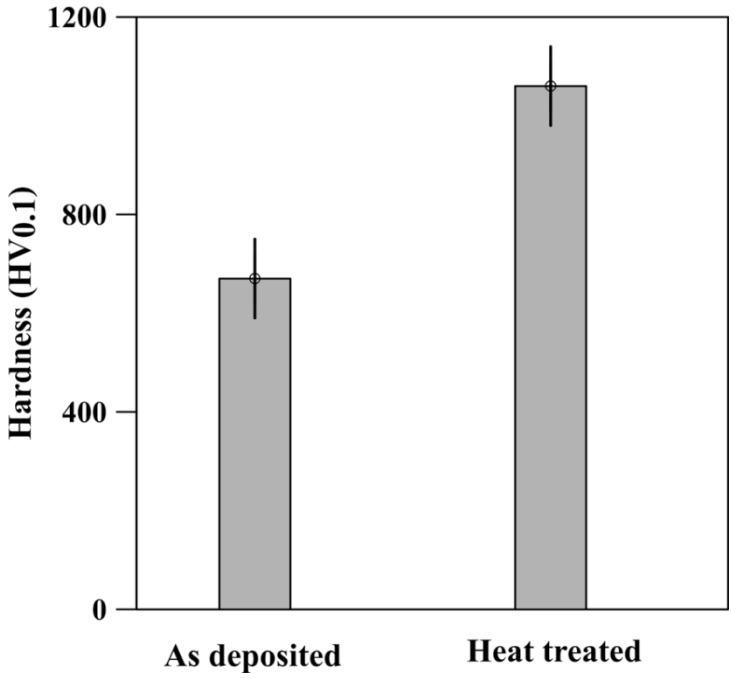

Figure 5.12 Microhardness obtained for as-deposited and heat-treated electroless Ni-P-B coating

5.3.5 Tribological characterization based on test parameters

5.3.5.1 Friction under different load and sliding velocity

The effect of load and sliding velocity under ambient and high temperature on the friction performance of as-deposited and heat-treated Ni-P-B coatings are studied. The experiments are arranged in an incremental manner by varying one factor at a time. The COF of as-deposited as well as heat-treated coatings as a function of load and sliding velocity separately under two

different working temperature are shown in Figure 5.13a and 5.13b respectively. The samples are slide with different loads by choosing a constant sliding velocity of 0.22 m/s. In general, COF increases with increase in applied load which is attributed to the increase in contact area and subsequent higher force required to break them. Similar observations have already been made by other researchers (Chowdhury et al., 2011). For a particular load however, COF decreases with increase in the operating temperature for as-deposited samples. The low friction may be due to the in situ oxide formation on sliding surfaces at high temperature. The oxide layer is soft and presents low shear properties resulting in lesser friction. Tests at RT for as-deposited coating show a monotonically increasing trend for COF with the applied load but for heat-treated coating it shows similar trend to that of test conducted at high temperature. For heat-treated coatings, COF increases with increase in load, quite similar to that of as-deposited coatings. Further, the test at RT for heat-treated coatings also reveals a similar trend as the high temperature tests which provides higher COF, may be because of higher hardness of heat-treated Ni-P-B samples.

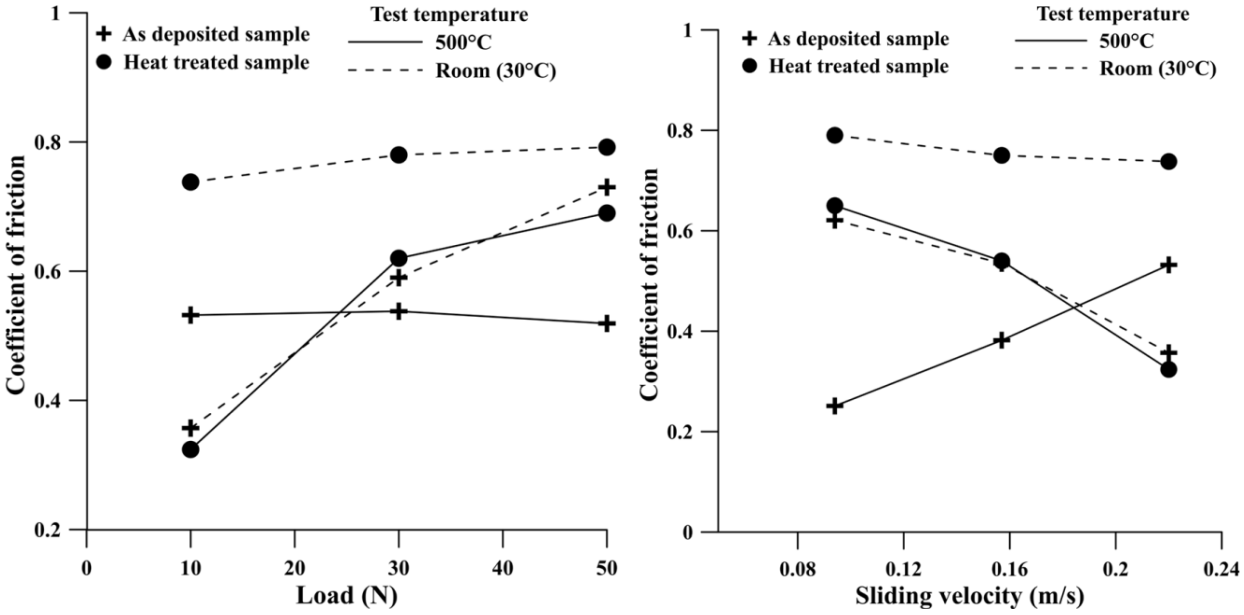

(a) (b)

Figure 5.13 Friction performance of Ni-P-B coating for room and high temperature under different (a) load and (b) sliding velocity

The sliding tests are conducted at a uniform load of 10 N. Except at 500°C test of as-deposited, increase in sliding velocity results in lowering of COF. However, apart from the 500°C test of as-deposited, highest level of sliding velocity (0.22 m/s) provides the lowest COF. Though as-deposited coating tested at high temperatures behave differently, as with the increase in velocity it shows an increased value of COF. The friction behavior of heat-treated coatings under room and high temperature for different sliding velocities are also included in Figure 5.13b. The effects of sliding velocity under both room and high temperature on COF are

analogous to the results of as-deposited coatings for room temperature application. Hence, it can be seen that both sliding velocity as well as operating temperature have a significant effect over the COF of Ni-P-B coatings. Now, during sliding, the contact points change rapidly depending on the sliding velocity as new points come in contact and existing contacts break. The more the area of contact, the higher is the friction at the interface. At higher operating temperature, the coating gets a real time heat-treatment and hence becomes hard. Due to increase in hardness, here it may have caused to increased COF at high temperature test of as-deposited samples. The decreasing trend of COF with sliding velocity may be due to the change of shear rate which can in turn affect the mechanical properties of the mating materials (Bhushan & Jahsman, 1978). Moreover, higher sliding velocity will contribute to a larger normal momentum transfer in the upward direction. This results in an increased separation between the coating and the counterface which further results in decreased real area of contact. This may also serve as an explanation for the lower friction coefficient at higher sliding velocity.

5.3.5.2 Wear under different load and sliding velocity

Wear behavior of Ni-P-B coatings is investigated under ambient and high temperature by varying the testing parameters viz. normal load and sliding velocity The effects of each parameter on the wear of the coating are investigated in detail here. Wear is represented by the ratio of weight loss to the distance traversed so that the effect of sliding speed on wear can be truly realized. The effect of load and sliding velocity on wear under two temperature for as-deposited along with heat-treated Ni-P-B coatings is shown in Figure 5.14a and 5.14b respectively. For Figure 5.14a, sliding velocity is fixed as 0.220 m/s whereas for Figure 5.14b, load is fixed as 10 N. From Figure 5.14a, it is found that wear rate increases with increase in applied load. Several researchers (Panja et al., 2016) have made similar observations for coatings tested at RT. For the current study, under RT for as-deposited coatings, wear is found to increase by almost four times within the load range 10–50 N. The same for heat-treated coatings is found to be eight times within the chosen load range. Whereas under elevated temperature conditions, within the same load range, the increase of wear is about eight times (500°C plot) for as-deposited coatings though for heat-treated coatings, the effects is less (nearer to three times). Under application of 10 N load, wear is found to be less also at test conducted at 500°C. Hence, the higher wear resistance found at 500°C can be attributed to the increase in hardness of the coating due to heat-treatment at the test temperature. This results can be further supported by post wear phase transformation and hardness study to understand and correlate the reason behind the better wear resistance of Ni-P-B coatings.

The relation between wear rate and sliding velocity for varying test temperature for a particular load (10 N) is shown in Figure 5.14b. It is found that under elevated temperature conditions wear reduces with increase in sliding speed. For variation of speed from 30-70 rpm, wear is found to decrease by sufficient amount in both room temperature as well as tests conducted at 500°C. Though there is a small exception occurs at 0.157 m/s sliding velocity. But

with further increment in velocity it again shows the usual trend. The behavior of as-deposited and heat-treated both of the coatings are very similar to each other.

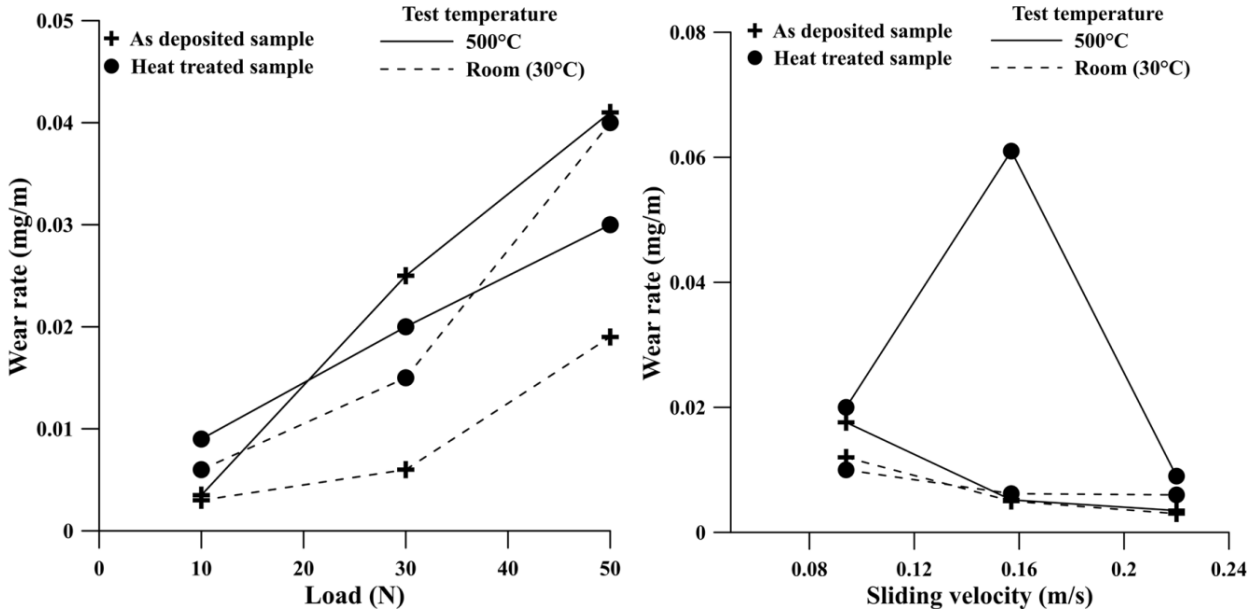

(a) (b)

Figure 5.14 Wear performance of Ni-P-B coating for room and high temperature under different (a) load and (b) sliding velocity

It is observed that the increase in load results in higher wear for any working temperature as in the case of as-deposited samples. Also similar to the as-deposited sample, increase in sliding velocity results in decrease in the wear rate of the heat-treated coating. However, when compared with that of the RT test, wear rate is observed to be higher in high temperature conditions. A direct comparison of the room and high temperature tribological performances of as-deposited as well as heat-treated EN coatings is shown in Figure 5.13 and 5.14. The comparison is presented for the best combination of applied load and sliding velocity (10 N and 0.220 m/s) as seen from the previous discussions. So, the further temperature profiling and detail discussion on as-deposited and heat-treated Ni-P-B coating is discussed in the next section based on selected load and velocity.

5.3.6 Study of tribological behavior of Ni-P-B coating at various test temperatures

5.3.6.1 Friction performance of as-deposited and heat-treated Ni-P-B coating at different test temperatures

COF of as-deposited and heat-treated Ni-P-B coating with respect to test temperature is presented in Figure 5.15. In ambient condition, the as-deposited coatings shows much lower

friction in compare to heat-treated case, it may be because of higher hardness of heat-treated Ni-P-B. Friction coefficient shows a lower value tested at RT and with the increase in temperature to 100°C it suddenly moves to 0.8 and thereafter with the further increase it gradually decreases as shown by Figure 5.15a. Material softening at higher temperature probably is the reason for that drop in COF. Heat-treated specimen shows a higher COF in RT and 100°C test in compare to as-deposited Ni-P-B. Coarse grained surface morphology because of heat-treatment causes to increase the surface roughness and accordingly the COF. But a reverse trend is noticed for 300°C and 500°C test temperature. As heat-treatment yields higher hardness and material softening is pronounced at higher test temperature, so those are the possible reason for the observation reported in Figure 5.15b. Present investigation with heat-treated Ni-P-B indicates higher COF at RT compared to elevated temperature (300°C and 500°C) test. It is therefore noteworthy to use Ni-P-B as coating for elevated temperature applications.

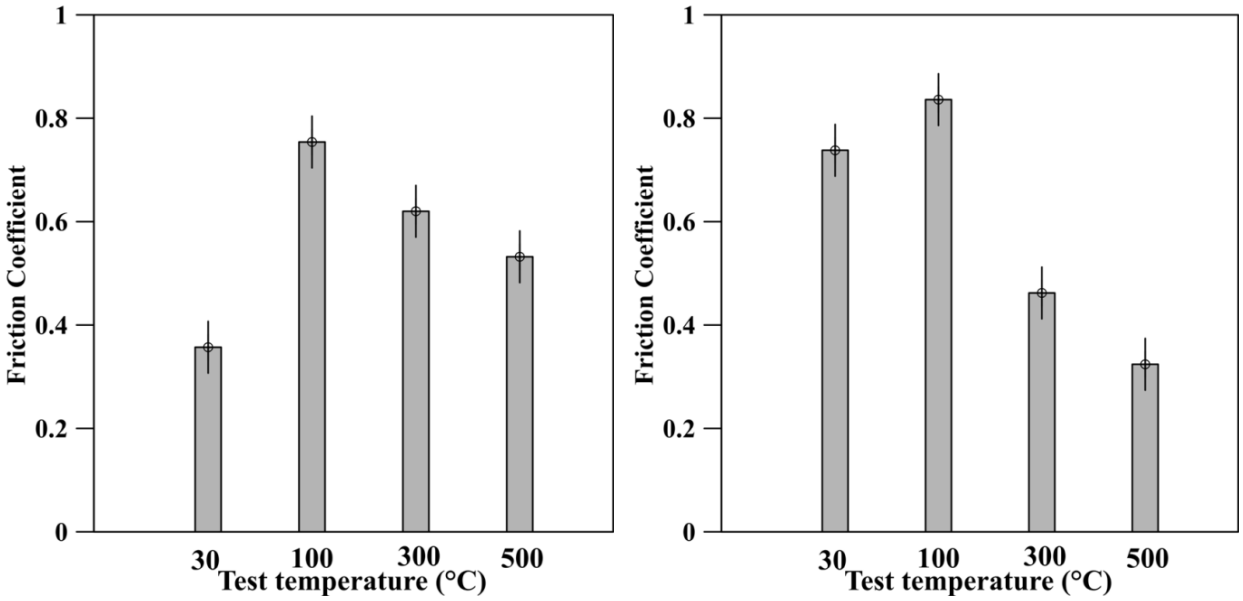

(a) (b)

Figure 5.15 Friction as a function of test temperature for (a) as-deposited and (b) heat-treated Ni-P-B coating

The variation of COF for Ni-P-B at different temperatures is inspected across the sliding distance to understand the underlying effects of running in period. Friction coefficient fluctuation for as-deposited and heat-treated Ni-P-B is presented in Figure 5.16a and 5.16b respectively. A huge variation in COF nearly about two times is observed for as-deposited samples tested at RT as shown in Figure 5.16a. The variation is decreased with the increase of test temperature and at 500°C, COF becomes stable. Heat-treatment samples tested at 30°C and 100°C (Figure 5.16b) provides higher COF than as-deposited one, may be because of higher hardness. But formation of surface oxides at higher temperature (500°C) causes to provide a lubricating effect that lowers down the COF.

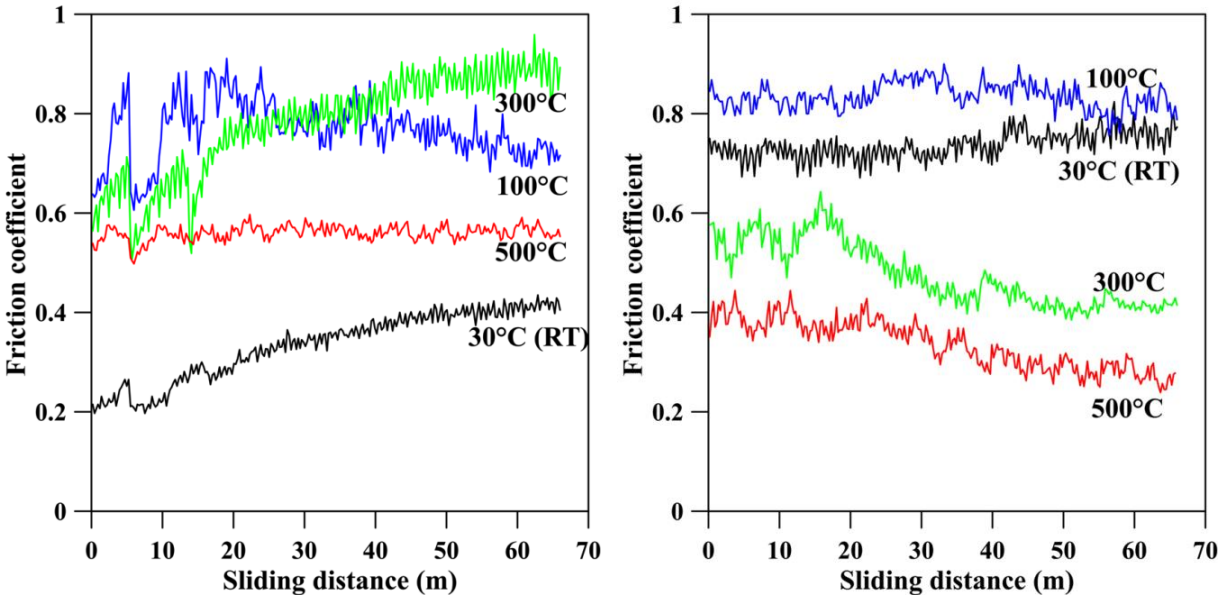

Figure 5.16 Evolution of COF of at room and elevated temperatures for (a) as-deposited and (b) heat-treated Ni-P-B coating

5.3.6.2 Wear performance of as-deposited and heat-treated Ni-P-B coating at different test temperatures

Wear rate of Ni-P-B as a function of test temperature is indicated by Figure 5.17. Each tests are carried out for a number of times to ensure appropriateness of the obtained results, which are illustrated as error plots in Figure 5.17. For both as-deposited (Figure 5.17a) and heat-treated (Figure 5.17b), case Ni-P-B shows better wear resistance. It may be because of the columnar structure of Ni-P-B coatings which helps to reduce the actual area of contact and thus reducing wear. In addition to that, harder coating surface of Ni-P-B (as marked by Figure 5.12) provides an incompatible surface contact with counterface material. For as-deposited Ni-P-B, RT test yields lowest wear rate may be because of the nanocrystalline structure and a high hardness value in its as-deposited condition. As temperature increase to 100°C, wear rate increases possibly due to microstructural alteration during the test. But further increase in test temperature shows a fall in wear rate perhaps because of phase transformation during the wear test as also reported by other researchers (Masoumi et al., 2012; Mukhopadhyay et al., 2018c). The effect of phase transformation during the wear test is negligible for heat-treated Ni-P-B samples. But heat-treated coating tested at 300-500°C shows better wear resistance because of achieving optimum nickel particle size as suggested by Masoumi et al. (2012). Overall, the wear resistance provided by Ni-P-B at 300 and 500°C is significant and it proves itself as a suitable coating material for adverse situation.

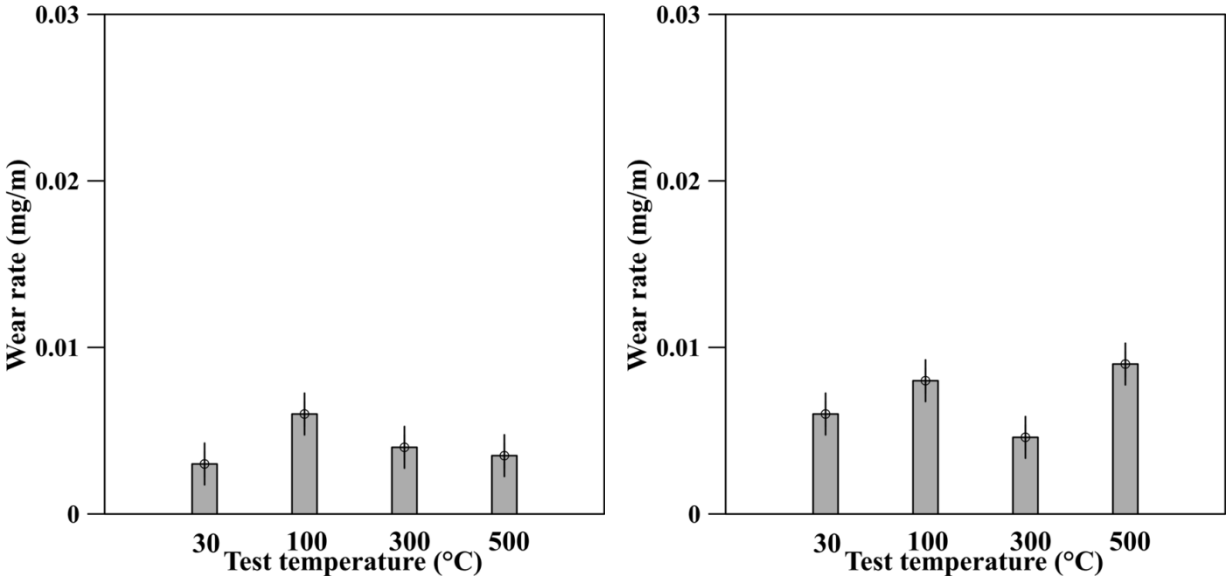

Figure 5.17 Wear as a function of test temperature for (a) as-deposited and (b) heat-treated Ni-P-B coating

SEM image indicating the wear along with the direction for Ni-P-B as-deposited coatings tested at 500°C is represented in Figure 5.18. The coating clearly exhibits linear wear tracks as soft coating is subjected to abrades by same hard counter face. Along with that, few removal of material in the form of pits and prows is also detectable which arise due to breakage of bonding in between coating and counter face asperities. Linear tracks are prominent which is an indication of abrasive wear pattern as well as pits and prows are symbolic for adhesive wear mechanism. So, the wear mechanism at 500°C for the coating is mostly governed by abrasive and partly by adhesive wear mechanism. The linear tracks and removal of coating is lesser in Ni-P-B in compare to Ni-P (indicated in chapter 3), as clearly visible from Figure 5.18a, satisfying the results as indicated by Figure 5.17a. The lesser wear compared to Ni-P may be because of the combined effects of higher hardness, columnar growth, formation of harder boride phases of Ni-P-B coating. The visible dark spots clearly indicates the formation of oxide layer during the test conducted at high temperature. Further to prove the fact as well as to indicate the other elemental distribution, line EDX (as shown by line AB in Figure 5.18a) is carried out. The results indicating the detail variation of each element across the chosen line (AB of approx 200 μm) is provided in Figure 5.18b for Ni-P-B coating. Presence of oxygen implies high temperature oxide formation as claimed by other researchers (Masoumi et al., 2012; Mukhopadhyay et al., 2018a; 2018b; 2018c) works in the field of high temperature coatings. Existence of nickel and the other primary coating elements proves the survival of those coatings at elevated temperature. Amount of Fe comes as a result of interaction with counterface material which may provide a mixed mechanical layer. It may be also the reason behind the lower wear rate at elevated temperature. It can be further analyzed through phase transformation study for worn out samples.

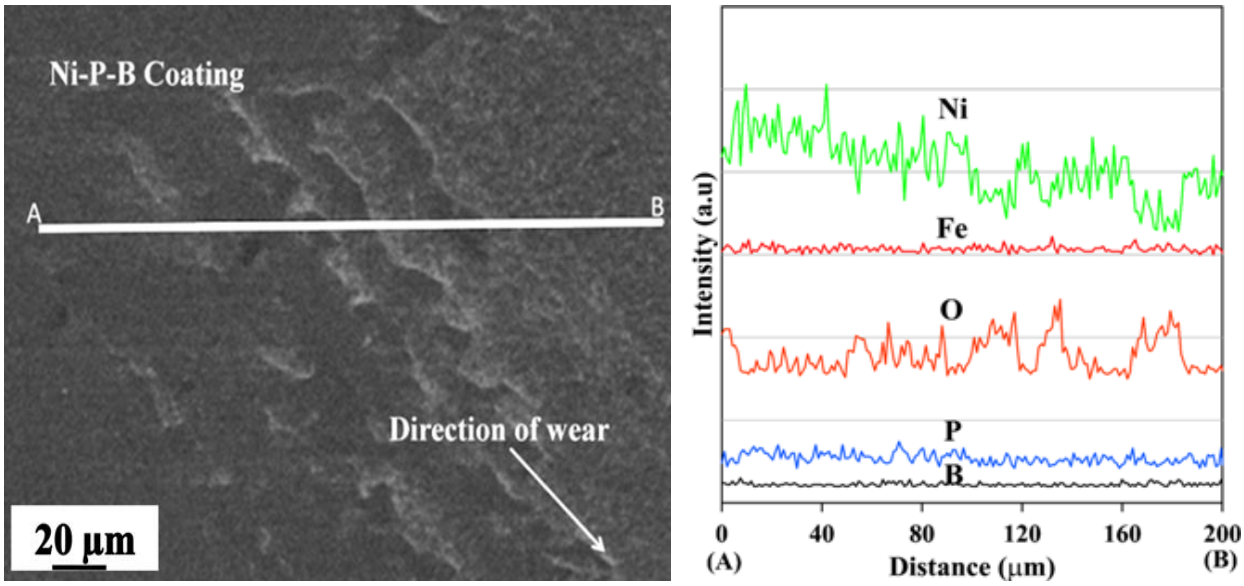

(a) (b)

Figure 5.18 Typical SEM image indicating the (a) line for EDX study in the direction of wear and (b) corresponding EDX line analysis for Ni-P-B coating

5.3.6.3 Wear mechanism study

Post wear test, both as-deposited and heat-treated Ni-P-B samples are subjected to SEM and EDX investigations to understand the mechanism and effects of wear respectively on the coating. Further a detailed study is consolidated by AFM and elemental mapping analysis for as-deposited and heat-treated coatings tested at 500°C. The effects of phase transformation because of elevated temperature test on the wear mechanism is imperative and corresponding study is investigated and presented in the next section. The as-deposited coating tested at room temperature shows a flattened nodular structure (Figure 5.19a). Most of the asperities are compressed under the application of load and few fragmented nodules are spread over the whole surface area of contact. This split particles playing the role of solid lubricants and causes to provide low COF and wear as indicated by Figure 5.15a and 5.17a respectively. The coating is mostly intact after the room temperature test as clearly visible in Figure 5.19a with a small number of patches. Removal of coating in the form of patches is an significant characteristics of adhesive wear. The intactness of the post test coatings are verified through EDX study (Figure 5.20a) which clearly indicates the existence of three major constituents Ni, P and B. The nodular morphology seems to disappear and rough surface with several pits and prows are observed for coating tested at 100°C (Figure 5.19b). This is a predominant features of adhesive wear which causes to increase the COF and wear of as-deposited samples and also justifies the results obtained in Figure 5.15a and 5.17a respectively. Mutual force of attraction between nickel and counter face material playing the lead role in material removal process as also supported by other researchers (Krishnaveni et al., 2005).

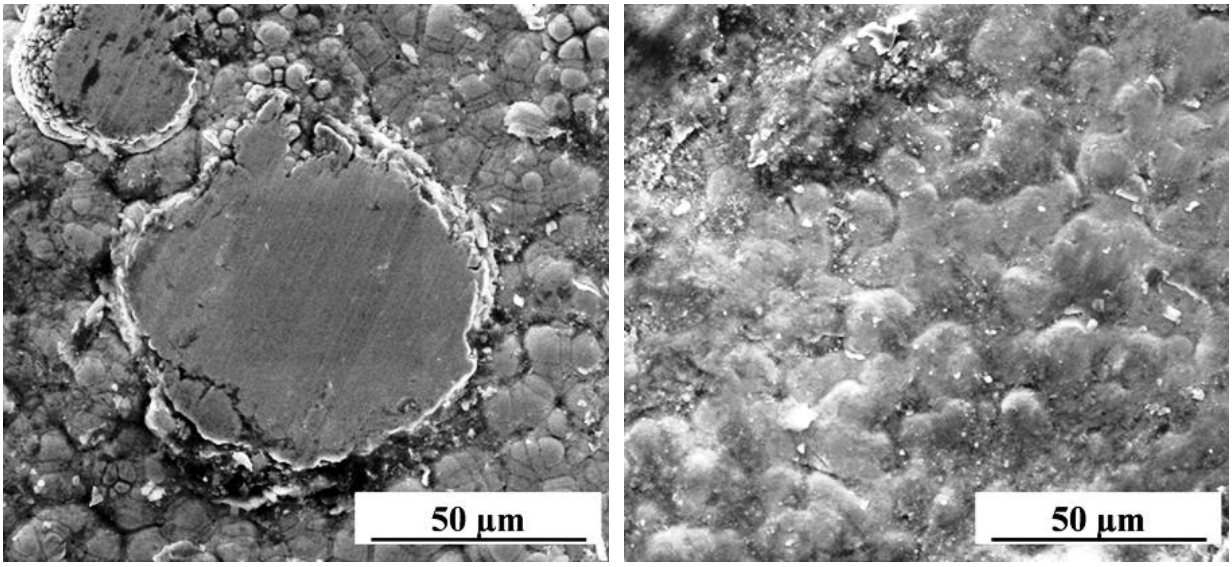

(a) (b)

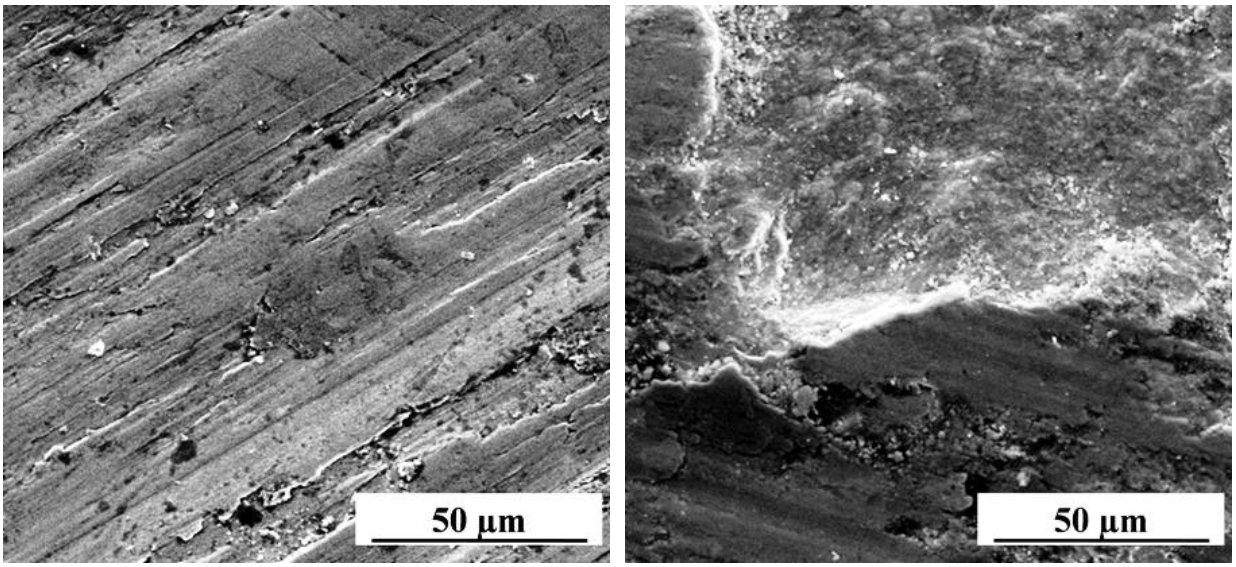

(c) (d)

Figure 5.19 SEM (secondary electron) micrograph of worn specimen of as-deposited electroless Ni-P-B coating tested at (a) 30°C (b) 100°C (c) 300°C and (d) 500°C

The presence of Fe along with the chief constituents in EDX study (Figure 5.20b) supports the claim of interaction of iron particles during 100°C test temperature. The nodular morphology of the coating is completely spoiled and high degree of plastic deformation in the direction of sliding is observed for the as-deposited Ni-P-B samples tested at 300°C.

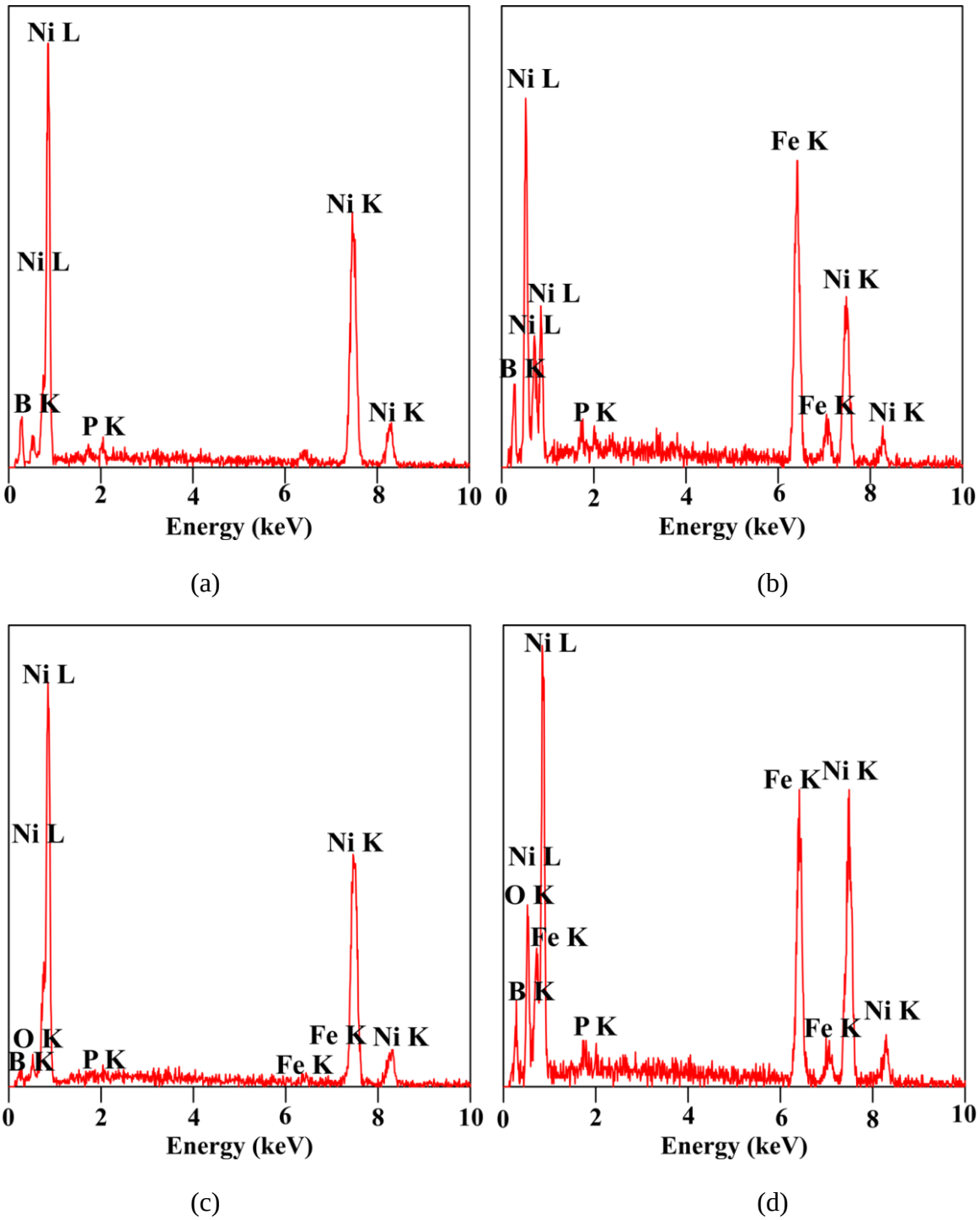

Figure 5.20 EDX spectrum of worn specimen of as-deposited electroless Ni-P-B coating tested at (a) 30°C (b) 100°C (c) 300°C and (d) 500°C

Figure 5.19c indicates deep grooves filled with flattened patches which is an indicative of occurrence of abrasive wear. Though the wear rate improves as shown in Figure 5.17a as compared to 100°C, it may be due to initiation of phase transformation which calls harder

phosphide and boride phases during elevated temperature test as well as fine scattered debris which acts like solid lubricants. Friction coefficient slightly decrease at 300°C, as indicated by Figure 5.15a, due to stable lubrication provided by the oxide layer formed during that test. Oxygen detection in the corresponding EDX study (Figure 5.20c) confirms the presence of oxide layer. The coating tested at 500°C shows deep grooves along with micro-ploughing (Figure 5.19d) which is again a sign of abrasive wear trend. Along with that few torn patches leading to adhesion and black spots indicating oxidation are clearly visible in Figure 5.19(d). Formation of tribo oxidative layer during the 500°C test decreases COF as presented in Figure 5.15a as well as yields COF with lesser fluctuation (Figure 5.16a). Presence of oxygen (Figure 5.20d) confirms the tribo oxidative layer as well as oxidation of the coating during the elevated test. Presence of Fe in the post test samples may be because of two reasons, either it because of adhesion (high mutual solubility of iron and nickel atoms) or diffusion of iron from the steel substrate during test. The chances of diffusion is very less as the test is subjected for a very short time. Hence, it can be confirmed that adhesive wear co-exist along with abrasive wear while governing the wear behavior of Ni-P-B coatings which is in agreement with the observation of other researchers (Staia et al., 2002).

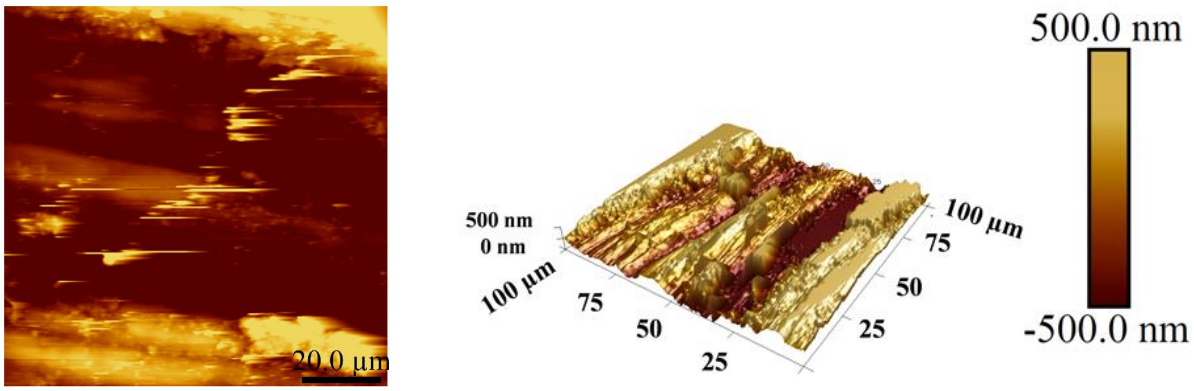

(a) (b)

Figure 5.21 AFM morphology (a) 2D and (b) 3D of as-deposited Ni-P-B coating tested at 500°C

To highlight the effects of elevated temperature test as well as to maintain brevity, samples post test 500°C are further considered for AFM and elemental mapping study and the corresponding results indicated by Figure 5.21 and 5.22 respectively. The 2D and 3D surface morphology of post test samples is represented by Figure 5.21a and b respectively. It clearly indicates a rough surface with deep grooves along with micro-ploughing. Wear tracks in the direction of sliding along with material removal is also noticeable. The elemental maps along with SE image of worn as-deposited Ni-P-B coating tested at 500°C is shown in Figure 5.22. SE image of worn out specimens also indicates the linear wear tracks, indicating abrasive wear trend, in the direction of sliding and its very close to that of Figure 5.18a. Uniform allocation of nickel, phosphorous and boron can be seen from the images (Figure 5.22) which mean the

survival of coating even after the wear test. The existence of oxygen proves the development of tribo-oxide film as discussed earlier. The oxide layer surrounds over the whole surface of the coating as evident from the mapped image (Figure 5.22) which is the main reason for lesser fluctuation and a reduced amount of COF. For the 500°C, iron shows very strong signal (Figure 5.22) in the image which implies occurrence of adhesive wear whose remnants can be experiential from torn patches on the coating post test.

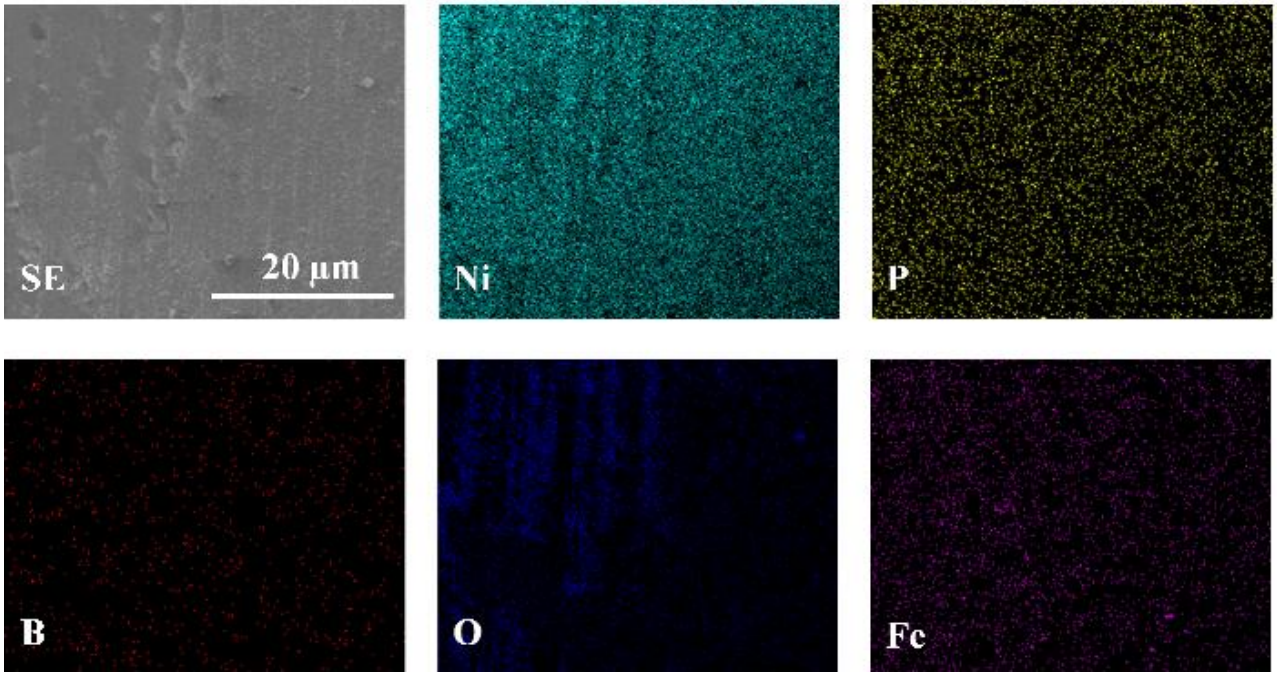

Figure 5.22 EDX maps of worn specimen of as-deposited Ni-P-B coating tested at 500°C

The wear mechanism of heat-treated Ni-P-B films at various temperatures (30°C, 100°C, 300°C and 500°C) are examined through SEM images and its corresponding EDX results. The friction and wear performances characteristics of heat-treated ternary coatings exhibited by Figure 5.15b, 5.16b and 5.17b are further consolidated through SEM micrographs (Figure 5.23) and EDX findings (Figure 5.24) of worn out samples. The nodular morphology is not visible rather several pits and prows, indicating adhesive wear pattern, are visible on the surface of heat-treated coating tested at room temperature (Figure 5.23a). These along with wear tracks are easily noticeable from the figure indicating the occurrence of abrasive wear phenomenon. Therefore, it can be concluded coating manifest clearly a mixed wear mechanism for test conducted at room temperature. EDX outcome (Figure 5.24a) refers post-wear elemental allocation which consists of original coating constituents, along with the presence of oxygen which comes because of previous heat-treatment process. Ploughing with torn patches in the direction of sliding can also be observed for coating tested at 100°C (Figure 5.23b) which again point towards a mixed wear mechanism. The severe adhesive wear and rough surface supports towards the high COF observed at this condition (Figure 5.15b).

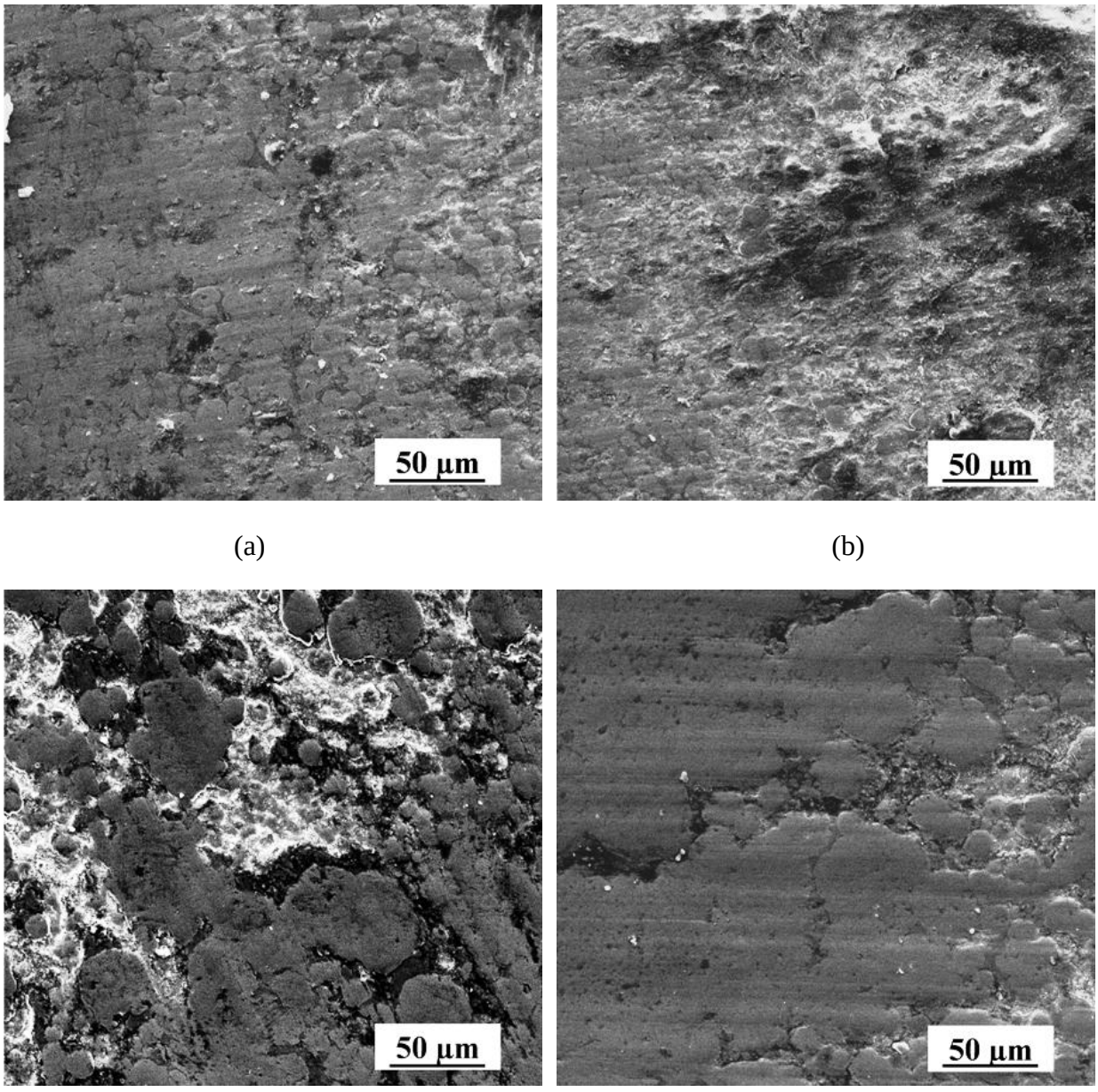

(a) (b)

(c) (d)

Figure 5.23 SEM (secondary electron) micrograph of worn specimen of heat-treated electroless Ni-P-B coating tested at (a) 30°C (b) 100°C (c) 300°C and (d) 500°C

The EDX of the post wear sample (Figure 5.24b) shows iron which yields abrasive wear owing to high mutual solubility of nickel and Fe atoms. The oxidation of wear zone may be represented by the EDX outcomes through the presence of oxygen. Micro-cutting and micro-ploughing together with torn patches (Figure 5.23c) are encountered in the wear test at 300°C. Though the coating surface appears to suffer ductile failure with high level of plasticity in the direction of sliding. EDX results again indicates the existence of oxygen and iron (Figure 5.24c).

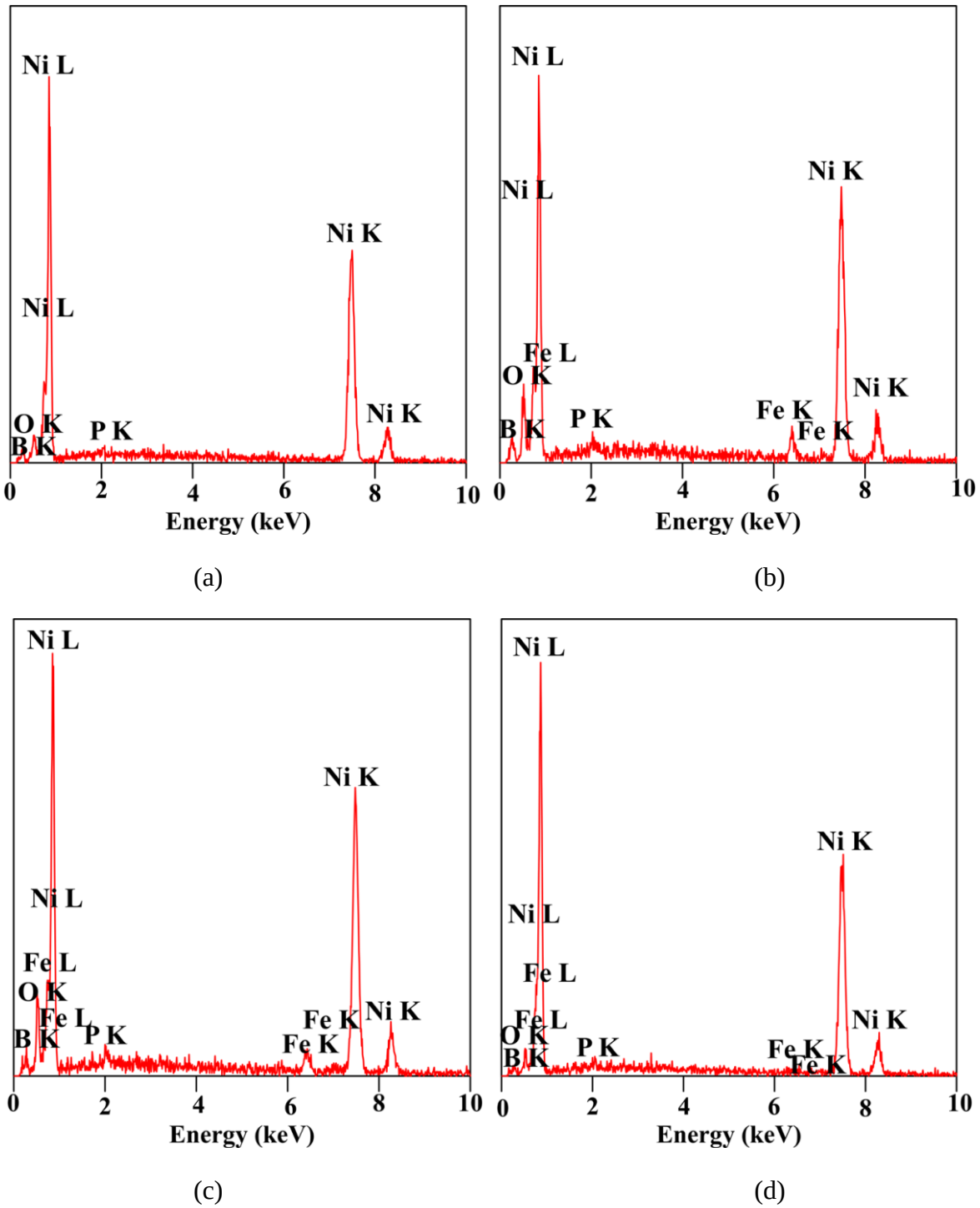

Figure 5.24 EDX spectrum of of worn specimen of heat-treated electroless Ni-P-B coating tested at (a) 30°C (b) 100°C (c) 300°C and (d) 500°C

Few parallel grooves along with micro-ploughing (Figure 5.23d) is visible on the surface of samples tested at 500°C. This indicates the occurrence of abrasive wear phenomenon. Fine coating particles are scattered over the whole region of contact in the form of wear debris and

some are getting pressed under the application of loads represented by some small spots in the post wear surface. Blackish regions in the post test surface which point toward heavy oxidation under 500°C (corresponds to NiO), as the similar observed by a number of researchers (Li et al., 2013; Masoumi et al., 2012; Alirezaei et al., 2013b; Franco et al., 2016). The presence of oxygen in the EDX spectrum (Figure 5.24d) also backing this claim.

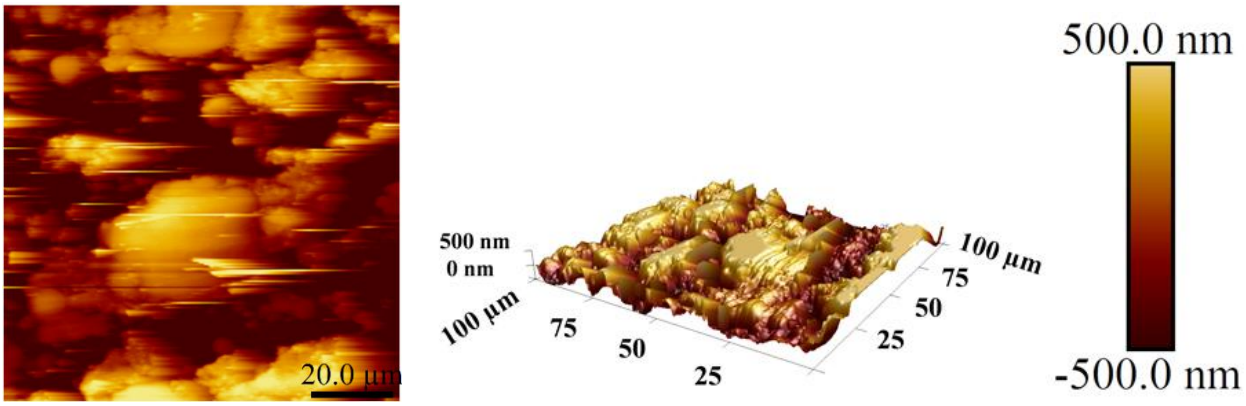

(a) (b)

Figure 5.25 AFM morphology (a) 2D and (b) 3D of heat-treated Ni-P-B coating tested at 500°C

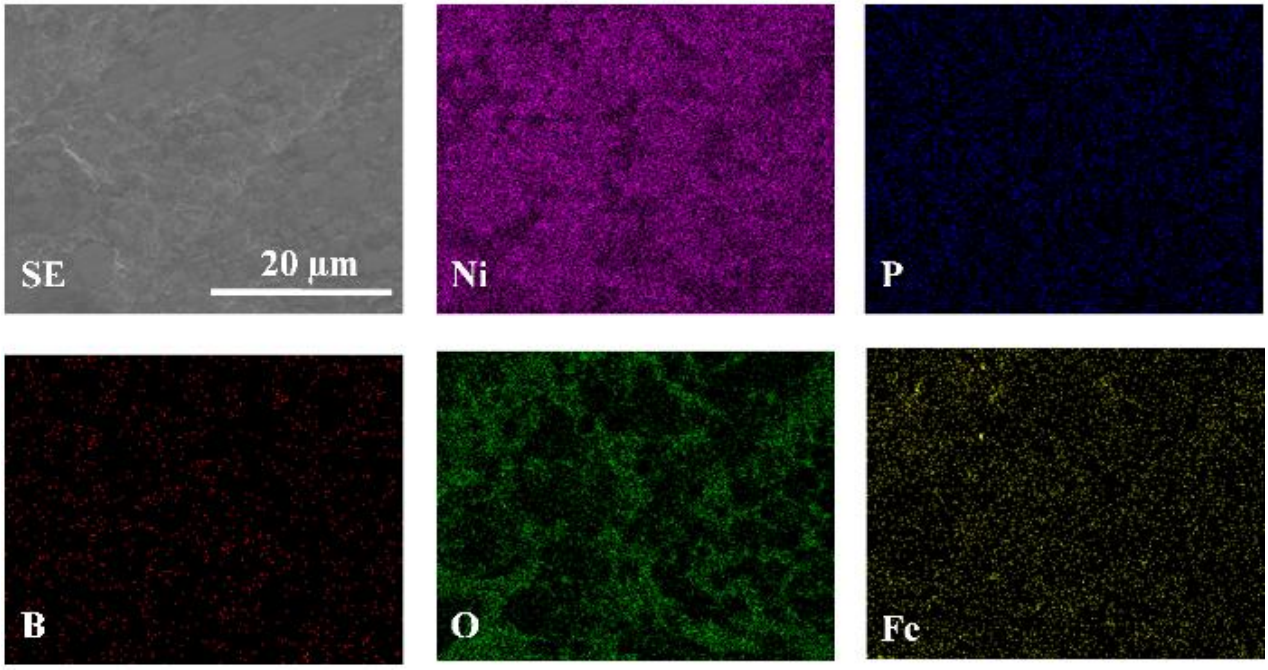

Figure 5.26 EDX maps of worn specimen of heat-treated Ni-P-B coating tested at 500°C

To understand the underlying facts of elevated temperature test in better way as well as to maintain brevity, heat-treated samples post test 500°C are consolidated via AFM and elemental mapping assessment and the corresponding results indicated by Figure 5.25 and 5.26

respectively. The 2D and 3D surface morphology of post test samples is represented by Figure 5.25a and 5.25b respectively. It clearly indicates a rough surface with deep grooves along with micro-ploughing. Wear tracks in the direction of sliding along with material removal is also noticeable. The elemental maps along with SE image of worn heat-treated Ni-P-B coating tested at 500°C is shown in Figure 5.26. SE image of worn out specimens also indicates the linear wear tracks, indicating abrasive wear trend, in the direction of sliding. Uniform allocation of nickel, phosphorous and boron can be seen from the images (Figure 5.26) which mean the survival of coating even after the wear test. The existence of oxygen proves the development of tribo-oxide film as discussed earlier. The oxide layer surrounds over the whole surface of the coating as evident from the mapped image which is the main reason for lesser fluctuation and a reduced amount of COF. For the 500°C, iron shows very strong signal (Figure 5.26) in the image which implies occurrence of adhesive wear whose remnants can be observed from torn patches on the coating post test.

5.3.6.4 Phase transformation and hardness change

Several researchers claim commencement of phase transformation because of in situ heat-treatment during elevated temperature test of EN coatings (Franco et al., 2016; Mukhopadhyay et al., 2018a; 2018c). Detailed XRD study of post wear Ni-P-B coatings are conducted to understand the reality of this claim. Phase transformation study of mainly as-deposited coatings tested at elevated temperature are examined and explained in Figure 5.27. Heat-treated specimens are excluded for XRD analysis, as they are already in crystalline state and so it is complicated to identify the effect of elevated temperature test. The samples subjected to room temperature test causes slight effects in crystal structure and observed similar to that presented by as-deposited coating as indicated in Figure 5.11. Wear behavior of as-deposited coatings during room temperature test is solely controlled by the plastic deformation occurs during the test as stated earlier. Figure 5.27a represents the phase structure of post wear Ni-P-B coatings tested at 100°C. Nickel peak (111) is getting sharper compared to as-deposited coating, may because of phase transformation. Microstructural changes occurs at 100°C is due to combination effect of plastic deformation and test temperature. Further crystallographic change is observed for coatings tested at 300°C , illustrated by Figure 5.27b. Crystalline Ni_2P along with Ni_3B and Ni_2B are visible which clearly indicates the phase transformation of the as-deposited coating during the 300°C wear test. The formation of phosphide and boride phases of nickel are accelerating with the increase in test temperature which reflects in Figure 5.27c. The existence of Fe in Figure 5.27b and 5.27c indicates the transfer of counterface material which ascribed to form a mixed mechanical layer. It acts as a barrier against the wear which leads to improvement in the tribological performance at elevated temperature. Formation of iron carbide at 500°C wear test is also attributed the crystallization phenomenon of as-deposited Ni-P-B coatings. High temperature during wear causes inter diffusion of iron to the surface, decrease of phosphorus and boron as individual element and results in precipitation of nickel phosphides and borides.

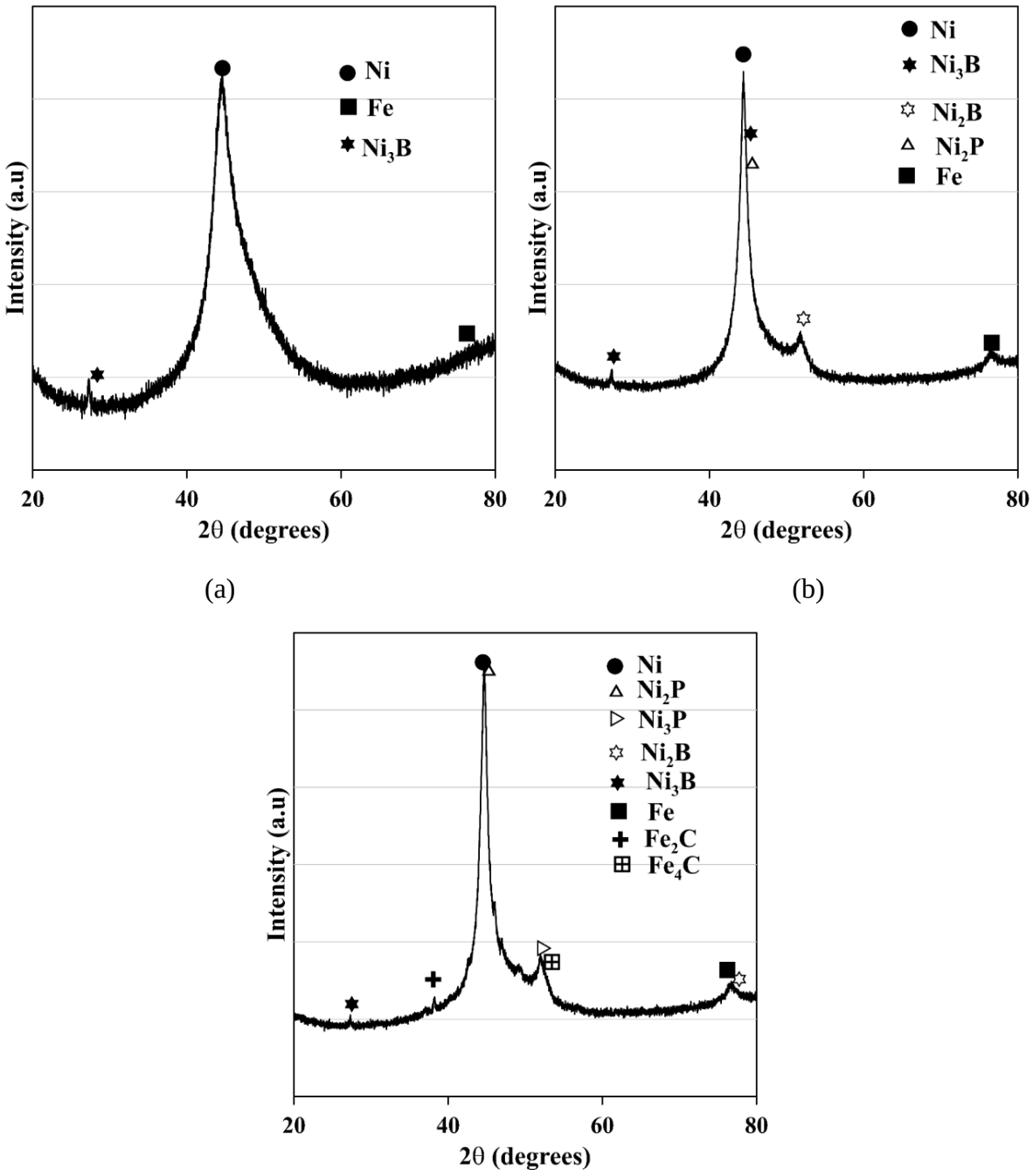

Figure 5.27 XRD analysis of as-deposited Ni-P-B coating post-wear test at (a) 100°C, (b) 300°C, and (c) 500°C

The results obtained through post wear XRD of as-deposited Ni-P-B coating is matching well the earlier results as it mentioned in the wear mechanism section. The point EDX (Figure 5.20c and 5.20d) clearly indicates the presence of inter diffused Fe particle that again

highlighted by Figure 5.19c and 5.19d respectively. The detailed wear mechanism also explains the EDX maps (Figure 5.22) of post wear test sample of as-deposited coatings tested at 500°C, clearly indicating the presence of each element including Ni, P and B, and thus justifying the existence of the coating at elevated temperature. The above discussion thus proves the phase transformation scenario as an outcome of short duration heat-treatment during the elevated temperature wear test. The present study provides a qualitative idea about high temperature tribology of Ni-P-B coatings, further studies such as X-ray photoelectron spectroscopy (XPS) can be conducted for through examination on oxide layer formation, that controls tribological performance of the coatings.

The change in hardness of the coatings after each test at different temperatures is measured and the percentage increase in hardness is represented by the plot in Figure 5.28. On an average there is an improvement of about 1-10% after each test. However, after 500°C test, there is a marked improvement (about 25%) in hardness of the as-deposited specimen. For heat-treated samples, up to 300°C, improvement in hardness is almost negligible. Beyond 300°C, improvement in hardness of the specimen is of the order of 5%. Hence, it can be concluded that the tests at elevated temperatures act as short duration heat-treatment, which have quite a positive impact on the hardness of the as-deposited coating. For heat-treated coatings, improvement in hardness is not that significant across the entire range of testing temperatures. It is interesting to note that there is a good correlation between the wear and hardness results which again satisfying the phase transformation results of as-deposited post wear specimen as indicated in Figure 5.27.

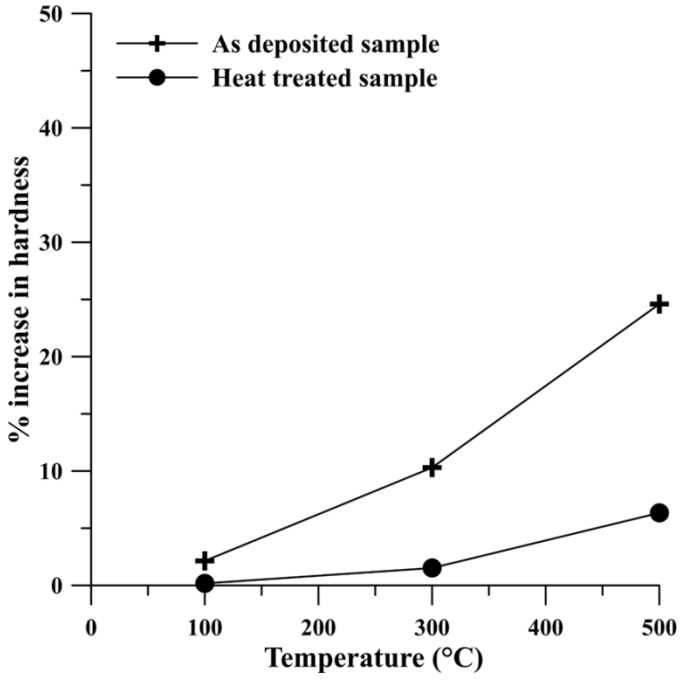

Figure 5.28 Percentage increase in hardness after high temperature tests of Ni-P-B coating

5.4 Conclusion

A combination of sodium hypophosphite and borohydride bath is used to develop electroless Ni-P-B coatings on carbon steel (AISI 1040) substrate. The rate of deposition is higher than that of Ni-P coating. The role of boron is dominating in Ni-P-B, as 3.5 wt% of B is present whereas P content is around 0.7 wt%. The developed low B range coating shows an nanocrystalline structure in as-deposited condition which further crystallizes on heating at 400°C. Cauliflower like appearance with closely compacted nodules is visible on the surface of the coatings. Grain coarsening causes to increase the granule dimension on heat-treatment. The as-deposited coating shows a hardness of $690HV_{0.1}$ which again increases upon heat-treatment. XRD results indicates the precipitation of hard inter metallic phases of nickel-phosphide and nickel-boron. As-deposited and heat-treated coatings are subjected to tribological test at room (30°C) and elevated (100°C, 300°C and 500°C) temperatures. A lower COF is observed for 500°C test in compare to 100°C and 300°C, can be credited to the oxide layer formation at high temperature which causes lubricating action. The developed Ni-P-B shows higher hardness as well as better wear resistance. This can be ascribed to the combination of columnar structure of Ni-P-B coatings and incompatible surface contact with counterface material. For as-deposited Ni-P-B, RT test yields lowest wear rate may because of the nanocrystalline structure and a high hardness value in its as-deposited condition. At elevated temperature (300°C and 500°C) coating shows better wear resistance. This can be attributed to several phenomenon such as formation of oxidative layer, mechanically mixed layer with inter diffused iron, wear mechanism, phase transformation and changes in microstructure during elevated wear test. Phase transformation as an outcome of short duration heat-treatment during the elevated temperature wear test is established. The existence of coating after wear test proves the stability of Ni-P-B in demanding situation.

This page is left blank intentionally

Chapter 6

High temperature tribology of Ni-P-Al_2O_3 coating

6.1 Need for Alumina (Al_2O_3) Inclusion

For better tribological, chemical, mechanical, physical, magnetic, and other properties from the same coatings, sometimes other particles are added into the chemical deposition process, giving rise to the idea of composite coatings. To meet the challenges for the development of material with enhanced characteristics such as high temperature sustainability, higher hardness, lubricity, wear and corrosion resistant etc. is the main cause behind the merger of particles. Many soft particles such as WS_2, MoS_2, PTFE (polytetrafluoroethylene), graphite as well as hard particles like WC, SiC, Al_2O_3, B_4C, TiO_2, diamond, etc. generally used as additional particles in Ni-P matrix (Gadhari and Sahoo, 2016; 2017). The properties of the composite coatings are generally related to and controlled by the second phase particles incorporated in the Ni-P deposit. The incorporation of nano size particles within Ni-P coatings significantly improves the coating properties and imparts new functional features to its performance. Several researchers have used the size of TiO_2 particles in the range of 15-300 nm, Al_2O_3 particles in the range of 5-15 µm, B_4C particles in the range of 5-11 µm and the SiC particles in the range of 40-600 nm. Each of the particles has a unique characteristic and because of that it affects the overall properties and performance of the developed coating. Friction coefficient of electroless nickel coating is increased due to missing of natural lubricity because of the addition of hard particles viz., B_4C (Ebrahimian-Hosseinabadi et al., 2006) and SiC (Araghi & Paydar, 2010) in the deposits.

In composite coatings, second phase particles act as barrier for plastic deformation of coated layer due to the application of load. As a result, an increase in hardness of Ni-P-Al_2O_3 composite coatings (Gadhari and Sahoo, 2016) is observed. Hardness of the composite coating depends on the amount of particles available in the coated layer, bonding strength of particles with coated layer and heat-treatment of the coating. The Al_2O_3 composite coatings heat-treated at 400°C have maximum hardness compared to coatings heat-treated above 400°C. The coating hardness increases due to formation of hard Ni_3P phase at a temperature of 400°C. The hardness of the coating reduces after 400°C due to excessive grain coarsening of coating structure and formation of cracks between consecutive grains. Wear resistance and hardness of a coated surface are correlated, though wear properties of the coatings are affected by many other factors such as the nature of the applied stress and the surface morphology. Phosphorus content and heat-treatment are the two main parameters that affect wear resistance a lot. An attractive force is

generated in between nickel atoms and the counterface material during the rubbing activity that causes the wear of electroless nickel phosphorus coating. Sometimes wear depth curve moves in negative direction which may be because of the formation of buildup oxide debris in between the coated sample and counterface material (Palaniappa & Seshadri, 2008). Gadhari and Sahoo (2016) made a detailed discussion on electroless composite coatings and corresponding tribological behavior under ambient condition.

A thorough literature survey reveals that despite a good number of studies on electroless Ni-P-Al_2O_3 coatings, there is a dearth in studies concerning its tribological behavior under elevated temperature. The current study is aimed to gather knowledge in that direction. The present chapter thus attempts to investigate the friction and wear behavior of hypophosphite reduced composite coating under high temperature. The same results are compared with room temperature condition. The morphology, composition, surface topography and microstructural evolution of the developed coating and worn surface were examined along with wear mechanism investigation. The present chapter deals with the development and high temperature tribological characteristics with wear mechanism of one of the composite variant of Ni-P i.e. Ni-P-Al_2O_3 coating.

6.2 Experimental Details

The way to develop the coating starting from substrate preparation and evaluation of the developed Ni-P-Al_2O_3 coating through several characterisations are same as mentioned earlier in chapter 2. The basic components and operating conditions of hypophosphite-reduced Ni-P composite coating is provided in Table 6.1, where 10g/L Al_2O_3 particles is added as a source of second phase particles (alumina). For better suspension and to avoid agglomeration of particles, the appropriate amount (0.2 gL-1) of surfactant (sodium dodecyl sulphate, SDS) is added into electroless Ni-P bath. Approximately 50 ml of electroless Ni-P solution containing with specified amount of second phase particles and surfactant is thoroughly mixed using magnetic stirrer to get better suspension of second phase particles (Al_2O_3 particles) in the electroless bath. At first Ni-P coating is deposited for one hour to prevent the porosity of the coating and to achieve good adhesion of coated layer with the substrate surface. After that the slurry of second phase particles, SDS and electroless solution (50 ml) is introduced into the same bath for a subsequent deposition of period two hours. It is very important to maintain the optimum agitation speed (150 rpm) of electroless bath. At lower agitation speed particles start agglomerating which results in decomposition of electroless bath. Similarly, at higher agitation speed, rate of particle incorporation is decreases due to insufficient time for particles to deposit on the coated surface. The pH of the solution is maintained at by continuous monitoring with a pH meter. All depositions are carried out for a period of three hours with mild agitation (stirred at 150 rpm) and same volume of the solution is used, so that the coating thickness and bath load remain approximately same for the entire specimen. As some heat-treated samples are required for the tests, some coated specimens undergo heat-treatment in the box furnace at 400ºC for 1 hour and

then cooled naturally. This particular temperature is selected as most researchers have acknowledged it as the best heat-treatment condition for Ni-P-Al_2O_3 coatings admired to tribological behavior.

Table 6.1: Bath composition and operating condition for Ni-P-Al_2O_3 composite coating

Bath chemical composition		**Operating conditions**	
$NiSO_4.6H_2O$ (Nickel Sulphate)	35 g/L	pH	4.5-5.0
$NaH_2PO_2.2H_2O$ (Sodium Hypophosphite)	20 g/L	Bath Temperature	85±2°C
Al_2O_3 Particles	10 g/L	Bath Volume	250 ml
$C_6H_5Na_3O_7.2H_2O$ (Tri Sodium Citrate)	15 g/L	Stirrer Speed	150 rpm
CH_3COONa (Sodium Acetate)	5 g/L	Deposition Time	3 Hours
$(CH_3COO)_2Pb.3H_2O$ (Lead Acetate)	2 mg/L	Annealing Temperature	400ºC
$C_{12}H_{25}NaO_4S$ (Sodium Dodecyl Sulphate)	0.2 g/L		

The detail of each of the characterisation performed is same as other coating variant and is mentioned earlier in chapter 2. Effect of test parameters such as load and sliding velocity on wear (in terms of mass loss/distance) and friction coefficient are evaluated under room temperature (30°C) and at high temperature (500°C) as following Table 3.2. From this analysis, suitable load and sliding velocity are decided after which they are subjected to a detail high temperature tribological tests by varying the temperature as mentioned in Table 3.3. Details XRD study of post wear Ni-P-Al_2O_3 coatings are conducted to understand the commencement of phase transformation because of in situ heat-treatment during elevated temperature test of as-deposited coatings. The changes in hardness due to high temperature test for both kind of samples are also examined to correlate the post test XRD results.

6.3 Results and Discussions

6.3.1 Ni-P-Al_2O_3 coating configuration

Al_2O_3 particles are added in the hypophophite reduced Ni-P matrix, for the deposition of Ni-P-Al_2O_3 coatings. Inclusion of Al_2O_3 particles in Ni-P matrix decreases the deposition rate compared to Ni-P coating. The deposition thickness versus time plot is presented in Figure 6.1. The deposition rate is very low for Ni-P-Al_2O_3 bath, about 6-10 μm/h. To achieve required thickness for tribological tests, instead of replenishment, double bath deposition technique (a total of 6h) is adapted for Ni-P-Al_2O_3 deposition.

Al_2O_3 added to the coating as a third particle is expected to have positive effect on the tribological behavior of the coating. Composition analysis of as-deposited and heat-treated Ni-P-Al_2O_3 coating is done using EDX and the spectrum shown in Figure 6.2. The analysis reveals that the Al content in terms of weight percentages, lie in the range of 8.7-8.9 and phosphorous content, in the range of 6.6-7.1 with oxygen close to 7.2-7.6 wt% while the remaining is nickel. This confirms that the developed coating is a composite mixing of nickel, phosphorous, Al_2O_3 as desired. Now, the phosphorus percentage of the deposit determines its crystallinity. In general, for the binary Ni-P alloy system, the coatings are seen to be amorphous in the high phosphorus (10-13 wt% P) range, while a mixture of nano-crystalline and amorphous phases exist for the medium phosphorus (6-9 wt% P) deposits. It has been seen from the literatures that incorporation of Al_2O_3 improves the crystallinity of the coatings due to the reduction in phosphorus content, and the coatings are transformed more to a mixture of amorphous and nano-crystalline phases. EDX of Ni-P-Al_2O_3 coating heat-treated at 400°C for 1 h is shown in Figure 6.2b and is very close to that of as-deposited case, except the presence of excess oxygen (around 10%). Hence, the formation of oxide scales due to heat-treatment could be confirmed from EDX results. Rest of the elements does not exhibit much variation in their composition.

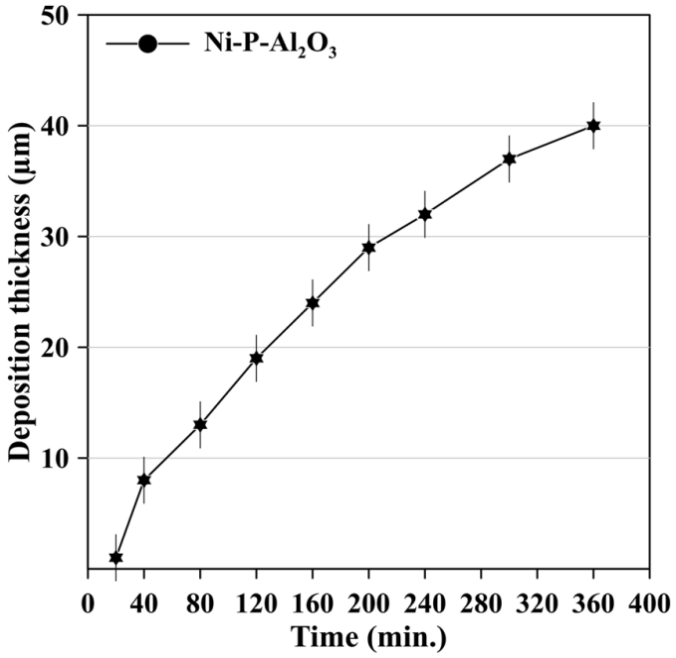

Figure 6.1 Deposition rate of Ni-P-Al_2O_3 coating

In addition to point elemental analysis, EDX line scan is also performed on the cross cut section of the coating for better understanding of elemental distribution. The detailed line scan is shown in Figure 6.3. The quantitative results indicating weight percentage of Ni, P, Al, O and Fe is given in table inside Figure 6.3a. Composition profiles of Ni, P, Al, O and Fe measured along the thickness of Ni-P-Al_2O_3 (Figure 6.3b) coatings are performed through line EDX for thorough understanding of the elemental variation across the cross section.

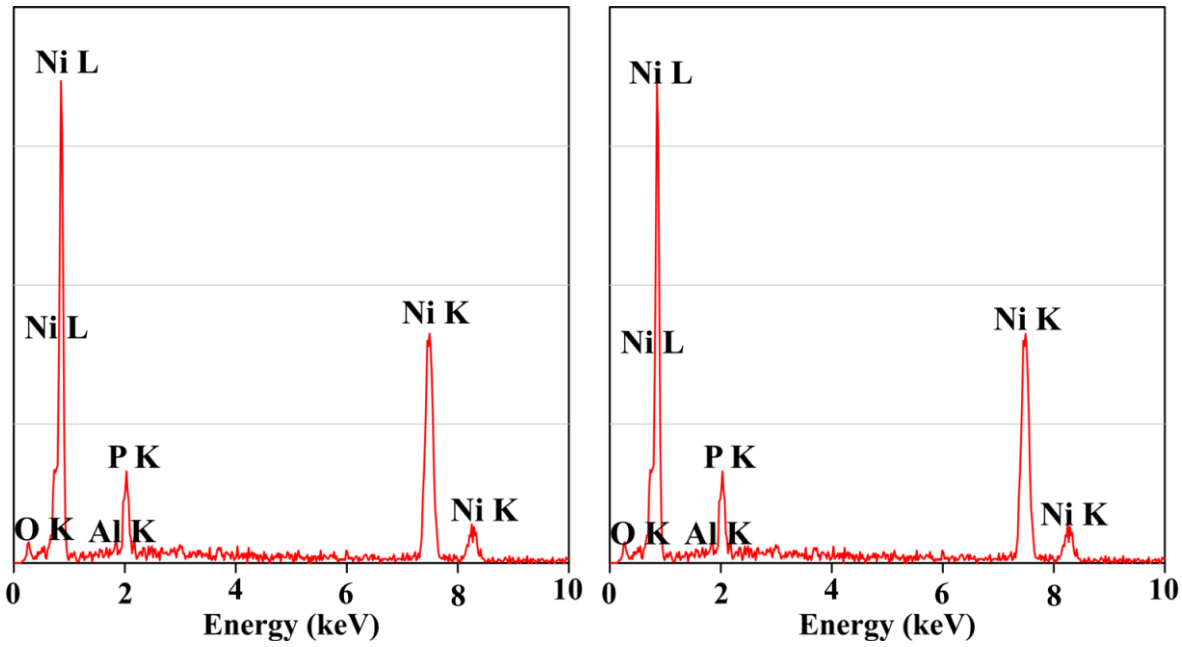

(a) (b)

Figure 6.2 EDX spectrum of (a) as-deposited and (b) heat-treated electroless Ni-P-Al_2O_3 coating

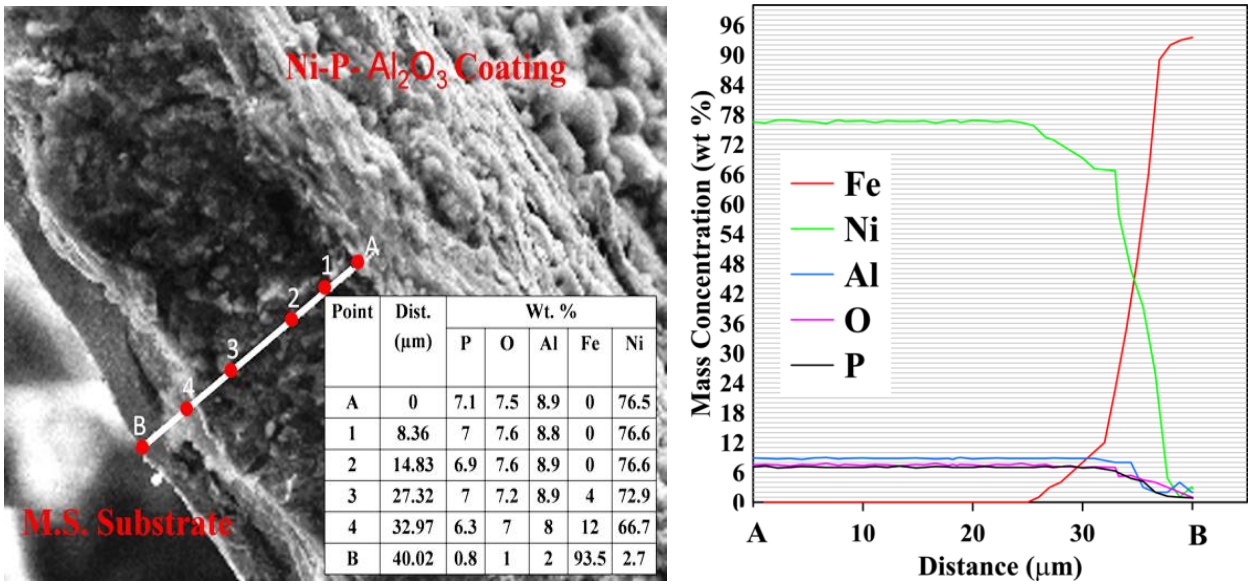

(a) (b)

Figure 6.3 (a) SEM image showing line EDX (quantitative analysis included in table) and (b) detailed composition profiles of elements presents measured along the thickness of the Ni-P-Al_2O_3 coating

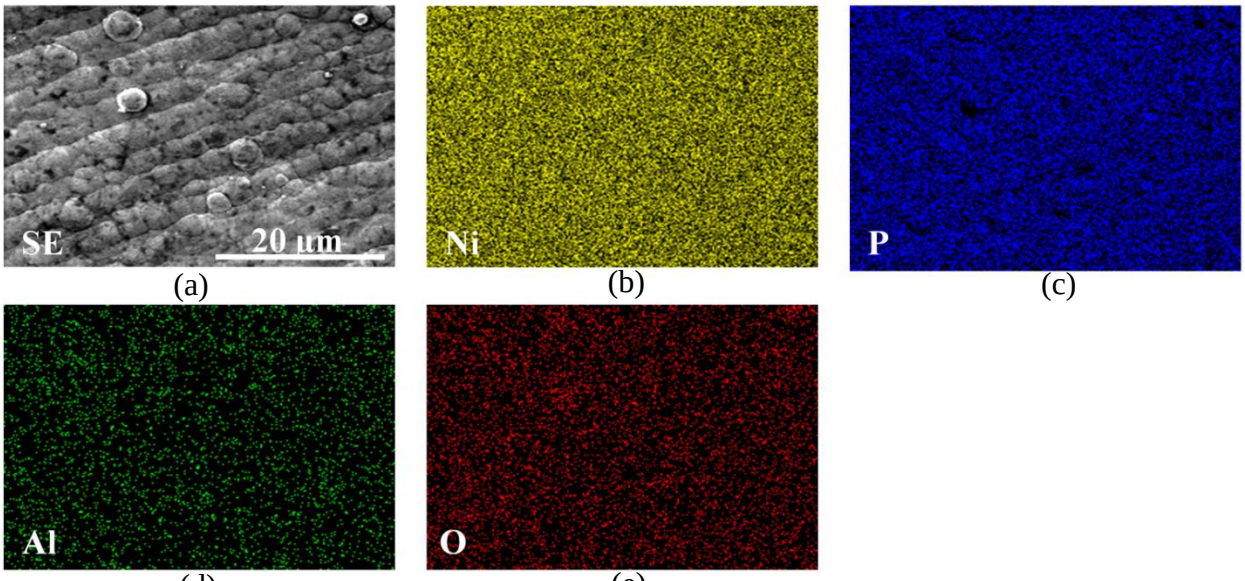

(a) (b) (c)

(d) (e)

Figure 6.4 EDX mapping analysis on the surface of the as-deposited Ni-P- Al_2O_3 coating

Moreover, to confirm the presence of individual elements in the respective coatings EDX mapping is carried out for as-deposited and heat-treated Ni-P-Al_2O_3 coating and presented in Figure 6.4 and Figure 6.5 respectively. The cross-sectional SE image of as-deposited and heat-treated coating layer is shown in Figure 6.4a and 6.5a respectively. EDX mapping proves that the nickel, phosphorus, aluminium and oxygen are uniformly and homogeneously distributed in the Ni-P-Al_2O_3 matrix as seen in Figure 6.4 for as-deposited and the same for heat-treated are presented in Figure 6.5.

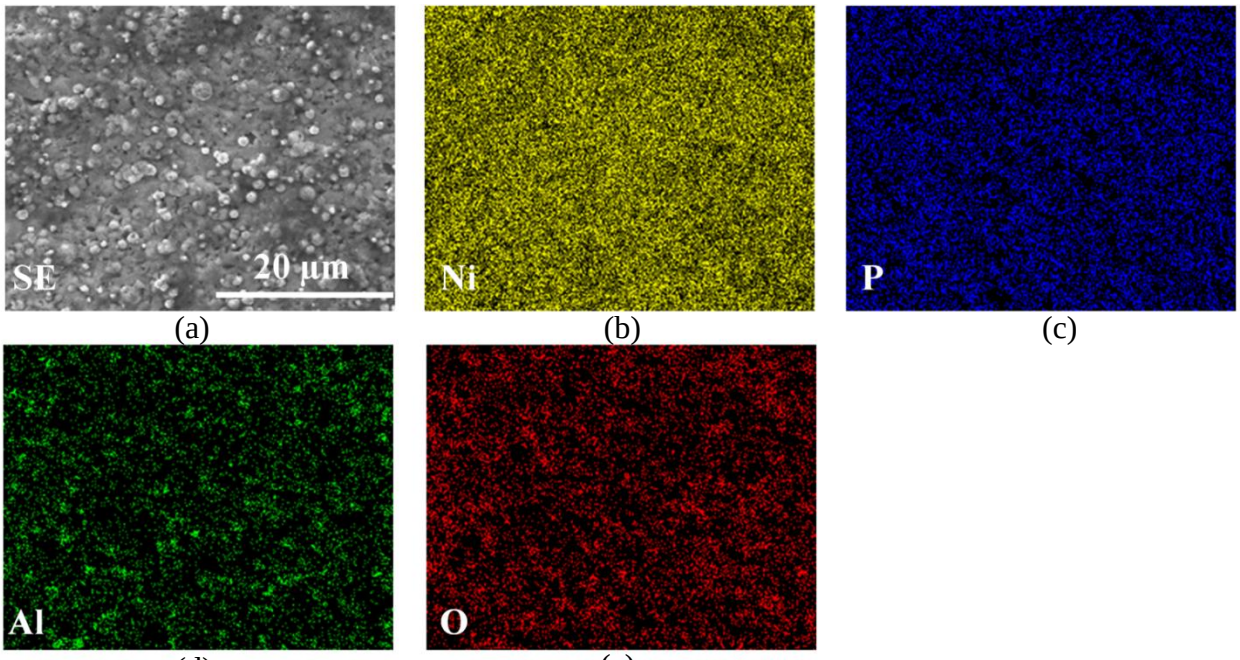

(a) (b) (c)

(d) (e)

Figure 6.5 EDX mapping analysis on the surface of the heat-treated Ni-P-Al_2O_3 coating

6.3.2 Surface texture of coating

Optical micrograph of as-deposited and heat-treated Ni-P-Al_2O_3 coating is presented in Figure 6.6. The same captured via scanning electron microscope is shown in Figure 6.7. From optical micrographs (Figure 6.6) it is confirmed that samples heat-treated at 400ºC exhibit more pores as compared to as-deposited sample, which might be due to the voids created by the release of trapped hydrogen gas and elimination temporary aluminum particles present on the coated surface during heat-treatment process. From SEM micrograph it is confirmed that as-deposited Ni-P-Al_2O_3 composite coatings have smooth surface and aluminium particles are almost uniformly embedded in the Ni-P layer (Figure 6.7a) In as-deposited condition, the nodules are almost flat and uniformly distributed. But when heat treated, the nodules grow in size giving rise to a coarse-grained structure as indicated both in optical and scanning microscope image. This indicates that in as-deposited condition the structure is a mixture of amorphous and microcrystalline structures which becomes crystalline with heat-treatment. The coating thickness is determined by observing the cross cut surface of the coated substrate in SEM as indicated by Figure 6.8. To get better and accurate result, the cross cut surface of the coated substrate is well ground. With proper alignment of substrate surface and by proper magnification index of microscope, thickness of the coating is accurately measured. It seems that the coating is connected closely to the substrate exhibiting good adhesion to the substrate. The coating thickness which lies in the range of 35-40 µm. For achieving the mentioned thickness Ni-P-Al_2O_3 is deposited for six hours with replenishment action with a single interval.

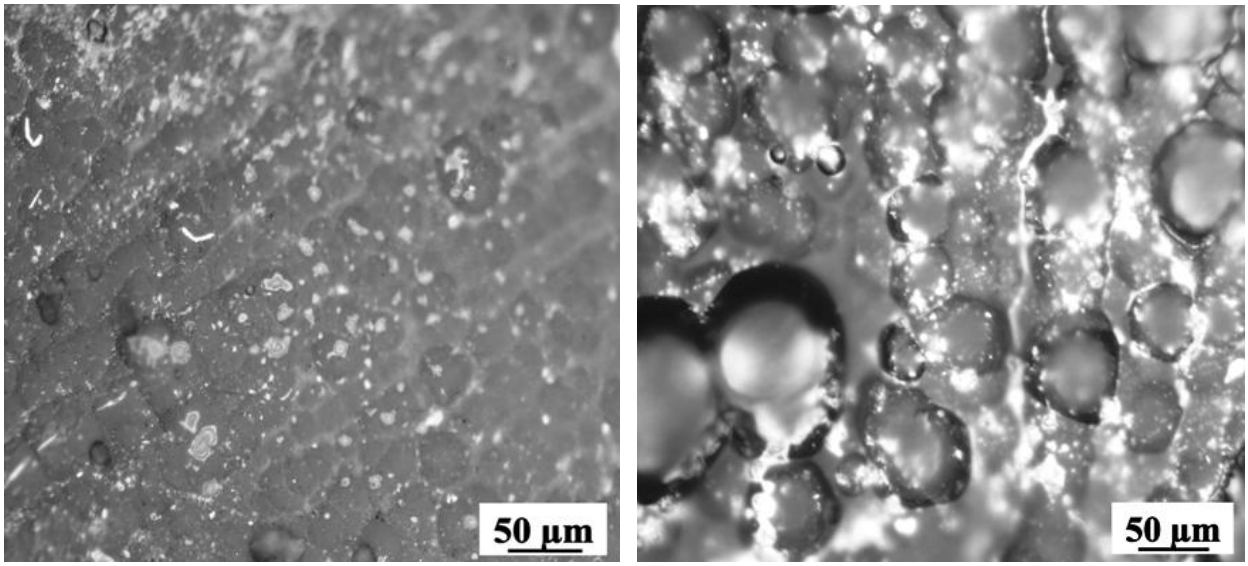

(a) (b)

Figure 6.6 Optical micrograph of (a) as-deposited and (b) heat-treated electroless Ni-P- Al_2O_3 coating

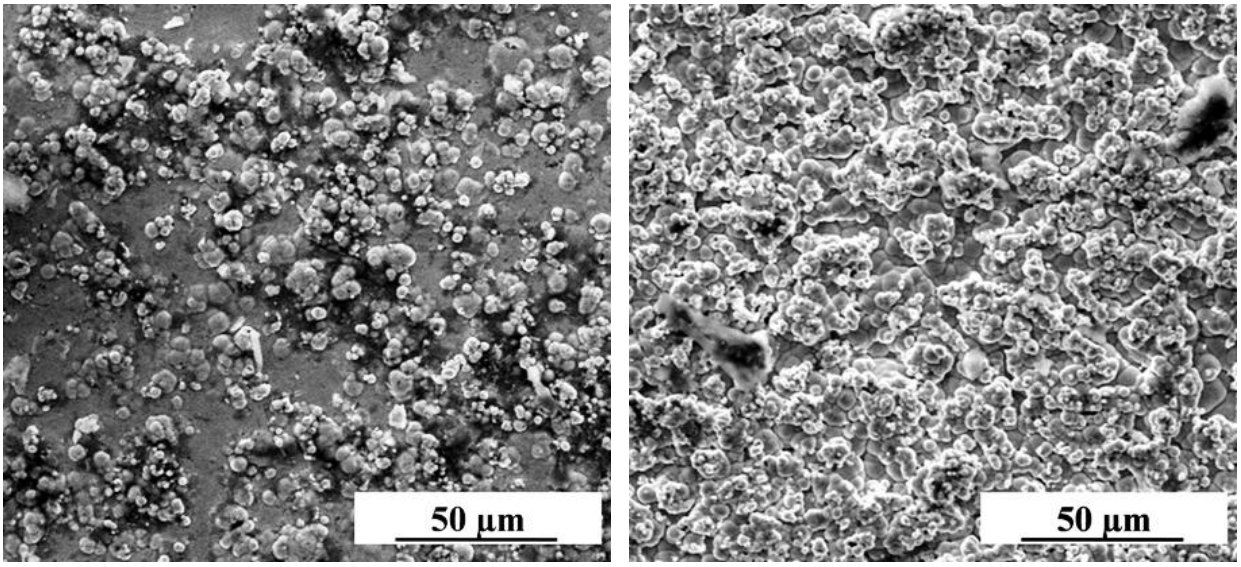

(a) (b)

Figure 6.7 SEM micrograph of (a) as-deposited and (b) heat-treated electroless Ni-P-Al_2O_3 coating

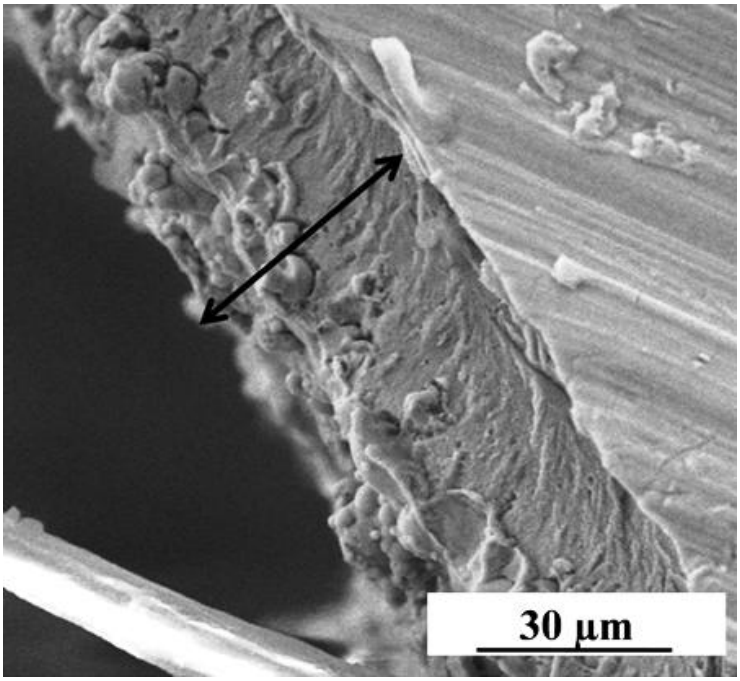

Figure 6.8 A cross-cut section of the Ni-P- Al_2O_3 coating

Further, surface texture of the coating of both as-deposited and heat-treated is investigated in more details through AFM and the corresponding plots appear in Figure 6.9 and 6.10 respectively. The AFM results reiterate the observations made through SEM. As usual nodular morphology for heat-treated coatings are observed. The figure corresponding to as-deposited coating is not showing any distinct feature. The 2D and 3D illustration of Ni-P-Al_2O_3

coatings in before and after heat-treatment conditions have been inspected with AFM in contact mode with a scan area of 10 μm × 10 μm. Nodular feature is very common in electroless deposition which arise due to fast nuclei creation and its successive growth. Apart from that bath constituents, coating environment and substrate surface mainly surface irregularities plays a deciding role in formation of nodule. The common nodular structure is formed by joining crystals each other on the surface of the substrate as clearly visible in Figure 6.10. The grain coarsening (supported further through XRD study) because of heat-treatment causes to increase the surface irregularities which indicates a higher roughness of heat-treated specimen compared to as-deposited samples. From the AFM observation (Figure 6.10), each grain of heat-treated samples consists of higher number of smaller grains analogous to diffused like morphology.

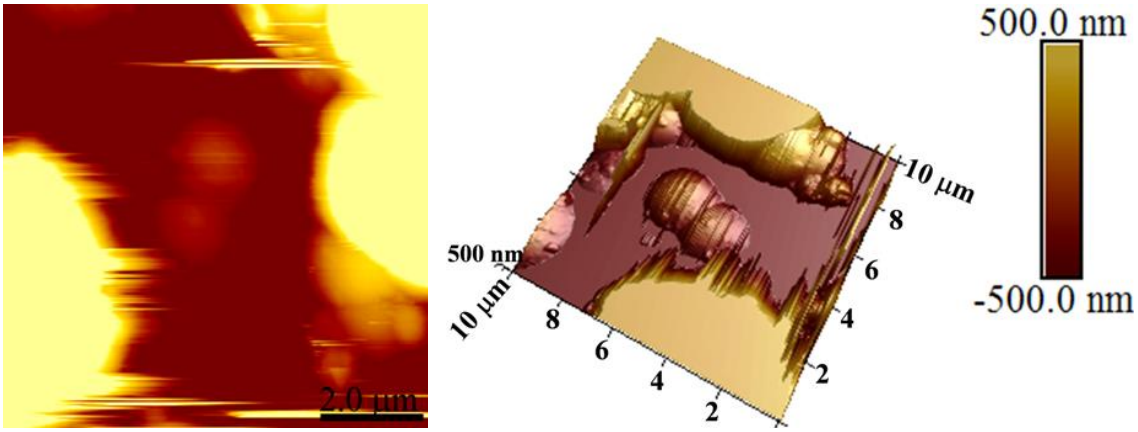

(a) (b)

Figure 6.9 Typical AFM morphologies of as-deposited Ni-P- Al_2O_3 surfaces in (a) 2D and (b) 3D

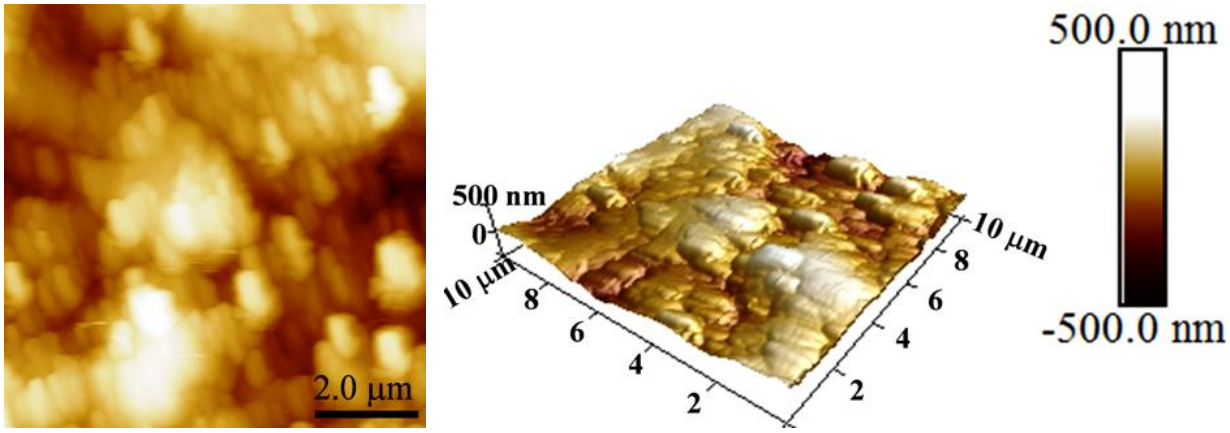

(a) (b)

Figure 6.10 Typical AFM morphologies of heat-treated Ni-P- Al_2O_3 surfaces in (a) 2D and (b) 3D

6.3.3 Structural aspects of Ni-P-Al_2O_3 coating

From XRD plots (Figure 6.11), it is confirmed that composite coatings have single broad peak. The broad peak corresponding to nano-crystalline phase composed of extremely fine nano meter scaled crystalline regions surrounded by amorphous grain boundaries. Hence, coatings have amorphous structure in as-deposited condition. For as-deposited samples, the presence of broad and single peak at 40–50° position shows the typical amorphous structure of electroless nickel composite coatings. Broad peak vanishes due to annealing, suggesting decomposition of Ni-P solid solution and formation of crystalline Ni and Ni_3P precipitates. XRD plots for heat-treated (at 400ºC) Al_2O_3 composite coating is shown in the same Figure 6.11. From the plot it is confirmed that the amorphous structure is converted into crystalline structure. Due to heat-treatment, hard phases of (Ni_3P) are seen at various diffraction angles. Some Al_2O_3 peaks are seen in heat-treated Al_2O_3 composite coating

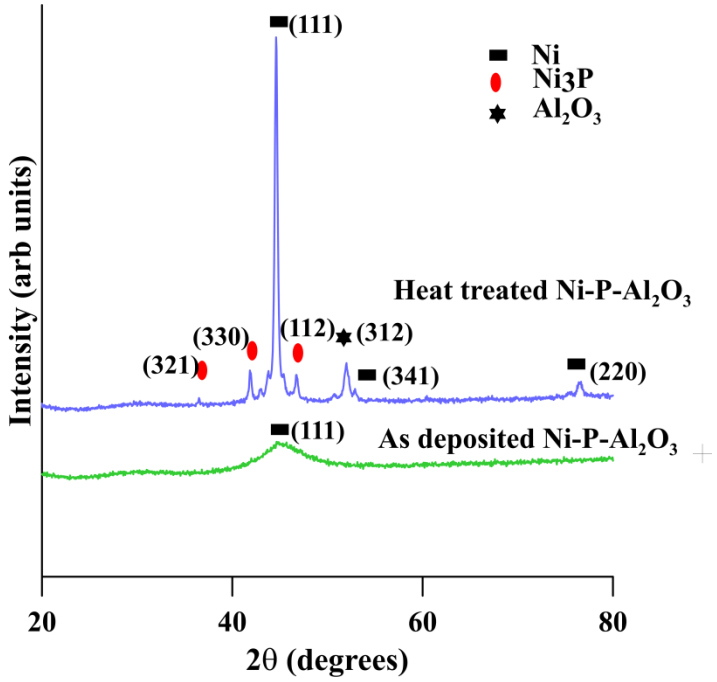

Figure 6.11 XRD spectra obtained for as-deposited and heat-treated electroless Ni-P-Al_2O_3 coating

6.3.4 Roughness and microhardness evaluation

The incorporation of Al_2O_3 particles has greater impact on the surface roughness of the composite coatings. Increase in amount of these particles increases the roughness of the composite coatings. For the amount of Al_2O_3 at the rate of 10g/L shows the roughness (R_a) of Ni-P-Al_2O_3 coating is close to 0.7. Which further slightly increases due to heat-treatment.

The incorporation of Al_2O_3 in Ni-P coatings is also reflected in the micro hardness results of the as-deposited coatings (Figure 6.12). When compared to that of Ni-P coatings which has as-deposited hardness around 600 $HV_{0.1}$ (as presented in chapter 3), Ni-P-Al_2O_3 coating is found to have hardness around 790 $HV_{0.1}$. This improvement in hardness is definitely due to the incorporation of Al_2O_3 which itself has a relatively higher hardness. There is a significant rise (more than 42%) in the average hardness of the coating post heat-treatment (400°C, 1h). This remarkable improvement in hardness is observed due to hard phases of (Ni_3P) along with few Ni and Al_2O_3 peaks of the EN matrix by Al_2O_3 addition as also reported by Gadhari et al. (2016). However, the hardness of the heat-treated Ni-P-Al_2O_3 coating is not so high when compared to that of heat-treated Ni-P coating (average hardness around 1000 $HV_{0.1}$) (as indicated in chapter 3). Moreover, since all the samples are subjected to a uniform deposition condition, a very low variation in micro-hardness between the specimens is ensured.

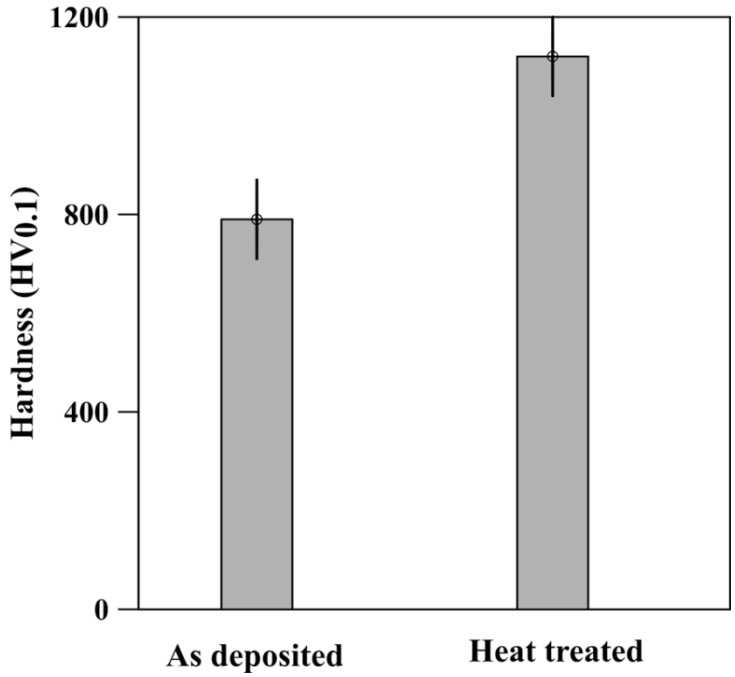

Figure 6.12 Microhardness obtained for as-deposited and heat-treated electroless Ni-P-Al_2O_3 coating

6.3.5 Tribological characterization based on test parameters

6.3.5.1 Friction under different load and sliding velocity

The effect of load and sliding velocity under ambient and high temperature on the friction performance of as-deposited and heat-treated Ni-P-Al_2O_3 coatings are studied. The experiments are arranged in an incremental manner by varying one factor at a time. The COF of as-deposited as well as heat-treated coatings as a function of load and sliding velocity separately under two different working temperature are shown in Figure 6.13a and 6.13b respectively. The samples are

slide in different load by choosing an uniform sliding velocity of 0.22 m/s. In general, COF increases with increase in applied load which is attributed to the increase in contact area and subsequent higher force required to break them. Similar observations have already been made by other researchers (Chowdhury et al., 2011). However, the test conducted at high temperature are not so much influenced by the different load and represent nearly similar COF results. In most of the combinations, as-deposited perform better in compare to heat-treated sample with respect to COF, it may because of higher hardness of heat-treated samples.

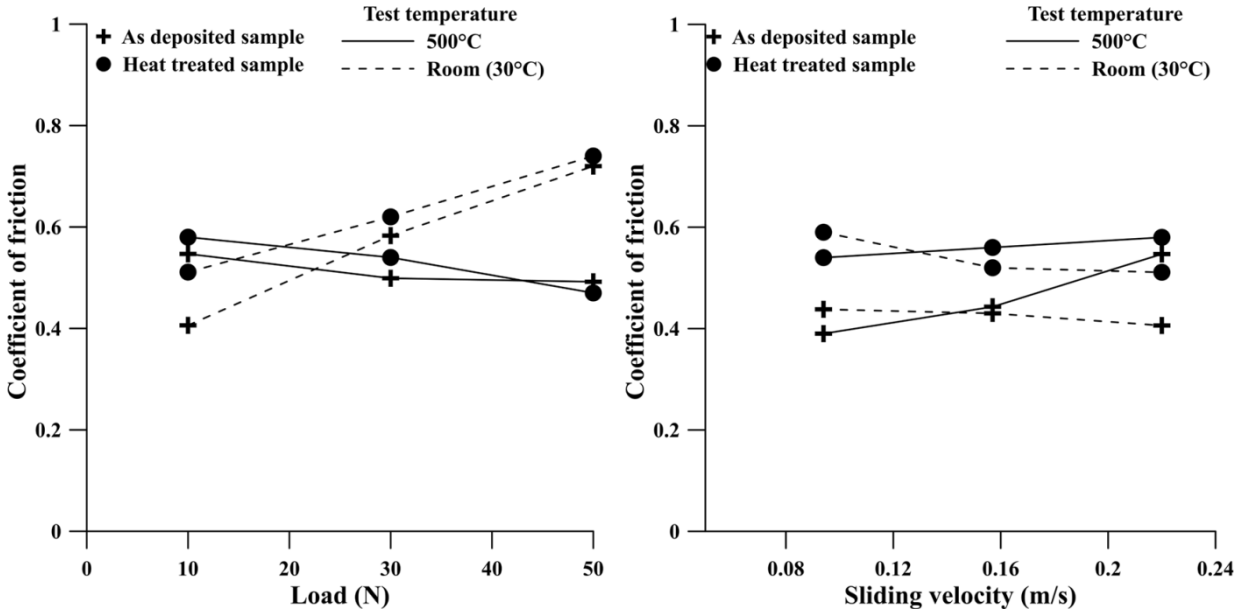

(a) (b)

Figure 6.13 Friction performance of Ni-P-Al_2O_3 coating for room and high temperature under different (a) load and (b) sliding velocity

The sliding tests are conducted at a uniform load of 10 N. Except at 500°C, increase in sliding velocity results in lowering of COF. Hence, it can be seen that both sliding velocity as well as operating temperature have a significant effect over the COF of EN coatings. Now, during sliding, the contact points change rapidly depending on the sliding velocity as new points come in contact and existing contacts break. The more the area of contact, the higher is the friction at the interface. The decreasing trend of COF with sliding velocity may be due to the change of shear rate which can in turn affect the mechanical properties of the mating materials (Bhushan & Jahsman, 1978). Moreover, higher sliding velocity will contribute to a larger normal momentum transfer in the upward direction. This results in an increased separation between the coating and the counterface which further results in decreased real area of contact. This may also serve as an explanation for the lower friction coefficient at higher sliding velocity. At higher operating temperature, the coating gets a real time heat-treatment and hence becomes hard. The friction behavior of heat-treated coatings under room and high temperature for different sliding

velocity are also included in Figure 6.13b. The effects of sliding velocity and high temperature on COF are analogous to the results of as-deposited Ni-P-Al_2O_3 coatings.

6.3.5.2 Wear under different load and sliding velocity

Wear behavior of Ni-P-Al_2O_3 coatings is investigated under ambient and high temperature by varying the testing parameters viz. normal load and sliding velocity The effects of each parameter on the wear of the coating are investigated in detail here. Wear is represented by the ratio of weight loss to the distance traversed so that the effect of sliding speed on wear can be truly realized. The effect of load and sliding velocity on wear under two temperature for as-deposited along with heat-treated Ni-P-Al_2O_3 coatings is shown in Figure 6.14a and 6.14b respectively. For Figure 3.14a, sliding velocity is fixed as 0.220 m/s whereas for Figure 6.14b, load is fixed as 10 N. From Figure 6.14a, it is found that wear rate increases with increase in applied load. For the current study, under RT for both as-deposited and heat-treated coatings, wear is found to increase by almost eight times within the load range 10–50 N. Whereas under elevated temperature conditions, within the same load range, the increase of wear is about five times (500°C plot) for as-deposited coatings though for heat-treated coatings, the effect is less. The change in wear rate because of load application is less at 500°C which can be attributed to the increase in hardness of the coating due to heat-treatment at the test temperature. This results can be further supported by post wear phase transformation and hardness study to understand and correlate the reason behind the better wear resistance of Ni-P-Al_2O_3 as-deposited coatings at high temperature (500°C) test.

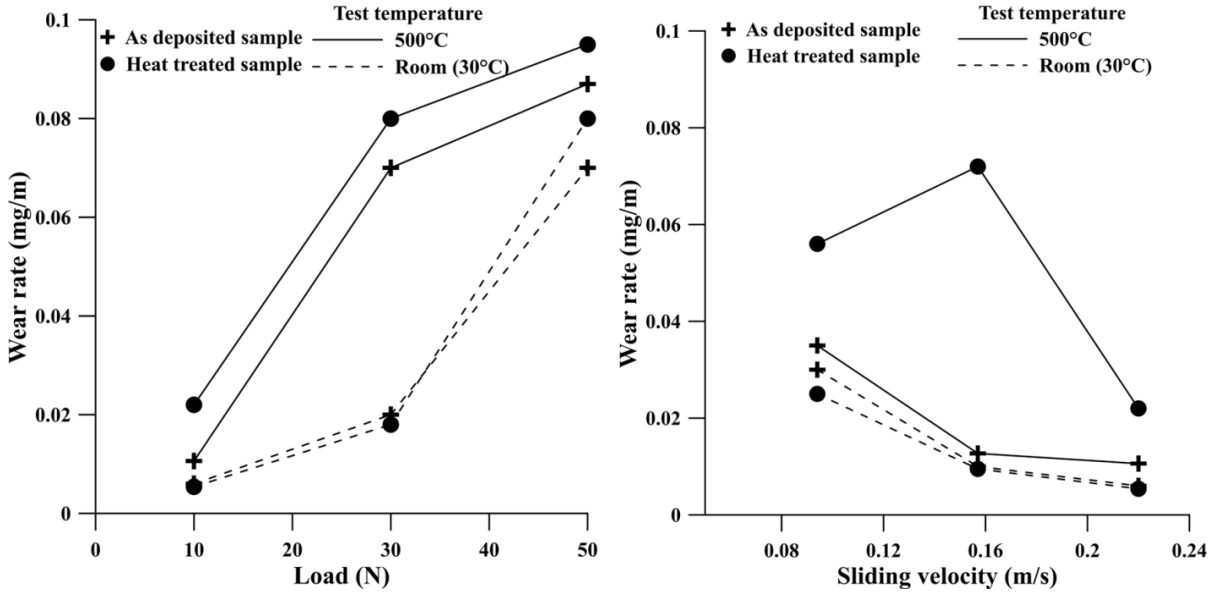

(a) (b)

Figure 6.14 Wear performance of Ni-P-Al_2O_3 coating for room and high temperature under different (a) load and (b) sliding velocity

The relation between wear rate and sliding velocity for varying test temperature for a particular load (10 N) is shown in Figure 6.14b. It is found that under elevated temperature conditions wear reduces with increase in sliding speed. For variation of speed from 30-70 rpm, wear is found to decrease by about 3-4 times in both room temperature as well as tests conducted at 500°C. The behavior of as-deposited and heat-treated both of the Ni-P-Al_2O_3 coatings are very similar to each other. It is observed that the increase in load results in higher wear for any working temperature as in the case of both as-deposited and heat-treated samples. Also similar to the as-deposited sample, increase in sliding velocity results in decrease in the wear rate of both the coating. A direct comparison of the room and high temperature tribological performances of as-deposited as well as heat-treated Ni-P-Al_2O_3 coatings is shown in Figure 6.13 and 6.14 respectively. The comparison is presented for the best combination of applied load and sliding velocity (10 N and 0.220 m/s) as seen from the previous discussions. So, further temperature profiling and detailed discussion on as-deposited and heat-treated Ni-P-Al_2O_3 coating is presented in the next section based on the selected load and velocity combination.

6.3.6 Study of tribological behavior of Ni-P-Al_2O_3 coating at various test temperatures

6.3.6.1 Friction performance of as-deposited and heat-treated Ni-P-Al_2O_3 coating at at different test temperatures

COF of as-deposited and heat-treated Ni-P-Al_2O_3 coating with respect to test temperature is presented in Figure 6.15. In ambient condition, the as-deposited coatings shows much lower friction compared to heat-treated case, which may be because of higher hardness of heat-treated Ni-P-Al_2O_3. Friction coefficient shows a lower value tested at RT and with the increase in temperature to 100°C it suddenly moves to 0.8 and thereafter with further increase in temperature it gradually decreases as shown by Figure 5.15a. Material softening at higher temperature is probably the reason for that drop in COF. Heat-treated specimen shows a higher COF at RT and at 100°C test compared to as-deposited Ni-P-Al_2O_3. Coarse grained surface morphology because of heat-treatment causes to increase the surface roughness and accordingly the COF. But a reverse trend is noticed for 300°C and 500°C test temperature. Present investigation with as-deposited and heat-treated Ni-P-Al_2O_3 indicates higher COF at 100°C compared to elevated temperature (300°C and 500°C) test. It is therefore noteworthy to use Ni-P-Al_2O_3 coating for elevated temperature applications with respect to frictional performances.

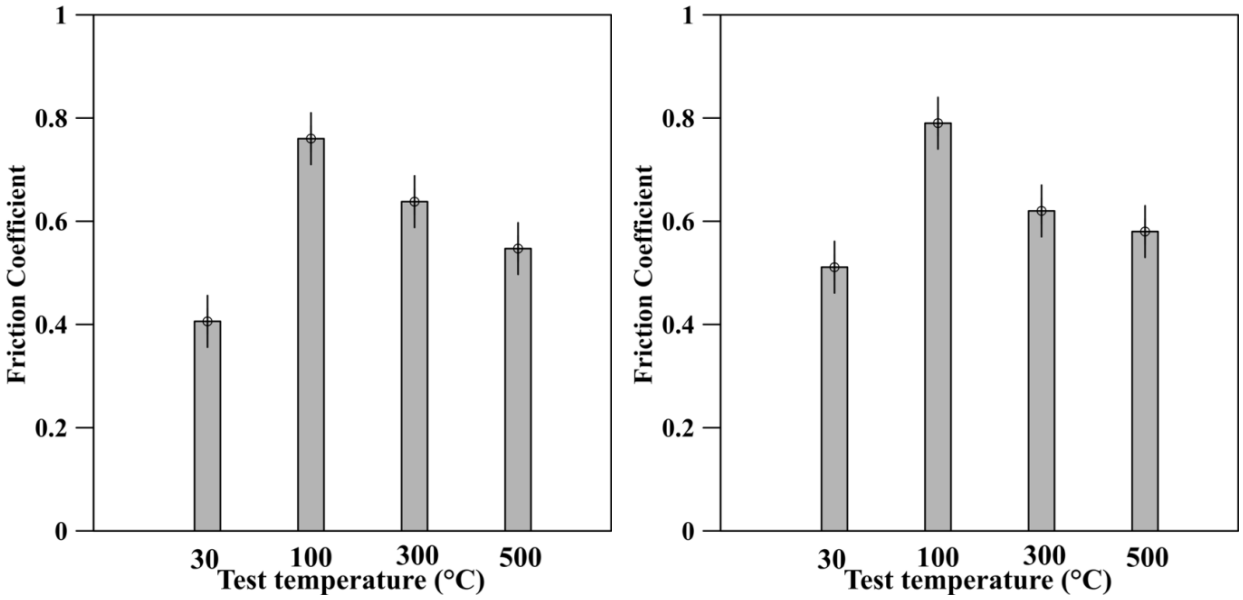

Figure 6.15 Friction as a function of test temperature for (a) as-deposited and (b) heat-treated Ni-P-Al_2O_3 coating

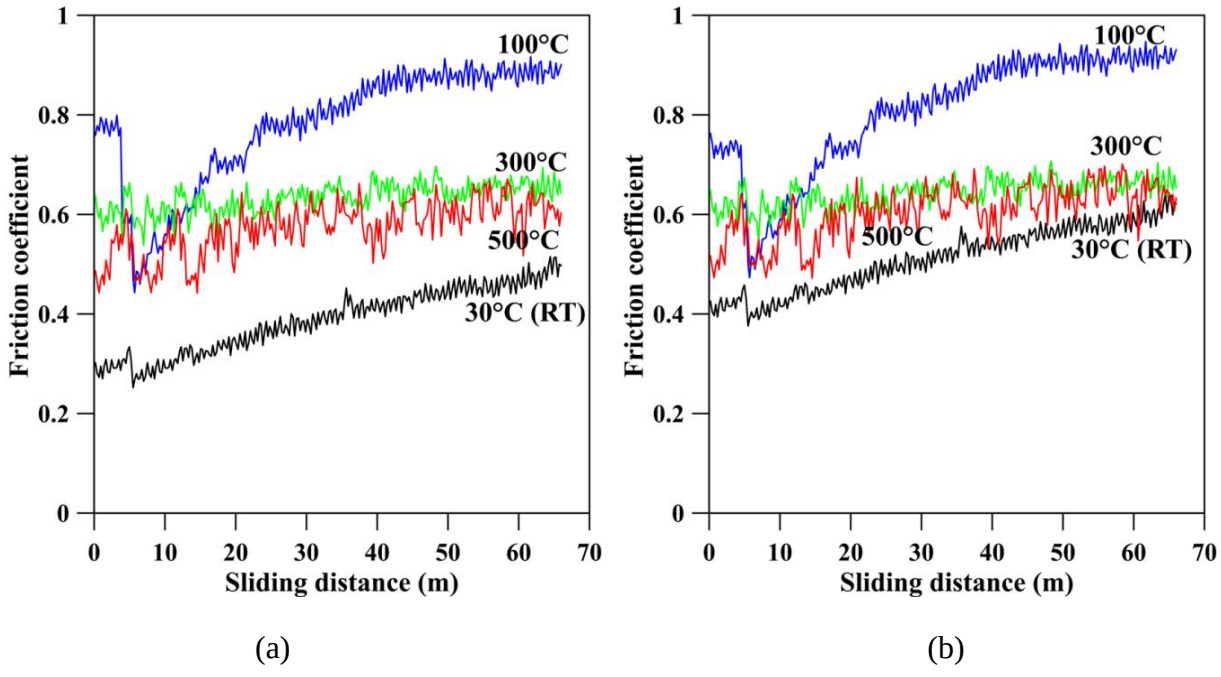

Figure 6.16 Evolution of COF of at room and elevated temperatures for (a) as-deposited and (b) heat-treated Ni-P- Al_2O_3 coating

The variation of coefficient of friction (COF) with distance traversed for tests conducted at different temperatures is illustrated in Figure 6.16. It is observed that for as-deposited sample

(Figure 6.16a), COF in general doesn't suffer huge variation with distances at all temperatures except at R.T and at 100°C. At. 100°C, COF variation by about 2 times is observed. Friction is also found to be lower for tests conducted at higher temperatures in compare to 100°C. For heat-treated case, the variation is analogous to as-deposited sample and the minimum value of friction belongs to test conducted at R.T followed by 500°C.

6.3.6.2 Wear performance of as-deposited and heat-treated Ni-P-Al_2O_3 coating at different test temperatures

Wear performance of Ni-P-Al_2O_3 coating both in as-deposited as well as heat-treated state at various testing temperature is studied. The experimental data is used to observe the wear behavior of electroless Ni-P-Al_2O_3 coatings through graphical representations. Here, wear is represented by the ratio of weight loss to the distance traversed. Figure 6.17 shows the wear rates at different test temperatures, both for as-deposited and heat-treated samples. Contrary to the common belief, it is observed that wear rate doesn't show a continuously increasing trend with the increase in test temperature. In case of as-deposited samples, wear rate increases with increase in test temperature and then suddenly drops at 500°C. For heat-treated samples, R.T. exhibits the lowest wear rate with a sudden jump in the wear rate at test temperature of 100°C, which is similar at 300°C, but slightly increases when tested at 500°C.

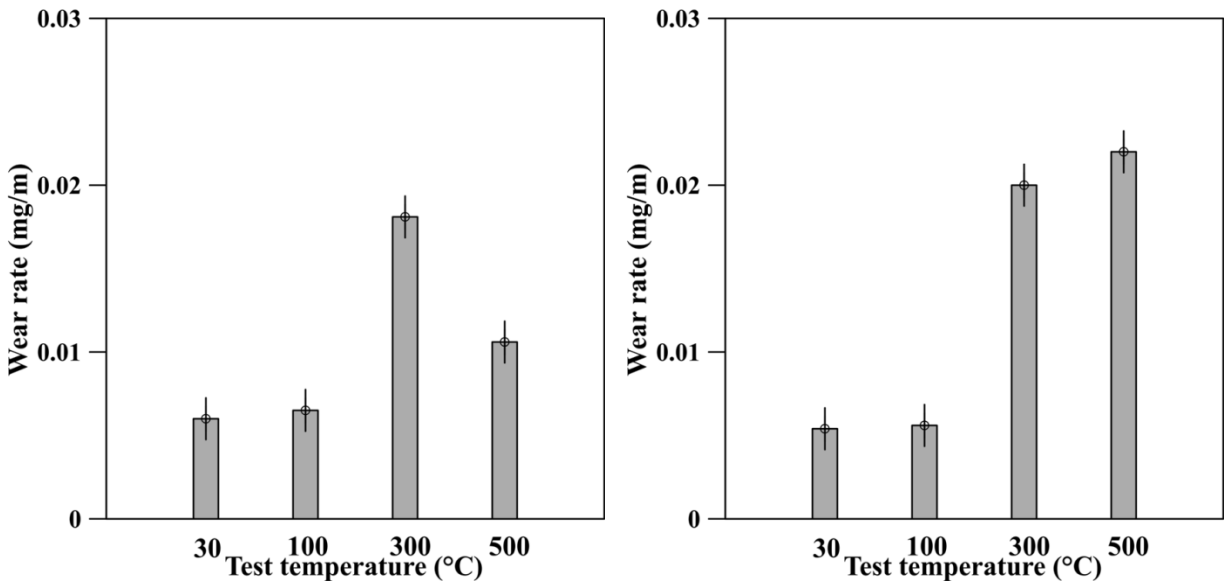

(a) (b)

Figure 6.17 Wear as a function of test temperature for (a) as-deposited and (b) heat-treated Ni-P-Al_2O_3 coating

SEM image indicating the wear along with the direction for Ni-P-Al_2O_3 as-deposited coatings tested at 500°C is represented in Figure 6.18. The coating clearly exhibits linear wear tracks as soft coating is subjected to abrades by same hard counter face. Along with that, few

removal of material in the form of pits and prows is also detectable which arise due to breakage of bonding in between coating and counter face asperities. Linear tracks are prominent which is an indication of abrasive wear pattern as well as pits and prows are symbolic for adhesive wear mechanism. So, the wear mechanism at 500°C for the coating is mostly governed by abrasive and partly by adhesive wear mechanism. The linear tracks and removal of coating is clearly visible from Figure 6.18a, satisfying the results as indicated by Figure 6.17a. The results indicating the detail variation of each element across the chosen line (AB of approx 200 µm) is provided in Figure 6.18b for Ni-P-Al_2O_3 coating. Existence of nickel and the other primary coating elements proves the survival of those coatings at elevated temperature. Amount of Fe comes as a result of interaction with counterface material which may provide a mixed mechanical layer. It may also be the reason behind the lower wear rate at elevated temperature of as-deposited coating as also reflected by Figure 6.17a.

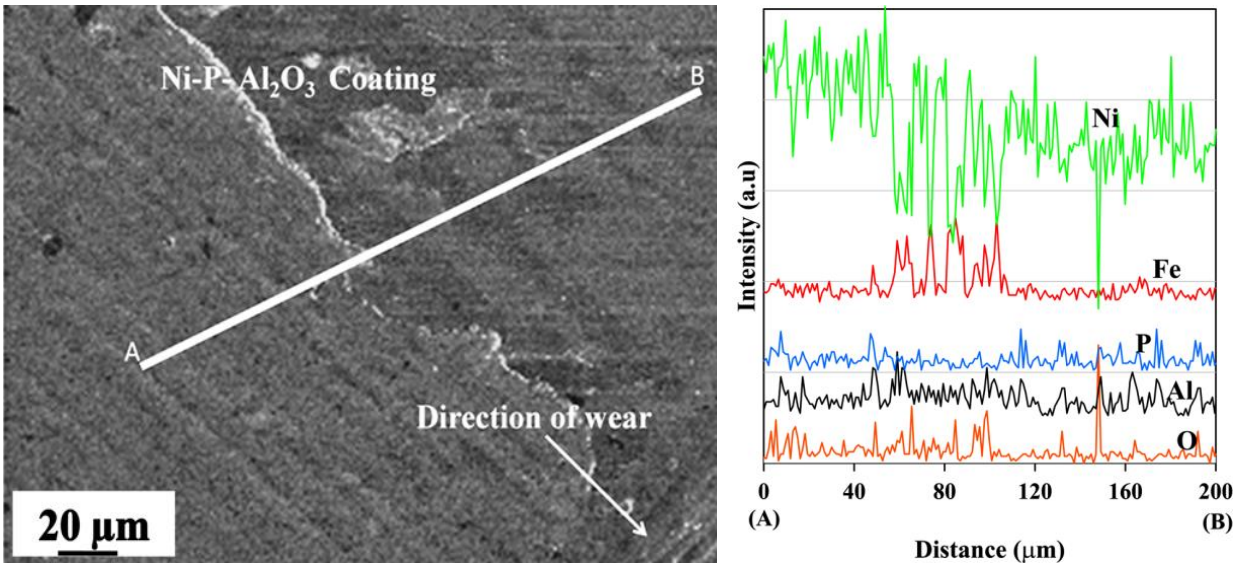

(a) (b)

Figure 6.18 (a) SEM image indicating the line for EDX study in the direction of wear and (b) corresponding EDX line analysis for Ni-P-Al_2O_3 coating

6.3.6.3 Wear mechanism study

In order to understand the underlying mechanisms defining the tribological behavior of the Ni-P-Al_2O_3 coating, the worn out surface of the samples are observed under SEM (Figure 6.19). This is also significant in assessing the wear mechanism via EDX (Figure 6.20) that the coating experiences with its counterpart. The as-deposited Ni-P-Al_2O_3 coatings exhibit linear wear tracks which indicate the occurrence of abrasive wear mechanism (Figure 6.19a). Abrasive wear occurs when hard rough surface or particles scratches across a softer surface. In the present case, the hard counterface having a defined roughness (Ra = 0.20) abrades the softer coating. Besides the wear track, small patches are also found to be distributed over the coating surface.

These small pits and prows are because of removal of material due to breakage (shear) of bonding between the coating and the counter face asperities. This indicates that adhesive wear mechanism is also partly responsible in governing the wear of the coating. The adhesive wear is mainly dependent on physical and chemical factors such as material properties, presence of corrosive atmosphere or chemicals, as well as the dynamics such as the velocity and applied load. The corresponding EDX is presented in Figure 6.20a.

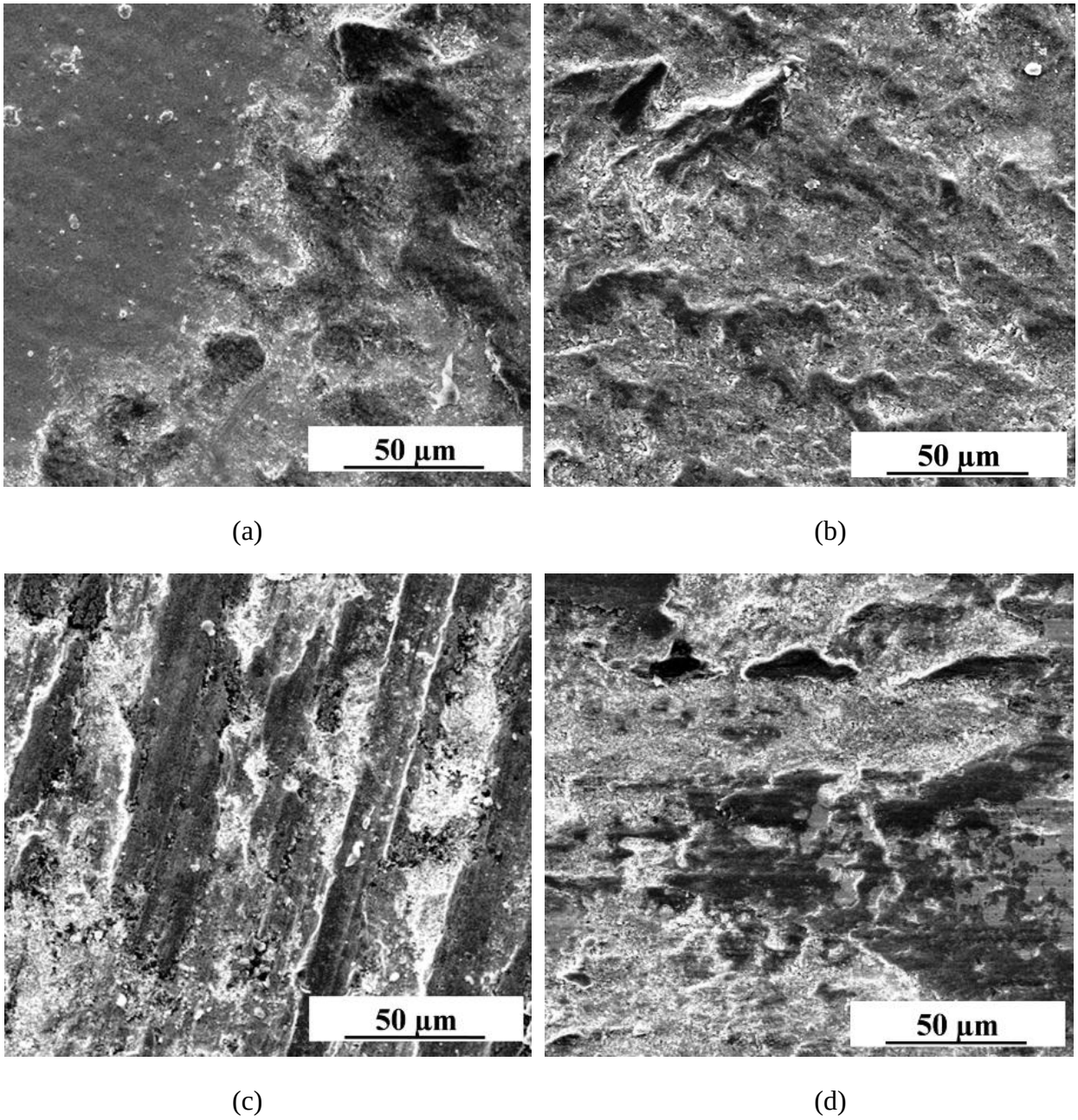

Figure 6.19 SEM (secondary electron) micrograph of worn specimen of as-deposited electroless Ni-P-Al_2O_3 coating tested at (a) 30°C (b) 100°C (c) 300°C and (d) 500°C

The nodular morphology of the coating is no longer visible post wear test. For Ni-P-Al_2O_3 samples tested at elevated temperature (100°C and 300°C), random torn patches typical to adhesion is visible which again directs towards adhesive wear mechanism. Now, adhesive wear is a very serious form of wear characterized by high wear rates and a large unstable friction coefficient (Stachowiak & Batchelor, 1993). Thus, the present analysis explains the abrupt rise in COF and wear rate of the samples tested particularly at 100°C as seen from Figure 6.15a and Figure 6.17a. Adhesive wear increases as the hardness of the bodies in contact decreases (Stachowiak & Batchelor, 1993). Now, it is quite natural that during sliding high amount of heat is generated at the interface which is further aided if the operating temperature is elevated. Thus, it can be said that the as-deposited sample during the test at 100°C is exposed to conditions which forces it to display a higher wear rate. Which further increases to 300°C, may be because of the same reason as stated earlier.

In both the sample, presence of Fe as indicated by EDX results (Figure 6.20b and 6.20c) which indicates adhesion as the chances of diffusion of Fe from the substrate is less (due to lesser test duration). But the presence of basic elements shows the existence of the coating at that elevated temperature tests. Few torn patches leads to adhesion, black spot indicating heavy oxidation are clearly visible in Figure 6.19(d). The relatively higher wear resistance at 500°C compared to 100°C and 300°C might have occurred due to the formation of harder phosphide phases. Coupled with this is the stable lubrication provided by the oxide layer formed during the test. The presence of oxide layer can be confirmed by the detection of oxygen in EDX results (Figure 6.20d). Presence of Fe in the post test samples may be because of two reasons, either it because of adhesion (high mutual solubility of iron and nickel atoms) or diffusion of iron from the steel substrate during test. The chances of diffusion is very less as the test is subjected for a very short time. Therefore, adhesive wear playing fraction responsibility in conjunction with the abrasive wear in governing the wear mechanism of as-deposited Ni-P-Al_2O_3 coating tested at 500°C.

To emphasize the effects of elevated temperature test as well as to maintain brevity, samples post test 500°C are further considered for AFM and elemental mapping study and the corresponding results indicated by Figure 6.21 and 6.22 respectively. The 2D and 3D surface morphology of post test Ni-P-Al_2O_3 samples is represented by Figure 6.21a and b respectively. It clearly indicates a deep grooves along with micro-ploughing. Wear tracks in the direction of sliding along with material removal is also noticeable. The elemental maps along with SE image of worn as-deposited Ni-P-Al_2O_3 coating tested at 500°C is shown in Figure 6.22. SE image of worn out specimens also indicates the linear wear tracks, indicating abrasive wear trend, in the direction of sliding and its very close to that of Figure 6.18a. Uniform allocation of nickel, phosphorous, aluminium and oxygen can be seen from the images (Figure 6.22) which mean the survival of coating even after the wear test.

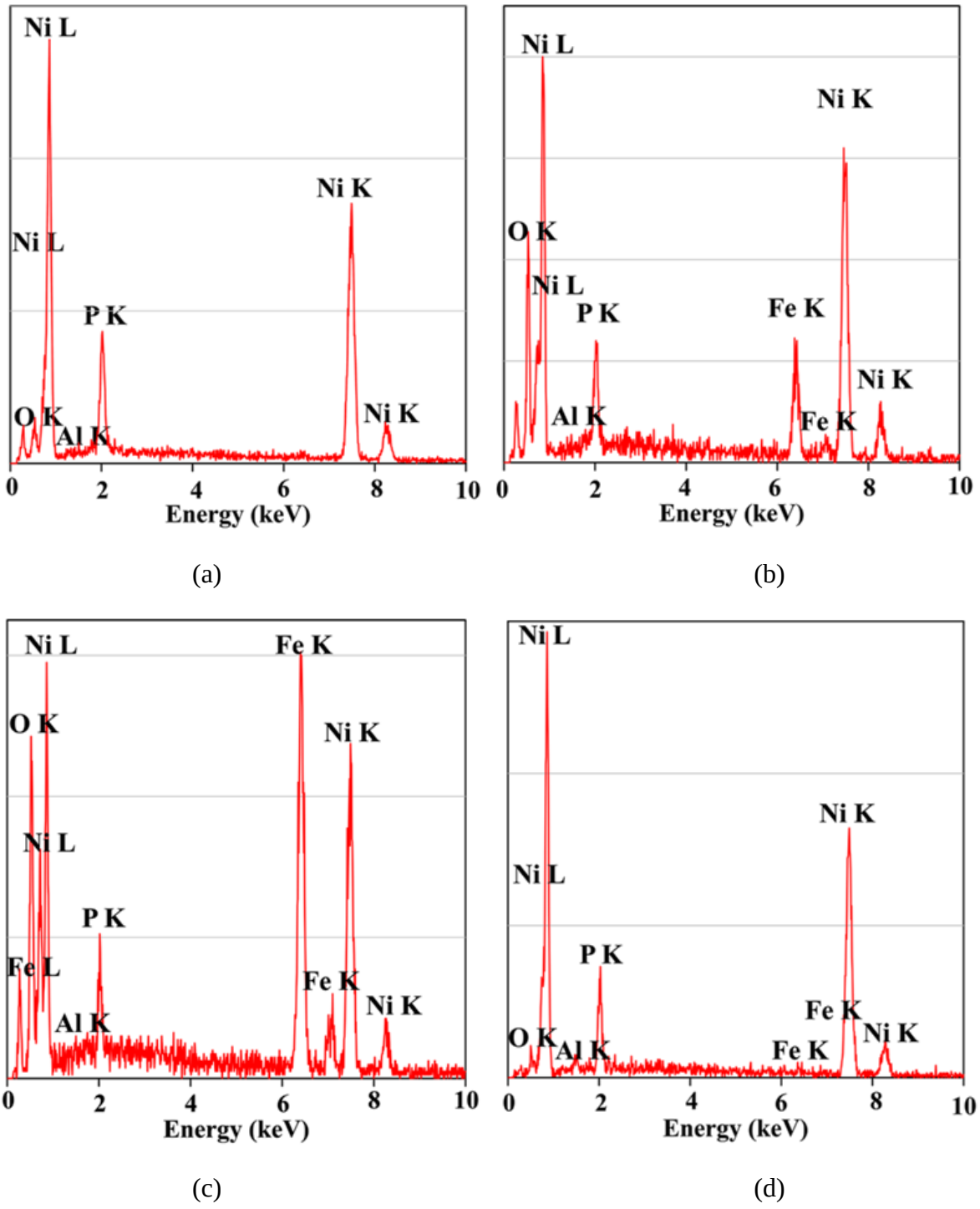

Figure 6.20 EDX spectrum of worn specimen of as-deposited electroless Ni-P-Al_2O_3 coating tested at (a) 30°C (b) 100°C (c) 300°C and (d) 500°C

The existence of oxygen proves the development of tribo-oxide film as discussed earlier, though it is very complicated to differentiate whether the oxygen is elemental or because of heat-treatment. The oxide layer surrounds over the whole surface of the coating as evident from the

mapped image (Figure 6.22) which is the main reason for lesser fluctuation and a reduced amount of COF. For the 500°C, iron shows very strong signal (Figure 6.22) in the image which implies occurrence of adhesive wear whose remnants can be experiential from torn patches on the Ni-P-Al_2O_3 coating post test.

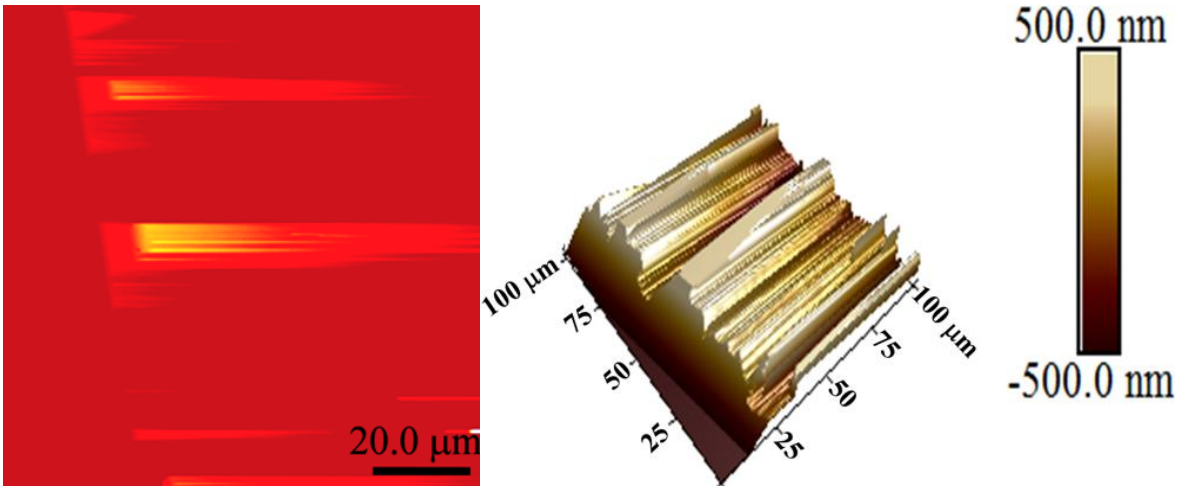

(a) (b)

Figure 6.21 AFM morphology (a) 2D and (b) 3D of as-deposited Ni-P- Al_2O_3 coating tested at 500°C

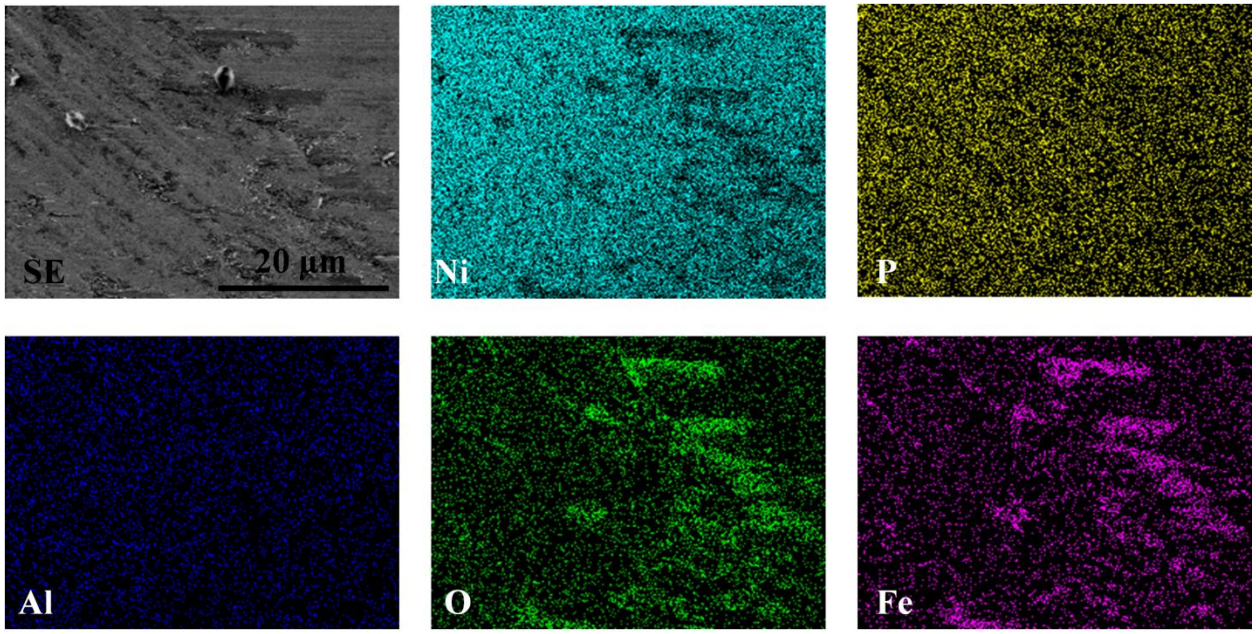

Figure 6.22 EDX maps of worn specimen of as-deposited Ni-P-Al_2O_3 coating tested at 500°C

Post wear test, heat-treated Ni-P-Al_2O_3 samples are subjected to SEM and EDX investigations to understand the mechanism and effects of wear respectively on coating. Further,

a detailed study is consolidated by AFM and elemental mapping analysis for as-deposited and heat-treated coating tested at 500°C. SEM micrographs (Figure 6.23) and EDX findings (Figure 6.24) of worn out heat-treated Ni-P samples at various temperatures (30°C, 100°C, 300°C and 500°C) are presented in this section.

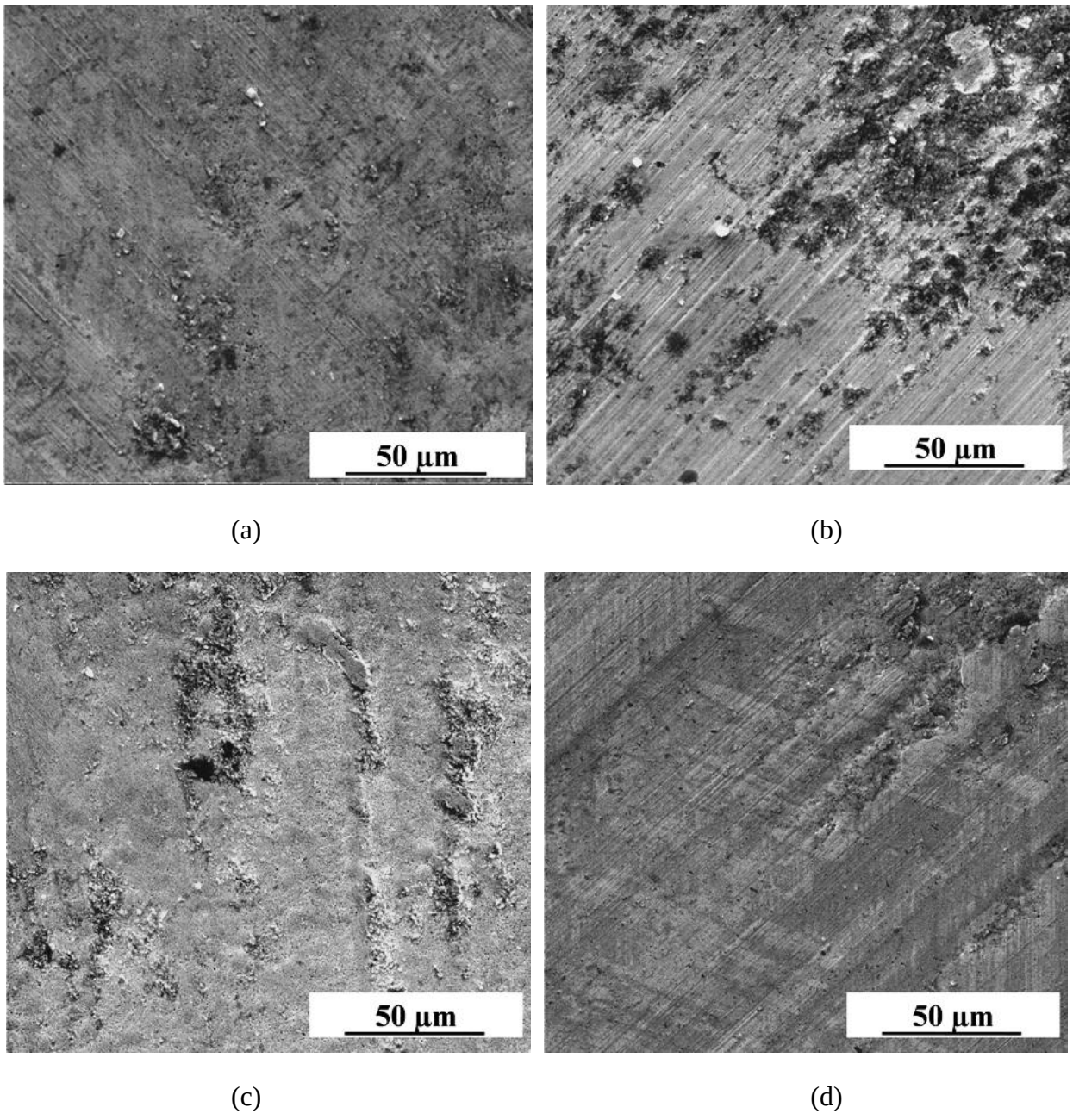

Figure 6.23 SEM (secondary electron) micrograph of worn specimen of heat-treated electroless Ni-P-Al_2O_3 coating tested at (a) 30°C (b) 100°C (c) 300°C and (d) 500°C

The heat-treated coating tested at room temperature shows a flattened nodular structure (Figure 6.23a). Most of the asperities are compressed under the application of load and few

fragmented nodules are spread over the whole surface area of contact. This split particles plays the role of solid lubricants and causes to provide low COF and wear as indicated by Figure 6.15b and 6.17b respectively.

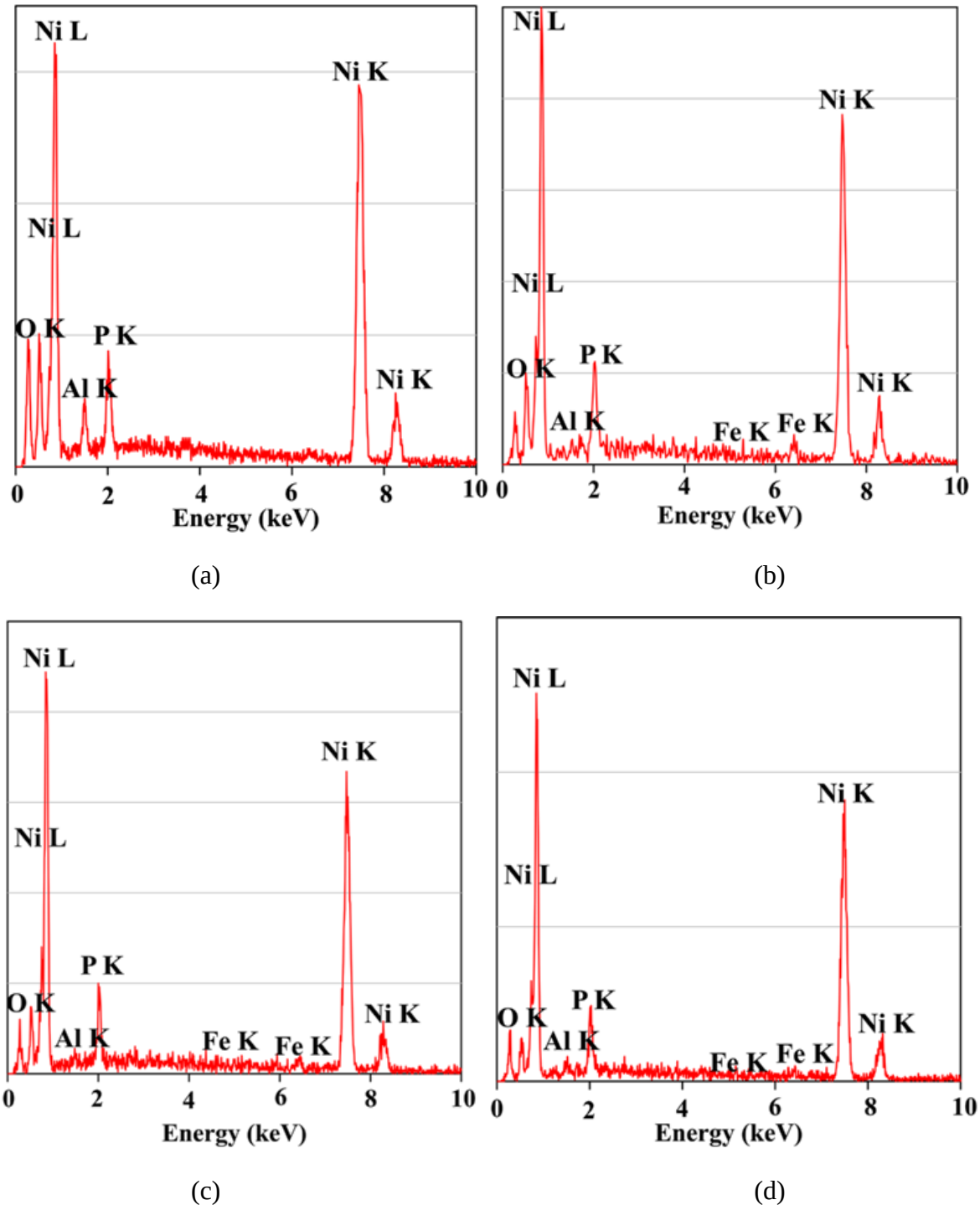

Figure 6.24 EDX spectrum of of worn specimen of heat-treated electroless Ni-P-Al_2O_3 coating tested at (a) 30°C (b) 100°C (c) 300°C and (d) 500°C

The coating is mostly intact after the room temperature test as clearly visible in Figure 6.23a with a small number of patches. Removal of coating in the form of patches is a significant characteristics of adhesive wear. The intactness of the post test coatings are verified through EDX study (Figure 6.24a) which clearly indicates the existence of four major constituents Ni, P, Al and O. The oxidation of wear zone may be represented by the EDX outcomes through the presence of higher oxygen. Micro-cutting and micro-ploughing together with torn patches (Figure 6.23b) are encountered in the wear test at 100°C. Though the coating surface appears to suffer ductile failure with high level of plasticity in the direction of sliding. EDX results again indicates the existence of oxygen and iron (Figure 6.24b). Ploughing with torn patches in the direction of sliding can also be observed for coating tested at 300°C (Figure 6.23c) which again point towards a mixed wear mechanism. The severe adhesive wear and rough surface supports towards the high COF observed at this condition (Figure 6.15b). The EDX of the post wear sample (Figure 6.24c) shows iron which yields abrasive wear owing to high mutual solubility of nickel and Fe atoms. The presence of micro cracks is noticed on the worn surface (Figure 6.23d) as a result of the shear stress transmitted to the sub-surface layer and the variation of the load experienced at the area of contact (Le´on et al., 2003). This type of morphological feature, commonly known as "prows", is reported for adhesive wear failure of EN coatings by several researchers (Staia et al., 1996; Gawne & Ma, 1987). All these evidences points towards the occurrence of adhesive wear phenomenon in the coatings. The EDX of the wear tested specimen (Figure 6.24d) also shows the presence of iron (Fe) peaks which have definitely come from the steel counterface. This indicates the high mutual solubility of nickel and iron atoms. The adhesive wear mechanism of Ni-P-Al_2O_3 coating is in agreement with literature reports belongs to hypophosphite reduced coatings (Staia et al., 2002). Overall, the wear mechanism encountered in the test is a mixture of adhesive and abrasive wear phenomena.

To realize the underlying facts of elevated temperature test in a better way as well as to maintain brevity, heat-treated samples post test 500°C are consolidated via AFM and elemental mapping assessment and the corresponding results are indicated by Figure 6.25 and 6.26 respectively. The 2D and 3D surface morphology of post test samples is represented by Figure 6.25a and 6.25b respectively. It clearly indicates a rough surface along with micro-ploughing. Wear tracks in the direction of sliding along with material removal is also noticeable. The elemental maps along with SE image of worn heat-treated Ni-P-Al_2O_3 coating tested at 500°C is shown in Figure 6.26. Uniform allocation of all the basic elements can be seen from the images (Figure 6.26) which mean the survival of coating even after the wear test. The existence of excess oxygen proves the development of tribo-oxide film as discussed earlier. The oxide layer surrounds over the whole surface of the coating as evident from the mapped image which is the main reason for lesser fluctuation and a reduced amount of COF compared to 100°C and 300°C tests. For the 500°C, iron shows very strong signal (Figure 6.26) in the image which implies occurrence of adhesive wear whose remnants can be observed from torn patches on the coating post test.

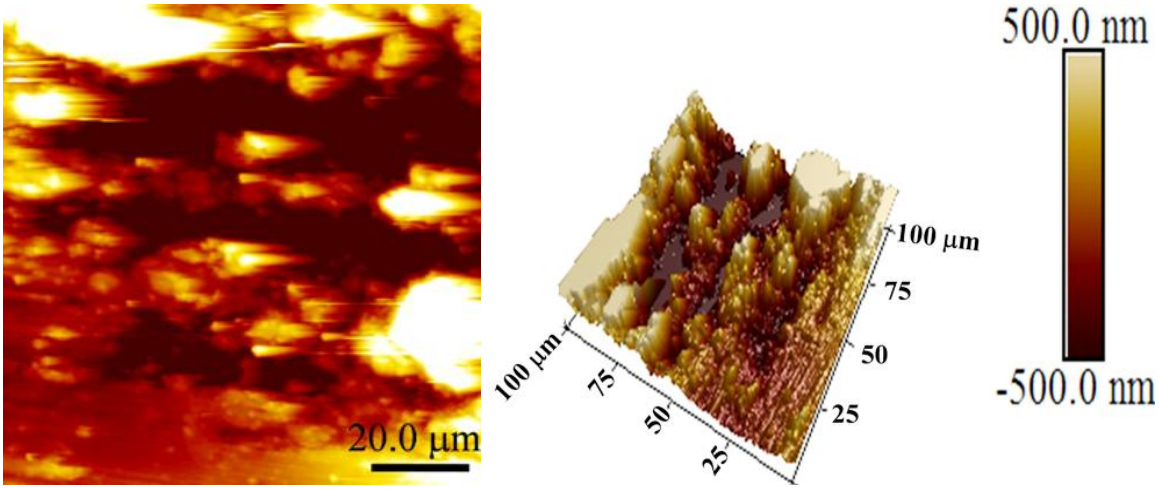

(a) (b)

Figure 6.25 AFM morphology (a) 2D and (b) 3D of heat-treated Ni-P-Al_2O_3 coating tested at 500°C

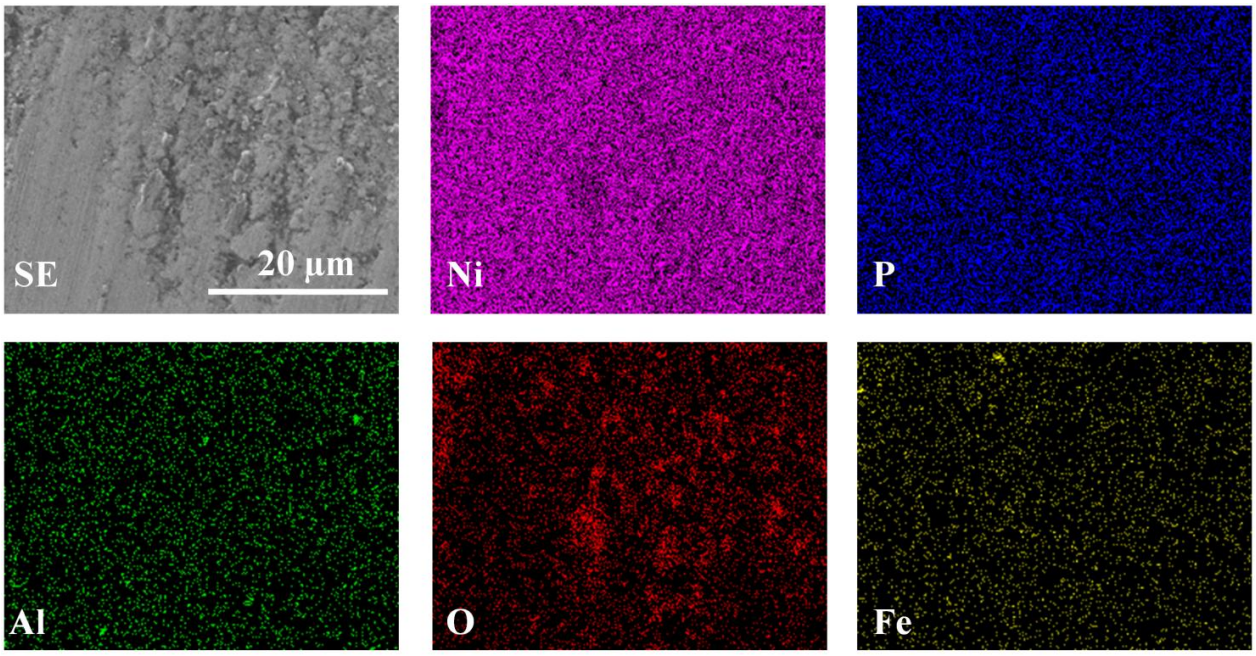

Figure 6.26 EDX maps of worn specimen of heat-treated Ni-P-Al_2O_3 coating tested at 500°C

6.3.6.4 Phase transformation and hardness change

Several researchers claim commencement of phase transformation because of in situ heat-treatment during elevated temperature test of EN coatings (Franco et al., 2016; Mukhopadhyay et al., 2018a; 2018c). Details XRD study of post wear Ni-P-Al_2O_3 coatings are conducted to understand the reality of the claim. Phase transformation study of mainly as-deposited coatings tested at elevated temperature are examined and explained in Figure 6.27.

Heat-treated specimens are excluded for XRD analysis, as they are in crystalline state, so complicated to identify the effect of elevated temperature test.

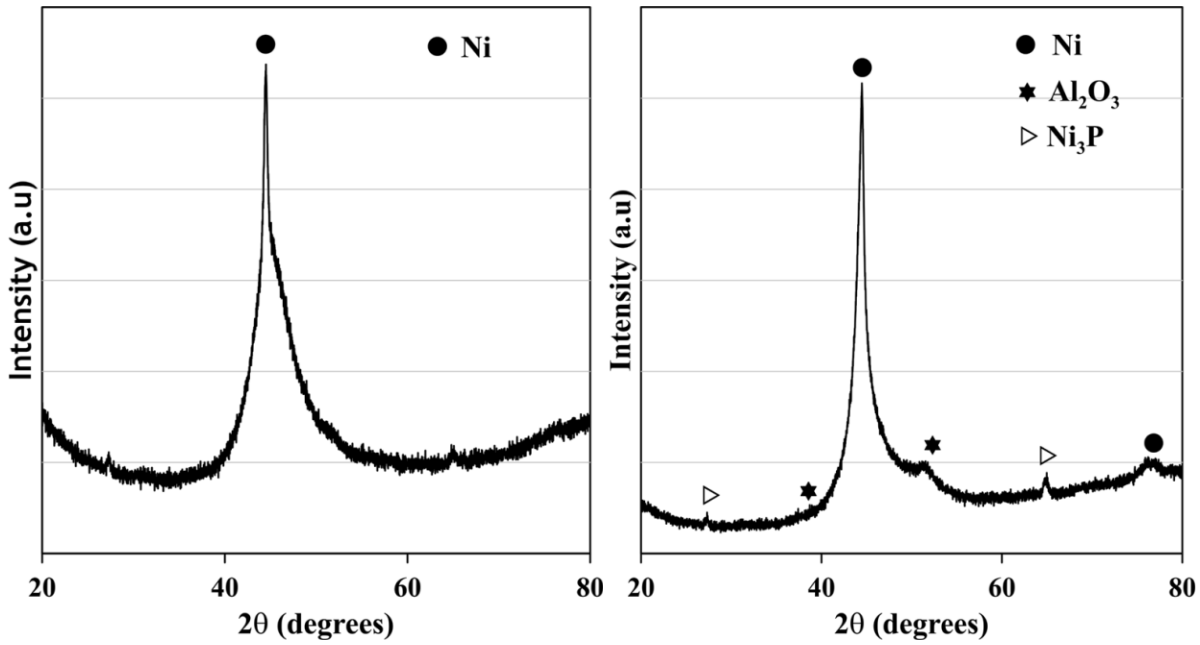

(a) (b)

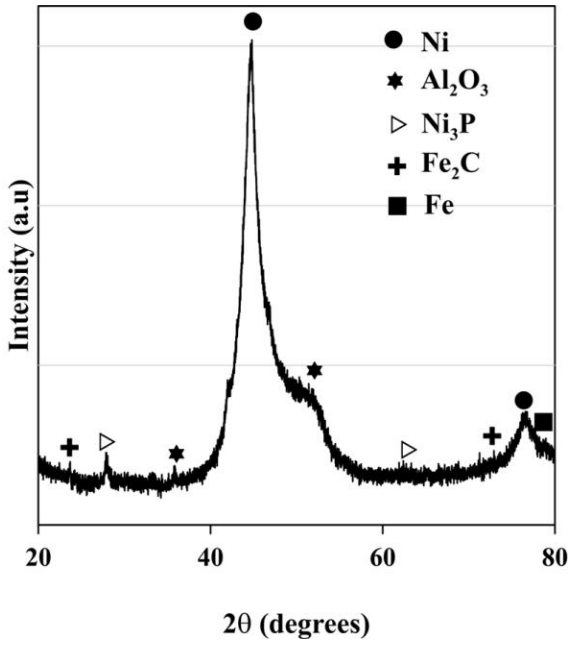

(c)

Figure 6.27 XRD analysis of as-deposited Ni-P-Al_2O_3 coating post-wear test at (a) 100°C, (b) 300°C, and (c) 500°C

The samples subjected to room temperature test causes trifling effects in crystal structure and observed similar to that presented by as-deposited coating as indicated in Figure 6.11. Wear behavior of as-deposited coatings during room temperature test is solely controlled by the plastic deformation occurs during the test as stated earlier. Figure 6.27a represents the phase structure of post wear Ni-P-Al_2O_3 coatings tested at 100°C. Nickel peak (111) is getting sharper compared to as-deposited coating, may because of phase transformation. Microstructural changes occurs at 100°C is due to combined effect of plastic deformation and test temperature. Further crystallographic change is observed for coatings tested at 300°C, and illustrated by Figure 6.27b. Crystalline Ni_3P along with few Ni and Al_2O_3 peaks are visible which clearly indicates the phase transformation of the as-deposited coating during the 300°C wear test. The formation of phosphide phases of nickel are accelerating with the increase in test temperature which reflects in Figure 6.27c. The existence of Fe in 5.27c indicates the transfer of counterface material which forms a mixed mechanical layer. Formation of iron carbide at 500°C wear test is also attributed the crystallization phenomenon of as-deposited Ni-P-Al_2O_3 coatings. High temperature during wear because of adhesion (high mutual solubility of iron and nickel atoms) of iron to the coating surface, decrease of phosphorus and aluminium as individual element and results in precipitation of nickel phosphides phases with Al_2O_3 peaks. The results obtained through post wear XRD of as-deposited Ni-P-Al_2O_3 coating is well confirmed the earlier results as mentioned in the wear mechanism section. The point EDX (Figure 6.20c and 6.20d) clearly indicates the presence of inter diffused Fe particle that again is highlighted by Figure 6.19c and 6.19d respectively. The detailed wear mechanism also explains the EDX maps (Figure 6.22) of post wear test sample of as-deposited coatings tested at 500°C, clearly indicating the presence of each element including Ni, P, Al and O, and thus justifying the existence of the coating at elevated temperature. The present discussion thus proves the phase transformation scenario as an outcome of short duration heat-treatment during the elevated temperature wear test. The current study provides a qualitative idea about high temperature tribology of Ni-P-Al_2O_3 coatings, further studies such as X-ray photoelectron spectroscopy (XPS) can be conducted for thorough examination on oxide layer formation, that controls tribological performance of the coatings.

The change in hardness of the Ni-P-Al_2O_3 coatings after each test at different temperatures is measured and the percentage increase in hardness is represented by the plot in Figure 6.28. It is observed that for as-deposited samples, the hardness increase is more for higher test temperature compared to the lower ones. In the case of heat-treated coatings, the test at 100°C yields negligible enhancement of hardness. Hence, it can be concluded that the tests at elevated temperatures act as short duration heat-treatment, which have quite a positive impact on the hardness of the as-deposited coating. The effect of the aforesaid heat-treatment is already proved through XRD study of the post wear samples where the formation of hard phosphide phases are visible as indicated in Figure 6.27.

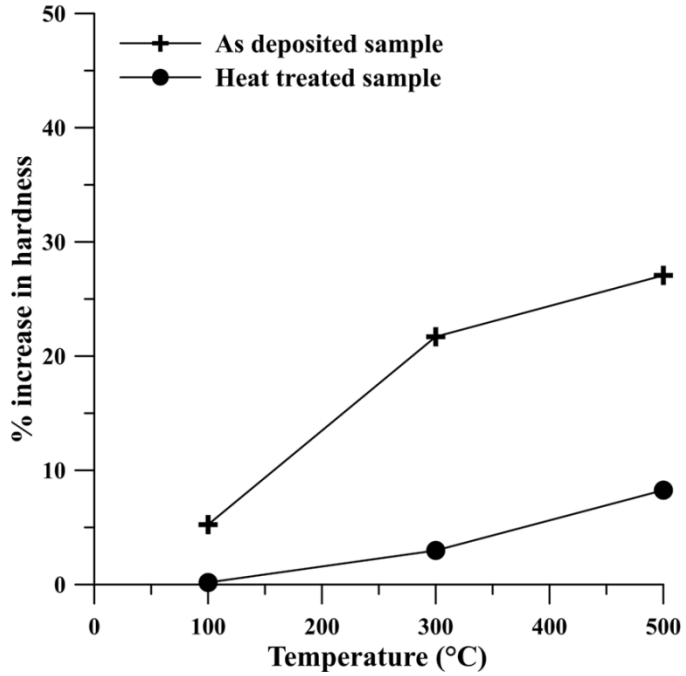

Figure 6.28 Percentage increase in hardness after high temperature tests of Ni-P-Al_2O_3 coating

6.4 Conclusion

This chapter attempts to present in a detailed manner the tribological behavior of electroless Ni-P-Al_2O_3 coatings under elevated temperature conditions. The coatings are developed in the laboratory and friction and wear tests are carried out in a pin on disc tribometer. Both the as-deposited and heat-treated coatings exhibit a uniform distribution of the constituent elements. Upon heat-treatment, the coatings turn crystalline with increase in the grain size. The Ni-P-Al_2O_3 coating showed an amorphous structure in the as-deposited state and exhibited a high hardness of approximately 790 $HV_{0.1}$. As temperature was raised to 400°C, the hardness increased to 1120 $HV_{0.1}$ due to the precipitation of Ni and Ni_3P in the amorphous matrix. Presence of stable Ni with Al_2O_3 peaks and Ni_3P was identified for the heat-treated deposits (400 °C/1 h). Ni-P-Al_2O_3 coatings are found to display good hardness and they are found to remain stable under elevated temperature tests. In fact the exposure to high temperature during the tests act like short duration heat-treatment inducing microstructural changes in the coating (especially for as-deposited coatings) which further increase the hardness of the coating.. Heat-treated coatings on the other hand display a stable tribological performance under elevated temperature tests. Friction performance of the coatings does not seem to be highly affected by the elevated operating temperatures. However, elevated temperature is found to affect the wear behavior of as-deposited coatings. The coating performance is very good for room temperature and up to 100°C, which further slightly degrade with the increase in temperature. Again applied load and sliding velocity also exhibit marginal influence over the friction and wear behavior behavior of the coatings particularly at higher temperatures. In high temperature tests it is observed that wear

rate increases with the increase in test temperature. The increase in applied load is also found to negatively impact the wear resistance of the coating. However, wear rate is almost inversely proportional to the sliding velocity under a constant value of load. Coefficient of friction does not seem to be affected very much under elevated temperature tests. The SEM micrograph of the worn surface of the coating reveals that both abrasive and adhesive wear phenomenon is present as wear mechanism for elevated temperature. Oxide formation is another interesting phenomenon for the coatings tested under elevated temperatures, though it is not clear particular to this coating, as oxygen itself is an element of the developed composite coating. Still considering the amount of oxygen detected, oxidation is a highly probable phenomena. Study of worn surface reveals that the wear is governed by both abrasive and adhesive wear mechanisms. Moreover, the formation of iron oxide on the coating at high temperature along with adhesion (high mutual solubility of iron and nickel atoms) of iron is observed which is also believed to influence the tribological behavior of the coating in high temperature.

This page is left blank intentionally

Chapter 7

Comparative study on tribological characterisation of Ni-P and its variants under room and high temperatures

7.1 Introduction

In the preceding chapters, the hypophosphite reduced coatings i.e. Ni-P, Ni-P-W and Ni-P-Al_2O_3 are developed and studied individually. Apart from that a hypophosphite and borohydride reduced combined coating Ni-P-B is also developed and studied exactly following the path as that of other developed coating. Each of the coating is evaluated based on several characterisations and finally tested under different temperatures to know its tribological appearance with related to wear mechanism. As each coating are subjected to similar kind of analysis, so it's quite interesting to know which one is best with regards to performance. The current chapter due with the systematic comparison of the tribological characteristics of developed Ni-P, Ni-P-W, Ni-P-B and Ni-P-Al_2O_3 coatings at room and various high temperatures. For better understanding, the comparison is initiated from the development of coating till its high temperature performance evaluation. The whole part of the comparison is divided into three broad parts as the first part belongs to the coating development with relevant composition as it effects the tribological behavior to large extent. The next part is microhardness of as-deposited and heat-treated coatings, as it directly affect the friction-wear performance of any coating. In the third part, the tribological performances of the coatings at different temperatures is compared. From these comparisons, the coating best suited for high temperature tribological applications is suggested.

7.2 Comparison based on Coating Configuration

Sodium hypophosphite is used as the reducing agent for Ni-P coating and its variants, which provides a stable bath with moderate deposition rate. The inclusion of alloying element or particles in the Ni-P matrix always causes to decrease the deposition rate. But the trend is reverse for Ni-P-B deposition where the deposition rate is better than that of Ni-P also, it is because of the use of borohydride as reducing agent in combination with hypophosphite. Though the deposition rate is high for borohydride as reducing agent, but bath is not stable. Plating rate is an important aspects for tribological behavior as it use to determine the growth of the nodules as well as the structure of the coating. For the high temperature tribological interaction the required thickness for each of the coating under the ranges of load and velocity is approximately 40μm.

So depending upon the stability of each coating and the deposition rate, the prime objective is to achieve the required thickness for better comparison under high temperature tribological tests. To understand the plating rate for all the developed coatings in a single place, the deposition thickness versus time plot is presented in Figure 7.1. Ni-P shows a moderate deposition rate such as 12-14 μm/h, but the inclusion of alloying element W in the Ni-P bath causes to decrease the deposition rate and so for incorporation of Al_2O_3 particles in the same bath. The deposition rate is very low for Ni-P-Al_2O_3 bath, where it seems to provide a deposition rate of 6-10 μm/h. The deposition rate for Ni-P-W lies in between the rate of Ni-P and Ni-P- Al_2O_3. But a completely reverse trend is observed for Ni-P-B deposition where it shows a deposition rate of 18-21 μm/h. The higher slope of Ni-P-B (as shown in Figure 7.1) may be because of using hypophosphite in combination with superior reducing agent, borohydride which provides higher reaction rate in compare to others.

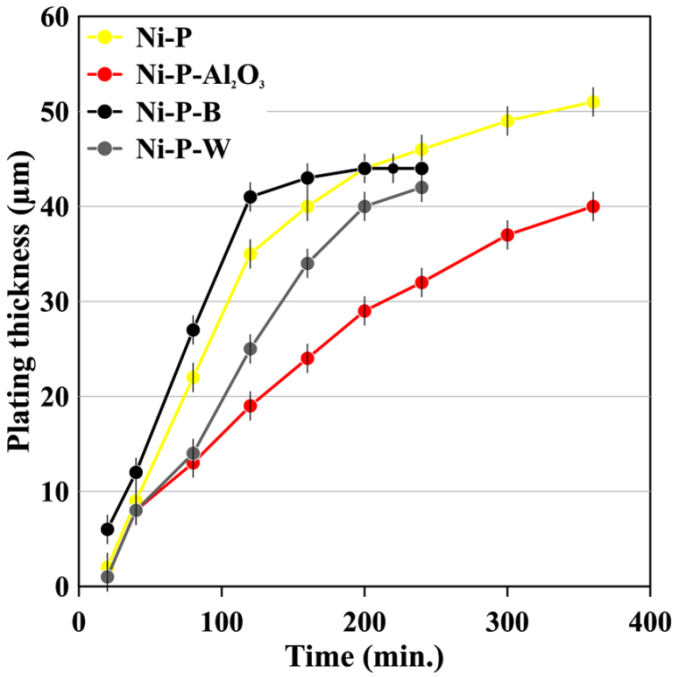

Figure 7.1 Plating rate comparison of Ni-P and its variants coatings

Compositional analysis is performed on several points on the surface of as-deposited and heat-treated Ni-P and its variants via EDX spectrum as indicated in individual chapters earlier. For better understanding of the deposition as well as to identify the elemental distribution, cross cut section is chosen where coating and substrate is visible. Line EDX is conducted on the cross cut section of Ni-P and its variants coatings and the result is illustrated in Figure 7.2. The quantitative results indicating weight percentage of each of the element present is given in table inside Figure 7.2. Composition profiles of all the element presents along with Ni and P are measured down the thickness of Ni-P and its variant (Figure 7.3) coatings are compared. The line EDX is used to indicate the adhesion in between the substrate and the coating as well as shows

the proper deposition of each of the variants of Ni-P and for detailed understanding of elemental variation across the coating cross section.

Therefore, based on coating configuration, it is observed that Ni-P-B coatings are better in comparison with Ni-P binary alloy or Ni-P-W ternary alloy or Ni-P-Al_2O_3 ternary composite coating with respect to plating rate. As well as from structural point of view Ni-P-B is found to provide columnar structure with cauliflower surface morphology which is used to provide better wear resistance.

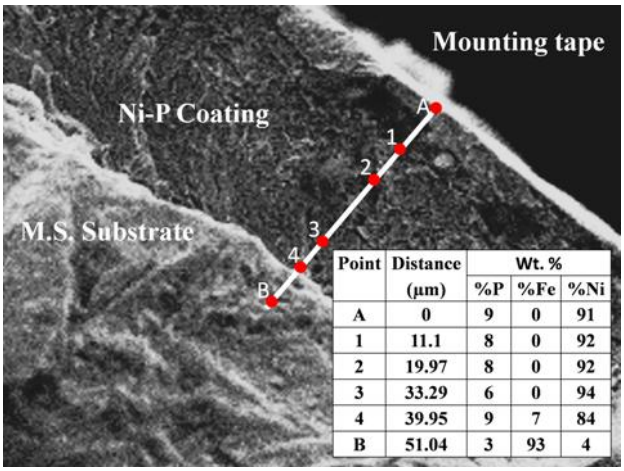

Point	Distance (µm)	Wt. %		
		%P	%Fe	%Ni
A	0	9	0	91
1	11.1	8	0	92
2	19.97	8	0	92
3	33.29	6	0	94
4	39.95	9	7	84
B	51.04	3	93	4

(a)

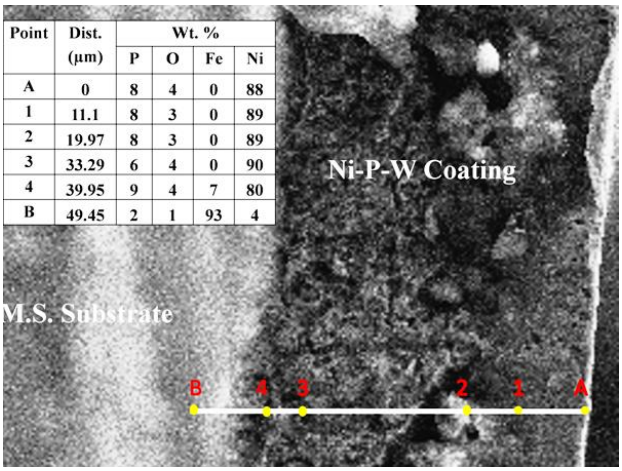

Point	Dist. (µm)	Wt. %			
		P	O	Fe	Ni
A	0	8	4	0	88
1	11.1	8	3	0	89
2	19.97	8	3	0	89
3	33.29	6	4	0	90
4	39.95	9	4	7	80
B	49.45	2	1	93	4

(b)

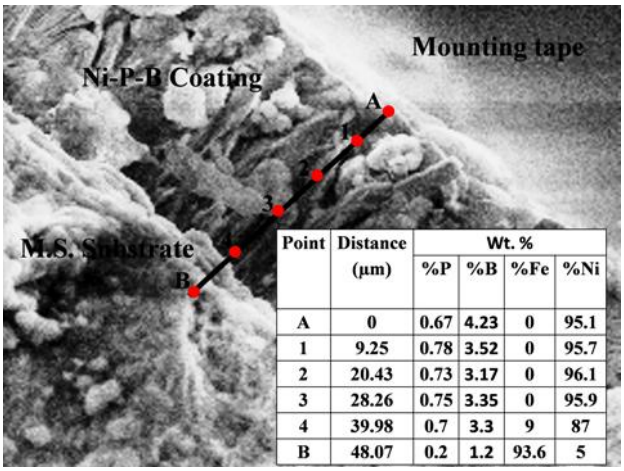

Point	Distance (µm)	Wt. %			
		%P	%B	%Fe	%Ni
A	0	0.67	4.23	0	95.1
1	9.25	0.78	3.52	0	95.7
2	20.43	0.73	3.17	0	96.1
3	28.26	0.75	3.35	0	95.9
4	39.98	0.7	3.3	9	87
B	48.07	0.2	1.2	93.6	5

(c)

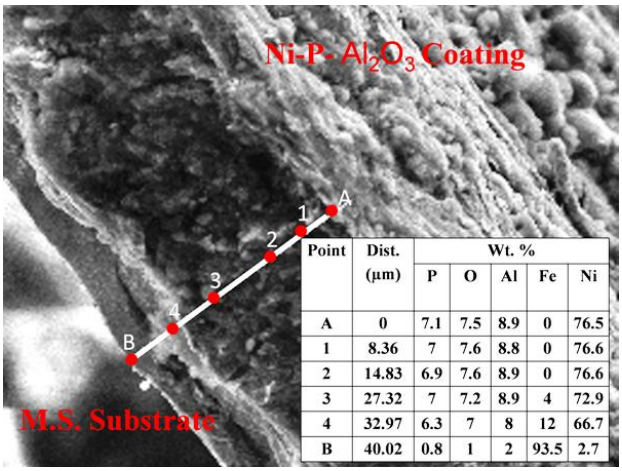

Point	Dist. (µm)	Wt. %				
		P	O	Al	Fe	Ni
A	0	7.1	7.5	8.9	0	76.5
1	8.36	7	7.6	8.8	0	76.6
2	14.83	6.9	7.6	8.9	0	76.6
3	27.32	7	7.2	8.9	4	72.9
4	32.97	6.3	7	8	12	66.7
B	40.02	0.8	1	2	93.5	2.7

(d)

Figure 7.2 SEM image showing line EDX (quantitative analysis included in table) for (a) Ni-P, (b) Ni-P-W, (c) Ni-P-B and (d) Ni-P-Al_2O_3

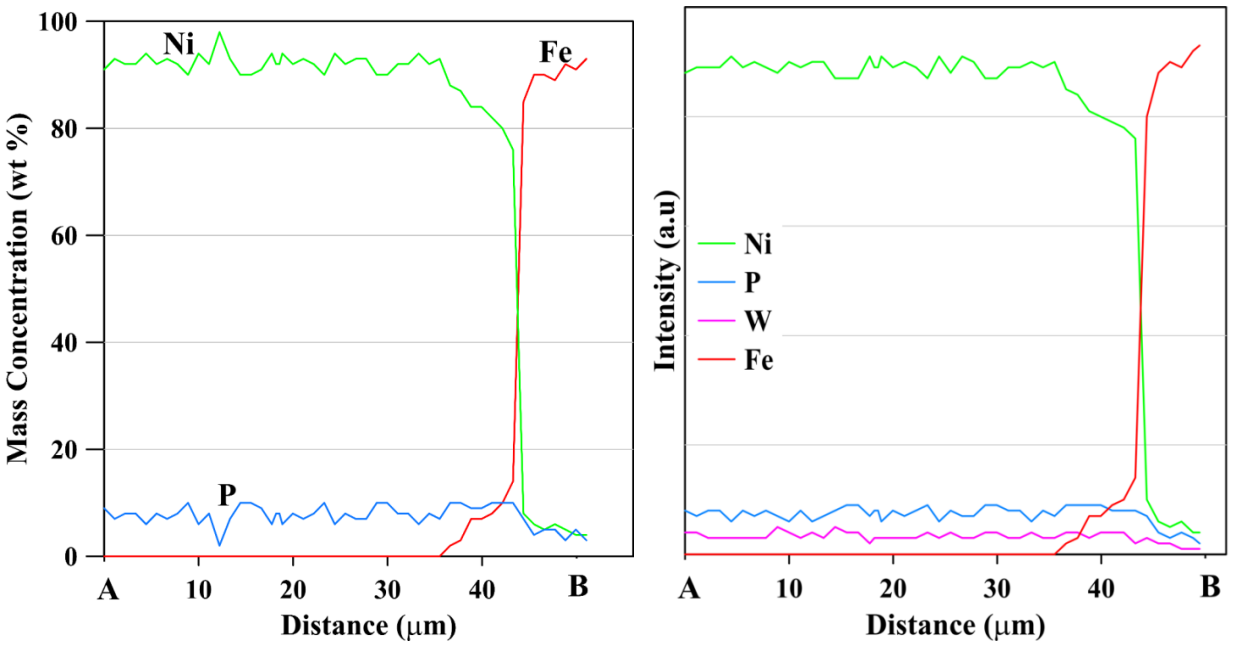

(a) (b)

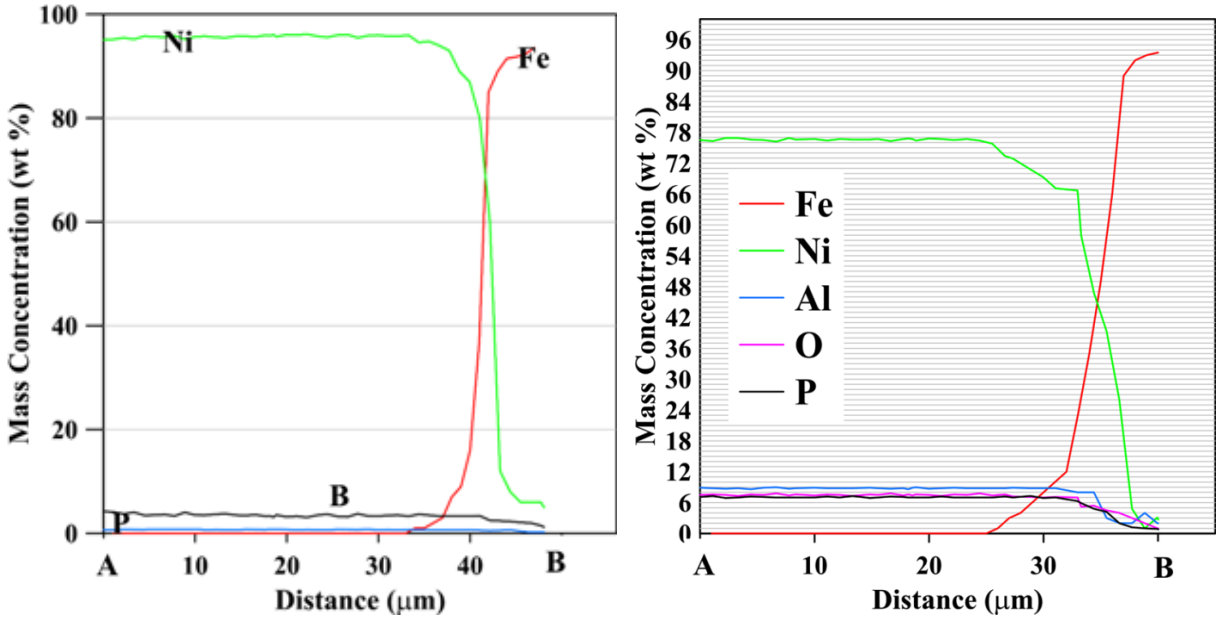

(c) (d)

Figure 7.3 Detailed composition profiles of elements presents measured along the thickness of the (a) Ni-P, (b) Ni-P-W, (c) Ni-P-B and (d) Ni-P-Al_2O_3

7.3 Comparison based on Microhardness

As tribological characteristics are largely dependent on the hardness, the microhardness of binary Ni-P and other ternary alloy variants such as Ni-P-W and Ni-P-B along with the ternary composite variant as Ni-P-Al_2O_3 coatings are compared. Each of the developed coatings are tested before and after the heat-treatment (400°C for 1 hour) and the same results as illustrated in Figure 7.4. All the coatings are developed by choosing a common substrate having hardness of 140 $HV_{0.1.}$ Substrate surface hardness is increased by multiple times in each of the cases by using a layer of Ni-P and its variants coatings and makes it suitable for further tribological interactions. Electroless deposition Ni-P provides average microhardness to be around 600 $HV_{0.1}$ which further increases because of heat-treatment to a hardness of 1000 $HV_{0.1}$. The deposition of alloying elements in the Ni-P matrix such as tungsten and boron gives rise to new Ni-P variants such as Ni-P-W and Ni-P-B respectively. Similarly inclusion of Al_2O_3 particles in Ni-P matrix causes to arise Ni-P-Al_2O_3 coating. In each of the cases it always increases of the hardness of as-deposited coatings than that of as-deposited Ni-P coating. The significant effect is noticed due to addition of Al_2O_3 particles in Ni-P matrix among all. Heat-treatment for each coatings has a positive effect on hardness as similar to Ni-P coating.

For Ni-P-W coatings, it is believed that inclusion of W promotes mechanical and thermal properties due to its relatively high hardness and high melting point of 3410°C (Wu et al., 2004). A similar observation is marked in Figure 7.4. Moreover, the incorporation of tungsten causes solid solution strengthening of the Ni-P matrix leading to a high hardness. On heat-treatment, the increase in microhardness is attributed to precipitation hardening caused by formation of Ni_3P as well as solid solution strengthening. Addition of boron in Ni-P matrix is found to provide better results than that of W addition, which may be the reason behind hardness increment. It may be concluded that developing coating through combined hypophosphite and borohydride bath is better than that from solely developed hypophosphite or borohydride bath. Electroless deposition Ni-P-B provides average microhardness of 690 $HV_{0.1}$ working with same substrate. The hardness obtained is nearly 15% more than that of Ni-P (as shown in Figure 7.4) and 3% higher compared to Ni-B (Mukhopadhyay et al., 2018c). Further the effect of heat-treatment at 400°C on the coating is studied. Heat-treatment causes increase of the hardness of Ni-P-B to 1080 $HV_{0.1}$. It is because of formation of hard boride and phosphide phases due to heat-treatment. The hardness of electroless Ni-P composite coatings increases in the presence of hard particles $Al_2O_{3.}$ In composite coatings, second phase particles act as barrier for plastic deformation of coated layer on the application of load. It results in increase in hardness of Ni-P-Al_2O_3 composite coatings (Alirezaei et al., 2007). Hardness of the composite coating is depending on the amount of particles available in the coated layer, bonding strength of particles with coated layer and heat-treatment of the coating. The Al_2O_3 composite coatings heat-treated at 400°C have maximum hardness as compared to other coatings in both as-deposited form or when heat-treated at 400°C. The properties of the composite coatings are generally related to and controlled by the second phase particles incorporated in the Ni-P deposit. After heat-treatment at 400°C for one hour,

coating hardness increases sharply. The coating hardness increases due to formation of hard Ni_3P phase at higher temperature.The effect of heat-treatment is prominent in Ni-P as it increases hardness by 67%, compared to other Ni-P variants coating, as shown in the figure.

Therefore, based on microhardness, it is observed that Ni-P-Al_2O_3 coatings are better in comparison with Ni-P binary alloy or Ni-P-W/Ni-P-B ternary alloy coatings. Ni-P-Al_2O_3 coatings in its both as-deposited as well as heat-treated condition provides higher hardness on comparison to other coatings in the corresponding conditions. Al_2O_3 is considered as hard particles and inclusion of the same in Ni-P matrix causes a hard variant of Ni-P, known as Ni-P-Al_2O_3 which is proved as best with respect to hardness.

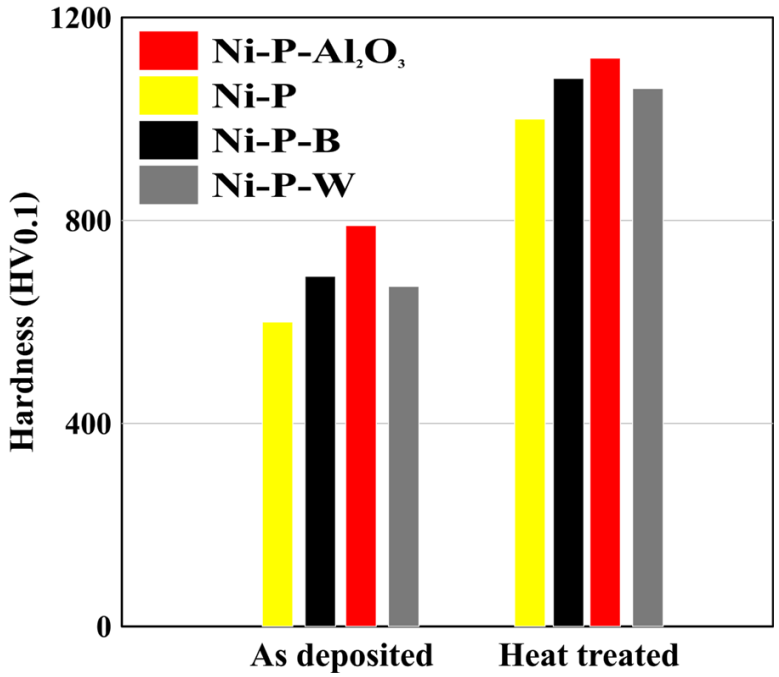

Figure 7.4 Comparison of microhardness of Ni-P and its variants coatings

7.4 Comparison based on Tribological Performance

In this section, a comparative study of the tribological behavior of as-deposited and heat-treated coatings is carried out at different temperatures. Basically, the response of the coatings to varying temperatures is observed by generating friction and wear plots of as-deposited and heat-treated coatings.

The friction performance of as-deposited and heat-treated coatings of Ni-P and its variants is represented by Figure 7.5. For both conditions, Ni-P shows lower friction coefficient. For room temperature tests each of the coating in its as-deposited condition provides lesser friction coefficient than that of heat-treated condition. Coarse grained surface morphology because of heat-treatment causes to increase the surface roughness and accordingly the COF. All of the coatings show an increasing trend for friction coefficient when temperature increases from 30°C to 100°C. But a reverse trend is noticed for 300°C and 500°C test temperature.

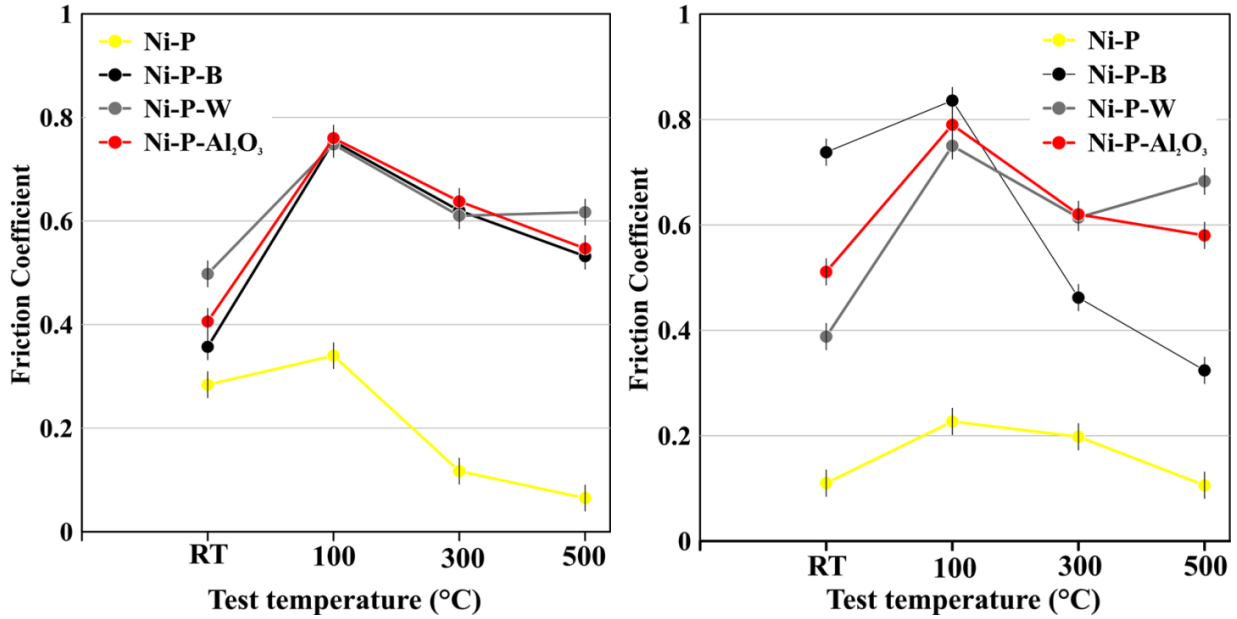

Figure 7.5 Comparison of friction performance for (a) as-deposited and (b) heat-treated electroless Ni-P and its variants coatings

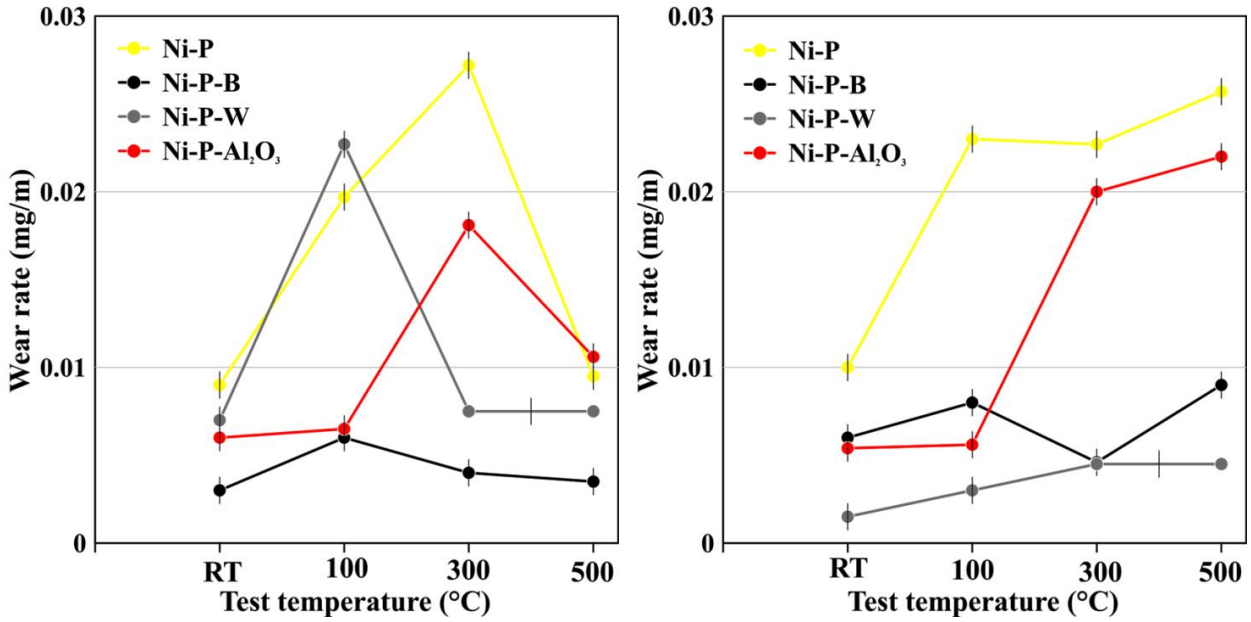

Figure 7.6 Comparison of wear performance for (a) as-deposited and (b) heat-treated electroless Ni-P and its variants coatings

Material softening at higher temperature is probably the reason for that drop in COF. Coatings tested at 500°C shows better results, may be because of the formation of surface oxides at higher temperature (500°C) which provide a lubricating effect that lowers down the COF. Overall, for frictional performance consideration, Ni-P in its room temperature as well as high temperature both perform better than its other variant coatings.

The wear performance of as-deposited and heat-treated coatings of Ni-P and its variants is represented by Figure 7.6. For both conditions, Ni-P shows high wear rate which may be due to lesser hardness as in both as-deposited and heat-treated case compared to other coatings as indicated by Figure 7.4. For as-deposited coating, Ni-P-B shows better results in room as well as high temperature case. But for heat-treated case, Ni-P-W provides better wear resistance compared to other coatings for all the temperature variations.

7.5 Selection of the Coatings based on Tribological Performance

At room temperature, Ni-P-B coatings exhibit high wear resistance while Ni-P shows low COF. Considering both wear and COF, Ni-P-B coatings may be suggested for room temperature applications. Further, at 100°C high wear resistance is observed for Ni-P-B in combination with Ni-P-Al_2O_3 coating while a low COF for Ni-P coatings. Overall, enhanced tribological behavior is observed for Ni-P-B coatings at 100°C. At 300°C, high wear resistance is seen for Ni-P-B while the binary Ni-P alloy shows low COF. Ni-P-B coating is suggested based on overall performance at 300°C. At 500°C, Ni-P-B coating shows better tribological characteristics both with respect to high wear resistance and low COF. So, if we consider the entire operating temperature domain i.e. 30°C-500°C, then Ni-P-B coatings would be preferable for as-deposited case.

For heat-treated coatings, at room temperature considering both wear and COF, Ni-P-W coatings may be suggested. Further, at 100°C, high wear resistance is observed for Ni-P-W which is very close to Ni-P-Al_2O_3 coating. Overall enhanced tribological behavior is experienced for Ni-P-W coatings at 100°C. At 300°C, high wear resistance is observed for Ni-P-B in conjunction with Ni-P-W while the binary Ni-P alloy show low COF. Ni-P-B coating is suggested based on overall performance at 300°C. At 500°C, Ni-P-W coatings show better tribological characteristics both with respect to high wear resistance. But Ni-P-B shows low COF at 500°C. So, if we consider the entire operating temperature domain i.e. 30°C-500°C, then Ni-P-W coatings would be preferable for heat-treated case. However, the performance of Ni-P-B in high temperature is also quite satisfactory.

7.6 Closure

The present chapter attempts to compare the hypophosphite reduced EN alloy and composite coatings based on coating configuration, microhardness and tribological behavior at different operating temperatures. From plating rate and structural point of view, Ni-P-B coating shows better plating rate as well as columnar structure with cauliflower surface morphology

which provides better wear resistance. The inclusion of alloying element causes to decrease bath deposition rate as well as increases the chances to make bath unstable Electroless Ni-P-Al_2O_3 coatings exhibit high hardness owing to deposition of hard Al_2O_3 particles in Ni-P matrix. Heat-treatment in each cases causes to increase the hardness of the as-deposited coatings, though the effect is higher for Ni-P coating. Considering the tribological behavior of the four coatings, it becomes difficult to identify a single one which outperforms the others in the entire operating temperature domain considered i.e. 30°C-500°C. But overall, Ni-P-B coatings have a high wear resistance at all the operating temperatures while its COF tends to be on the higher side at room temperature (30°C) and 100°C. But at high temperatures of 300°C or 500°C, oxide formation causes to impart self lubricating capabilities and that helps to drop the COF. For heat-treated coatings Ni-P-W performs better with regards to wear resistance because of solid solution strengthening effects of tungsten in nickel matrix. Heat-treatment causes to increase COF but at high temperature the oxide formation is causes to provide lubrication effect and corresponding drop in high temperature COF.

This page is left blank intentionally

Chapter 8

Conclusion and future scope

Hypohosphite reduced Ni-P and its few variants under alloy (Ni-P-W and Ni-P-B) and composite (Ni-P-Al_2O_3) category are developed and tribological characterisation are performed systematically. The prime aim is to evaluate the tribological performance of the developed Ni-P and its variants under room and high temperature. Apart from Ni-P-B, Ni-P and all the other variants show an amorphous structure in as-deposited condition which turns crystalline on heat-treatment. Ni-P shows very stable bath with moderate deposition rate which further decrease due to incorporation of third particles viz. W or Al_2O_3 . Though a reverse trend regarding the bath stability and deposition rate is observed for Ni-P-B, as because of use of borohydride in combination with hypophosphite as reducing agent where the former is known to provide higher reaction rate. The as-deposited coatings shows roughness which is very close to that of substrate that again increases slightly due to heat-treatment because of inflation in grain size. As-deposited Ni-P provides hardness around 600 $HV_{0.1}$ which further increases by incorporation of boron or tungsten or Al_2O_3 particles in the Ni-P matrix. The incorporation of Al_2O_3 in the Ni-P matrix is significant among all and it provides higher hardness among all the developed Ni-P variants. Heat-treatment causes to increase hardness of the each of the as-deposited coatings by precipitation of hard nickel phosphide phases. For Ni-P-B, the hard boride phases are also formed in conjunction with phosphide phases. But the effect of heat-treatment is found to be higher for Ni-P coating in compared to other coatings. XRD analysis Ni-P coating is found to be largely amorphous in the as-deposited phase which is represented by a series of small peaks very close to each other. After heat-treatment (400°C, 1hr) the coating turns crystalline with the formation of nickel phosphide phases, the major phase being Ni_3P. Addition of W improves the crystallinity of Ni-P-W coating representing a mixture of amorphous and nano crystalline phases but with heat-treatment it turns crystalline with the formation of nickel phosphide and Ni-W solid solution. Incorporation of B in Ni-P gives rise to low-B range Ni-P-B coating which shows nano crystallite structure. Heat treatment helps in formation of borides and phosphide phases which clearly indicates the phase transformation that leads to higher hardness. The amorphous structure of as deposited Ni-P-Al_2O_3 coating is converted into crystalline structure due to heat treatment through formation of hard Ni_3P phases along with some Al_2O_3 peaks at various diffraction angles. The presence of metastable phases in coatings may be because of incomplete transformation from the originally amorphous structure to the crystalline Ni and Ni_3P stable phases after heat treatment.

Both as-deposited as well as heat-treated coatings have been investigated for friction and wear under room and high temperature conditions by varying applied load (10-50 N) and sliding

velocity (0.094-0.22 m/s). It is found that the COF of the as-deposited coating mostly increases with increase in load. This increase in COF may be attributed to the increase in contact area and subsequent higher force required to break them. The decreasing trend of COF with sliding velocity may be due to the change of shear rate which can in turn affect the mechanical properties of the mating materials. Moreover, higher sliding velocity will contribute to a larger normal momentum transfer in the upward direction. This results in an increased separation between the coating and the counterface which further results in decreased real area of contact. A direct comparison of the room and high temperature tribological performances of as-deposited as well as heat-treated EN coatings is performed with respect to varying load and velocity. The comparison is presented for the best combination of applied load and sliding velocity (10 N and 0.220 m/s) as seen from the previous discussions. The further temperature profiling and detail discussion on as-deposited and heat-treated Ni-P and its variants coatings is discussed in the next phase based on selected load (10 N) and velocity (0.22 m/s).

Friction and wear performance of electroless Ni-P and its variants coatings is evaluated at room (30°C) and elevated (100°C, 300°C and 500°C) temperatures. Now, heat-treated coatings are harder than as-deposited coatings and are anticipated to exhibit better wear resistance compared to the latter. Again, at elevated temperature testing, the samples are expected to undergo a simultaneous heat-treatment cycle (short duration) and as a result get somewhat harder. Hence, tests are conducted both on as-deposited samples as well as heat-treated (400°C, 1 hr) samples at various temperatures. The results of elevated temperature tests particularly at 500°C exhibit comparatively lower COF than the others. This may be because of the in situ heat-treatment due to the exposure to the elevated test temperature which results in improved hardness of the coating. The heat-treated coatings also display almost analogous friction characteristics. The worn surface displays a ploughing effect, coating detachment and cracks which indicate that both adhesion and abrasion phenomena govern the wear mechanism. The top surface of the EN coating after elevated tribology tests consists of a mechanically mixed layer of oxidation products. After the tests, the hardness increase of the as-deposited coatings is quite high compared to the heat-treated ones. The effect of the short duration heat-treatment, because of high temperature tests is proven through XRD as well as hardness study of the post wear samples where the formation of hard phosphide phases are visible that causes to increase hardness as well as represents better wear resistance Overall the EN coatings have potential to perform under elevated temperature conditions.

From the current work, it would be possible to judge the suitability of hypophosphite reduced coatings for high temperature tribological applications. Depending on the requirement such as anti-wear, anti-friction or both it would be possible to select the suitable alloy or composite coating. Moreover, introduction of W, B or Al_2O_3 in Ni-P coatings affect their crystallinity and degree of crystallization at different temperatures. A preliminary investigation is carried out in present study where high temperature tribological characteristics of hypophosphite reduced alloys or composite are studied revealing its relevant wear mechanisms. The choice of a

particular variant depends upon several factors and it is better to say that choice depends on the requirement. So for the coating and relevant industries, the following recommendations may be made for proper selection of hypophosphite reduced coating variants:

(i) At lower or room temperature, Ni-P exhibit low COF. Therefore, it would not be economical to go for further complexities and deposit other variants regarding frictional behavior. Though for high hardness, Ni-P-Al_2O_3 is preferred choice. But considering both wear and COF, Ni-P-B or Ni-P-W coatings may be suggested as Ni-P shows lower wear resistance.

(ii) Overall enhanced tribological behavior is seen for Ni-P-W coatings within temperature range of 30°C to 100°C.

(iii) Ni-P-B coating is suggested based on overall performance at 300°C. At 500°C, Ni-P-B coating show better tribological characteristics both with respect to high wear resistance and low COF. But for same temperature domain, Ni-P-W coatings would be preferable for heat-treated case.

So considering the entire operating temperature domain i.e. 30°C-500°C, Ni-P-B coatings would be preferable for tribological performance.

While completing the experiments, there emerge certain issues which require further examination utilizing advanced equipment. The inter-diffusion between coating and substrate material at high temperatures and their impact on the tribological performances should be additionally explored. Such phenomenon may essentially influence the tribological properties and can be analyzed using glow discharge optical emission spectroscopy (GDOES) of crosscut segments. The role of oxides of Ni or W could also be studied intricately utilizing micro-Raman analysis or X-ray photoelectron spectroscopy (XPS).

Analysis of the mechanical properties of the counterface disc is not carried out and the focus has been mainly on the analysis of tribological behavior of the coatings and associated wear mechanisms. Future investigations might be coordinated towards the assessment of mechanical properties of EN 31 plate at raised temperatures alongside the variation of its hardness which would encourage a more profound knowledge into friction and wear conduct of Ni-P-(W, B or Al_2O_3)/EN 31 tribo-pair. The friction and wear characteristics evaluated in the present work are specific to electroless Ni-P, Ni-P-B, Ni-P-W or Ni-P-Al_2O_3 coatings sliding against EN 31 disc at high temperature and are expected to vary for some other configuration of tribo-test setup used. The other variations of Ni-P can also be investigated as well as the present coating with other combination of coating composition is also a option for further study. Apart from that duplex and nano coatings based on hypophosphite reduction may be a choice for future works related to high temperature suitable coating. Selection of a particular mechanical application where sliding at high temperature is included especially in the hot metal working industry might be investigated in future for assessment of the present coatings.

This page is left blank intentionally

References

Agarwala, R. C., & Agarwala, V. (2003). *Sadhana*, **28**(3-4), 475-493.

Alirezaei, S., Monirvaghefi, S. M., Saatchi, A., Ürgen, M., & Motallebzadeh, A. (2013a). *Surf. Eng.*, **29**(4), 306-311.

Alirezaei, S., Monirvaghefi, S. M., Saatchi, A., Ürgen, M., & Motallebzadeh, A. (2013b). *Trans. IMF*, **91**(4), 207-213.

Anik, M., & Körpe, E. (2007). *Surf. Coat. Technol.*, **201**, 4702–4710.

Anik, M., Körpe, E., & Şen, E. (2008). *Surf. Coat. Technol.*, **202**(9), 1718-1727.

Apachitei, I., Duszczyk, J., Katgerman, L., & Overkamp, P. J. B. (1998). *Scripta Materialia*, **38**(9), 1347-1353.

Araghi, A., & Paydar, M. H. (2010). *Mater. Des*., **31**(6), 3095-3099.

Ashassi-Sorkhabi, H., & Rafizadeh, S. H. (2004). *Surf. Coat. Technol*., **176**(3), 318-326.

Ashassi-Sorkhabi, H., Dolati, H., Parvini-Ahmadi, N., & Manzoori. (2002). *Appl. Surf. Sci.*, **185**, 155-160.

Aydeniz, A. I., Göksenli, A., Dil, G., Muhaffel, F., Calli, C., & Yüksel, B. (2013). *Materiali in tehnologije*, **47**(6), 803-806.

Balaraju, J. N., & Rajam, K. S. (2005). *Surf. Coat. Technol.*, **195**(2), 154-161.

Balaraju, J. N., & Rajam, K. S. (2008). *J. Alloy. Compd.*, **459**, 311–319.

Balaraju, J. N., & Rajam, K. S. (2009). *J. Alloy. Compd*., **486**(1), 468-473.

Balaraju, J. N., Jahan, S. M., Anandan, C., & Rajam, K. S. (2006). *Surf. Coat. Technol.*, **200,** 4885-4890.

Balaraju, J. N., Manikandanath, N. T., & Grips, VKW. (2012). *Surf. Coat. Technol.*, **206**, 2682-2689.

Balaraju, J. N., Priyadarshi, A., Kumar, V., Manikandanath, N. T., Kumar, P. P., & Ravisankar, B. (2016). *Mater. Sci. Technol.*, **32**(16), 1654-1665.

Balaraju, J. N., Raman, N., & Manikandanath, N. T. (2014). *Trans. IMF*, **92**(3), 169-176

Beygi, H., Vafaeenezhad, H., & Sajjadi, S. A. (2012). *Appl. Surf. Sci.*, **258**(19), 7744-7750.

Biswas, A., Das, S. K., & Sahoo, P. (2017). *Surf. Coat. Technol.*, **328**, 102-114.

Bonin, L., & Vitry, V. (2016). *Surf. Coat. Technol.*, **307**, 957-962.

Bouanani, M., Cherkaoui, F., Fratesi, R., Roventi, G., & Barucca, G. (1999). *J. Appl. Electrochem*., **29**(5), 637-645.

Brenner, A., & Riddell, G. E. (1946). *J. Res. Nat. Bur. Standards*, **37**(1), 31–34.

Chen, L. J., Chen, M., Zhou, H. D., & Chen, J. M. (2008). *Appl. Surf. Sci.*, **255**, 3459–3462

Contreras, A., León, C., Jimenez, O., Sosa, E., & Pérez, R. (2006). *Appl. Surf. Sci.*, **253**, 592–599

Das, S. K., & Sahoo, P. (2011a). *Mater. Des.*, **32**(4), 2228-2238.

Das, S. K., & Sahoo, P. (2011b). *Port. Electrochim. Acta.*, **29(**4), 211-231.

Das, S. K., & Sahoo, P. (2012). *Adv. Mech. Eng.*, **4**, 703168, 11pp.

DellaCorte, C. (1996). *Surf. Coat. Technol., **86**,* 486-492.

Dervos, C. T., Novakovic, J., & Vassiliou, P. (2004). *Mater. Lett.*, **58**(5), 619-623.

Dong, D., Chen, X. H., Xiao, W. T., Yang, G. B., & Zhang, P. Y. (2009). *Appl. Surf. Sci.*, **255**(15), 7051-7055.

Duari, S., Mukhopadhyay, A., Barman, T. K., & Sahoo, P. (2016). *J. Mol. Eng. Mater.*, **04**(04), 1640013, 13pp.

Duari, S., Mukhopadhyay, A., Barman, T. K., & Sahoo, P. (2017). *Surfaces and Interfaces*, **6**, 177-189.

Duncan, R. N., & Arney, T. L. (1984). *Plat. Surf. Finish.*, **71**(12), 49-54.

Ebrahimian-Hosseinabadi, M., Azari-Dorcheh, K., & Vaghefi, S. M. (2006). *Wear*, **260**, 123–127.

Farzaneh, A., Ehteshamzadeh, M., Ghorbani, M., & Mehrabani, J. V. (2010). *J. Coat. Technol. Res.*, *7*(5), 547-555.

Franco, M., Sha, W., Aldic, G., Malinov, S., & Çimenoğlu, H. (2016). *Tribol. Int.*, **97**, 265-271.

Gadhari, P., & Sahoo, P. (2016). *Surf. Rev. Lett.*, **23**(01), 1550082, 14 pp.

Gadhari, P., & Sahoo, P. (2017). *Silicon*, **9***(5), 761-774*

Gaurilow, G.G. (1979). *Chemical (electroless) nickel plating*, Portcullis press, Redhill.

Gawne, D. T., & Ma, U. (1987). *Wear*, **120**(2), 125-149.

Ghaderi, M., Rezagholizadeh, M., Heidary, A., & Monirvaghefi, S. M. (2016a). *Prot. Met. Phys. Chem. Surf.*, **52**(5), 854-858.

Ghaderi, M., Rezagholizadeh, M., Vaghefi, S. M., & Heidary, A. (2016b). *Prot. Met. Phys. Chem. Surf.*, **52**(3), 538-542.

Gou, Y. N., Huang, W.J., Chen, W.B., Tan, G.F., & Xue, Y. (2010). *Corrosion and Protection*, **31**(3):225-228.

Guo, Z., Keong, K. G., & Sha, W. (2003). *J. Alloy. Compd*., **358**(1), 112-119.

He, X. M., Liu, X. B., Wang, M. D., Yang, M. S., Shi, S. H., Fu, G. Y., & Chen, S. F. (2011). *Appl. Surf. Sci.*, **258**(1), 535-541.

Higgs, C.E. (1974*). Electrodep. and Surf. Treat.*, **2**(4), 315-326.

Hosseini, J., & Bodaghi, A. (2013). *Port. Electrochim. Acta*,, **31**(1), 11-20.

Hu, X., Jiang, P., Wan, J., Xu, Y., & Sun, X. (2009). *J. Coat. Technol. Res.*, **6**(2), 275-281.

Huang, L., Gao, Y., & Zheng, Z. (2007). *J. of Funct. Mater.*, **38**(4), 683-687.

Huang, Y. S., Zeng, X. T., Hu, X. F., & Liu, F. M. (2004). *Electrochim. Acta*, **49**(25), 4313-4319.

Jappes, J. W., Ramamoorthy, B., & Nair, P. K. (2005). *J Mater Process Technol.*, **169**(2), 308-313.

John, S. S., Srinivasan, K. N., Kavimani, P. M., Krishnan, K. H., Praveen, J., Ganesan, M., & Electroless, N. P. (2005). *Plating Surf. Finish*, **92**(5), 62.

Keong, K. G., & Sha, W. (2002). *Surf. Eng.*, **18**(5), 329-343.

Keong, K. G., Sha, W., & Malinov, S. (2003). *Surf. Coat Technol.*, **168**(2), 263-274.

Krishnaveni, K., Narayanan, T. S., & Seshadri, S. K. (2005). *Surf. Coat. Technol.*, **190**(1), 115-121.

León, O. A., Staia, M. H., & Hintermann, H. E. (2003). *Surf. Coat. Technol.*, **163**, 578- 584.

Li, Z., Chen, Z., Liu, S., Zheng, F., & Dai, A. (2008). *Trans. Nonferrous Met. Soc. China*, **18**(4), 819-824.

Li, Z., Wang, J., Lu, J., & Meng, J. (2013). *Appl. Surf. Sci.*, **264**, 516-521.

Li, Z., Wang, B., & Guan, H. (2006). *Corrosion and Protection*, **27**(8), 326-328.

Liu, G. J., Zhang, W. Q., Yu, Z. T., & Ning, X. (2011). *Adv. Mater. Res.*, **217**, 897-900.

Liu, H., Guo, R. X., & Liu, Z. (2012). *Trans. Nonferrous Met. Soc. China*, **22**(12), 3012-3020.

Liu, H., Lv, Y. Y., Liu, Z., & Thompson, G. E. (2016). *Tribol. Int.*, **103**, 343-351.

Liu, J., Wang, X., Tian, Z., Yuan, M., & Ma, X. (2015). *Appl. Surf. Sci.*, **356**, 289-293.

Loto, C. A. (2016). *Silicon*, **8**(2), 177-186.

Makkar, P., Agarwala, R. C., & Agarwala, V. (2013). *Ceram. Int.*, **39**(8), 9003-9008.

Mallory, G. O., & Hajdu, J. B. (1990). *Electroless plating: fundamentals and applications*. William Andrew, New York, USA.

Masoumi, F., Ghasemi, H. R., Ziaei, A. A., & Shahriari, D. (2012). *Int. J. Adv. Manuf. Technol.*, **62**(9-12), 1063-1070.

Martyak, N. M., & Drake, K. (2000). *J. Alloy. Compd*., **312**, 30-40.

Mellor, B.G. (2006). *Surface coatings for protection against wear*. Cambridge, Woodhead publishing limited.

Mukhopadhyay, A., Barman, T. K., & Sahoo, P. (2018a), *Proc. IMechE. Part J: J. Eng. Tribol.*, **232(11)**, 1450-1466.

Mukhopadhyay, A., Barman, T. K., & Sahoo, P. (2018b), *Surf. Rev. Lett.*,1850175, 14 pp.

Mukhopadhyay, A., Barman, T. K., & Sahoo, P. (2018c), *Tribol. T.*, **61(1)**, 41-52.

Mukhopadhyay, A., Duari, S., Barman, T. K., & Sahoo, P. (2015). *J. Manuf. Technol. Res.*, **7**(1/2), 1-24.

Mukhopadhyay, A., Duari, S., Barman, T. K., & Sahoo, P. (2016). *J. Inst. Eng. India Ser. D*, **97**(2), 215-231.

Mukhopadhyay, A., Duari, S., Barman, T. K., & Sahoo, P. (2017). *J. Inst. Eng. India Ser. D*, **98**(2), 255-268.

Niksefat, V., & Ghorbani, M. (2015). *J. Alloy Compd.*, **633**, 127-136.

Novák, M., Vojtěch, D., Novak, P., & Vítů, T. (2011). *Appl. Surf. Sci.*, **257**(23), 9982-9985.

Oraon, B., Majumdar, G., & Ghosh, B. (2006). *Mater. Des.*, **27**(10), 1035-1045.

Oraon, B., Majumdar, G., & Ghosh, B. (2007). *Mater. Des.*, **28**, 2138-2147.

Oraon, B., Majumdar, G., & Ghosh, B. (2008). *Mater. Des.*, **29**(7), 1412-1418.

Osaka, T., Sawai, H., Otoi, F., & Nihei, K. (1982). *Metal Finish*, **80**(8), 31-35.

Pal, S., Sarkar, R., & Jayaram, V. (2018). *Metall. Mater. Trans. A*, **49**(8), 3217–3236.

Pal, S., Verma, N., Jayaram, V., Biswas, S. K., & Riddle, Y. (2011). *Mater. Sci. Eng. A*, **528**(28), 8269-8276.

Palaniappa, M., & Seshadri, S. K. (2007). *Mater. Sci. Eng. A.*, **460-461**, 638-648.

Palaniappa, M., & Seshadri, S. K. (2008). *Wear*, **265**(5), 735-740.

Panja, B., & Sahoo, P. (2014). *IJSEIMS*, **2**(2), 53-69.

Panja, B., Das, S. K., & Sahoo, P. (2016). *Surf. Rev. Lett.*, **23**(05), 1650040, 18pp.

Parkinson, R. (1997). *Properties and Applications of Electroless Nickel*. Nickel Development Institute, NiDI Technical Series, (10081).

Qu, S., Huang, X., & Cai, G. (2011). *Adv. Mater. Res*., **179**,:334-338.

Ramalho, A., & Miranda, J. C. (2005). *Wear*, **259**(7-12), 828-834.

Riddle, Y. W., & Bailer, T. O. (2005). *JOM*, **57**(4), 40-45.

Roman, A., Chicot, D., & Lesage, J. (2002). *Surf. Coat Technol*., **155**(2-3), 161-168.

Roy, S., & Sahoo, P. (2012a). *Port. Electrochim. Acta*., **30**(3), 203-220.

Roy, S., & Sahoo, P. (2012b). *Trib. in Industry*, **34**(4), 186-197.

Roy, S., & Sahoo, P. (2013). *J. of Coatings*, 608140, 13pp.

Sahoo, P. (2008a). *Tribol. Online*, **3**(1), 6-11.

Sahoo, P. (2008b). *Surf. Interf. Anal.*, **40**(12), 1552-1561.

Sahoo, P. (2009). *Mater. Des.*, **30**(4), 1341-1349.

Sahoo, P., & Das, S. K. (2011). *Mater. Des.*, **32**(4), 1760-1775.

Sahoo, P., & Roy, S. (2017). *IJSEIMS*, **5**(1), 1-15.

Sankara Narayanan, & Seshadri, S. K. (2004). *J. Alloy. Compd.*, **365**, 197–205

Sankara Narayanan, T. S. N., Baskaran, I., Krishnaveni, K., & Parthiban, S. (2006). *Surf. Coat. Technol.*, **200**(11), 3438-3445.

Sankara Narayanan, T. S. N., Krishnaveni, K., & Seshadri, S. K. (2003). *Mater. Chem. Phys.*, **82**(3), 771-779.

Schwartz, M., & Mallory, G. O. (1976). *J. of Electrochem. Soc*., **123**(5), 606-614.

Selvi, V. E., Chatterji, P., Subramanian, S., & Balaraju, J. N. (2014). *Surf. Coat. Technol.*, **240**, 103-109.

Serin, I. G., & Göksenli, A. (2015). *Surf. Rev. Lett*., **22**(05), 1550058.

Sliney, H.E. (1992). *Solid lubricants, in: friction, lubrication and wear technology*, ASM Handbook, New York.

Srinivasan, K. N., & John, S. (2005). *Surf. Eng.*, **21**(2), 156-160.

Srinivasan, K. N., Meenakshi, R., Santhi, A., Thangavelu, P. R., & John, S. (2010). *Surf. Eng.*, **26**(3), 153-158.

Staia, M. H., Castillo, E. J., Puchi, E. S., Lewis, B., & Hintermann, H. E. (1996). *Surf. Coat. Technol.*, **86**, 598-602.

Staia, M. H., Enriquez, C., & Puchi, E. S. (1997). *Surf. Coat. Technol.*, **94**, 543-548.

Staia, M. H., Conzono, A., Cruz, M. R., Roman, A., Lesage, J., Chicot, D., & Mesmacque, G. (2002). *Surf. Eng.*, **18**(4), 265-269.

Straffelini, G., Colombo, D., & Molinari, A. (1999). *Wear*, **236**(1-2), 179-188.

Sudagar, J., Lian, J., & Sha, W. (2013). *J. Alloy. Compd*., **571**, 183-204.

Tsai, Y., Wu, F., Chen, Y., Peng, P., Duh, J., & Tsai, S. (2001). *Surf. Coat. Technol.*, **146**, 502-507.

Vaghefi, S. Y. M., & Vaghefi, S. M. M. (2011). *Neural Comput. Appl.*, **20**(7), 1055-1060.

Vargas Mendoza, L., Barba, A., Bolarin, A., & Sanchez, F. (2006). *Surf. Eng.*, **22**(1), 58-62.

Velez, M., Quinones, H., Di Giampaolo, A. R., Lira, J., & Grigorescu, I. C. (1999). *Int. J. Refract. Met. H.*, **17**(1), 99-102.

Venkatkrishna, P. G. & Sankara Narayanan, T. S. N. (2013). *Eur. J. Sci. Res.*, **82**, 506-514.

Venkatkrishna, P. G., Mohamed Nazirudeen, S. S., & Sankara Narayanan, T. S. N. (2014). *Int. J. Eng. Technol.*, **6**, 1059-1064.

Vitry, V., & Bonin, L. (2017a). *Electrochim. Acta*, **243**, 7–17.

Vitry, V., & Bonin, L. (2017b). *Surf. Coat. Technol.*, **311**, 164–171.

Vitry, V., Kanta, A. F., & Delaunois, F. (2010). *Mater. Sci. Eng. B*, **175**(3), 266-273.

Vitry, V., Kanta, A. F., & Delaunois, F. (2011). *Surf. Coat. Technol.*, **206**(7), 1879-1885.

Vitry, V., Kanta, A. F., Dille, J., & Delaunois, F. (2012a). *Surf. Coat. Technol.*, **206**(16), 3444-3449.

Vitry, V., Sens, A., Kanta, A. F., & Delaunois, F. (2012b). *Appl. Surf. Sci.*, **263**, 640-647.

Vitry, V., Sens, A., Kanta, A. F., & Delaunois, F. (2012c). *Surf. Coat. Technol.*, **206**(16), 3421-3427.

Voevodin, A. A., & Zabinski, J. S. (2005). *Compos. Sci. Technol.*, **65**(5), 741-748.

Wang, X. R., Hu, X. G., & Li, W. Y. (2012). *Appl. Mech. Mater.*, **117**, 1276-1279.

Wu, F. B., Tien, S. K., Chen, W. Y., & Duh, J. G. (2004). *Surf. Coat. Technol.*, **177**, 312-316.

Wu, Y., Liu, H., Shen, B., Liu, L., & Hu, W. (2006). *Tribol Int.*, **39**(6), 553-559.

Yating, W., Bin, S., Lei, L., & Wenbin, H. (2008). *J Mater Process Technol.*, **205**(1), 207-213.

Yu, H. S., Luo, S. F., & Wang, Y. R. (2001). Surf. Coat. Technol., **148**(2-3), 143-148.

Zhang, W. X., Jiang, Z. H., Li, G. Y., Jiang, Q., & Lian, J. S. (2008). Appl. Surf. Sci., **254**(16), 4949-4955.

Zhao, G. G., & Deng, F. M. (2005). *Key Eng. Mater.*, **280**, 1445-1448.

Zhou, Q. J., He, J. Y., Li, J. X., Chu, W. Y., & Qiao, L. J. (2006a). *Mater. Lett.*, **60**(3), 349-351.

Zhou, Q. J., He, J. Y., Sun, D. B., Chu, W. Y., & Qiao, L. J. (2006b). *Scripta Materialia.*, **54,** 603-608.

This page is left blank intentionally

Publication from the Thesis

Applied Physics A (2019) 125:520
https://doi.org/10.1007/s00339-019-2816-1

Applied Physics A
Materials Science & Processing

Tribological behavior of autocatalytic Ni–P–B coatings at elevated temperatures

Sanjib Kundu[1] · Suman Kalyan Das[1] · Prasanta Sahoo[1]

Received: 9 April 2019 / Accepted: 12 July 2019

Abstract

Ni–P–B coatings are produced directly on surface of carbon steel (AISI 1040) using electroless plating technique. The effects of temperature on the friction and wear behavior of Ni–P–B alloy coatings have been investigated. Tribological tests are conducted at four temperatures (30, 100, 300 and 500 °C) under constant load and sliding speed in a pin-on-disk apparatus. Results show that Ni–P–B coatings sustain the elevated temperatures with minimal effect on friction and wear performances. Ni–P–B coating is found to exhibit the maximum hardness among the binary Ni–P and Ni–B coatings with as-deposited hardness reaching around 700HV. Heat treatment increases the hardness as well as wear resistance by precipitation of boride and phosphide phases of nickel. Room temperature test shows mostly adhesive wear pattern but finally, it leads to a mixture of abrasive–adhesive wear mechanism. Friction and wear of Ni–P–B is overall governed by the formation of oxidative layer, mechanically mixed layer with iron (from ferrous counter face), wear mechanism, phase transformation and changes in microstructure during elevated wear test. Phase transformation and corresponding micro-structural changes occurring during elevated test duration help in providing better wear resistance to the coating.

1 Introduction

Brenner and Riddell invented [1] the electroless deposition in 1946; since then, it got immense attention due to its ability to produce coatings that have outstanding corrosion and wear resistance. Among all types of deposition, electroless nickel (EN) has gained enormous popularity due to its ability to provide a hard, wear and corrosion-resistant surface [2, 3]. Reducing agents (i.e., hypophosphite, borohydride or dimethylamine borane and hydrazine) play the deciding role in grouping of electroless nickel coatings. Essential characteristics of hypophosphite-reduced electroless nickel baths (Ni–P) are: ease of control, low cost and good corrosion resistance. Whereas, borohydride-based baths (Ni–B) provide better reduction efficiency as well as plating rate but probability of decomposition and cost of operation are higher. The major advantages of borohydride-reduced baths are its hardness and better wear resistance in the as-deposited condition [4]. Both electroless Ni–P and Ni–B coatings are found to be amorphous in as-deposited condition but get transformed to crystalline structure with heat treatment through precipitation of hard particles such as nickel phosphide (Ni_3P) and nickel boride (Ni_3B) phases, respectively [5–7]. Cauliflower-type surface morphology and columnar growths of Ni–B enhance lubricity and thus improve the wear properties (comparable with hard chromium) due to reduction in the contact area [8, 9]. Ni–B coating has decent anti-corrosive (0.058 mm/year) properties but not satisfactory in comparison to Ni–P (0.019 mm/year). Heat treatment in vacuum provides an improvement in hardness but it is also associated with increase in corrosion rate (0.135 mm/year) for Ni–B coating [10].

High-temperature conditions present an adverse situation for most of the tribological applications such as bearings, turbines, heat exchangers, control valves, extruders etc. [11]. Exposures to elevated temperature cause decomposition as well as rapid degradation of liquid lubricant as the same is mostly limited to operate within 350 °C [12]. The demand of high-temperature solid-lubricating coatings (Cs-compounds coating, sulfate coatings, NASA-PS coatings, other multi-phase coatings, etc.) is very crucial for those applications [13]. EN coatings has already proven its suitability to act as wear reduction alternative to those harshest conditions, as nickel can sustain a temperature up to 1480 °C (melting point) and with oxidation resistance

✉ Prasanta Sahoo
psjume@gmail.com; prasanta.sahoo@jadavpuruniversity.in

[1] Department of Mechanical Engineering, Jadavpur University, Kolkata 700 032, India

Published online: 18 July 2019

Surfaces and Interfaces 14 (2019) 192–207

Contents lists available at ScienceDirect

Surfaces and Interfaces

journal homepage: www.elsevier.com/locate/surfin

Friction and wear behavior of electroless Ni-P-W coating exposed to elevated temperature

Sanjib Kundu, Suman Kalyan Das, Prasanta Sahoo*

Department of Mechanical Engineering, Jadavpur University, Kolkata – 700 032, India

ARTICLE INFO

Keywords:
Electroless ni-p-w
Friction
Wear
Hardness, high temperature

ABSTRACT

The present study evaluates the effect of operating temperature on the tribological behaviour of electroless Ni-P-W coating developed over mild steel. The constituent of the coating is found to be uniformly distributed. The incorporation of tungsten increases the as-deposit hardness (670 $HV_{0.1}$) of Ni-P coatings besides improving its crystallinity. The friction and wear tests are carried out under elevated temperature (100 to 500 °C) in a pin-on-disc setup. The results reveal that Ni-P-W coating (especially heat treated ones) display a stable friction and wear behaviour even when subjected to elevated working temperature. The as-deposited coating on the other hand shows increased wear resistance particularly when tested at 300 and 500 °C which is due to microstructural changes induced in the coating because of exposure to high temperature. This is also supported by the excellent hardness shown by the samples after test (46% increase in hardness after testing at 500 °C compared to as-deposited hardness). The applied load and sliding velocity exhibit marginal influence over the friction behavior of the coating especially for heat treated coatings. Study of worn surface reveals that the wear is governed by both abrasive and adhesive mechanisms. Moreover, the formation of oxide layers on the coating at high temperature is also believed to influence the tribological behavior of Ni-P-W coatings.

1. Introduction

The main function of coatings is basically to provide protection to the component surface against phenomena viz. wear and corrosion [1]. However, keeping in mind the industrial demands, a need for thermal resistant coatings have cropped up lately. Now, mechanical parts undergoing tribological interactions under elevated temperature require coatings which would possess low friction characteristics, high corrosion resistance and high wear resistance and at the same time maintain its properties under high temperature. As electroless nickel has already established itself as a material suitable for tribological applications [2], its candidature as a thermal resistant coating seems to be worth exploring.

Electroless deposition has been acknowledged due to its ability to coat any material with uniform thickness. Various metals like nickel, gold, copper etc. can be deposited by this method. However, deposition of nickel as proposed by Brenner and Riddell [3] has gained immense popularity due to its superior tribological properties. In case of electroless nickel (EN) coatings, base material which is also known as substrate acts like electrode where both the oxidation and reduction reactions take place. It is an autocatalytic process where the substrate develops a potential when it is immersed in electroless bath that contains a source of metallic ions, reducing agent, complexing agent, stabilizer and other components [2].

Electroless Ni-P deposit is a supersaturated alloy in the as-deposited state, and can be strengthened by the precipitation of nickel phosphide crystallites by suitable heat treatment. However, the hardness of Ni-P film degrades with excessive heat treatment due to grain coarsening. Another method to enhance the strength and properties of the coating is to incorporate certain metals and particulates into it. Tungsten and its alloys are recognized due to their specific tribological, magnetic, electrical and electro-erosion properties. They may compete even with ceramics and graphite by virtue of their high thermal resistance. It has been observed that incorporation of tungsten in EN coatings increases its wear resistance which has brought it in focus of numerous investigations [4–11]. This could be attributed to the solid solution strengthening by provided by tungsten into nickel matrix. The addition of tungsten into nickel enhances its properties like hardness and high temperature stability. The as-deposited Ni-P and Ni-P-W coatings exhibit amorphous structure. Phosphorus and tungsten are dissolved in the nickel matrix and exhibit a (111) preferred orientation under phase structure analysis. Microhardness of as-deposited Ni-P-W deposit is found to be above 600 HV. Heat treatment at 400°C for 1 h increases the hardness to above 1000 HV. The presence of tungsten retards the

* Corresponding author.
E-mail addresses: psjume@gmail.com, prasanta.sahoo@jadavpuruniversity.in (P. Sahoo).

https://doi.org/10.1016/j.surfin.2018.12.007
Received 8 June 2018; Received in revised form 12 December 2018; Accepted 15 December 2018
Available online 17 December 2018

Silicon
DOI 10.1007/s12633-016-9450-8

ORIGINAL PAPER

Tribological Behaviour of Electroless Ni-P Deposits Under Elevated Temperature

Sanjib Kundu[1,2] · Suman Kalyan Das[1,2] · Prasanta Sahoo[1,2]

Received: 13 June 2016 / Accepted: 28 July 2016

Abstract Electroless Ni-P (EN) coatings have already proven their aptness for improving the tribological performance of the base material. This is possible due to their high hardness, good wear resistivity and corrosion resistance. However, the performance evaluation of the EN coatings under high temperature or the assessment of their thermal stability is yet to be conducted. The present work deals with the study of tribological characteristics viz. friction and wear of EN coatings at elevated temperatures (100 °C, 300 °C and 500 °C) by varying the tribological testing parameters viz. applied load and sliding velocity. A detailed study of the tribological behaviour of the coating is undertaken individually for the as-deposited and heat treated samples. The results obtained are compared among each other and also with that of the room temperature (RT) tests of the coating. It is found that the friction coefficient (COF) and wear rate of EN coatings mostly increases with increase in load for all the test temperatures. However, for variation in sliding velocity, both COF and wear rate show a reverse trend. The as-deposited samples show lesser wear rate particularly at high temperature, which may be because of the in situ heat treatment received during the test. The as-deposited coatings yield better results especially when the test temperature is kept above or near the phase transformation temperature of the coating. The surface morphology, composition of coatings and crystalline structure are studied with the help of scanning electron microscopy, energy dispersed X-ray analysis and X-ray diffraction analysis respectively. The coating displays a nodular morphology and is amorphous in the as-deposited phase. With heat treatment, the coating turns crystalline. A mixed adhesive and abrasive wear mechanism is observed for the EN coatings tested at elevated temperature. Adhesive wear is accompanied by micro-cracks. Tribo-oxidation is confirmed from energy dispersive X-ray spectrometry.

Keywords Electroless Ni-P · Coating · Friction · Wear · Elevated temperature

1 Introduction

Brenner and Riddell [1] first developed electroless coating, as a result of a chemical reaction between a reducing agent present in the solution and the metal ions. EN coatings have a wide range of industrial uses due to their excellent mechanical, electrical, physical, corrosion, hardness, friction and wear resistance properties [2]. Electroless Ni-P (EN) coatings are an autocatalytic deposition of a Ni-P alloy from an aqueous solution onto a substrate without the application of electric current. The electroless bath typically comprises an aqueous solution of metal ions, complexing agents, reducing agents and stabilizers, operating in a specific metal ion concentration, temperature and pH range [3]. Electroless nickel coatings are very uniform and they follow the surface profile of the substrate rather than just filling the spaces between surface asperities. Thus, in general the roughness of the coating does not vary much from the roughness of the substrate. The deposition rate, properties of coated components and the structural behavior of deposits

✉ Prasanta Sahoo
psjume@gmail.com; psahoo@mech.jdvu.ac.in

[1] Department of Mechanical Engineering, Jadavpur University, Kolkata 700 032, India

[2] Centre of Excellence on Phase Transformation and Product Characterization, TEQIP-II, Jadavpur University, Kolkata 700032, India

Published online: 22 October 2016

Available online at www.sciencedirect.com

ScienceDirect

Materials Today: Proceedings 4 (2017) 379–387

materialstoday: PROCEEDINGS

www.materialstoday.com/proceedings

5th International Conference of Materials Processing and Characterization (ICMPC 2016)

Tribological performance of electroless Ni-(high) P coatings under elevated testing temperature

Sanjib Kundu[a,b], Suman Kalyan Das[a], Prasanta Sahoo[a,b]*

[a]*Mechanical Engineering Department, Jadavpur University, Kolkata 700032, India*
[b]*Centre of Excellence on Phase Transformation and Product Characterisation, TEQIP-II, Jadavpur University, Kolkata 700032, India*

Abstract

The ambient temperature is expected to play a significant role in the tribological performance of electroless Ni-P coatings. Moreover, the performance of Ni-P coatings is found to be largely dependent on the phosphorous content of the coatings. Hence, the present study aims to evaluate the tribological performance of Ni-(high)P coating under elevated testing temperatures. Both as-deposited as well as heat treated samples are developed for the performance evaluation. Coatings are tested under constant load and speed but at temperatures ranging from room temperature (R.T.) to 500°C. It is found that friction in general decreases at elevated temperatures compared to R.T. tests. Wear doesn't show a consistent trend with change in test temperature. The wear rate of as-deposited coatings increases with increase in temperature up to 400°C test temperature beyond which it again decreases. In case of heat treated coatings, the wear rate remains almost same except at 200°C test temperature where a higher wear rate is observed. The hardness results show good correlation with the wear results. The as-deposited coatings are found to exhibit a higher increase in hardness after the tests compared to already heat treated coatings. The microstructure characterization of the coating is performed using SEM (Scanning Electron Microscopy), EDX (Energy Dispersive X-Ray Analysis) and XRD (X-Ray Diffraction Analysis). It is found that the coating in general exhibited a nodular structure and exhibit amorphous structure in as-deposited condition which turns crystalline with heat treatment. The wear mechanism is found to be predominantly abrasive in nature.

Selection and peer-review under responsibility of Conference Committee Members of 5th International Conference of Materials Processing and Characterization (ICMPC 2016).

Keywords: Electoless; Ni-P; Coating; High Temperature; Wear; Friction;

* Corresponding author. Tel.: +91-9831434636;
E-mail address: psjume@gmail.com

Selection and peer-review under responsibility of Conference Committee Members of 5th International Conference of Materials Processing and Characterization (ICMPC 2016).

Influence of load and temperature on tribological behaviour of electroless Ni-P deposits

S Kundu[1, 2], **S K Das**[1] **and P Sahoo**[1, 2]

[1]Mechanical Engineering Department, Jadavpur University, Kolkata 700032
[2]Centre of Excellence on Phase Transformation and Product Characterisation, TEQIP-II, Jadavpur University, Kolkata 700032, India

E-mail: skundu_me@rediffmail.com

Abstract. Electroless Ni-P coatings have shown tremendous potential as tribology material at room temperature. However, the performance of the same in high temperature field needs to be evaluated as investigation reveals the softening of most of the coating materials. In the current study, both as-deposited as well as heat treated samples are developed for the performance evaluation. Coatings are tested under different loads with a constant speed and at temperatures ranging from room temperature (R.T.) to 500°C. Tribological tests are carried out on a pin-on-disc tribotester by selecting a wear track diameter of 60 mm for 5 minutes. Wear is reported in the form of wear rate by following Archard's equation. The microstructure characterization of the coating is performed using SEM (Scanning Electron Microscopy), EDX (Energy Dispersive X-Ray Analysis) and XRD (X-Ray Diffraction Analysis). Coating is developed with phosphorous weight percentages around 9% on cylindrical mild steel samples and the deposition thickness is observed to be around 50 µm. The as-deposited coating is found to be amorphous in nature and hardness of the as-deposited coating is found to be around 585$HV_{0.1}$. Friction coefficient increases initially with the increase in temperature from room temperature up to 100°C but thereafter gradually decrease with the increase in temperature. Initial increase in temperature (up to 100°C) provides higher rate of wear compared to room temperature but with further increase it drops in most of the cases. Wear rate increases with the increase in temperature but as it crosses or nears the phase transformation temperature (around 340°C), the scenario gets reversed. From X-ray diffraction analysis, it is found that coating is amorphous in as-deposited condition but transforms into a crystalline structure with heat treatment.

1. Introduction

To meet the challenging needs of a variety of industrial applications, Brenner and Riddell [1,2] discovered electroless nickel (EN) technology in 1946. EN coatings have got wide range of industrial applications because of their excellent mechanical, electrical, physical, corrosion, hardness, friction and wear resistance properties [3]. Electroless Ni-P coating is an autocatalytic deposition of a Ni-P alloy from an aqueous solution unto a substrate without the application of electric current. The substrate develops a potential when it is dipped in electroless solution called bath The electroless bath usually consisting of metal ions, reducing agents, complexing agents and stabilizers. Due to the developed potential, both positive and negative ions are attracted towards the substrate surface and release their energy through charge transfer process The process relies on the presence of a reducing agent, for example sodium hypophosphite in case of Ni-P which reacts with the metal ions to deposit metal. The bath used to operate at a particular level of metal ion and reducing agents concentration,

BLB-International Journal of Science & Technology
Special Issue November 2015 (ISSN 0976-3074)

Friction and wear trends of electroless Ni-P coatings under high temperature test conditions

Sanjib Kundu[1,2*], Suman Kalyan Das[1], Prasanta Sahoo[1,2]

[a]Department of Mechanical Engineering, Jadavpur University, Kolkata-700032, India

[b]Centre of Excellence on Phase Transformation and Product Characterisation, TEQIP-II, Jadavpur University, Kolkata 700032, India

Abstract:

Electroless nickel coating is already recognized as a coating of choice across various domains due to its distinct set of properties. However, the performance of the same in high temperature field needs to be evaluated as investigation reveals the softening of most of the coating materials in high temperature domain. This paper aims to investigate the tribological behaviour of electroless Ni-P coating under high temperature, dry condition and analyze the trends of wear rate and friction coefficient with the variation in tribo testing parameters such as the applied normal load (N) and sliding speed (rpm) Electroless Ni-P coating is developed with phosphorous weight percentages around 9% on cylindrical mild steel samples and the deposition thickness is observed to be around 50 μm. The as-deposited coating is found to be amorphous in nature and hardness of the as-deposited coating is found to be around 585$HV_{0.1}$. The friction and wear tests are carried out on a pin-on-disc type tribotester at a temperature of 500°C with a wear track diameter of 60mm for 10minutes. In high temperature tests it is observed that wear rate and friction coefficient is directly proportional with the applied load under a constant value of speed. However, both friction and wear exhibit an inverse relationship with speed under a constant applied load. In case of friction, high temperature tests yield a lower value compared to room temperature tests. To study the surface morphology and analyze the composition of the deposits, scanning electron microscopy and energy dispersed X-ray analysis are used respectively.

Keywords: *Electroless nickel, friction, high temperature, wear.*

I. INTRODUCTION

Electroless coating is a term used for a set of coatings which can be developed without the use of electric current. The coating occurs chemically when a substrate is introduced in a solution containing the metal ions to be coated and a suitable reducing agent [1]. On heating the solution, metal ions get reduced and get deposited on the substrate together with an element of the reducing agent. These types of coating can be deposited virtually over any material (conductor or non-conductor). Moreover, the coatings formed are uniform even for intricate geometries also. Electroless nickel is the popular variant among this segment of coatings. Electroless nickels have the added advantages of being hard and wear resistant besides being corrosion resistant as well. Electroless Ni-P coatings are popularly used for corrosion resistant applications [2]. It is found that the corrosion resistance of Ni-P coatings increases with the increase in phosphorous content [1, 3]. Ni-P exhibit good hardness in as-deposited condition which can be increased by suitable heat treatment. Electroless Ni-B coatings are harder than Ni-P coatings and when heat treated achieve hardness equivalent to hard chromium coatings [4].

The properties of electroless nickel coatings can be customized by adding suitable ternary elements viz. tungsten, copper, tin, cobalt, etc. or by incorporation of certain particles viz. boron carbide, silicon carbide, boron nitride, PTFE, etc. giving rise to composite coatings.

Electroless nickel coatings are found to be suitable for tribological based applications due to their smoothness and high wear resistance. At room temperature the primary mechanisms behind material displacement are adhesive and abrasive wear for surfaces under dry, non-lubricated conditions and the wear rate will vary depending on the dominant mechanism [2, 5-8]. On heat treatment of electroless Ni-P coatings beyond 300°C, hard phases of nickel phosphides are formed which inhibit the propagation of dislocation in the crystal lattice thereby contributing to higher wear resistance. At higher thermal treatments, a

Optimization Studies on Electroless Nickel Coatings: A Review

Sanjib Kundu, Jadavpur University, Kolkata, India

Prasanta Sahoo, Jadavpur University, Kolkata, India

Suman Kalyan Das, Jadavpur University, Kolkata, India

ABSTRACT

Electroless nickel coating is a novel method of coating which can be developed in various combinations of alloys and composites each having its unique set of characteristics. Electroless nickel coatings are mainly used for wear and corrosion resistant properties. However, additional characteristics like smoothness of deposit, low friction, descent plating rate, electrical and magnetic properties also make them suitable for a host of applications. The properties of electroless nickel coatings depend mainly on the electroless solution ingredients as well as deposition conditions. Important deposition parameters include bath temperature, concentration of nickel source, concentration of reducing agent, pH of the solution, concentration of surfactants, and so on. Moreover, heat treatment is found to modify the microstructure of the coating and influence certain properties viz. hardness, wear resistance, corrosion resistance, etc. A large number of works have been published by the researchers on the evaluation of electroless nickel coating performance on the basis of hardness, roughness, corrosion resistance, friction and wear resistance for various types of coatings and substrates. Several approaches are proposed in the literatures to solve the problems related with optimization of these parameters. It is felt that a review of the various approaches developed would help to compare their main features and their relative advantages or limitations which will enable to choose the most suitable approach for a particular application and also throw light on aspects that needs further attention. In this regard, the present paper presents a review on the developments done on the optimization of electroless nickel coatings to increase its efficiency.

Keywords: *ANN, DOE, Electroless Coatings, Optimization, Parameters, Process, Review, RSM, Taguchi*

1. INTRODUCTION

Electroless coatings, developed by Brenner and Riddell (1946) are formed as a result of a chemical reaction between reducing agent present in the solution and the metal ions. The reducing agent reduces the metallic ions in the solution while itself getting oxidised. In contrast to the electro-deposition method, electroless nickel requires no external source of electricity. Continuous build-up of the deposit occurs as the metal being coated; itself acts as the catalyst for

DOI: 10.4018/ijmmme.2014100101

Available online at www.sciencedirect.com

ScienceDirect

Procedia Engineering 97 (2014) 1698 – 1706

Procedia Engineering

www.elsevier.com/locate/procedia

12th GLOBAL CONGRESS ON MANUFACTURING AND MANAGEMENT, GCMM 2014

Properties of electroless nickel at elevated temperature-a review

Sanjib Kundu[a,b,*], Suman Kalyan Das[a] and Prasanta Sahoo[a,b]

[a]*Department of Mechanical Engineering, Jadavpur University, Kolkata-700032, India*
[b]*Centre of Excellence on Phase Transformation and Product Characterisation, TEQIP-II, Jadavpur University, Kolkata 700032, India*

Abstract

Electroless nickel (EN) deposits are classified as anefficient class of coatings used mainly to enhance the surface performance characteristics of a range of substrates. Electroless coating differs from conventional electrolytic coating on the basis of uniform deposition, coating of nonconductive materials and operation without the aid of electricity. Severalinvestigations devoted to the engineering facetsof EN and their technologies along with the applications have been published. Co-deposition of inert elements such as silicon carbide, Teflon or boron improved the mechanical properties of EN deposits. Furthermore, introduction of a third element (forming alloy of Ni-P-X/Ni-B-X; X=Cu, W, Mo, Sn, etc.) is also found to enhance the coating performance.The improvementin tribological featuresdone with modification of the bath formulation and the coatingprocedurehas persisted as a key research interest in investigators. Application of coating in high temperature field again reveals the softening of the material and deterioration in the wear resistant activity causing the shortening of life of the component. In brief, the performance of EN depends upon various process parameters, composition, heat treatment, operating temperature, etc. In the present work, an effort has been made to review the properties of EN coating at elevated temperature.

Selection and peer-review under responsibility of the Organizing Committee of GCMM 2014

Keywords:Electroless nickel, coating, properties, elevated temperature, review

1. Introduction

Electroless coating developed by Brenner and Riddell [1]is a chemical reduction process, which depends on the catalytic reduction of a metallic ion from an aqueous solution, and the subsequent deposition of the metal without the use of electrical energy [2].This coating method can coat electrically conductive materials including graphite as well as fabrics and insulators like plastics, rubber etc. Broadclassifications of electroless nickel are shown in Table 1.Electroless nickel (EN) coating which possesses some distinct collection of properties (Table 2) has assumed huge commercial importance among the variants of electroless coatings. EN coating has unique physicochemical and

* Corresponding author. Tel.: +91-923-166-0855; fax: +91-33-2414-6890.
E-mail address: skundu_me@rediffmail.com

Selection and peer-review under responsibility of the Organizing Committee of GCMM 2014
doi:10.1016/j.proeng.2014.12.321

Chapter 4
Friction and Wear Characteristics of Heat Treated Electroless Ni–P–W Coatings Under Elevated Temperature

Sanjib Kundu, Suman Kalyan Das and Prasanta Sahoo

4.1 Introduction

Brenner and Riddell [1] proposed a process of coating without any external current, known as electroless deposition in which electroless nickel (EN) became very popular. Since invention, it is widely used because it provides uniformity concerning deposit, low porosity and requires low process temperature [2]. The as-deposited Ni–P perhaps is invigorated through growth of nickel phosphide crystallites under satisfactory heating conditions. Yet, higher heat treatment period or heating [3] temperatures impair the solidity of Ni–P covering because of grain coarsening [4].

A typical electroless solution consists of supplying agent of nickel, reducing agent, complexing agent, stabilizer, surfactant, buffering agent, etc. The function of nickel source is to supply the nickel ions for deposition on the substrate while reducing agent supplied the requisite electrons intended for the reduction procedure of nickel [2]. Complexing agents are used to inhibit the breakdown of the solution as well as to make the bath stable. Stabilizers/inhibitors are also provided to avoid the random disintegration of the plating bath. Addition of surfactant results in better surface finish and increased hardness [5]. Moreover, existence of surfactant favours the film deposition reaction between the bath solution and the dipped substrate surface [5] which results in improved surface finish. Buffering agents are used to control the pH of the bath [2]. Primarily coating follows substrate roughness profile with marginal fluctuations. Surface roughness of the coating is hugely affected by the level of reducing agent [6]. It is seen to again decrease with heat treatment [7]. Chloride baths provide smoother surface than that developed from sulphate-based bath [8]. Several optimization methods [9] are employed to know the proper

S. Kundu (✉) · S. K. Das · P. Sahoo
Mechanical Engineering Department, Jadavpur University, Kolkata 700032, India
e-mail: skundu_me@rediffmail.com

P. Sahoo and J. P. Davim (eds.), *Advances in Materials, Mechanical and Industrial Engineering*, Lecture Notes on Multidisciplinary Industrial Engineering,
https://doi.org/10.1007/978-3-319-96968-8_4